DEVELOPMENT AND APPLICATION OF PHOTO-CLICK REAGENTS FOR SPATIAL AND TEMPORAL CONTROL OF STRAIN-PROMOTED ALKYNE-AZIDE CYCLOADDITIONS (SPAAC).

by

CHRISTOPHER DANIEL MCNITT

(Under the Direction of Vladimir V. Popik)

ABSTRACT

Catalyst-free strain-promoted alkyne-azide cycloaddition (SPAAC) has become an increasingly popular ligation strategy in the areas of material functionalization, immobilization, nano medicine, and labeling of various biological substrates. We have developed a new Oxa-dibenzocyclooctyne (ODIBO) that displays exceptional reaction kinetics with azides. ODIBO can be readily prepared by the photochemical decarbonylation of corresponding cyclopropenones (photo-ODIBO). Not only is ODIBO one of the most reactive cyclooctynes reported to date, but it also shows dramatic increase in the rate of cycloaddition in neutral aqueous solutions. We have done extensive studies comparing ODIBO to the most commonly used cyclooctynes in the literature DIBO, ADIBO, and BCN. Rate constants for all cyclooctynes in various conditions were determined as well as the stabilities of each cyclooctyne to hydrolysis, pH, and glutathione. These properties are vital for being able to choose the correct cyclooctyne for a specific application. We then applied a variety of different photo-caged cyclooctynes and cyclooctynes for application in the field of surface functionalization, nano-medicine, and drug delivery.

INDEX WORDS: SPAAC, Copper-Free Click Chemistry, Photo-Click, Cyclopropenones, Cyclooctyne, Azide, Click-Chemistry, Bioorthogonal Ligation, Oxadibenzocyclooctyne,

DEVELOPMENT AND APPLICATION OF PHOTO-CLICK REAGENTS FOR SPATIAL AND TEMPORAL CONTROL OF STRAIN-PROMOTED ALKYNE-AZIDE CYCLOADDITIONS (SPAAC).

by

CHRISTOPHER DANIEL MCNITT

B.S., Florida State University, 2009

A Dissertation Submitted to the Graduate Faculty of The University of Georgia in Partial Fulfillment of the Requirements for the Degree

DOCTOR OF PHILOSOPHY

ATHENS, GEORGIA

2016

DEVELOPMENT AND APPLICATION OF PHOTO-CLICK REAGENTS FOR SPATIAL AND TEMPORAL CONTROL OF STRAIN-PROMOTED ALKYNE-AZIDE CYCLOADDITIONS (SPAAC).

by

CHRISTOPHER DANIEL MCNITT

Major Professor:	Vladimir V. Popik
Committee:	Robert S. Phillips
	Ryan Hili

Electronic Version Approved:

Suzanne Barbour
Dean of the Graduate School
The University of Georgia
December 2016

ACKNOWLEDGEMENTS

I would like to thank my advisor Dr. Popik for his guidance and wisdom. I have deeply enjoyed my time doing research under your tutelage. Also, I would like to thank my committee members Dr. Phillips and Dr. Hili for your help whenever needed. To all former and current group members Dr. Alexander Kuzmin, Dr. Emmanuel Nekongo , Dr. Selvanathan Arumugam, Dr. Natalia Zhegalova, Dr. Dewey A. Sutton, Nannan Lin, Joshua A. Valencia, Kun Wang and Masha Sutton thank you for being amazing labmates. Last I would like to thank all the undergraduates that worked under me Virginia, Max and Chris. I hope you all enjoyed your time in the lab as much as I have.

TABLE OF CONTENTS

Page

LIST OF TABLES

Page

LIST OF FIGURES

Page

LIST OF SCHEMES

CHAPTER 1

INTRODUCTION

The use of photo-labile protecting groups for spatial and temporal control of bioorthogonal ligation is of great interest. An exemplar of this is the use of cyclopropenones as a photo-labile protecting group for cyclooctynes. Upon photolysis, the cyclopropenone quantitatively releases carbon monoxide and generates an alkyne. The newly generated cyclooctyne can then readily react with an azide to form a stable triazole.

Also, the spatial and temporal control of the photodecarbonylation of cyclopropenones is extremely valuable in surface functionalization and photo-patterning. Thus development of new, easier to make photo-caged cyclooctynes that display faster reaction kinetics are of a great interest for bioorthogonal labeling and surface chemistry. Faster rates allow for the use of lower concentrations of cyclooctyne at biological conditions as well as potential *in vivo* applications.

This dissertation is structured as follows. Chapter one reviews the development of cyclooctynes and photo-caged cyclooctynes for bioorthogonal ligation. Chapter two and three describe the development of a new photo-caged cyclooctyne, and a comprehensive examination of the stabilities and kinetics verses a variety of other cyclooctynes. Chapter four describes the application of various photo-caged cyclooctynes and cyclooctynes in a variety of fields including surface functionalization and drug delivery.

1.01 Bioorthogonal Ligation Strategies

Scientists have long striven to understand the interactions of various biomolecules within subcellular environments. The development of tools for understanding these interactions is of

extreme importance. One major breakthrough in the field of cell biology happened with the revolutionary development of green fluorescent protein (GFP).[1] Before this development there were no convenient methods of imaging living cells.[2-3] Since its discovery several other variants have also been developed to further enhance the applicability of this method.[4-6] Unfortunately, GFP is limited to use on proteinaceous biomolecules.[7] To address this problem, researchers worked on new strategies for imaging non-proteinaceous biomolecules.

One strategy for targeting and labeling small biomolecules is bioorthogonal ligation. In this strategy, a chemical reporter is inserted through enzymatic or metabolic labeling. Then, before imaging, the chemical reporter is reacted with a bioorthogonal counterpart that has a detectable substituent attached (Figure 1.01). These are two principle components that make-up the chemistry of bioorthogonal ligation.[8]

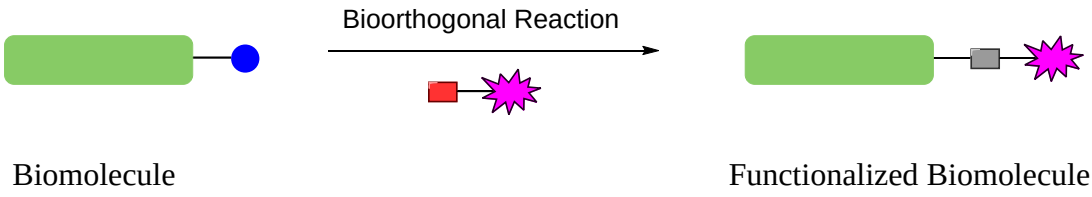

Figure 1.01 General example of bioorthogonal reaction. The green biomolecule has a unique chemical repoter (blue circle) and is reacted with its counterpart (red rectangle) that has a detectable substituent attached (magenta polygon) to form a covalent bond (grey rectangle).

The first category includes the earliest attempts for bioorthogonal ligation. This category revolves around polar reactions between nucleophiles and electrophiles. These techniques include aldehyde and ketone condensations and the Staudinger ligation.[8-13] There are several limitations with these two strategies, which limit their application. Aldehyde and ketone condensations are not true bioorthogonal reactions. This causes non-specific labeling of

biomolecules, and the products are susceptible to hydrolysis.[8, 12] The Staudinger ligation struggles from slow reaction kinetics as well as poor phosphine stability.[14-15]

The second category, where much of the current research is focused on is the use of various cycloaddition reactions. There are two main types of cycloadditions reactions used. The first is 1,3-dipolar cycloaddtions[8, 11-13, 16-17] between alkynes and 1,3-dipoles and the second is the Diels-Alder reaction[8, 12, 16, 18] between alkenes and a conjugated dienes like tetrazine. The Diels-Alder reaction shows excellent kinetics compared to 1,3-dipolar cycloaddtions, but suffers from stability in aqueous environments.[18]

The field of bioorthogonal chemistry is too large to cover all aspects. This literature review focuses on highlighting the development of cyclooctynes, various 1,3-dipoles, and their design for selectivity in bioconjugation.

1.02 Azides Handle as Chemical Reporters

The most prominent chemical reporter in bioorthogonal ligation is the azide. Azides are relatively inert, and can be easily incorporated into biological systems without perturbation and cytotoxicity.[9] They can be incorporated into biological system in a variety of ways including metabolic incorporation with azidosugars,[19] genetic incorporation with orthogonal synthetase/tRNA pairs,[20-21] and pre- and post- synthetic modification of oligonucleotides.[22] This makes the azide the most versatile chemical reporter available.

1.03 Cyclooctynes for Bioorthogonal Ligation

The discovery of the copper catalyzed cycloaddition of terminal alkynes and azides (CuAAC) to give 1,4-triazoles by Sharpless and Meldal independently has become staple in all fields of chemistry.[23-24] Its fast reaction rates, selectivity, high yields, and small amount of catalyst make it the most prominent click reaction discovered.[25] Unfortunately, CuAAC does

have some major drawbacks in biological applications because of the cytotoxicity of copper.[26-28] A solution to alleviate the use of copper for cell labeling was developed by Bertozzi *et. al*. with the Staudinger ligation.[9] A modification of the Staudinger reaction, the Staudinger ligation works by using an electrophilic trap to react with an aza-ylide that forms during the reaction to make a covalent bond with the biomolecule. Unfortunately, the reaction kinetics are extremely slow and the phosphine precursor is easily oxidized.[11]

It was known that cyclooctynes react spontaneously with azides to form triazoles and could be a potential way to remove the use of copper for bioorthiognal ligation.[29] Bertozzi *et. al*. were the first to explore applying cyclooctynes as potential click reagents in strain-promoted alkyne-azide cycloadditions (SPAAC).[30] The first example of SPAAC (Figure 1.02) was with cyclooctyne (OCT) **1.01** for labeling the surface of JURKAT cells that were incubated with N-azidoacetylmannosamine (Ac_4ManNAz).[30] The sluggish rate of OCT SPAAC reaction prompted Bertozzi *et. al*. to develop a faster reacting cyclooctyne. A difluorocyclooctyne (DIFO) **1.02** (Figure 1.02) was synthesized and displayed enhanced rates (0.052 $M^{-1}s^{-1}$) which were over 20 times faster than OCT **1.01**.[31-32] Bertozzi *et. al*. then applied DIFO **1.02** to a variety of *in vivo* labeling experiments.[31, 33-34] The most notable application of DIFO **1.02** was done in the *in vivo* labeling of zebra fish embryos.[35] The amenability to optical imaging makes zebra fish an excellent choice for visualization of glycan trafficking throughout the embryos development. Three different DIFO-Fluorophore derivatives were synthesized with varying excitation and emission wavelengths. Incubation of zebra fish embryos with N-azidoacetylgalactosamine (Ac_4GalNAz) followed by incubation with one DIFO-Fluorophore led to surface glycan functionalization. This was done multiple times and masterfully showed the movement of surface glycans throughout the development of zebra fish. One of the most active time regions

was around 60 hours post fertilization when an explosion of fluorescence was observed in the jaw region as surface glycans began to be produced. A drawback of DIFO was shown when live mice were administered Ac_4ManNAz to label cell-surface sialic acids and injected with DIFO.[30] When Western blots of organ lystates and serum were conducted there was a strong labeling around 65 kDa in an azide independent manner. This was determined as unwanted labeling of mouse serum albumin which is the most abundant serum protein. These experiments completed by Bertozzi *et. al*. brought the use of cyclooctynes into the forefront of bioorthogonal ligation.

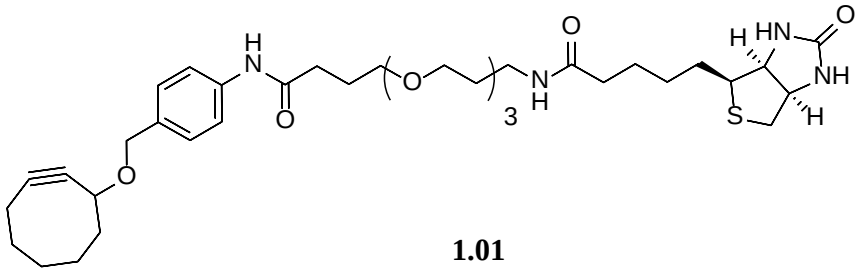

1.01

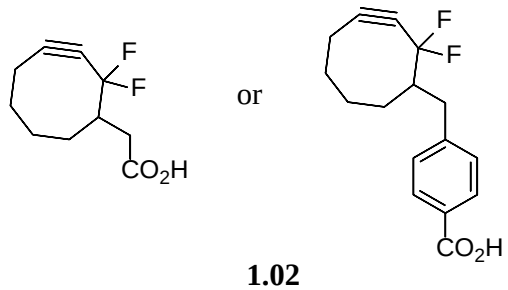

1.02

Figure 1.02 First and second generation of cyclooctynes for bioorthogonal ligation.

With the groundwork laid for cyclooctynes, intense focus was put on developing new cyclooctynes that displayed increased reactivity (Figure 1.03). Boons *et. al.* developed dibenzocyclooctyne (DIBO) **1.03** which showed moderate reactivity towards azides (0.06 $M^{-1}s^{-1}$).[36] DIBO's utility was shown by successfully labeling JURKAT cells that were incubated with Ac_4ManNAz. Unfortunately, a major drawback of DIBO is its highly hydrophobic nature. This

has lead to a variety of more hydrophilic derivatives to be developed. Boons *et. al*. synthesized a sulfated DIBO derivative (S-DIBO) **1.04** which significantly improved the water solubility (Figure 1.03).[37] An added benefit of S-DIBO was that the negative charge of the sulfates prohibited S-DIBO from passing through the cell membrane. This makes S-DIBO ideal for selective labeling of cell surfaces. Another derivative of DIBO to improve water solubility was developed by Gowlkowski.[38] He developed a tetra-ethylene glycol functionalized DIBO (THE-DIBO) **1.05** which can be used for intracellular labeling because the absence of the negatively charged sulfates (Figure 1.03).

A significant improvement in the dibenzocyclooctyne family came with the development of aza-dibenzocyclooctynes (ADIBO) **1.06** (Figure 1.03).[39-40] Simultaneously developed by our group and the van Delft group, an exocyclic amide was incorporated into the cyclooctyne ring to improve water solubility. An added benefit to this modification was a significant increase in reactivity towards azides (0.30 $M^{-1}s^{-1}$). ADIBO **1.06** also shows excellent stability with being able to be stored for long periods of time and slow reactivity towards thiols. With its unique combination of fast rate and stability ADIBO **1.06** is the most robust cyclooctyne developed to date. A very similar lactam derivative (BARAC) **1.07** was synthesized by Bertozzi *et. al*. (Figure 1.03).[41] The slight structural change from exo- to endocyclic amide caused a 3 times increase in reactivity but significant reduction in stability. BARAC **1.7** must be stored from light, oxygen, and kept in the freezer. Another way to enhance the reactivity of SPAAC while significantly shortening the synthesis was achieved by van Delft *et. al*. with bicyclononyne (BCN) **1.08**.[42] The addition of the cyclopropyl group caused moderate increase in reactivity (0.14 $M^{-1}s^{-1}$), but without the addition of phenyl rings. This allowed BCN derivatives **1.08** to be significantly less hydrophobic compared to the various dibenzocyclooctynes (Figure 1.03).

Bertozzi *et. al*. also developed a hydrophilic aza-cyclooctyne derivative (DIMAC) **1.09.**[43] Unfortunately, its reactivity is very close to that of cyclooctyne **1.10** (0.003 $M^{-1}s^{-1}$) which limits applicability (Figure 1.03).

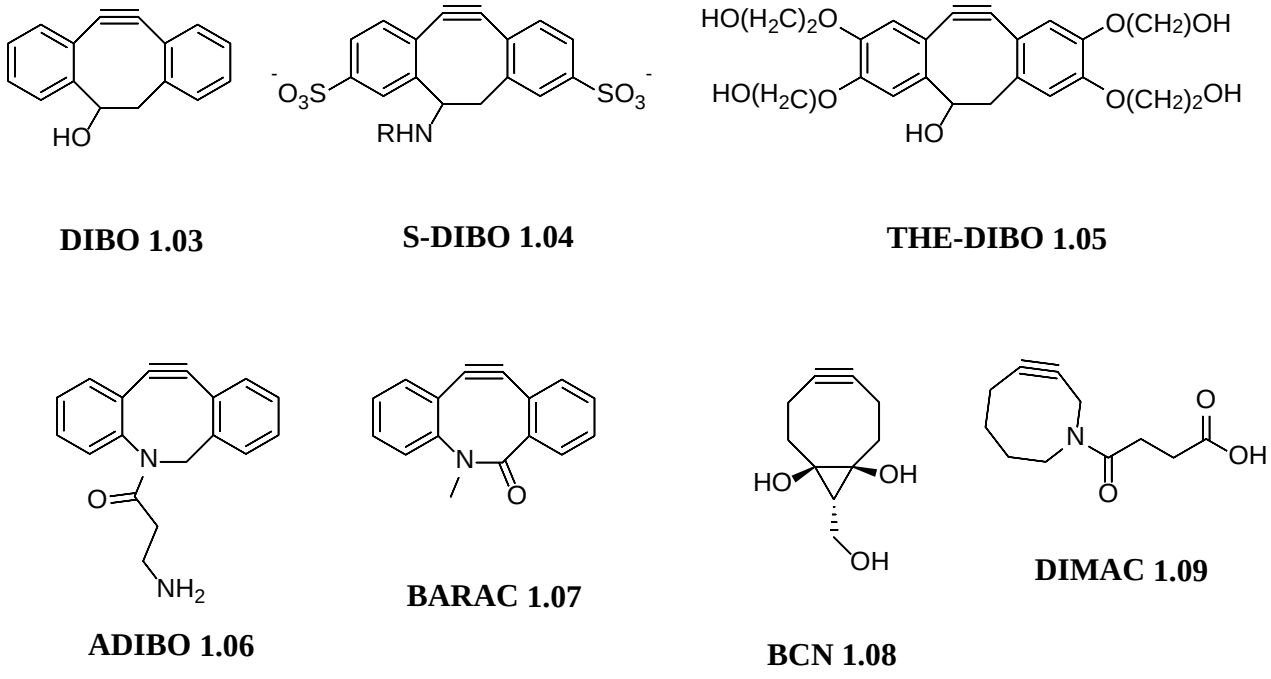

DIBO 1.03 **S-DIBO 1.04** **THE-DIBO 1.05**

ADIBO 1.06 **BARAC 1.07** **BCN 1.08** **DIMAC 1.09**

Figure 1.03 Various derivatives of cyclooctynes developed for SPAAC in bioorthogonal ligation.

1.04 Structural Effects on Cyclooctyne Reactivity

It continues to be a challenge to modify cyclooctynes for improved reactivity while not sacrificing the stability. The most prominent strategy to increase the reactivity of SPAAC is distortion of the alkyne bond angle.[44-47] A general distortion/interaction theory for 1,3-dipolar cycloaddition reactivity was developed by Hook *et. al*.[45] This states that the differences in the energy ($\Delta E_d^{\ddagger}$) required in the 1,3-dipole and it's dipolarophile into its transition state control the

barrier heights for different dipoles.[44] In Hook's *et. al.* analysis they determined that cyclooctyne's **1.10** (Figure 1.04) transition state structure occurs earlier than acetylene with phenyl azide. The energy required to overcome the activation barrier is 16.2 kcal/mol for acetylene with phenyl azide and 8.0 kcal/mol with cyclooctyne **1.10** and phenyl azide. This huge difference in energy is the reason for the spontaneity of SPAAC.

Almost all the cyclooctynes discussed so far rely on the strategy of distortion of the alkyne bond angle (Figure 1.04). The addition of extra sp^2 centers into the cyclooctyne ring by the addition of two phenyl rings has been the most successfully way in increasing the reactivity.[36, 39-41] Even though the ortho hydrogens to the alkyne decrease the reactivity because of steric interference, DIBO **1.03**, ADIBO **1.06**, and BARAC **1.07** offer 24 to 375 fold increases in reactivity compared to the parent cyclooctyne **1.10**.[46-47] The second most prominent way of distortion of the alkyne bond is fusion of a ring to the 5 and 6 position of cyclooctyne.[42, 48-49] The most well known example of this is BCN **1.08** which has a 70 fold increase in reactivity compared to cyclooctyne.[42] COMBO **1.11** which is a variant of the dibenyzlcyclooctyne family displays a 96 fold increase in reactivity.[48] A recently synthesized cyclooctyne PYRROC **1.12** that contains a C_2-symmetry axis reported similar rates as BCN.[49] Bertozzi *et. al.* further validated that distortion of the alkyne bond angle can lead to significant increases in reactivity by finding crystal structures of various cyclooctynes.[46] In their work BARAC **1.07**, the fastest cyclooctyne they examined had bond angles of 153°. Cyclooctyne **1.10**, the slowest reacting, has bond angles of 159°. These large differences in the bond angles of the alkynes explain their differences in reactivity of SPAAC.

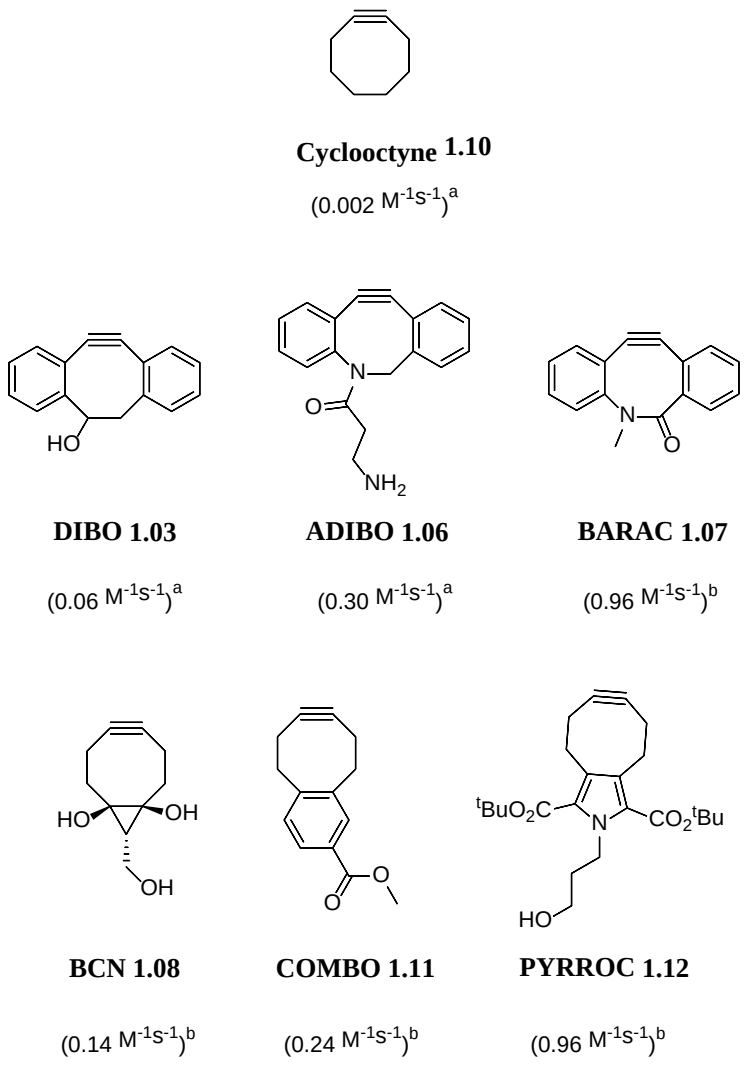

Figure 1.04 Various cyclooctynes modified by introducing further distortion of alkyne bond angle. [a] Rates determined in methanol. [b] Rates determined in acetonitrile.

Another strategy proposed by Alabugin *et. al*. involves modifying cyclooctynes with σ^* acceptors which will lower the transition state energy of the 1,3-dipole and increasing the rate of SPAAC.[50-51] Two ways to achieve this involve reducing unfavorable interactions[47, 52] and maximizing stabilizing effects.[53] It has been reported that the ability of a chemical bond to donate into an acceptor increases upon its distortion.[53] A strategically placed acceptor on the cyclooctyne core could lead to increased reactivity through stabilization of the transition state

1,3-dipole. In their previous work they investigated vicinal fluorines ability as $\sigma^*_{C\text{-}F}$ acceptors to an alkyne-π system to enhance reactivity. DIFO **1.02** which has two propargylic fluorines shows increased reactivity based on the polarization of the triple bond. This causes a 2 kcal/mol decrease in LUMO which lowers the activation barrier compared to cyclooctyne **1.10**.[44-45] Alabugin *et. al*. proposed that DIFO also experiences rate enhancement from partial hyperconjugative assistance. They further proposed that increased hyperconjugative assistance could be achieved by incorporation of one or two σ^* acceptors into the cyclooctyne ring with the propargylic fluorines.

A variety of cyclooctynes have been synthesized that incorporate the use of this hyperconjugative assistance (Figure 1.05).[43, 54-56] Unfortunately, the effect of the stabilization have very little effects on the rate of the click reaction. Cyclooctyne derivative **1.13** shows the fastest rate enhancement with only a rate increase of 3.5 times that of cyclooctyne **1.10**.[54] Potentially if better σ^* acceptor could be incorporated into the ring, hyperconjugative assistance could cause more prominent rate enhancement.

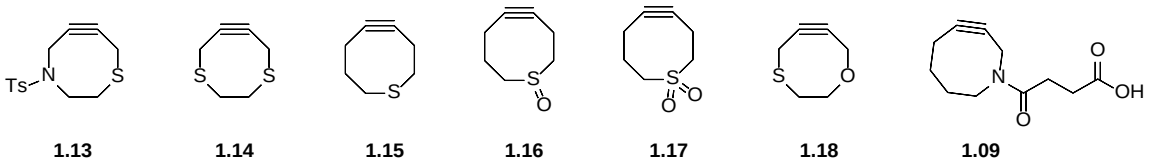

1.13 **1.14** **1.15** **1.16** **1.17** **1.18** **1.09**

Figure 1.05 Cyclooctynes designed on the principal of transition state stabilization.

1.05 Modifying Reactivity with Different 1,3-Dipoles

Cyclooctynes reactivity in bioorthogonal ligation can also be highly modified by changing the chemical reporter. Nitrones, an alternative 1,3-dipole were first examined by Pezacki *et al.*[57] They examined various functionalized nitrones to find the ideal conditions for

strained-promoted alkyne-nitrone cycloaddition (SPANC), which affords an isoxazoline. They used DIBO as their strained cyclooctyne and concluded that nitrones with electron withdrawing substituents exhibited a higher rate of reactivity versus ones without. They also found that cyclic nitrones exhibited the higher reactivity with DIBO versus linear nitrones. They observed rates up to 25 times faster ($1.5 \pm 0.1\ M^{-1}s^{-1}$) with DIBO than benzyl azide ($0.06\ M^{-1}s^{-1}$). Perzacki *et. al*. later investigated further improving the reaction kinetics of nitrones and determined that the reactivity was sensitive to functionalization of the nitrogen atom.[58] They also determined that functionalization of the α-carbon had little effect on the reactivity. Through these modifications they were able to synthesize acyclic nitrones that exhibited higher reactivity than any cyclic nitrone previously. Major drawbacks of these developed acyclic nitrones were significant decreases in their stability in aqueous environments. Cyclic nitrones have emerged as the go to choice for biological conditions because of their higher stability and exceptionally fast reaction kinetics.

Boons and van Delft were the first to apply nitrones in protein functionalization.[59] They determined that N-terminal serine residues would be ideal for insertion of nitrones. They showcased SPANC by functionalizing chemokine interleukin-8 (IL-8) protein which is a small size and has a N-terminal serine residue. Using a one-pot, three-step protocol for site specific modification, they were successfully able to functionalize IL-8 with a DIBO derivative with PEG_{2000} attached (Scheme 1.01).

Scheme 1.01 Functionalization of IL-8 with a DIBO

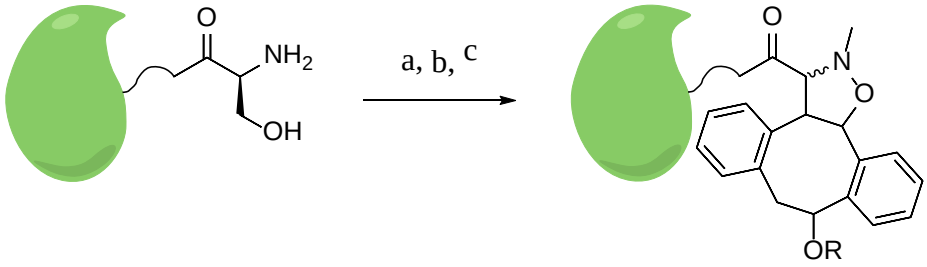

General protocol for one-pot functionalization: a) 1. $NaIO_4$, NH_4OAc buffer, pH 6.9, rt , 1 hr; 2. *p*-$MeOC_6H_4SH$, rt, 2 hr; b) *p*-$MeOC_6H_4NH_2$, MeNHOH·HCl, rt, 20 min; c) functionalized cyclooctyne, rt, 20 hrs.

Even with the exceptional reactivity of SPANC, it has only found limited applicability in cellular labeling.[60-64] The lower stability of nitrones compared to that of azides, and the requirements of an N-terminal serine residue has hindered the applications of this 1,3-dipole. Also, almost all SPANC must be done at pH 6.8 (NH_4OAc buffer), and the product isoxazoline is susceptible to side reactions like rearrangements under mild conditions.[65-66] For SPANC to be a prominent bioorthogonal click reaction the nitrone must be stable in biological conditions and after the cycloaddition a permanent covalent bond must be formed.

Boons *et. al*. also looked into nitrile oxides (Scheme 1.02) in strained promoted nitrile oxide cycloaddition (SPANOC) .[67] SPANOC forms a much more stable isoxazole ring compared to that of SPANC. Their strategy for nitrile oxide generation worked by an *in situ* generation of oximes with hydroxyl amine that can then be easily oxidized with [bis(acetoxy)iodo]benzene (BAIB). The reaction rates observed for nitrile oxides with DIBO ranged from 2.15 ± 0.03 $M^{-1}s^{-1}$ to 8.47 ± 0.03 $M^{-1}s^{-1}$. These are very comparable to that of SPANC.[57-59] Boons *et. al*. successfully achieved SPANOC by functionalization of the

glycoprotein fetuin. The sialic acid on the protein was used to insert the nitrile oxide by oxidation to the C-7 aldehyde which then could be converted to the nitrile oxide.

Scheme 1.02 SPAAC vs SPANOC with DIBO **1.03**

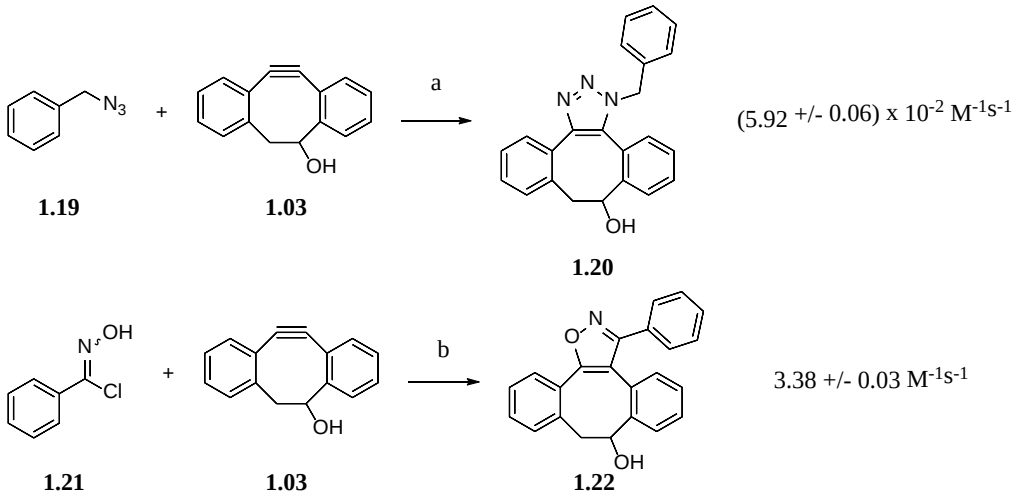

1.19 **1.03** **1.20**

1.21 **1.03** **1.22**

Reagents and Conditions: a) Et_3N, MeOH, 25.0 ± 0.1 °C; b) MeOH, 25.0 ± 0.1.

The low yields (~50 %) of oxidation reported by Boons *et. al*. limit the applicability of SPANOC.[67] A solution to this was reported by van Delft *et. al*. where they used phenyliodide bis(trifluoroacetate) (PIFA) for oxidation of oximes to nitrile oxides.[68] This drastically improved the yields of SPANOC with BCN (~90 %). Unfortunately, SPANOC has found very limited applicability in biological conditions because of difficulty to use *in vitro* as well as the stability of oximes in biological environments. It has found some utility in solid-phase modification of DNA and RNA.[69-70]

Diazo compounds have also been suggested as a potential 1,3-dipole. Boons *et. al*. first observed rates similar to azides when he investigated *N*-benzyl-2-diazoacetamide (3.11 ± 0.03 x 10^{-2} $M^{-1}s^{-1}$) with DIBO.[67] With no advantage over azides, diazo compounds have not been used

in cellular experiments. Recently, investigation into how the modification of diazos can significantly alter their reactivity with cyclooctynes.[71-72] Raines *et. al.* determined that functionalize of diazo compounds with an electron deficient substituent slows the rate of cycloaddition and electron rich substituents accelerate the rate of the 1,3-dipolar cycloaddition. This would allow selectivity for multi-component systems with azides and diazo 1,3-dipoles. Potentially in the future diazo compounds may find a place in bioorthogonal click chemistry.

1.06 Modifying Reactivity of SPAAC with Various Ring Sizes

An alternative strategy to modify the reactivity of SPAAC has been to adjust the ring size of the cycloalkyne. Modifying the ring size will cause drastic changes to the distorted alkyne bond which will cause significant rate changes. Most modifications to cycloalkynes have been to decrease the ring size for increased reactivity. This was first investigated in the 70's by Krebs *et. al.* and they reported that 3,3,6,6-tetramethylthiacycloheptyne (TMTH) was stable and reacted with benzyl azide.[73-74] Bertozzi *et. al.* set to synthesize TMTH **1.23** and various other thiocycloalkyne derivatives to test their potential for SPAAC (Figure 1.06).[75] When a fused aryl ring **1.24** was synthesized this caused significant reduction in stability leading to trimerization upon formation. Two other thiocyclooctyne **1.25** and **1.26** derivatives were synthesized but struggled with slow second order rate constants. It was determined that TMTH was the best candidate and had a second order rate constant of 4.0 ±0.4 $M^{-1}s^{-1}$ in acetonitrile, which is exceptionally fast.

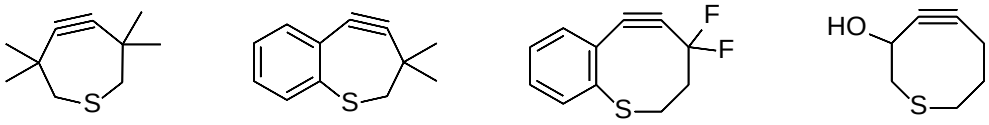

1.23 **1.24** **1.25** **1.26**

Figure 1.06 Variable thiocycloalkynes synthesized to improve the reactivity SPAAC.

Bertozzi *et. al*. showcased the selectivity of TMTH **1.23** by labeling the small protein barstar from ***B. cenocepacia*** (11.7kDa) in a methionine auxotrophic *E. coli* in which the methionine residues were replaced with azidohomoalanine residues (barstar-AHA). The modified barstar-AHA and a non modified methionine derivative were treated with TMTH and only the barstar-AHA showed a change in mass by LCMS. Unfortunately, TMTH **1.23** is highly susceptible to hydration in biological conditions, nucleophilic attack from endogenous thiols, as well as not easily modifiable for functionalization.

Another modification to improve the potential of cycloheptynes was the synthesis of dibenzoselenacycloheptyne **1.28** by Bertozzi *et. al*.[76] Their strategy hinged on the fact that the larger size of selenium compared to that of sulfur would allow for the addition of fused aryl rings. This would further increase the reactivity of SPAAC but potentially still be stable enough for biological conditions. The synthesis of dibenzoselenacycloheptynes **1.28** proved difficult by traditional strategies such as didehydrohalogenation. Using the same strategy as our group with photo-DIBO[77], they were able to synthesize cyclopropenone **1.27** by a Friedel-Crafts alkylation with tetrachlorocyclopropene followed by subsequent hydrolysis of the reaction mixture.

Unfortunately, upon photolysis of the cyclopropenone the alkyne could not be isolated (Scheme 1.03). Further studies revealed that the endocyclic selenium was not enough to

overcome the increased diradical character caused by the distortion of the alkyne bond angle. Upon formation of **1.28** proton abstraction would occur forming an alkene. When **1.27** was irradiated in the presence of azide both an alkene and triazole product was isolated. The rate of proton abstraction was on the same time scale as the reaction with benzyl azide which made photo-triggered dibenzoselenacycloheptyne unsuitable for bioorthogonal ligation.

Scheme 1.03 Irradiation of Photo-Dibenzoselenacycloheptyne **1.27**

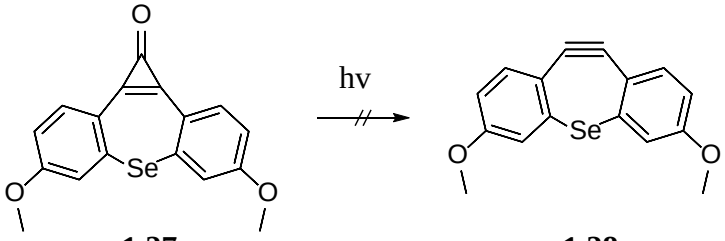

1.27 **1.28**

Recently, a new dibenzosilacyclohept-4-yne **1.30** has been synthesized to further improve on cycloheptynes for SPAAC.[78] The synthesis of dibenzosilacyclohept-4-yne again uses the strategy by our group of a Friedel-Crafts alkylation with tetrachlorocyclopropene followed by subsequent hydrolysis of the reaction mixture to form a cyclopropenone **1.29**. Unfortunately, the cycloheptyne **1.30** could not be isolated and the cycloheptyne still struggled from stability in aqueous media.

The reaction kinetics of the new cycloheptyne were studied with benzyl azide (Scheme 1.04). The second-order rate constants were determined to be 22.5 ± 0.7 M^{-1} s^{-1} and 15.8 ± 0.9 M^{-1} s^{-1} in methanol and acetonitrile. This makes dibenzosilacyclohept-4-yne one of the fastest SPAAC reactions to date. Interestingly, tetrazines also reacted (Scheme 1.04) in a [4+2] cycloaddition. The second-order rate constant was determined to be 2.58 ± 0.15 x10^2 M^{-1} s^{-1} in acetonitrile with 3,6-bis(methoxycarbonyl)-1,2,4,5-tetrazine. This result was very surprising

because diaryl fused cyclooctynes like DIBO are known to not react with tetrazines **1.32**. Even with these various augmentations to the cycloheptyne with various endocylic hetero atoms cycloheptynes are still not viable in biological conditions.

Scheme 1.04 General Photo-Click Reaction of **1.29** with Azides and Tetrazines

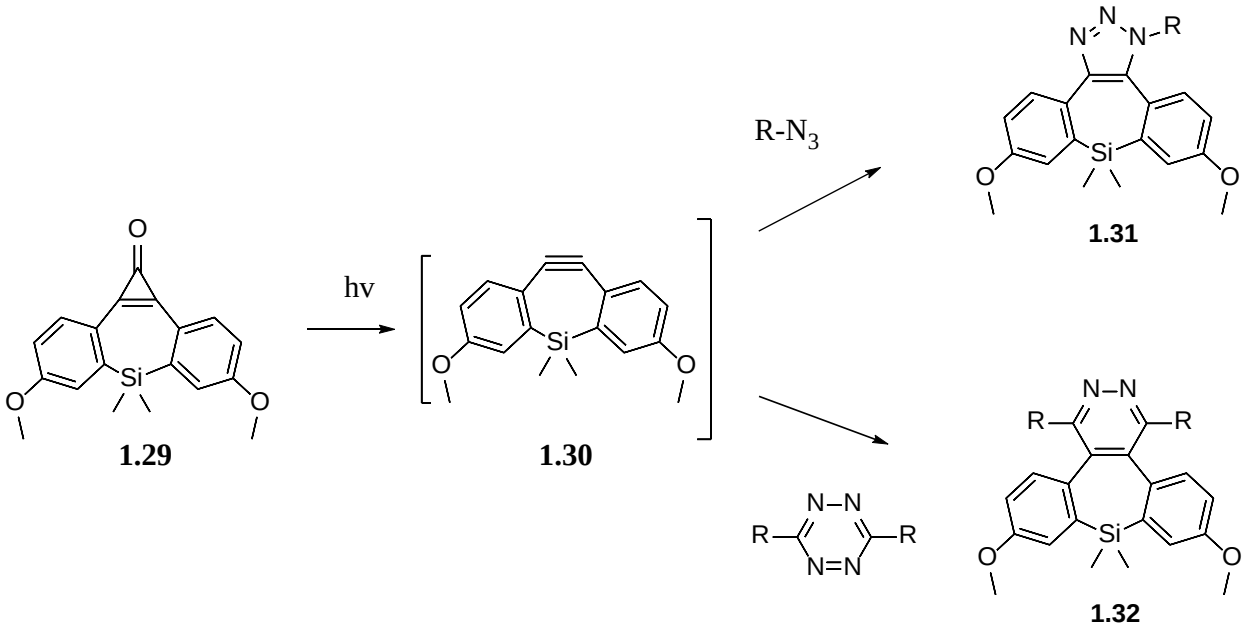

Even though it seems counterintuitive cyclononynes have been explored for their potential in SPAAC. Dudley *et. al*. developed a benzocyclononyne (BONO) with a second order rate constant of 1.5 x10^{-4} $M^{-1}s^{-1}$ with benzyl azide.[52] Their reasoning was that cyclooctynes are suseptible to nucleophilic attack by endogenous nucleophiles like glutathione and modification of a cyclononyne would significantly reduce this from happening. This would lead to significantly less background labeling during *in vitro* experiments. Unfortunately, the draw-back of the extremely slow second order rate constant requires the use of large amounts of cyclononyne to be used and long reactions times.

1.07 Photo-Labile Protecting Groups (Cyclopropenones)

Photo-labile protecting groups have been applied for spatial and temporal control of SPAAC in cell labeling. The most widely used photo-labile protecting group for SPAAC is cyclopropenone.[37, 76-79] Not only does the cyclopropenone give spatial and temporal control of the click reaction, but it also prevents side reactions occurring with endogenous thiols. Cyclooctynes are known to react with nucleophilic thiols in biological systems and can cause significant increases in background noise.[80] The non-specific labelling can be reduced by blocking thiols with iodoacetamide prior to conjugation, but it is not ideal.[81] Cyclopropeneones are a convenient protecting group that are stable to thiols which allow for expanding SPAACs application in bioorthogonal ligation.

When cyclopropenone is irradiated, photodecarbonylation occurs to produce an alkyne (Scheme 1.05). The first time cyclopropenones were reported in the literature was in the 1950's by Breslow *et. al.*[82] and Vol'pin *et. al.*[83]. Since then, cyclopropenones have been widely studied for their unique structure and potential aromatic character.[84-88] Cyclopropenones are optimal for photo-click reactions because of their thermal stability and high quantum yields of photodecarbonylation.[87-93]

Scheme 1.05 Photodecarbonylation of Cyclopropenones

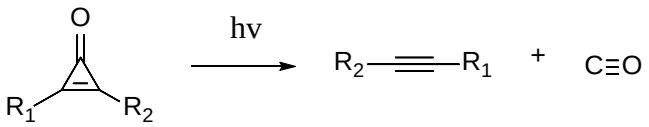

Mechanistically the photodecarbonylation of cyclopropenones is not fully understood. It is known that an intermediate forms that is a resonance hybrid of a zwitterionic structure and ketenylcarbene (Scheme 1.06). Geerlings and Nguyen suggest that the photodecarbonylation is a

ground-state process.[94] Their reasoning for this was that it required a significant amount of energy to promote an electron to the lowest excited state, and this state lies above the highest-lying excited state. This would make it impossible to have a mechanistic pathway that went along the excited state.

Scheme 1.06 Mechanism of Photodecarbonylation

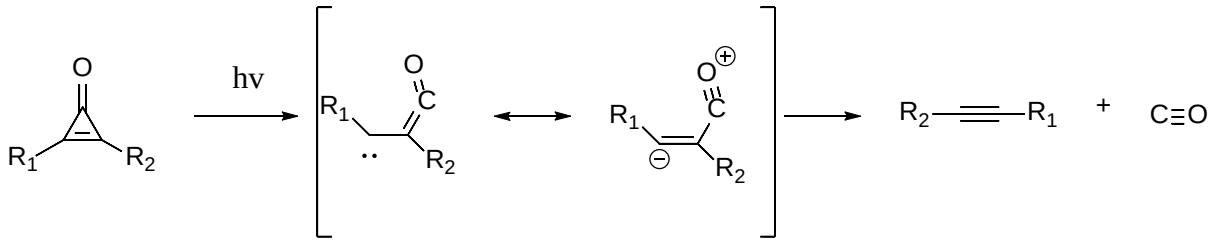

Alternatively, Mataga *et. al.* have done picosecond experiments on diphenylcyclopropenone with 20 ps time resolution.[95] In their experiments they found that upon excitation at 295 nm that the time-resolved absorption spectra of diphenyl acetylene and the time-resolved absorption spectra of diphenylcyclopropenone were nearly the same. This meant an electronically excited state of diphenyl acetylene was formed upon photolysis of the diphenylcyclopropenone. Also, it was suggested that a different photodecarbonylation pathways can occur for the S_1 and S_2 excited state. The S_1 excitation of diphenylcyclopropenone leads to a ground state diphenyl acetylene and the S_2 excitation forms leads to an excited state diphenyl acetylene. Further investigation into the possibility of photodecarbonylation being an adiabatic process was conducted by Tahara *et. al.* using femtoseconed experiments on diphenylcylopropenone.[96] They determined that if they excite into the S_2 then the diphenyl acetylene is formed in the S_2 state and relaxes to the S_1 through internal conversion. Intersystem crossing then occurs to the T_1 and then the diphenyl acetylene relaxes to the ground state through internal conversion (Figure 1.07). The experimental evidence provided in their work is in complete disagreement with Geerlings and Nguyen.

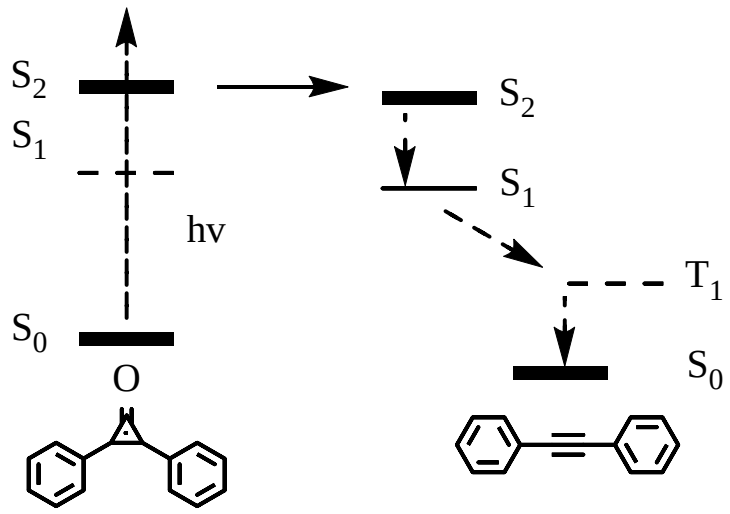

Figure 1.07 General scheme of photodecarbonylation of diphenylcyclopropenone.

Our group has also investigated the mechanism of photodecarbonylation of cyclopropenones using bis-p-anisylcyclopropenone and several naphtyl derivatives.[97] When irradiating diphenyl cyclopropenone the product alkynes absorption is close to overlapping with the excitation wavelength and can lead to excitation. We have shown that previous complex photo-dynamics and observation of excited states of acetylenic products were caused by this direct excitation of the product due to imperfect experimental design. Using DFT calculations and laser flash photolysis studies we determined that when creating a larger absorption shift between cyclopropenone and alkyne there was no longer an observed excited alkyne product. Photodecarbonylation was determined to be step-wise process, with the intermediate in the excited state, and the product was formed in the ground state.

1.08 Photo- SPAAC

The first use of cyclopropenones for potential photo-click use in SPAAC was showcased by our group. by synthesizing photo-triggered DIBO (photo-DIBO) derivatives **1.34a** (Scheme 1.07).[77] This was done using a simple Friedel-Crafts alkylation of 3,3'-bisbutoxybibenzyl with tetrachlorocyclopropene in the presence of aluminum chloride in dichloromethane subsequently

followed by hydrolysis of the reaction mixture to afforded mostly the mono butoxy cyclopropenone **1.34a**.

Scheme 1.07 Synthesis of Photo-DIBO **1.34** and Photodecarbonylation

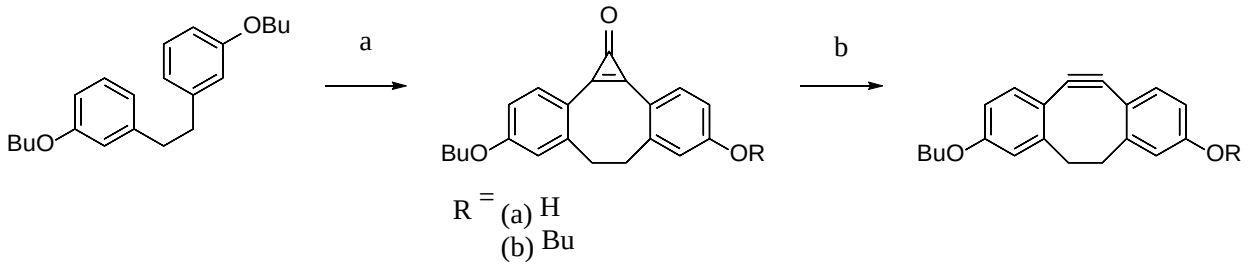

1.33 **1.34** **1.35**

Reagents and Conditions: a) C_3Cl_4, $AlCl_3$, CH_2Cl_2, 23 % (a), 12 % (b); b) 355 nm, MeOH, 86 % (b).

Cyclopropenones **1.34a,b** display unique UV spectra with two close lying bands (λ_{max} = 331 and 347 nm, log$\varepsilon \approx 4.5$) which upon photolysis at 350 nm results in decarbonylation (Φ_{355} = 0.33) and quantitative formation of the cyclooctynes **1.35a,b**. The cyclopropenones showed exceptional stability in aqueous media and were inert to reactions with azides. The rate of reaction of cyclooctynes **1.35a,b** with various azides displayed very similar rates to that of DIBO (*vide supra*). The rate found for cyclooctyne **1.35a** and benzyl azide was 5.67 ± 0.27 $M^{-1}s^{-1}$.

A biotin derivative **1.36** (Figure 1.08) was synthesized and the applicability of the system was tested with JURKAT cells. The cells showed no changes in viability when incubated with **1.36** and when irradiated with 350 nm light. Finally, the spatial and temporal control of photo-SPAAC was visualized in cell labeling experiments with Chinese hamster ovary (CHO) cells. CHO cells were incubated with Ac_4ManNAz for three days, then incubated with **1.36,** and then were irradiated for *in situ* decarbonylation to functionalize the CHO surface. The photo-triggered click reaction was successful in only functionalizing the surfaces of CHO cells that had been irradiated with compound **1.36** and that had been incubated with Ac_4ManNAz.

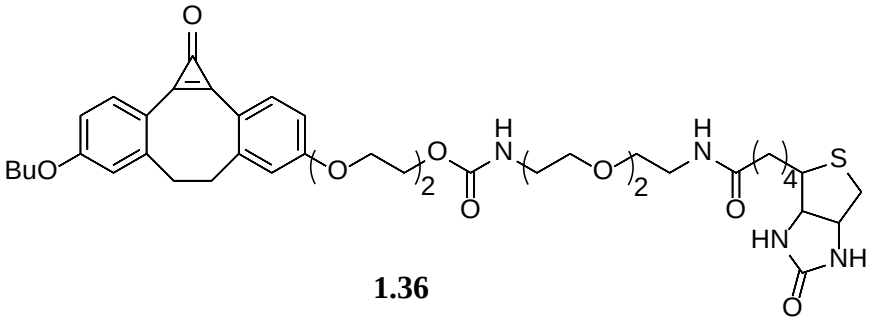

1.36

Figure 1.08 Structure of photo-DIBO with biotin attached.

Several other photo-caged cyclooctyne derivatives have been synthesized based on ADIBO. The first was synthesized by Starke and co-workers and takes three steps to get to the cyclopropenone product (Scheme 1.08).[98] A drawback of the strategy used in the preparation of cyclopropenone **1.40** is that upon photolysis and generation of the alkyne **1.41** there is an ortho-methoxy substituent that hinders reactivity. ADIBO derivative **1.41** has a second order rate constant of 8.0 $x10^{-3}$ $M^{-1}s^{-1}$ which is significantly slower than that of other ADIBO derivatives (*vide supra*). [98]

Scheme 1.08 Synthesis of ADIBO **1.41**

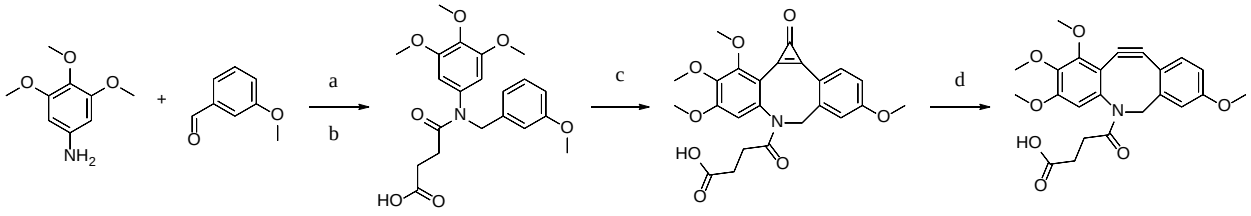

1.37 **1.38** **1.39** **1.40** **1.41**

Reagents and Conditions: a) $NaBH_4$, MeOH, 99 %; b) succinic anhydride, DMAP, NEt_3, $CHCl_3$, 83 %; c) C_3Cl_4, $AlCl_3$, CH_2Cl_2, 28 %; d) 350 nm, MeCN, 96%.

Another photo-caged ADIBO derivative was synthesized by Rutjes and co-workers.[79] Their strategy used a much simpler 3-methoxy aniline **1.42** starting material that would alleviate the problem of having an ortho-methoxy group to the cyclopropenone **1.44** (Scheme 1.09). The

second-order rate constant of ADIBO **1.45** is 0.62 $M^{-1}s^{-1}$ which is comparable to other ADIBO derivatives (*vide supra*).

Scheme 1.09 Synthesis of ADIBO **1.45**

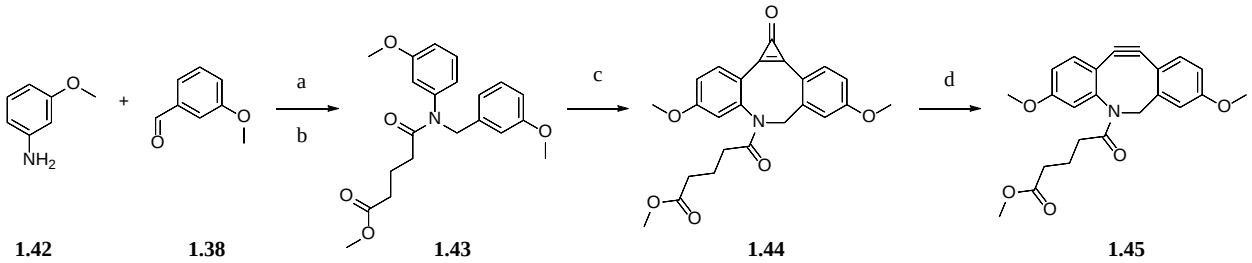

1.42 **1.38** **1.43** **1.44** **1.45**

Reagents and Conditions: a) $NaBH_4$, MeOH, 98 %; b) $ClCO_2C_3H_6CO_2Me$, Et_3N, CH_2Cl_2, 54 %; c) C_3Cl_4, $AlCl_3$, CH_2Cl_2, 30 %; d) 350 nm, MeCN 35%.

1.09 Multi-Click Functionalization.

There have been a variety of multi-functionalization strategies developed for the use of cross-linking and immobilization of substrates. Many of these strategies use multi-orthogonal click reactions to attach substrates.[99-109] While extremely selective, these strategies lead to complexity in substrate preparation. A more convent way to achieve multi-click functionalization would use only one type of click reaction.[110-112] SPAAC is extremely selective and its reactivity with azides makes it the perfect choice. Initially, strategies were developed using only CuAAC. Carell[113-114] and Aucagne[115] separately developed functionalization strategies that used silyl protecting groups of terminal alkynes to selectively do CuAAC with various substrates. The lability of the protecting groups and use of copper are major drawbacks.

A better strategy would incorporate the use of a small molecule that could go through SPAAC with two or more substrates. Unfortunately, initial dual-click functionalization systems were designed by coupling SPAAC and CuAAC together. This was first achieved by Wolfbeis *et. al.*[116] They bound cyclooctyne to the C-terminus of a small peptide chain with a terminal

alkyne bound to the N-terminus **1.46** (Figure 1.09). They showcased the feasibility of the system by taking azido-modified silica nano-particles and dual clicking the beads to a coumarin FRET pair. In the second example, they modified BSA with both cyclooctyne and a terminal alkyne and selectively bound two different FRET pairs to the surface of the BSA. This strategy is limited by the reaction order. SPAAC must be done first and then the CuAAC can be done or there will be cross contamination.

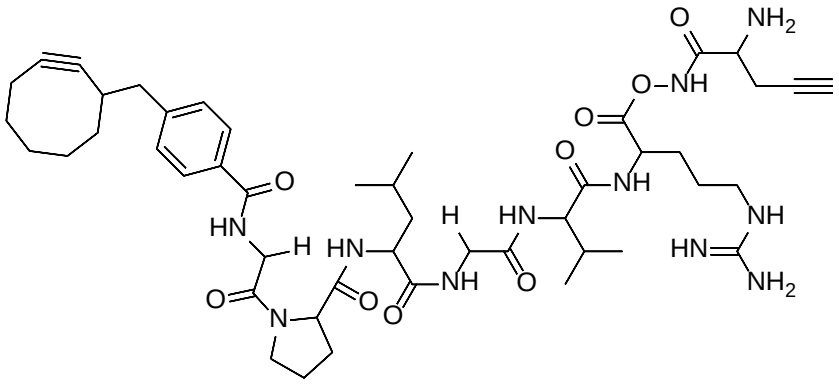

1.46

Figure 1.09 Structure of dual click peptide.

Another mixed functionalization strategy was reported by Dudley *et. al.*[117] Using the previously developed BONO **1.47** (Scheme 1.10) they attached a terminal alkyne that could be used for CuAAC. The reaction pairs were coupled through a carbamate functionality that could be cleaved to release the substrates if desired. The advantage of their strategy was there was no restriction on the order of SPAAC and CuAAC (Scheme 1.10). The slow second-order rate constant of BONO 1.5 $x10^{-4}$ $M^{-1}s^{-1}$ with azides paired with the extremely high reactivity of CuAAC afforded the selectivity. They successfully showcased this by reacting BONO **1.47** with benzyl azide and 4-(azidobutyl)benzamide using SPAAC or CuAAC first. No matter what order the click chemistry was used they attained the mixed triazole product.

Scheme 1.10 Dual Click with SPAAC (BONO) and CuAAC

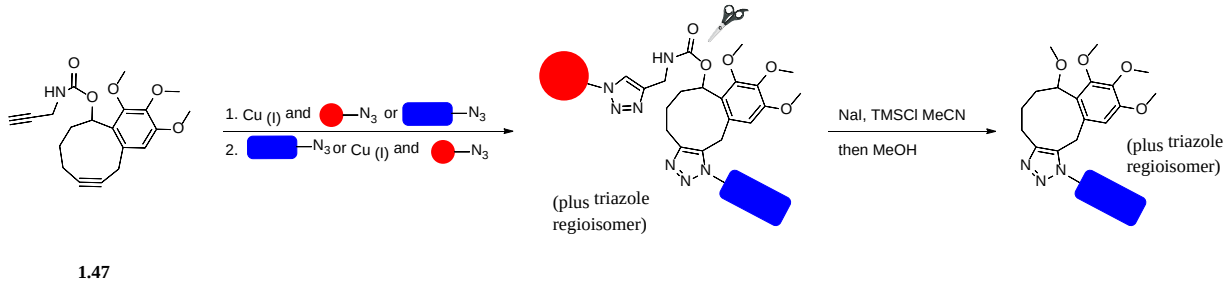

1.47

The use of alkyne protecting groups has also been developed for selective dual click functionalization. Selective protection of the cyclooctynes allows for CuAAC to easily be done first which is a limitation of other methods (*vide supra*). In synthetic chemistry, metal complexes are common for alkyne protection.[118] This strategy to protect cyclooctynes involves formation of the metal complex and then insert a terminal alkyne for CuAACA (Scheme 1.11, A). Hosoya *et. al*. was the first to investigate this strategy by developing a copper metal complex that could protect cyclooctynes.[119] They found out that $(MeCN)_4CuBF_4$ works as an exceptional protecting group (Scheme 1.11 B). An added bonus of using this copper complex is that it also catalyzed the CuAAC with addition of tris(benzyltriazolylmethyl)amine (TBTA) and they could easily remove the copper complex with ammonia. Another strategy was developed by Workeintin *et. al.*[120] They used the traditional di-cobalt-hexacarbonyl complex for protection of BCN (Scheme 1.11 B). Their strategy for removal was the use of nitro-methane to regenerate the alkyne. While these two strategies allow for more customization of the dual-click CuAAC/SPAAC they require extreme deprotection conditions and would not be viable for biological experiments.

Scheme 1.11 Protecting Groups for Dual-Click Functionalization

A

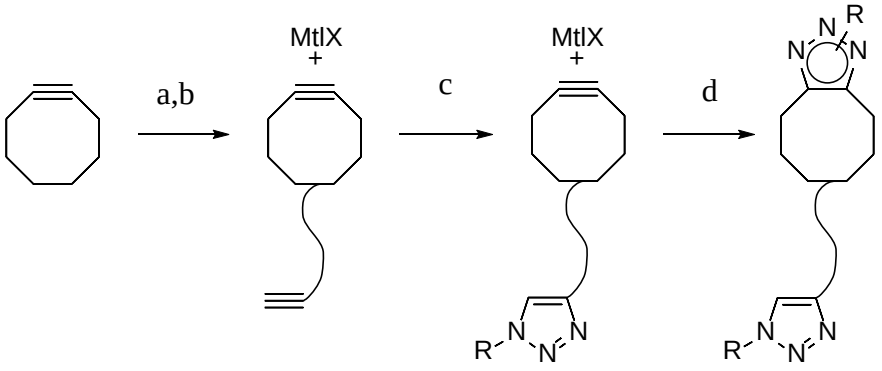

General Strategy for Cyclooctyne Protection: a) protection of cyclooctyne with metal complex; b) attachment of terminal alkyne; c) CuAAC; d) deprotection and SPAAC

B

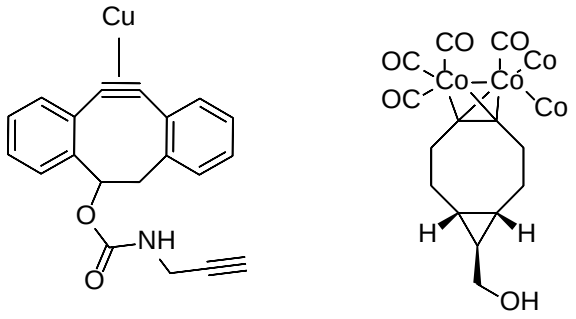

Copper Protection Cobalt Protection

A tri-click functionalization was developed by Jones *et. al.*[121] Their goal was to use the amino acid lysine to develop a complex multi-click reagent. They were able to functionalize the lysine with MOFO, a terminal alkyne, and a protected thiol **1.48** (Figure 1.10). Jones *et. al.* showcased the system by sequential click reactions with biotin azide and a septendecuple fluoro lipid derivative. They then deprotected the thiol and then proceeded to functionalize BSA which was functionalized with maleimide. This allowed for the rapid conjugation of complex systems

very easily. The drawback of the system is that the order of click must be CuAAC, SPAAC, and thiol. This could leave to potential limitations in conjugation experiments.

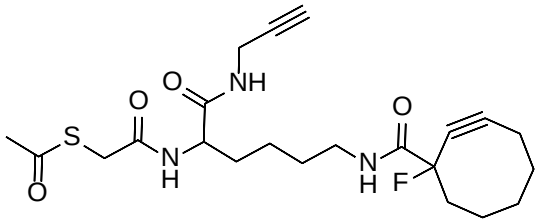

1.48

Figure 1.10 Structure of lysine tri-click scaffold.

Eventually a much simpler solution of dual click functionalization was developed and it use photo-labile protecting gruops. Our group achieved this by coupling a cyclooctyne to a photo-activated cyclooctyne (Scheme 1.12).[122] The irradiation of the cyclopropenone after the first SPAAC reaction had completed allows for complete selectivity. We showcased the applicability of the system for selective conjugation by functionalizing BSA-azide and reacting with crosslinked ADIBO/photo-DIBO **1.49**. After purification of the BSA the mixture was irradiated with 350 nm light, and reacted with an azido fluorescein dye. The results concluded that the BSA had been successfully functionalized with the aizdo fluorescein by this dual click strategy. We next showed that this strategy could be applied for protein immobilization by reacting ADIBO/photo-DIBO **1.X** with azide functionalized silica beads. The mixture was then irradiated and the beads were reacted with BSA-azide and it was determined that they had successfully bound 93 % of the BSA to the silica beads.

Scheme 1.12 Photo-SPAAC and SPAAC Dual-Click Functionalization

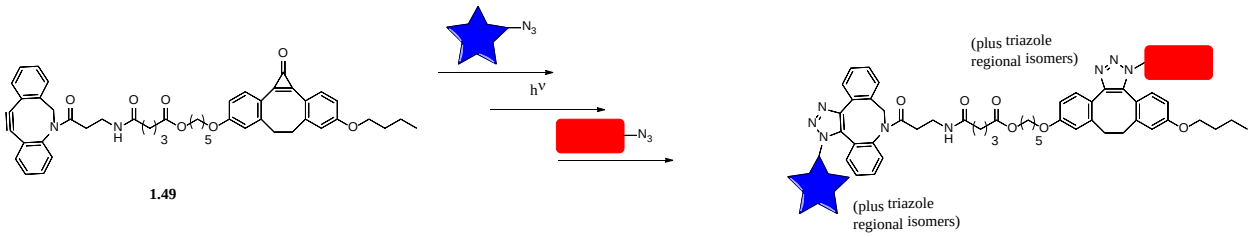

Another interesting dual-click platform that only uses SPAAC was developed by Hosoya *et. al*. where they were able to achieve functionalization of two substrates with a bis reactive cyclooctyne.[123] The Sondheimer diyne[124] **1.50** is the most atom economical of the double SPAAC cross-linkers because two reactive cyclooctynes are within one ring. They showcased the applicability of the of Sondheimer diyne **1.50** by synthesizing an azido-HaloTag that was reacted with a GST-fused HaloTag protein bound on the GSH Sepharose resin to give azido-HaloTag-GST-resin **1.52** (Scheme 1.13). The fluorescence modification of the azido-HaloTag-GST-resin was studied by mixing it with the Sondheimer diyne **1.50** and an azido-conjugated tetraethylsulforhodamine (TESRA) derivative **1.51**. SDS-PAGE confirmed that they were successful in the dual click of the azido-HaloTag-GST-resin **1.52** with the Sondheimer diyne **1.50** and azido TESRA fluorophore **1.51** with 40% efficiency to form dual click product **1.53**. If they procedure was done stepwise by adding the azido-HaloTag-GST-resin and Sondheimer diyne **1.50** first, washing the mixture, and then adding the azido TESRA fluorophore **1.51** they could increase the functionalization efficiency to 45%.

Scheme 1.13 Sondheimer Diyne as a Linchpin

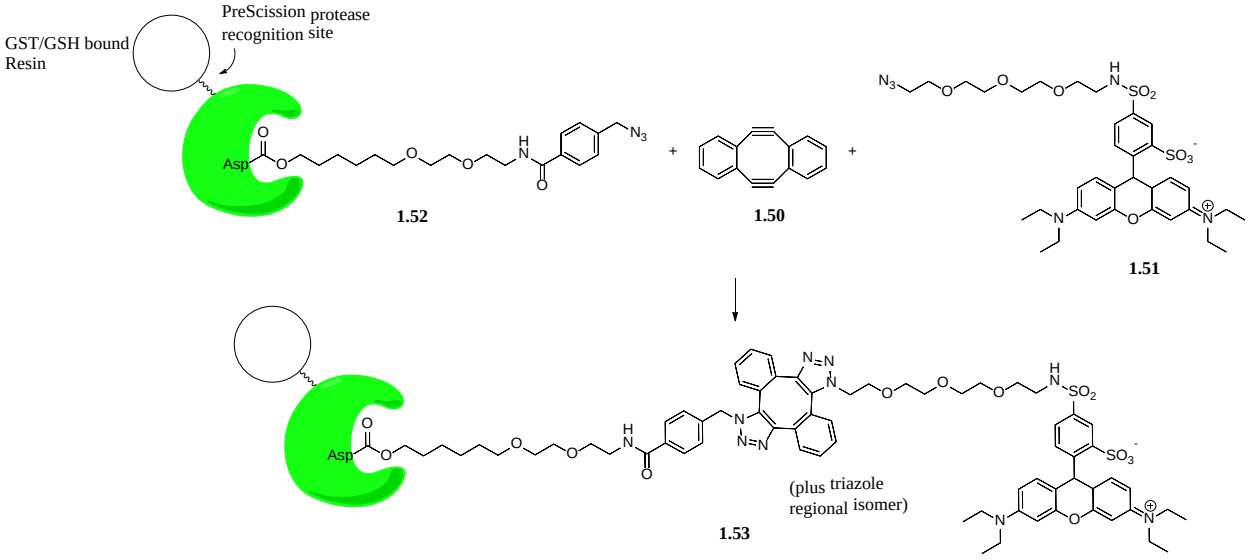

Reagents and Conditions: Compounds **1.50**, **1.51**, and **1.52** were incubated together in PBS (10% DMSO)

The prevalence of the Sondheimer diyne **1.50** as a cross-linker for biological use has increased significantly since Hosoya's work. Spring showed that the Sondeheimer diyne could be used for *in situ* stapling of peptides which allows for rapid selection of peptides with novel structures or biological activities.[125] Other methods rely on CuAAC[126-132] or a two-component approach to create photo-switchable[133-139], reversible[139-141], and dynamic linkers[139, 142]. These methods suffer from the need of multiple purifications which is not optimal for peptide screening.

Recently, we have published a photo-caged variant of the Sondheimer diyne **1.556a** that allows for spatial and temporal control as well as drastically improved stability (Scheme 1.14).[143] The Sondheimer diyne **1.50** completely decomposes in the neat form in over two days and has a half life of 10 minutes in neutral aqueous solutions (1mM in PBS, pH 7.4, r.t). When the Sondheimer diyne **1.54a** is protected as a bis-cyclopropenone **1.56a** (photo-DIBOD) it becomes

completely bench stable and stable in aqueous solvent. The synthesis was accomplished by taking Sondheimer diyne **1.54a** (Scheme 1.14) and doing a Hu-Prakesh reaction which generates difluorocarbene which upon hydrolysis of the bis-difluorocyclopropenes afforded the bis-cyclopropeonones **1.56a**. Two other derivatives were also synthesized, 2,8-di-butoxy **1.56b** and a 2,8-bis-[tetra(ethylene glycol)] **1.56c** to improve the low water solubility of the highly hydrophobic compounds. Unfortunately, these attempts were futile as there were no improvements in the solubility.

Scheme 1.14 Synthesis of Photo-DIBOD **1.56**

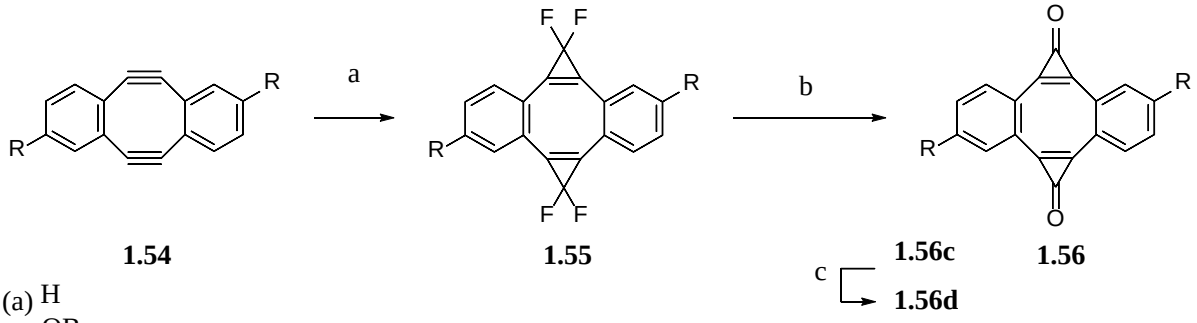

1.54 **1.55** **1.56c** **1.56** **1.56d**

R = (a) H
(b) OBu
(c) $O(OCH_2H_4)_4OAc$
(d) $O(OCH_2H_4)_4OH$

Reagents and Conditions: a) $TMSCF_3$, NaI, 110 °C, THF, **1.55a** 60%, **1.55b** 80%, **1.55c** 25%; b) wet silica gel, **1.56a** 81%, **1.56b** 73%; c) K_2CO_3 , MeOH (**1.56c** 53% yield over 2 steps, b, and c).

To overcome solubility problems for photo-crosslinking, nanocrystalline suspensions were used. Garcia-Garibay has shown that diphenyl cyclopropenone nanocyrstalline suspensions not only can efficiently be decarbonylated, but also display increased quantum yields because of a "quantum chain reaction".[144-148] We were successfully able to use the nanocrystalline suspensions in the photo-crosslinking of azido-BSA with an azido rhodamine derivative. SDS-PAGE confirmed that only irradiated samples were cross-linked with the rhodamine dye.

A limitation of the Sondheimer diyne **1.50** for dual-click functionalization is that it can be difficult to use non symmetrical azides. Most of the applications of the Sondheimer diyne have been limited to large biomolecules where sterics allow for two different azides to react. A mono cyclopropenone derivative (MC-DIBOD) **1.57** was developed by our group and allows for reaction between two different azides selectively (Scheme 1.15). MC-DIBOD **1.57** can easily be prepared from the irradiation of photo-DIBOD **1.56** because of a large difference in the quantum yield of decarbonylation between photo-DIBOD **1.56** (Φ_{350}=0.05) and MC-DIBO **1.57** (Φ_{350}=0.006). The quantum yield of the triazole **1.58** is (Φ_{350}=0.09). These changes in quantum yield allow for selective photo-crosslinking between multiple azides.

Scheme 1.15 Selective Irradiation of Photo-DIBOD **1.56**

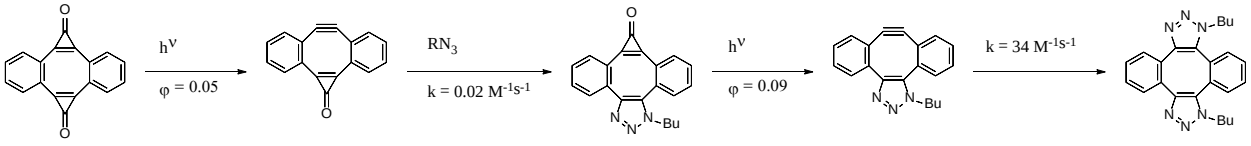

1.56 **1.57** **1.58** **1.59** **1.60**

MC-DIBOD **1.57** also allowed our group to examine the rate of the second SPAAC reaction of the Sondheimer diyne. In the work by Hosoya he had determined that the second SPAAC reaction of the Sondheimer diyne proceeded significantly faster than the first.[123] MC-DIBOD **1.57** was reacted with butyl azide and isolated to give triazole **1.58**. The mono cyclopropenone triazole **1.58** was then irradiated to form intermediate **1.59** and reacted with butyl azide to give di-triazole **1.60**. The second-order rate constant for this reaction was determined to be 34 ± 1 M^{-1} s^{-1} by following the decay of the alkyne peak in UV-spectroscopy. This is the fastest reported cyclooctyne rate to date. The applicability of MC-DIBOD **1.57** was showcased by photo-crosslinking azido-BSA with an azido rhodamine derivative. Any order of reacting MC-DIBOD **1.57** with BSA or rhodamine azide had no effect on the photo-crosslinking.

1.10 SPAAC Activated Fluorogenic Cyclooctynes

Extensive study into cyclooctynes has lead researchers to design SPAAC reagents that become flurogenic upon formation of the triazole. This would significantly simplify their use because attaching a fluorescence probe would no longer be required. This was first achieved by Bertozzi *et. al.*[149] They synthesized a BARAC derivative which is conjugated with coumarin (CoumBARAC) **1.61** (Scheme 1.16). The coumBARAC triazole **1.62** has a fluorescence quantum yield (Φ_f ~ 0.04) ~10 times that of the coumBARAC **1.61** (Φ_f ~ 0.003). With a extremely large stoke shift coumBarac triazole **1.62** can be excited at 340 nm and emits at 438 nm.

Scheme 1.16 Fluorescence CoumBARAC activated by SPAAC

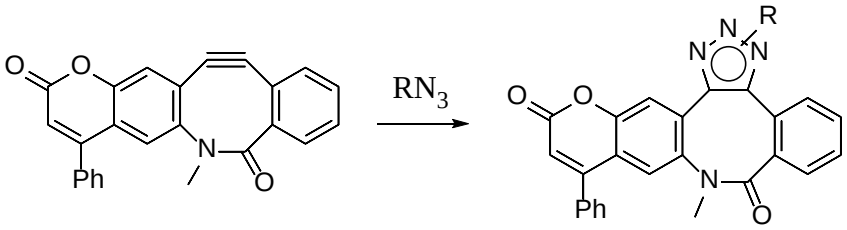

1.61 **1.62**

Reagents and Conditions: Reaction of **1.61** with azides leads to formation of triazole **1.62** which becomes fluorogenic.

In the attempt to develop a MC-DIBOD derivative for dual click functionalization Boons *et. al*. serendipitously developed a SPAAC activated fluorogenic cyclooctyne (Fl-DIBO) **1.63** (Scheme 1.17).[150] The highly symmetrical Fl-DIBO **1.63** when excited at 420 nm is weakly fluorescent (Φ_f = 0.002) and emits at 548 nm. Upon formation of triazole, Fl-DIBO **1.64** has a ~60 fold increase in fluorescence (Φ_f = 0.112) and emission at 491 nm (excitation 370 nm). This result was very surprising, because this is the only known case of a photostable and fluorescent cyclopropenone.

Scheme 1.17 General Reactivity of **1.63** with Azide to Form a Fluorescent Triazole

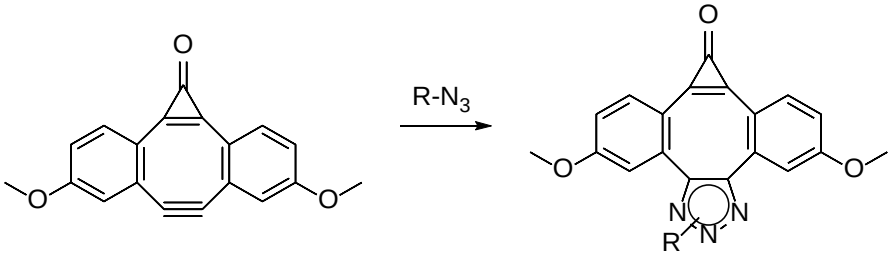

1.63 **1.64**

To showcase the ability of their system, Boons *et. al.* functionalized BSA protein with an azide and incubated it with Fl-DIBO **1.63**.[150] After SDS-PAGE proved that functionalization of BSA protein had occurred (Scheme 1.18). Fl-DIBO **1.63** has also been applied for the detection of NaN_3.[151] It is known that NaN_3 is a carcinogen and can cause extensive harm to your health.[152] When Fl-DIBO was mixed in the presence of various ions it was extremely sensitive towards NaN_3 and had detection limits of 10 μM.

Scheme 1.18 Functionalization of BSA with Fl-DIBO **1.63**

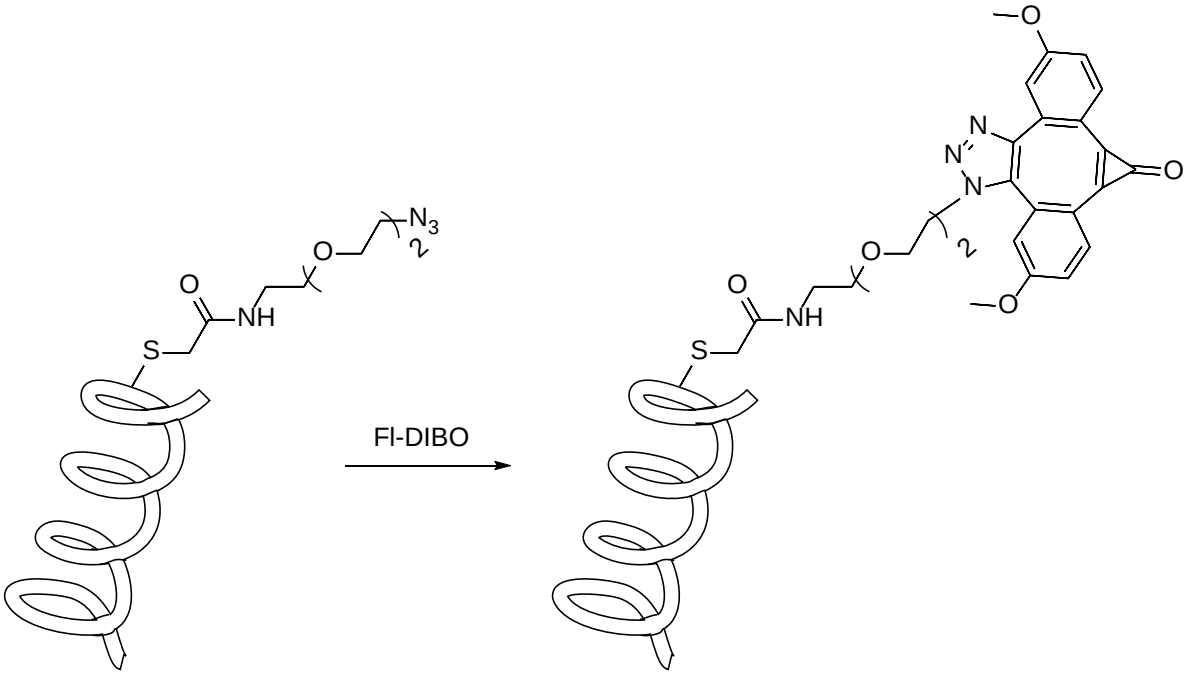

1.64 **1.65**

Reagents and Conditions: Fl-DIBO **1.63** was incubated with **1.64** in PBS to afford conjugated BSA **1.65**.

1.11 Conclusion

As seen from the examples above there have been many strategies used to modify the reactivity of cyclooctynes. The incorporation of more sp^2 centers and σ^* acceptors have allowed researchers to push the limits between reactivity and stability. The use of different 1,3-dipoles has also been looked into to further reaction rates. Cyclopropenones have become pivotal for spatial and temporal control of SPAAC and dual-click functionalization. The application of SPAAC seems endless because of selectivity and mild reaction conditions. This means that the development of new SPAAC reagents will continue to be a goal for researchers.

1.12 References

1. Chalfie, M.; Tu, Y.; Euskirchen, G.; Ward, W. W.; Prasher, D. C. Green Fluorescent Protein as a Marker For Gene Expression. *Science*, **1994,** *263*, 802-805.

2. Tsien, R. Y. The Green Fluorescent Protein. *Annu. Rev. Biochem.*, **1998,** *67*, 509-544.

3. Giepmans, B. N. G.; Adams, S. R.; Ellisman, M. H.; Tsien, R. Y. The Fluorescent Toolbox for Assessing Protein Location and Function. *Science*, **2006,** *312*, 217-224.

4. Heim, R.; Prasher, D. C.; Tsien, R. Y. Wavelength Mutations and Posttranslational Autoxidation of Green Fluorescent Protein. *Proc. Natl. Acad. Sci. USA*, **1994,** *91*, 12501-12504.

5. Ormö, M.; Cubitt, A. B.; Kallio, K.; Gross, L. A.; Tsien, R. Y.; Remington, S. J. Crystal Structure of the Aequorea Victoria Green Fluorescent Protein. *Science*, **1996,** *273*, 1392-1395.

6. Wachter, R. M.; King, B. A.; Heim, R.; Kallio, K.; Tsien, R. Y.; Boxer, S. G.; Remington, S. J. Crystal Structure and Photodynamic Behavior of the Blue Emission Variant Y66H/Y145F of Green Fluorescent Protein. *Biochemistry*, **1997,** *36*, 9759-9765.

7. Remington, S. J. Green Fluorescent Protein: a Perspective. *Protein Sci.*, **2011,** *20*, 1509-1519.

8. Patterson, D. M.; Nazarova, L. A.; Prescher, J. A. Finding the Right (Bioorthogonal) Chemistry. *ACS Chem. Bio.*, **2014,** *9*, 592-605.

9. Saxon, E.; Bertozzi, C. R. Cell Surface Engineering by a Modified Staudinger Reaction. *Science*, **2000,** *287*, 2007-2010.

10. Cornish, V. W.; Hahn, K. M.; Schultz, P. G. Site-Specific Protein Modification Using a Ketone Handle. *J. Am. Chem. Soc.*, **1996,** *118*, 8150-8151.

11. Sletten, E. M.; Bertozzi, C. R. From Mechanism to Mouse: A Tale of Two Bioorthogonal Reactions. *Acc. Chem. Res.*, **2011,** *44*, 666-676.

12. King, M.; Wagner, A. Developments in the Field of Bioorthogonal Bond Forming Reactions—Past and Present Trends. *Bioconjugate Chem.*, **2014,** *25*, 825-839.

13. Debets, M. F.; van der Doelen, C. W. J.; Rutjes, F. P. J. T.; van Delft, F. L. Azide: A Unique Dipole for Metal-Free Bioorthogonal Ligations. *ChemBioChem*, **2010,** *11*, 1168-1184.

14. van Berkel, S. S.; van Eldijk, M. B.; van Hest, J. C. M. Staudinger Ligation as a Method for Bioconjugation. *Angew. Chem. Int. Ed.*, **2011,** *50*, 8806-8827.

15. Schilling, C. I.; Jung, N.; Biskup, M.; Schepers, U.; Brase, S. Bioconjugation viaazide-Staudinger ligation: an overview. *Chem. Soc. Rev.*, **2011,** *40*, 4840-4871.

16. Debets, M. F.; van Berkel, S. S.; Dommerholt, J.; Dirks, A. T.; Rutjes, F. P.; van Delft, F. L. Bioconjugation With Strained Alkenes and Alkynes. *Acc. Chem. Res.*, **2011,** *44*, 805-815.

17. Jewett, J. C.; Bertozzi, C. R. Cu-Free Click Cycloaddition Reactions in Chemical Biology. *Chem. Soc. Rev.*, **2010,** *39*, 1272-1279.

18. Šečkutė, J.; Devaraj, N. K. Expanding room for tetrazine ligations in the in vivo chemistry toolbox. *Curr. Opin. Chem. Biol.*, **2013,** *17*, 761-767.

19. Vocadlo, D. J.; Hang, H. C.; Kim, E.-J.; Hanover, J. A.; Bertozzi, C. R. A Chemical Approach for Identifying O-GlcNAc-Modified Proteins in Cells. *Proc. Natl. Acad. Sci. USA*, **2003,** *100*, 9116-9121.

20. Kiick, K. L.; Saxon, E.; Tirrell, D. A.; Bertozzi, C. R. Incorporation of Azides Into Recombinant Proteins for Chemoselective Modification by the Staudinger Ligation. *Proc. Natl. Acad. Sci. USA*, **2002,** *99*, 19-24.

21. Tanrikulu, I. C.; Schmitt, E.; Mechulam, Y.; Goddard, W. A.; Tirrell, D. A. Discovery of Escherichia Coli Methionyl-tRNA Synthetase Mutants for Efficient Labeling of Proteins with Azidonorleucine in Vivo. *Proc. Natl. Acad. Sci. USA*, **2009,** *106*, 15285-15290.

22. Gramlich, P. M. E.; Wirges, C. T.; Manetto, A.; Carell, T. Postsynthetic DNA Modification through the Copper-Catalyzed Azide–Alkyne Cycloaddition Reaction. *Angew. Chem. Int. Ed.*, **2008,** *47*, 8350-8358.

23. Rostovtsev, V. V.; Green, L. G.; Fokin, V. V.; Sharpless, K. B. A Stepwise Huisgen Cycloaddition Process: Copper(I)-Catalyzed Regioselective "Ligation" of Azides and Terminal Alkynes. *Angew. Chem. Int. Ed.*, **2002,** *41*, 2596-2599.

24. Tornøe, C. W.; Christensen, C.; Meldal, M. Peptidotriazoles on Solid Phase: [1,2,3]-Triazoles by Regiospecific Copper(I)-Catalyzed 1,3-Dipolar Cycloadditions of Terminal Alkynes to Azides. *J. Org. Chem.*, **2002,** *67*, 3057-3064.

25. Kolb, H. C.; Finn, M. G.; Sharpless, K. B. Click Chemistry: Diverse Chemical Function from a Few Good Reactions. *Angew. Chem. Int. Ed.*, **2001,** *40*, 2004-2021.

26. Burrows, C. J.; Muller, J. G. Oxidative Nucleobase Modifications Leading to Strand Scission. *Chem. Rev.*, **1998,** *98*, 1109-1152.

27. Wang, Q.; Chan, T. R.; Hilgraf, R.; Fokin, V. V.; Sharpless, K. B.; Finn, M. G. Bioconjugation by Copper(I)-Catalyzed Azide-Alkyne [3 + 2] Cycloaddition. *J. Am. Chem. Soc.*, **2003,** *125*, 3192-3193.

28. Gaetke, L. M.; Chow, C. K. Copper Toxicity, Oxidative Stress, and Antioxidant Nutrients. *Toxicology*, **2003,** *189*, 147-163.

29. Krebs, A.; Wilke, J., Angle Strained Cycloalkynes. In *Wittig Chemistry*, Springer Berlin Heidelberg: Berlin, Heidelberg, 1983; pp 189-233.

30. Agard, N. J.; Prescher, J. A.; Bertozzi, C. R. A Strain-Promoted [3 + 2] Azide−Alkyne Cycloaddition for Covalent Modification of Biomolecules in Living Systems. *J. Am. Chem. Soc.*, **2004,** *126*, 15046-15047.

31. Codelli, J. A.; Baskin, J. M.; Agard, N. J.; Bertozzi, C. R. Second-Generation Difluorinated Cyclooctynes for Copper-Free Click Chemistry. *J. Am. Chem. Soc.*, **2008,** *130*, 11486-11493.

32. Sletten, E. M.; de Almeida, G.; Bertozzi, C. R. A Homologation Approach to the Synthesis of Difluorinated Cycloalkynes. *Org. Lett.*, **2014,** *16*, 1634-1637.

33. Chang, P. V.; Prescher, J. A.; Sletten, E. M.; Baskin, J. M.; Miller, I. A.; Agard, N. J.; Lo, A.; Bertozzi, C. R. Copper-Free Click Chemistry in Living Animals. *Proc. Natl. Acad. Sci. USA*, **2010,** *107*, 1821-1826.

34. Baskin, J. M.; Prescher, J. A.; Laughlin, S. T.; Agard, N. J.; Chang, P. V.; Miller, I. A.; Lo, A.; Codelli, J. A.; Bertozzi, C. R. Copper-Free Click Chemistry for Dynamic in Vivo Imaging. *Proceedings of the National Academy of Sciences,* **2007,** *104*, 16793-16797.

35. Laughlin, S. T.; Baskin, J. M.; Amacher, S. L.; Bertozzi, C. R. In Vivo Imaging of Membrane-Associated Glycans in Developing Zebrafish. *Science,* **2008,** *320*, 664-667.

36. Ning, X.; Guo, J.; Wolfert, M. A.; Boons, G.-J. Visualizing Metabolically Labeled Glycoconjugates of Living Cells by Copper-Free and Fast Huisgen Cycloadditions. *Angew. Chem. Int. Ed.*, **2008,** *47*, 2253-2255.

37. Friscourt, F.; Ledin, P. A.; Mbua, N. E.; Flanagan-Steet, H. R.; Wolfert, M. A.; Steet, R.; Boons, G.-J. Polar Dibenzocyclooctynes for Selective Labeling of Extracellular Glycoconjugates of Living Cells. *J. Am. Chem. Soc.*, **2012,** *134*, 5381-5389.

38. Golkowski, M.; Ziegler, T. Synthesis of Tetra(2-hydroxyethoxy)-Substituted Dibenzocyclooctyne Derivatives as Novel, Highly Hydrophilic Tool Compounds for Strain-Promoted Alkyne-Azide Cycloaddition Applications. *Synthesis*, **2013,** *45*, 1207-1214.

39. Kuzmin, A.; Poloukhtine, A.; Wolfert, M. A.; Popik, V. V. Surface Functionalization Using Catalyst-Free Azide−Alkyne Cycloaddition. *Bioconjugate Chem.*, **2010,** *21*, 2076-2085.

40. Debets, M. F.; van Berkel, S. S.; Schoffelen, S.; Rutjes, F. P. J. T.; van Hest, J. C. M.; van Delft, F. L. Aza-Dibenzocyclooctynes for Fast and Efficient Enzyme PEGylation via Copper-Free (3+2) Cycloaddition. *Chem. Commun.*, **2010,** *46*, 97-99.

41. Jewett, J. C.; Sletten, E. M.; Bertozzi, C. R. Rapid Cu-Free Click Chemistry with Readily Synthesized Biarylazacyclooctynones. *J. Am. Chem. Soc.*, **2010,** *132*, 3688-3690.

42. Dommerholt, J.; Schmidt, S.; Temming, R.; Hendriks, L. J. A.; Rutjes, F. P. J. T.; van Hest, J. C. M.; Lefeber, D. J.; Friedl, P.; van Delft, F. L. Readily Accessible Bicyclononynes for Bioorthogonal Labeling and Three-Dimensional Imaging of Living Cells. *Angew. Chem. Int. Ed.*, **2010,** *49*, 9422-9425.

43. Sletten, E. M.; Bertozzi, C. R. A Hydrophilic Azacyclooctyne for Cu-Free Click Chemistry. *Org. Lett.*, **2008,** *10*, 3097-3099.

44. Ess, D. H.; Jones, G. O.; Houk, K. N. Transition States of Strain-Promoted Metal-Free Click Chemistry: 1,3-Dipolar Cycloadditions of Phenyl Azide and Cyclooctynes. *Org. Lett.*, **2008,** *10*, 1633-1636.

45. Schoenebeck, F.; Ess, D. H.; Jones, G. O.; Houk, K. N. Reactivity and Regioselectivity in 1,3-Dipolar Cycloadditions of Azides to Strained Alkynes and Alkenes: A Computational Study. *J. Am. Chem. Soc.*, **2009,** *131*, 8121-8133.

46. Gordon, C. G.; Mackey, J. L.; Jewett, J. C.; Sletten, E. M.; Houk, K. N.; Bertozzi, C. R. Reactivity of Biarylazacyclooctynones in Copper-Free Click Chemistry. *J. Am. Chem. Soc.*, **2012,** *134*, 9199-9208.

47. Chenoweth, K.; Chenoweth, D.; Goddard Iii, W. A. Cyclooctyne-Based Reagents for Uncatalyzed Click Chemistry: A Computational Survey. *Org. Biomol. Chem.*, **2009,** *7*, 5255-5258.

48. Varga, B. R.; Kállay, M.; Hegyi, K.; Béni, S.; Kele, P. A Non-Fluorinated Monobenzocyclooctyne for Rapid Copper-Free Click Reactions. *Chem. Eur. J.*, **2012,** *18*, 822-828.

49. Grost, C.; Berg, T. PYRROC: The First Functionalized Cycloalkyne that Facilitates Isomer-Free Generation of Organic Molecules by SPAAC. *Org. Biomol. Chem.*, **2015,** *13*, 3866-3870.

50. Gold, B.; Shevchenko, N. E.; Bonus, N.; Dudley, G. B.; Alabugin, I. V. Selective Transition State Stabilization via Hyperconjugative and Conjugative Assistance: Stereoelectronic Concept for Copper-Free Click Chemistry. *J. Org. Chem.*, **2012,** *77*, 75-89.

51. Gold, B.; Dudley, G. B.; Alabugin, I. V. Moderating Strain without Sacrificing Reactivity: Design of Fast and Tunable Noncatalyzed Alkyne–Azide Cycloadditions via Stereoelectronically Controlled Transition State Stabilization. *J. Am. Chem. Soc.*, **2013,** *135*, 1558-1569.

52. Tummatorn, J.; Batsomboon, P.; Clark, R. J.; Alabugin, I. V.; Dudley, G. B. Strain-Promoted Azide-Alkyne Cycloadditions of Benzocyclononynes. *J Org Chem*, **2012,** *77*, 2093-2097.

53. Alabugin, I. V.; Gilmore, K. M.; Peterson, P. W. Hyperconjugation. *WIREs Comput. Mol. Sci.*, **2011,** *1*, 109-141.

54. Ni, R.; Mitsuda, N.; Kashiwagi, T.; Igawa, K.; Tomooka, K. Heteroatom-embedded Medium-Sized Cycloalkynes: Concise Synthesis, Structural Analysis, and Reactions. *Angew. Chem. Int. Ed.*, **2015,** *127*, 1206-1210.

55. Hagendorn, T.; Brase, S. A New Route to Dithia- and Thiaoxacyclooctynes via Nicholas Reaction. *RSC Adv.*, **2014,** *4*, 15493-15495.

56. Schuhmacher, H.; Beile, B.; Meier, H. 1-Thiacyclooct-4-yne (=5,6-Didehydro-3,4,7,8-tetrahydro-2H-thiocin), and Its Sulfoxide and Its Sulfone. *Helv. Chim. Acta.*, **2013,** *96*, 228-238.

57. McKay, C. S.; Moran, J.; Pezacki, J. P. Nitrones as Dipoles for Rapid Strain-Promoted 1,3-Dipolar Cycloadditions with Cyclooctynes. *Chem. Commun.*, **2010,** *46*, 931-933.

58. McKay, C. S.; Chigrinova, M.; Blake, J. A.; Pezacki, J. P. Kinetics Studies of Rapid Strain-Promoted [3 + 2]-Cycloadditions of Nitrones with Biaryl-Aza-Cyclooctynone. *Org. Biomol. Chem.*, **2012,** *10*, 3066-3070.

59. Ning, X.; Temming, R. P.; Dommerholt, J.; Guo, J.; Ania, D. B.; Debets, M. F.; Wolfert, M. A.; Boons, G.-J.; van Delft, F. L. Protein Modification by Strain-Promoted Alkyne–Nitrone Cycloaddition. *Angew. Chem. Int. Ed.*, **2010,** *49*, 3065-3068.

60. McKay, C. S.; Blake, J. A.; Cheng, J.; Danielson, D. C.; Pezacki, J. P. Strain-Promoted Cycloadditions of Cyclic Nitrones with Cyclooctynes for Labeling Human Cancer Cells. *Chem. Commun.*, **2011,** *47*, 10040-10042.

61. Colombo, M.; Sommaruga, S.; Mazzucchelli, S.; Polito, L.; Verderio, P.; Galeffi, P.; Corsi, F.; Tortora, P.; Prosperi, D. Site-Specific Conjugation of ScFvs Antibodies to Nanoparticles by Bioorthogonal Strain-Promoted Alkyne–Nitrone Cycloaddition. *Angew. Chem. Int. Ed.*, **2012,** *51*, 496-499.

62. Temming, R. P.; Eggermont, L.; van Eldijk, M. B.; van Hest, J. C. M.; van Delft, F. L. N-Terminal Dual Protein Functionalization by Strain-Promoted Alkyne-Nitrone Cycloaddition. *Org. Biomol. Chem.*, **2013,** *11*, 2772-2779.

63. MacKenzie, D. A.; Sherratt, A. R.; Chigrinova, M.; Kell, A. J.; Pezacki, J. P. Bioorthogonal Labelling of Living Bacteria Using Unnatural Amino Acids Containing Nitrones and a Nitrone Derivative of Vancomycin. *Chem. Commun.*, **2015,** *51*, 12501-12504.

64. Sherratt, A. R.; Chigrinova, M.; MacKenzie, D. A.; Rastogi, N. K.; Ouattara, M. T. M.; Pezacki, A. T.; Pezacki, J. P. Dual Strain-Promoted Alkyne–Nitrone Cycloadditions for Simultaneous Labeling of Bacterial Peptidoglycans. *Bioconjugate Chem.*, **2016,** *27*, 1222-1226.

65. Spears, R. J.; Fascione, M. A. Site-Selective Incorporation and Ligation of Protein Aldehydes. *Org. Biomol. Chem.*, **2016,** *14*, 7622-7638.

66. MacKenzie, D. A.; Sherratt, A. R.; Chigrinova, M.; Cheung, L. L. W.; Pezacki, J. P. Strain-Promoted Cycloadditions Involving Nitrones and Alkynes — Rapid Tunable Reactions for Bioorthogonal Labeling. *Current Opinion in Chemical Biology*, **2014,** *21*, 81-88.

67. Sanders, B. C.; Friscourt, F.; Ledin, P. A.; Mbua, N. E.; Arumugam, S.; Guo, J.; Boltje, T. J.; Popik, V. V.; Boons, G.-J. Metal-Free Sequential [3 + 2]-Dipolar Cycloadditions using Cyclooctynes and 1,3-Dipoles of Different Reactivity. *J. Am. Chem. Soc.*, **2011,** *133*, 949-957.

68. Jawalekar, A. M.; Reubsaet, E.; Rutjes, F. P. J. T.; van Delft, F. L. Synthesis of Isoxazoles by Hypervalent Iodine-Induced Cycloaddition of Nitrile Oxides to Alkynes. *Chem. Commun.*, **2011,** *47*, 3198-3200.

69. Singh, I.; Freeman, C.; Madder, A.; Vyle, J. S.; Heaney, F. Fast RNA Conjugations on Solid Phase by Strain-Promoted Cycloadditions. *Org. Biomol. Chem.*, **2012,** *10*, 6633-6639.

70. Singh, I.; Heaney, F. Solid Phase Strain Promoted "Click" Modification of DNAvia[3+2]-Nitrile Oxide-Cyclooctyne Cycloadditions. *Chem. Commun.*, **2011,** *47*, 2706-2708.

71. McGrath, N. A.; Raines, R. T. Diazo Compounds as Highly Tunable Reactants in 1,3-Dipolar Cycloaddition Reactions with Cycloalkynes. *Chem. Sci.*, **2012,** *3*, 3237-3240.

72. Gold, B.; Aronoff, M. R.; Raines, R. T. Decreasing Distortion Energies without Strain: Diazo-Selective 1,3-Dipolar Cycloadditions. *J. Org. Chem.*, **2016,** *81*, 5998-6006.

73. Krebs, A.; Kimling, H. 3.3.6.6-Tetramethyl-1-Thiacyclopheptin Ein Ssolierbares Siebenring-Acetylen. *Tetrahedron Lett.*, **1970,** *11*, 761-764.

74. Kimling, H.; Krebs, A. *Liebigs Ann. Chem.*, **1974**, 2074-.

75. de Almeida, G.; Sletten, E. M.; Nakamura, H.; Palaniappan, K. K.; Bertozzi, C. R. Thiacycloalkynes for Copper-Free Click Chemistry. *Angew. Chem. Int. Ed.*, **2012,** *51*, 2443-7.

76. de Almeida, G.; Townsend, L. C.; Bertozzi, C. R. Synthesis and Reactivity of Dibenzoselenacycloheptynes. *Org. Lett.*, **2013,** *15*, 3038-3041.

77. Poloukhtine, A. A.; Mbua, N. E.; Wolfert, M. A.; Boons, G. J.; Popik, V. V. Selective Labeling of Living Cells by a Photo-Triggered Click Reaction. *J. Am. Chem. Soc.*, **2009,** *131*, 15769-15776.

78. Martinek, M.; Filipova, L.; Galeta, J.; Ludvikova, L.; Klan, P. Photochemical Formation of Dibenzosilacyclohept-4-yne for Cu-Free Click Chemistry with Azides and 1,2,4,5-Tetrazines. *Org Lett*, **2016,** *18*, 4892-4895.

79. Debets, M. F.; Prins, J. S.; Merkx, D.; van Berkel, S. S.; van Delft, F. L.; van Hest, J. C. M.; Rutjes, F. P. J. T. Synthesis of DIBAC Analogues with Excellent SPAAC Rate Constants. *Org. Biomol. Chem.*, **2014,** *12*, 5031-5037.

80. Beatty, K. E.; Fisk, J. D.; Smart, B. P.; Lu, Y. Y.; Szychowski, J.; Hangauer, M. J.; Baskin, J. M.; Bertozzi, C. R.; Tirrell, D. A. Live-Cell Imaging of Cellular Proteins by a Strain-Promoted Azide–Alkyne Cycloaddition. *ChemBioChem*, **2010,** *11*, 2092-2095.

81. van Geel, R.; Pruijn, G. J. M.; van Delft, F. L.; Boelens, W. C. Preventing Thiol-Yne Addition Improves the Specificity of Strain-Promoted Azide–Alkyne Cycloaddition. *Bioconjugate Chem.*, **2012,** *23*, 392-398.

82. Breslow, R.; Haynie, R.; Mirra, J. The Sythesis of Diphenylcyclopropenone. *J. Am. Chem. Soc.*, **1959,** *81*, 247-248.

83. Vol'pin, M. E.; Koreshkov, Y. D.; Kursanov, D. N. *Dokl. Akad. Nauk SSSR, Ser. Khim.*, **1959,** *3*, 560.

84. Benson, R. C.; Flygare, W. H.; Oda, M.; Breslow, R. Microwave Spectrum, Substitutional Structure, and Stark and Zeeman Effects in Cyclopropenone. *J. Am. Chem. Soc.*, **1973,** *95*, 2772-2777.

85. Mueller, C.; Schweig, A.; Vermeer, H. Theory and Application of Photoelectron Spectroscopy. 51. Thiirene Dioxides. Electronic Structure. *J. Am. Chem. Soc.*, **1975,** *97*, 982-987.

86. Staley, S. W.; Norden, T. D.; Taylor, W. H.; Harmony, M. D. Electronic Structure of Cyclopropenone and its Relationship to Methylenecyclopropene. Evaluation of Criteria for Aromaticity. *J. Am. Chem. Soc.*, **1987,** *109*, 7641-7647.

87. Komatsu, K.; Kitagawa, T. Cyclopropenylium Cations, Cyclopropenones, and HeteroanaloguesRecent Advances. *Chem. Rev.*, **2003,** *103*, 1371-1428.

88. Potts, K. T.; Baum, J. S. Chemistry of Cyclopropenones. *Chem. Rev.*, **1974,** *74*, 189-213.

89. Dehmlow, E. V.; Neuhaus, R.; Schell, H. G. Cyclopropenonchemie, X. 2-Alkoxy-3-alkylcyclopropenone. *Chem. Ber.*, **1988,** *121*, 569-571.

90. Ciabattoni, J.; Nathan, E. C. Di-Tert-Butylcyclopropenone and Substituted Di-Tert-Butyl-Cyclopropenyl Cations. *J. Am. Chem. Soc.*, **1969,** *91*, 4766-4771.

91. Poloukhtine, A.; Popik, V. V. Highly Efficient Photochemical Generation of a Triple Bond: Synthesis, Properties, and Photodecarbonylation of Cyclopropenones. *J. Org. Chem.*, **2003,** *68*, 7833-7840.

92. Fessenden, R. W.; Carton, P. M.; Shimamori, H.; Scaiano, J. C. Measurement of the Dipole Moments of Excited States and Photochemical Transients by Microwave Dielectric Absorption. *J. Phys. Chem.*, **1982,** *86*, 3803-3811.

93. Chapman, O. L.; Gano, J.; West, P. R.; Regitz, M.; Maas, G. Acenaphthyne. *J. Am. Chem. Soc.*, **1981,** *103*, 7033-7036.

94. Nguyen, L. T.; De Proft, F.; Nguyen, M. T.; Geerlings, P. Theoretical Study of Cyclopropenones and Cyclopropenethiones: Decomposition Via Intermediates. *J. Chem. Soc. Perkin Trans. 2,* **2001**, 898-905.

95. Hirata, Y.; Mataga, N. Picosecond Dye Laser Photolysis Study of Diphenylcyclopropenone in Solution: Formation of the Electronically Excited States of Diphenylacetylene. *Chem. Phys. Lett.*, **1992,** *193*, 287-291.

96. Takeuchi, S.; Tahei Tahara, S. Femtosecond Absorption Study of Photodissociation of Diphenylcyclopropenone in Solution: Reaction Dynamics and Coherent Nuclear Motion. *J. Phys. Chem.*, **2004,** *120*, 4768-4776.

97. Poloukhtine, A.; Popik, V. V. Mechanism of the Cyclopropenone Decarbonylation Reaction. A Density Functional Theory and Transient Spectroscopy Study. *J. Phys. Chem. A.*, **2006,** *110*, 1749-1757.

98. Starke, F.; Walther, M.; Pietzsch, H.-J. A Novel Dibenzoazacyclooctyne Precursor in Regioselective Copper-Free Click Chemistry. An Innovative 3-Step Synthesis. *ARKIVOC*, **2010,** *xi*, 350-359.

99. Yi, L.; Sun, H.; Itzen, A.; Triola, G.; Waldmann, H.; Goody, R. S.; Wu, Y.-W. One-Pot Dual-Labeling of a Protein by Two Chemoselective Reactions. *Angew. Chem. Int. Ed.*, **2011,** *50*, 8287-8290.

100. Chan, D. P. Y.; Owen, S. C.; Shoichet, M. S. Double Click: Dual Functionalized Polymeric Micelles with Antibodies and Peptides. *Bioconjugate Chem.*, **2013,** *24*, 105-113.

101. Goswami, L. N.; Houston, Z. H.; Sarma, S. J.; Jalisatgi, S. S.; Hawthorne, M. F. Efficient Synthesis of Diverse Heterobifunctionalized Clickable Oligo(Ethylene Glycol) Linkers: Potential Applications in Bioconjugation and Targeted Drug Delivery. *Org. Biomol. Chem.*, **2013,** *11*, 1116-1126.

102. Durmaz, H.; Sanyal, A.; Hizal, G.; Tunca, U. Double Click Reaction Strategies for Polymer Conjugation and Post-Functionalization of Polymers. *Polym. Chem.*, **2012,** *3*, 825-835.

103. Glassner, M.; Oehlenschlaeger, K. K.; Gruendling, T.; Barner-Kowollik, C. Ambient Temperature Synthesis of Triblock Copolymers via Orthogonal Photochemically and Thermally Induced Modular Conjugation. *Macromolecules*, **2011,** *44*, 4681-4689.

104. Durmaz, H.; Dag, A.; Altintas, O.; Erdogan, T.; Hizal, G.; Tunca, U. One-Pot Synthesis of ABC Type Triblock Copolymers via in situ Click [3 + 2] and Diels−Alder [4 + 2] Reactions. *Macromolecules*, **2007,** *40*, 191-198.

105. Galibert, M.; Dumy, P.; Boturyn, D. One-Pot Approach to Well-Defined Biomolecular Assemblies by Orthogonal Chemoselective Ligations. *Angew. Chem. Int. Ed.*, **2009,** *48*, 2576-2579.

106. Kempe, K.; Hoogenboom, R.; Jaeger, M.; Schubert, U. S. Three-Fold Metal-Free Efficient ("Click") Reactions onto a Multifunctional Poly(2-oxazoline) Designer Scaffold. *Macromolecules,* **2011,** *44*, 6424-6432.

107. Ehlers, I.; Maity, P.; Aubé, J.; König, B. Modular Synthesis of Triazole-Containing Triaryl α-Helix Mimetics. *Eur. J. Org. Chem.,* **2011,** *2011*, 2474-2490.

108. Sun, X.-L.; Stabler, C. L.; Cazalis, C. S.; Chaikof, E. L. Carbohydrate and Protein Immobilization onto Solid Surfaces by Sequential Diels−Alder and Azide−Alkyne Cycloadditions. *Bioconjugate Chem.*, **2006,** *17*, 52-57.

109. Deng, X.; Friedmann, C.; Lahann, J. Bio-orthogonal "Double-Click" Chemistry Based on Multifunctional Coatings. *Angew. Chem. Int. Ed.*, **2011,** *50*, 6522-6526.

110. Delaittre, G.; Guimard, N. K.; Barner-Kowollik, C. Cycloadditions in Modern Polymer Chemistry. *Acc. Chem. Res.*, **2015,** *48*, 1296-1307.

111. Shieh, P.; Bertozzi, C. R. Design Strategies for Bioorthogonal Smart Probes. *Org. Biomol. Chem.,* **2014,** *12*, 9307-9320.

112. Tang, W.; Becker, M. L. "Click" Reactions: A Versatile Toolbox for the Synthesis of Peptide-Conjugates. *Chem. Soc. Rev.*, **2014,** *43*, 7013-7039.

113. Burley, G. A.; Gierlich, J.; Mofid, M. R.; Nir, H.; Tal, S.; Eichen, Y.; Carell, T. Directed DNA Metallization. *J. Am. Chem. Soc.*, **2006,** *128*, 1398-1399.

114. Gramlich, P. M. E.; Warncke, S.; Gierlich, J.; Carell, T. Click–Click–Click: Single to Triple Modification of DNA. *Angew. Chem. Int. Ed.*, **2008,** *47*, 3442-3444.

115. Valverde, I. E.; Delmas, A. F.; Aucagne, V. Click à La Carte: Robust Semi-Orthogonal Alkyne Protecting Groups for Multiple Successive Azide/Alkyne Cycloadditions. *Tetrahedron*, **2009,** *65*, 7597-7602.

116. Kele, P.; Mezö, G.; Achatz, D.; Wolfbeis, O. S. Dual Labeling of Biomolecules by Using Click Chemistry: A Sequential Approach. *Angew. Chem. Int. Ed.*, **2009,** *48*, 344-347.

117. Ramsubhag, R. R.; Dudley, G. B. Orthogonal dual-click diyne for CuAAC and/or SPAAC couplings. *Org Biomol Chem*, **2016,** *14*, 5028-31.

118. Hegedus, L. S.; Soderberg, B. C. G., *Transition Metals in the Synthesis of Complex Organic Molecules*. University Science Books: Saulsalito, CA, 2009.

119. Yoshida, S.; Hatakeyama, Y.; Johmoto, K.; Uekusa, H.; Hosoya, T. Transient Protection of Strained Alkynes from Click Reaction via Complexation with Copper. *J. Am. Chem. Soc.*, **2014,** *136*, 13590-13593.

120. Gobbo, P.; Romagnoli, T.; Barbon, S. M.; Price, J. T.; Keir, J.; Gilroy, J. B.; Workentin, M. S. Expanding the Scope of Strained-Alkyne Chemistry: A Protection-Deprotection Strategy Via the Formation of a Dicobalt-Hexacarbonyl Complex. *Chem. Commun.*, **2015,** *51*, 6647-6650.

121. Beal, D. M.; Albrow, V. E.; Burslem, G.; Hitchen, L.; Fernandes, C.; Lapthorn, C.; Roberts, L. R.; Selby, M. D.; Jones, L. H. Click-Enabled Heterotrifunctional Template for Sequential Bioconjugations. *Org. Biomol. Chem.*, **2012,** *10*, 548-554.

122. Arumugam, S.; Popik, V. V. Sequential "Click" - "Photo-Click" Cross-Linker for Catalyst-Free Ligation of Azide-Tagged Substrates. *J. Org. Chem.*, **2014,** *79*, 2702-2708.

123. Kii, I.; Shiraishi, A.; Hiramatsu, T.; Matsushita, T.; Uekusa, H.; Yoshida, S.; Yamamoto, M.; Kudo, A.; Hagiwara, M.; Hosoya, T. Strain-Promoted Double-Click Reaction for Chemical Modification of Azido-Biomolecules. *Org. Biomol. Chem.*, **2010,** *8*, 4051-4055.

124. Wong, H. N. C.; Garratt, P. J.; Sondheimer, F. Unsaturated Eight-Membered Ring Compounds. XI. Synthesis of Sym-dibenzo-1,5-cyclooctadiene-3,7-diyne and Sym-dibenzo-1,3,5-cyclooctatrien-7-yne, Presumably Planar Conjugated Eight-Membered Ring Compounds. *J. Am. Chem. Soc.*, **1974,** *96*, 5604-5605.

125. Lau, Y. H.; Wu, Y.; Rossmann, M.; Tan, B. X.; de Andrade, P.; Tan, Y. S.; Verma, C.; McKenzie, G. J.; Venkitaraman, A. R.; Hyvönen, M.; Spring, D. R. Double Strain-Promoted Macrocyclization for the Rapid Selection of Cell-Active Stapled Peptides. *Angew. Chem. Int. Ed.*, **2015,** *54*, 15410-15413.

126. Torres, O.; Yüksel, D.; Bernardina, M.; Kumar, K.; Bong, D. Peptide Tertiary Structure Nucleation by Side-Chain Crosslinking with Metal Complexation and Double “Click” Cycloaddition. *ChemBioChem*, **2008,** *9*, 1701-1705.

127. Lau, Y. H.; de Andrade, P.; Quah, S.-T.; Rossmann, M.; Laraia, L.; Skold, N.; Sum, T. J.; Rowling, P. J. E.; Joseph, T. L.; Verma, C.; Hyvonen, M.; Itzhaki, L. S.; Venkitaraman, A. R.; Brown, C. J.; Lane, D. P.; Spring, D. R. Functionalised Staple Linkages for Modulating the Cellular Activity of Stapled Peptides. *Chem. Sci.*, **2014,** *5*, 1804-1809.

128. Lau, Y. H.; de Andrade, P.; Skold, N.; McKenzie, G. J.; Venkitaraman, A. R.; Verma, C.; Lane, D. P.; Spring, D. R. Investigating Peptide Sequence Variations for 'Double-Click' Stapled P53 Peptides. *Org. Biomol. Chem.*, **2014,** *12*, 4074-4077.

129. Lau, Y. H.; Wu, Y.; de Andrade, P.; Galloway, W. R. J. D.; Spring, D. R. A Two-Component 'Double-Click' Approach to Peptide Stapling. *Nat. Protocols*, **2015,** *10*, 585-594.

130. Kawamoto, S. A.; Coleska, A.; Ran, X.; Yi, H.; Yang, C.-Y.; Wang, S. Design of Triazole-Stapled BCL9 α-Helical Peptides to Target the β-Catenin/B-Cell CLL/lymphoma 9 (BCL9) Protein–Protein Interaction. *J. Med. Chem.*, **2012,** *55*, 1137-1146.

131. Ingale, S.; Dawson, P. E. On Resin Side-Chain Cyclization of Complex Peptides Using CuAAC. *Org. Lett.*, **2011,** *13*, 2822-2825.

132. Scrima, M.; Le Chevalier-Isaad, A.; Rovero, P.; Papini, A. M.; Chorev, M.; D'Ursi, A. M. CuI-Catalyzed Azide–Alkyne Intramolecular i-to-(i+4) Side-Chain-to-Side-Chain Cyclization Promotes the Formation of Helix-Like Secondary Structures. *Eur. J. Org. Chem.*, **2010,** *2010*, 446-457.

133. Nevola, L.; Martín-Quirós, A.; Eckelt, K.; Camarero, N.; Tosi, S.; Llobet, A.; Giralt, E.; Gorostiza, P. Light-Regulated Stapled Peptides to Inhibit Protein–Protein Interactions Involved in Clathrin-Mediated Endocytosis. *Angew. Chem. Int. Ed.*, **2013,** *52*, 7704-7708.

134. Jafari, M. R.; Lakusta, J.; Lundgren, R. J.; Derda, R. Allene Functionalized Azobenzene Linker Enables Rapid and Light-Responsive Peptide Macrocyclization. *Bioconjugate Chem.*, **2016,** *27*, 509-514.

135. Lee, Y.-J.; Han, S.; Lim, Y.-b. Simultaneous Stabilization and Multimerization of a Peptide α-Helix by Stapling Polymerization. *Macromol. Rapid Commun.*, **2016,** *37*, 1021-1026.

136. Wójcik, P.; Berlicki, Ł. Peptide-Based Inhibitors of Protein–Protein Interactions. *Bioorg. Med. Chem. Lett.*, **2016,** *26*, 707-713.

137. Cardote, T. A. F.; Ciulli, A. Cyclic and Macrocyclic Peptides as Chemical Tools To Recognise Protein Surfaces and Probe Protein–Protein Interactions. *ChemMedChem*, **2016,** *11*, 787-794.

138. Mart, R. J.; Allemann, R. K. Azobenzene Photocontrol of Peptides and Proteins. *Chem. Commun.*, **2016,** *52*, 12262-12277.

139. Lau, Y. H.; de Andrade, P.; Wu, Y.; Spring, D. R. Peptide Stapling Techniques Based on Different Macrocyclisation Chemistries. *Chem. Soc. Rev.*, **2015,** *44*, 91-102.

140. Brown, S. P.; Smith, A. B. Peptide/Protein Stapling and Unstapling: Introduction of s-Tetrazine, Photochemical Release, and Regeneration of the Peptide/Protein. *J. Am. Chem. Soc.*, **2015,** *137*, 4034-4037.

141. Chen, X.; He, Y.; Kim, Y.; Lee, M. Reversible, Short α-Peptide Assembly for Controlled Capture and Selective Release of Enantiomers. *J. Am. Chem. Soc.*, **2016,** *138*, 5773-5776.

142. Haney, C. M.; Loch, M. T.; Horne, W. S. Promoting Peptide [Small Alpha]-Helix Formation with Dynamic Covalent Oxime Side-Chain Cross-links. *Chem. Commun.*, **2011,** *47*, 10915-10917.

143. Sutton, D. A.; Yu, S.-H.; Steet, R.; Popik, V. V. Cyclopropenone-Caged Sondheimer Diyne (dibenzo[a,e]cyclooctadiyne): A Photoactivatable Linchpin for Efficient SPAAC Crosslinking. *Chem. Commun.*, **2016,** *52*, 553-556.

144. Doan, S. C.; Kuzmanich, G.; Gard, M. N.; Garcia-Garibay, M. A.; Schwartz, B. J. Ultrafast Spectroscopic Observation of a Quantum Chain Reaction: The Photodecarbonylation of Nanocrystalline Diphenylcyclopropenone. *J. Phys. Chem. Lett.*, **2012,** *3*, 81-86.

145. Hernández-Linares, M. G.; Guerrero-Luna, G.; Pérez-Estrada, S.; Ellison, M.; Ortin, M.-M.; Garcia-Garibay, M. A. Large-Scale Green Chemical Synthesis of Adjacent Quaternary Chiral Centers by Continuous Flow Photodecarbonylation of Aqueous Suspensions of Nanocrystalline Ketones. *J. Am. Chem. Soc.*, **2015,** *137*, 1679-1684.

146. Kuzmanich, G.; Gard, M. N.; Garcia-Garibay, M. A. Photonic Amplification by a Singlet-State Quantum Chain Reaction in the Photodecarbonylation of Crystalline Diarylcyclopropenones. *J. Am. Chem. Soc.,* **2009,** *131*, 11606-11614.

147. Kuzmanich, G.; Natarajan, A.; Chin, K. K.; Veerman, M.; Mortko, C. J.; Garcia-Garibay, M. A. Solid-State Photodecarbonylation of Diphenylcyclopropenone: A Quantum Chain Process Made Possible by Ultrafast Energy Transfer. *J. Am. Chem. Soc.*, **2008,** *130*, 1140-1141.

148. Nielsen, A.; Kuzmanich, G.; Garcia-Garibay, M. A. Quantum Chain Reaction of Tethered Diarylcyclopropenones in the Solid State and Their Distance-Dependence in Solution Reveal a Dexter S2–S2 Energy-Transfer Mechanism. *J. Phys. Chem. A,* **2014,** *118*, 1858-1863.

149. Jewett, J. C.; Bertozzi, C. R. Synthesis of a Fluorogenic Cyclooctyne Activated by Cu-Free Click Chemistry. *Org. Lett.,* **2011,** *13*, 5937-5939.

150. Friscourt, F.; Fahrni, C. J.; Boons, G.-J. A Fluorogenic Probe for the Catalyst-Free Detection of Azide-Tagged Molecules. *J. Am. Chem. Soc.,* **2012,** *134*, 18809-18815.

151. Wang, K.; Friscourt, F.; Dai, C.; Wang, L.; Zheng, Y.; Boons, G.-J.; Wang, S.; Wang, B. A Metal-Free Turn-on Fluorescent Probe for the Fast and Sensitive Detection of Inorganic Azides. *Bioorg. Med. Chem. Lett.,* **2016,** *26*, 1651-1654.

152. Kleinhofs, A.; Owais, W. M.; Nilan, R. A. Azide. *Mutat. Res. Rev. Genet.*, **1978,** *55*, 165-195.

CHAPTER 2

PHOTOCHEMICAL GENERATION OF OXA-DIBENZOCYCLOOCTYNE (ODIBO) FOR METAL-FREE CLICK LIGATIONS

2.01 Introduction

The project goal was to reduce the enormous amount of synthetic steps required in preparing photo-caged cyclooctynes, and simultaneously improve the reactivity of the cyclooctyne that is being generated after photodecarbonylation. The use of cyclopropenones as a photo-cage allows for spatial and temporal control of SPAAC as well as protection of the alkyne from unwanted side reactions like nucleophilic attack of endogenous nucleophiles. It was envisioned that photo-oxa-dibenzocyclooctynes (photo-ODIBO) would a be perfect scaffold for this process (Figure 2.01). Coupling of two aromatic moieties by an ether formation will allow for a significant reduction in the number of steps as well as allow for easy functionalization of the photo-ODIBO/ODIBO core.

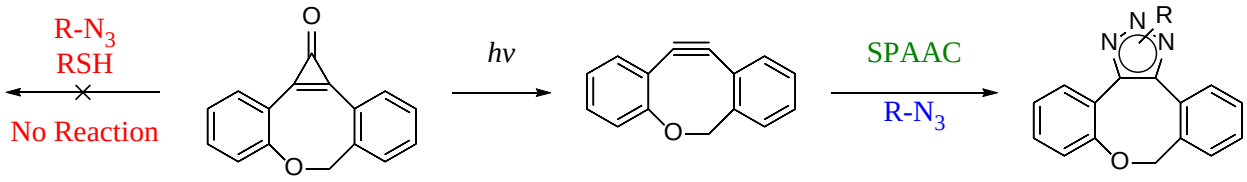

Figure 2.01 General Scaffold of photo-ODIBO

2.02 Synthesis of Photo-ODIBO Derivatives

The first target cyclopropenone **2.03** (Scheme 2.01), which can be prepared from the commercially available 3-hydroxybenzyl alcohol, was synthesized in three steps. The benzyl alcohol is converted to the benzyl bromide with phosphorus tribromide in dichloromethane to afford **2.01**. Next, compound **2.01** is reacted in a Williamson ether synthesis with 3-

methoxyphenol in DMF to afford benzyl ether **2.02**. Lastly, using a Friedel-Crafts alkylation with tetrachlorocyclopropene followed by hydrolysis with 5% HCl afforded cyclopropenone **2.03**. Unfortunately, the yield of the cyclopropenone reaction was extremely low (11 %) because polymerization was more favorable. This also caused major reproducibility and purification problems.

Scheme 2.01

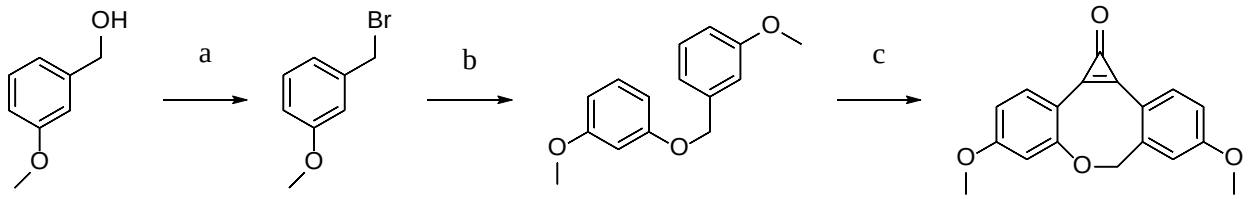

2.01 **2.02** **2.03**

Reagents and Conditions*:* a) PBr_3, CH_2Cl_2 73%; b) 3-methoxyphenol, K_2CO_3, DMF, 61 %; c) C_3Cl_4, $AlCl_3$, CH_2Cl_2, 11%.

To alleviate the problem of polymerization during the Friedel-Crafts alkylation and increase reproducibility, a t-butyl group was used to block polymerization from happening (Scheme 2.02). The synthesis starts with benzyl bromide **2.01** reacting with 4-tert-butylphenol in a Williamson ether synthesis in DMF to afford ether **2.04**. Next, Friedel-Crafts alkylation with tetrachlorocyclopropene followed by hydrolysis with 5% HCl afforded photo-ODIBO **2.05** in a much higher yield (29%). The use of the tert-butyl moiety was extremely efficient in stopping polymerization during the Friedel-Crafts alkylation and the reaction worked consistently.

Scheme 2.02

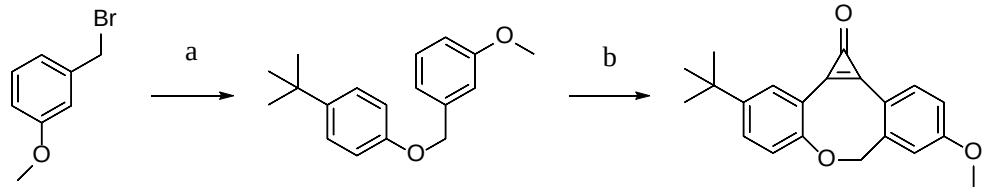

2.01 **2.04** **2.05**

Reagents and Conditions: a) 4-tert-butylphenol, K_2CO_3, DMF, 60%; b) C_3Cl_4, $AlCl_3$, CH_2Cl_2, 29%.

Lastly, a derivative of photo-ODIBO that could be easily functionalized with handles for various future applications was synthesized (Scheme 2.03). To do this, a simple TBDMS protecting group was used and removed after cyclopropenone formation. The first step of the synthesis starts with protection of the commercially available 3-hydroxybenaldehyde with TBDMS-Cl to afford **2.06**. Next, **2.06** was reduced with $NaBH_4$ in methanol to afford **2.07** which can then be coupled in a Mitsunobu reaction with 4-tert-butylphenol to afford **2.08**. With the ether of **2.08** a Friedel-Crafts alkylation reaction with tetrachlorocyclopropene in CH_2Cl_2 followed by hydrolysis in 5% HCl afforded photo-ODIBO-TBDMS **2.09**. The removal of the TDBDMS can be done with TBAF in THF to afford the pre-functionalized photo-ODIBO-OH **2.10**. In five synthetic steps and a total 20% yield large quantities of photo-ODIBO-OH **2.10** can be synthesized.

Scheme 2.03

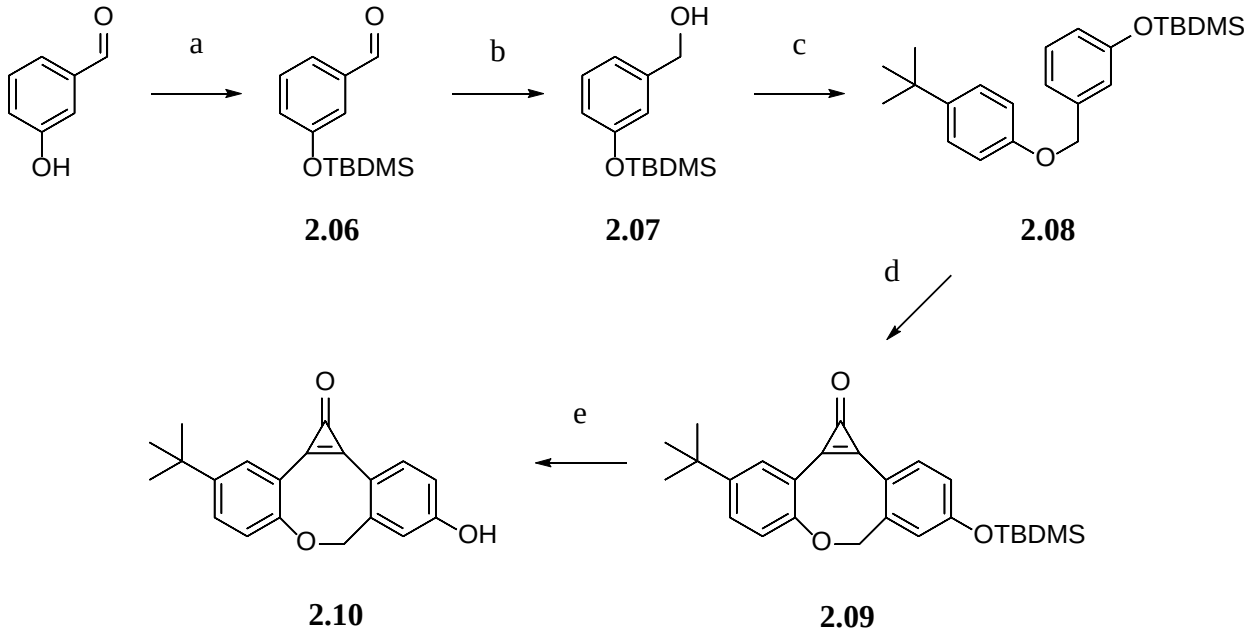

2.06 **2.07** **2.08**

2.10 **2.09**

Reagents and Conditions: a) TBDMS-Cl, imidazole, CH_2Cl_2, 97%; b) $NaBH_4$, MeOH, 91%; c) 4-tert-butylphenol, K_2CO_3, DMF, 66%; d) C_3Cl_4, $AlCl_3$, CH_2Cl_2, 43%; e) TBAF, THF, 80%.

After completing the synthesis of photo-ODIBO derivatives **2.03**, **2.05**, and **2.10**, characterization of the formation of the alkyne and triazole were needed to authenticate the photochemical and chemical reactions. Photo-ODIBO **2.05** (Scheme 2.04) was irradiated for 15 minutes in methanol (350 nm) to successfully form ODIBO **2.11**. Next, ODIBO **2.11** was mixed with benzyl azide to form triazole **2.12**. Interestingly, only one isomer of triazole was isolated. This may be attributed to steric hindrance between the tert-butyl substituent and the large benzyl group of the azide. Lastly, kinetic experiments with photo-ODIBO derivatives **2.03** and **2.10** were carried out by *in situ* generation of the corresponding alkynes **2.13** and **2.14** before mixing with organic azides.

Scheme 2.04

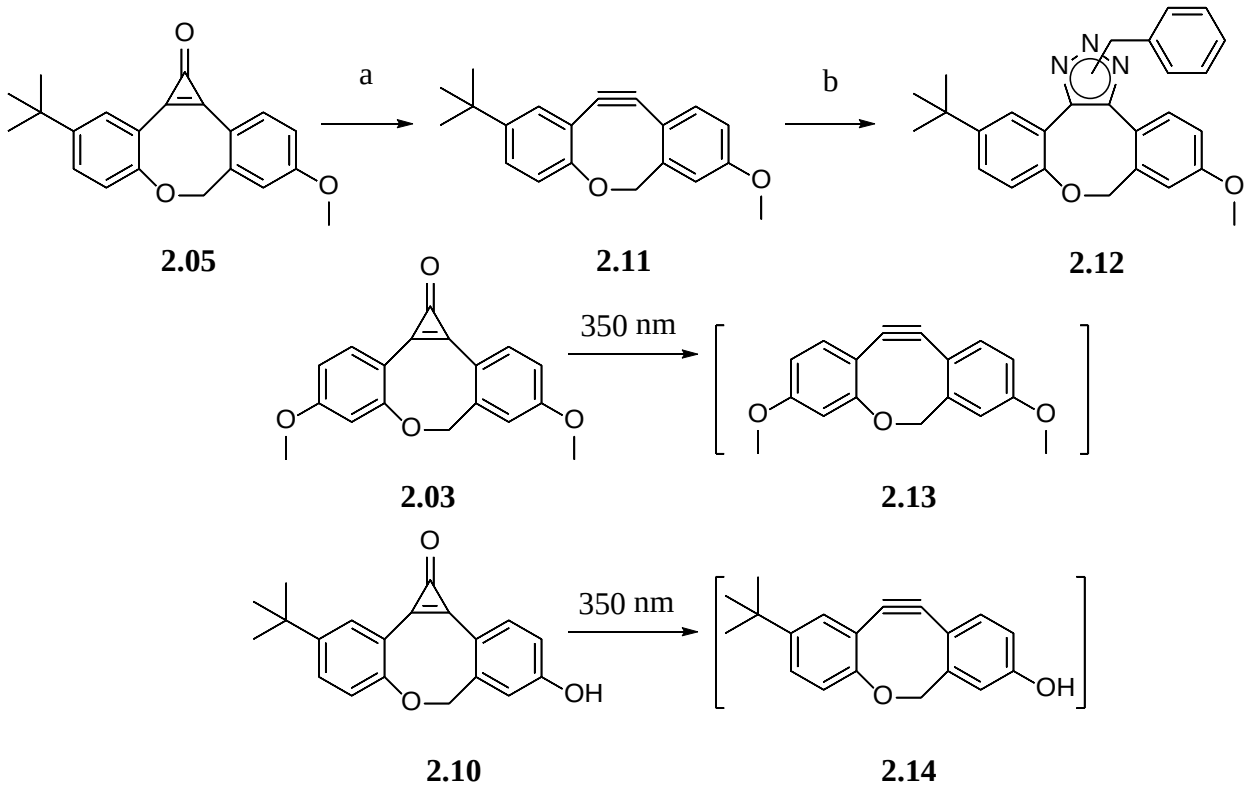

2.05 **2.11** **2.12**

2.03 **2.13**

2.10 **2.14**

Reagents and Conditions: a) 350 nm, MeOH, 88%; b) BnN_3, CH_2Cl_2, 85%

2.03 Properties of photo-ODIBO and ODIBO Derivatives

The photo-ODIBO derivatives **2.03**, **2.05**, and **2.10** are all white crystalline compounds that are bench stable if stored away from light. Each derivative shows remarkable stability to elevated temperatures. Photo-ODIBO derivative **2.05** melts at 160-163 °C and shows no signs of decarbonylation, and when refluxed in *o*-dichlorobenzene for six hours it is completely recovered. All three cyclopropenones are stable in methanol, PBS, and TRIS buffers. Also, the cyclopropenones do not react with azides and are stable to endogenous nucleophiles like glutathione (10 mM) under ambient conditions.

The UV spectra of the photo-ODIBO derivatives in methanol display three close-lying intense bands (λ_{max} = 308, 330, 343 nm, log ε ~ 3.9) that are characteristic for similar cyclopropenone derivatives.[1] Photo-ODIBO **2.05** (Figure 2.01) upon irradiation with 350 nm

light shows efficient decarbonylation (ϕ = 0.16). Upon disappearance of the characteristic cyclopropenone peak quantitative formation of ODIBO is observed (Figure 2.01). All ODIBO derivatives show a hypsochromic shift compared to their cyclopropenone precursors (λ_{max} = 290, 308, 323 nm, log $\varepsilon \sim 4.1$). Also, when ODIBO derivatives react with azides, disappearance of the characteristic alkyne peak can be observed by UV (Figure 2.01). This system allows convenient monitoring of the decarbonylation as well as the SPAAC reaction with UV.

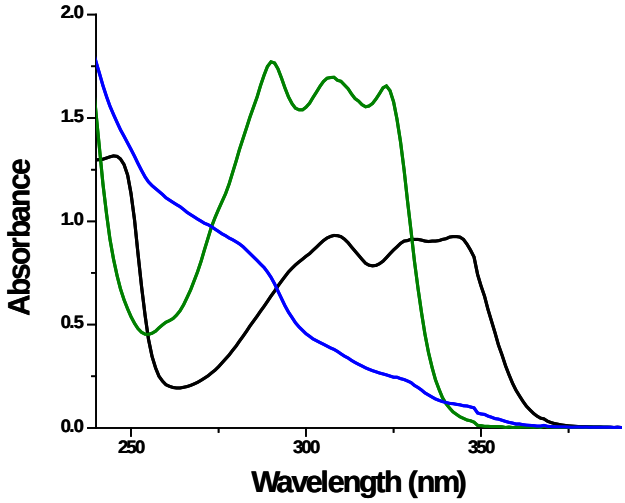

Figure 2.02 UV Spectrum of 115 µM solutions of photo-ODIBO **2.05** (black line), ODIBO **2.11** (green line), and triazole **2.12** (blue line) in MeOH.

ODIBO derivatives **2.11**, **2.13**, and **2.14** are stable for long term storage in the freezer (0 °C). They are also stable when dissolved into methanol, PBS, and TRIS. ODIBO derivatives hydrate slowly under elevated temperatures. The half-lifetime of hydration is ~ 20 minutes at 75 °C and the half-lifetime with 10 mM glutathione is ~50 minutes. These exceptional stabilities showcase that even after deprotection, ODIBO is extremely robust.

2.04 Kinetics of ODIBO Derivatives

Studying the reactivity of the newly synthesized ODIBO derivatives was done by UV spectroscopy. Various concentrations of organic azides were mixed with 115 µM of ODIBO **2.11** at 25.0 ± 0.1 °C in methanol and aqueous solutions. Reactions were conducted under pseudo-first order conditions with the organic azides in excess. The consumption of starting material was monitored by following the decay of the characteristic alkyne peak at 323 nm. The experimental data fits the single exponential equation well, and linear dependence of the pseudo-first order rate constants on azide concentration were analyzed by the least square method to obtain biomolecular rate constants (Figure 2.02, Table 2.01)

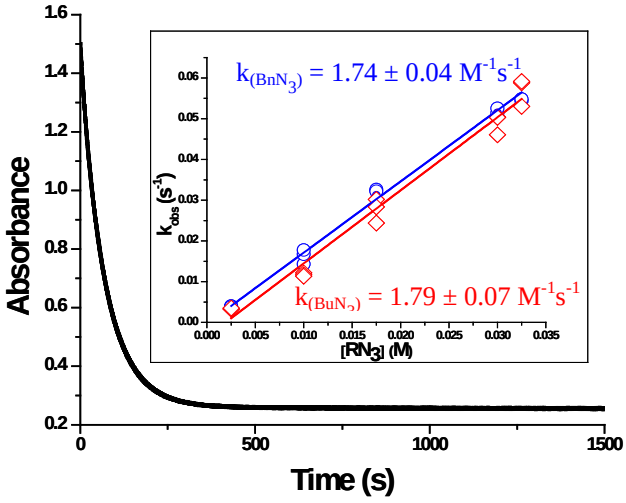

Figure 2.03 Reaction of 115 µM of ODIBO **2.11** with 10 mM of BnN_3 in MeOH at 25 °C. The inset illustrates the linear dependence of the observed rates on azide concentration.

The rate of reaction of ODIBO **2.11** with benzyl azide (BnN_3) in methanol was determined to be 1.74 ± 0.04 $M^{-1}s^{-1}$ which makes ODIBO **2.11** one of the fastest cyclooctyne reported. ODIBO **2.11** is two times faster than the previously fastest reported reacting cyclooctyne BARAC[2]. It is important to note that BARAC was not measured under the same

conditions as ODIBO **2.11** and used in a much less accurate NMR technique. So a direct comparison must be used with some caution. Next, because the reaction of azides and cyclooctynes is mostly used for biological application, the rate enhancement in water was studied (Figure 2.03, Table 2.01). ODIBO **2.11** was reacted in an aqueous methanol solution with various organic azides. The reactions still follow first order law and shows linear dependence on the azide concentration.

To explore the effect of the water concentration on the rate of SPAAC, the reaction was monitored with 2.5 mM of BnN_3 at various water concentrations (Figure 2.03). Conservative extrapolation of the trend suggests that ODIBO **2.11** could proceed at rates of 2-3 x 10^2 $M^{-1}s^{-1}$. The acceleration of the reaction can be attributed to higher polarity and/or donor-acceptor interaction with the solvent. However, it is also possible that rate enhancement could be caused by formation of inhomogenous solution such as micro emulsions or aggregates of azide. To test this, first, the concentration of ODIBO **2.11** was lowered to 800 nM in 35.75 M of water (Figure 2.03). The reaction kinetics of a single concentration of benzyl azide (2.5 mM) was monitored, and a near identical rate was calculated when compared to the original. Next, a more hydrophilic ODIBO derivative and azide were used to study the SPAAC reactivity. ODIBO **2.14** with 1-amino-8-azido-3,5-dioxaoctane (TEG-N_3) were examined in a variety of solvents (Table 2.01). The second order rate constant in methanol was very similar to that of other organic azides with with ODIBO **2.11** (Table 2.01). The SPAAC reaction of ODIBO **2.14** increased to 11.3 ± 0.2 $M^{-1}s^{-1}$ in water (19:1 water: methanol) compared to 1.43 ± 0.4 $M^{-1}s^{-1}$ in methanol. The effect was less pronounced than benzyl azide but still showed a significant increase in reactivity.

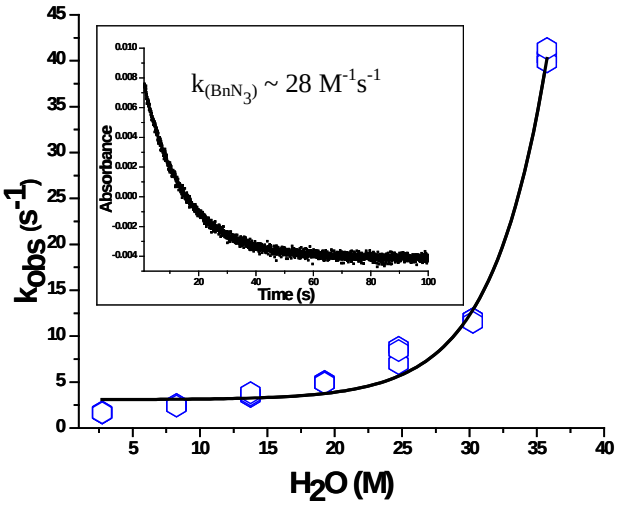

Figure 2.04 Dependence of the rate of ODIBO **2.11** with various water concentrations in aqueous methanol (Bimolecular rate constants were evaluated from a rate measured at 2.5 mM of BnN_3 and 115 µM ODIBO **2.01**). The inlet shows the kinetics of ODIBO **2.11** at 800 nM (35.75 M of water).

Table 2.01 Rates of ODIBO derivatives with organic azides.

ODIBO	Solvent	Azide	Rate ($M^{-1}s^{-1}$)
2.11	MeOH	BnN_3	1.74 ± 0.04
2.11	MeOH	n-BuN_3	1.79 ± 0.07
2.11	MeOH	TEG-N_3	1.96 ± 0.03
2.11	Water-MeOH-THF[a]	BnN_3	45.1 ± 2.6
2.11	Water-MeOH-THF[a]	n-BuN_3	28.6 ± 1.3
2.11	Water-THF	TEG-N_3	7.2 ± 0.1
2.13	MeOH	BnN_3	2.22 ± 0.1[d]
2.14	MeOH	TEG-N_3	1.43 ± 0.04
2.14	Water-MeOH[b]	TEG-N_3	8.91 ± 0.07[d]
2.14	Water-MeOH[c]	TEG-N_3	11.3 ± 0.02[d]

[a] 13:4:3, water: MeOH, THF; [b] 7:3, water: MeOH; [c] 19:1 water: MeOH; [d] Evaluated rated from a single azide concentration.

2.05 Conclusion

The development of a photo-caged cyclopropenone that could be synthesized quickly and display increased reactivity was achieved. Photo-OIBO derivatives show remarkable stability to various conditions such as elevated temperature, endogenous nucleophiles like glutathione, and no reactivity towards azides. Cyclopropenones allow for spatial and temporal control, and once the cyclopropenone is irradiated efficient photo-decarbonylation occurs to generate a cyclooctyne. ODIBO is a fast reacting cyclooctyne with rates as high as 45.1 ± 2.6 $M^{-1}s^{-1}$ in an aqueous solution. Also, ODIBO displays excellent stabilities when compared to the rate

enhancement. This exceptionally fast reactivity will allow ODIBO to be used in a variety of labeling experiments. The next goal will be to optimize and apply photo-ODIBO and ODIBO in cell ligation experiments and surface functionalization.

2.06 Experimental Section

Materials and Methods

All organic solvents were dried and freshly distilled before use; Tetrahydrofuran was distilled from sodium/benzophenone ketyl. Other reagents were obtained from Aldrich or VWR and used as received unless noted. Flash chromatography was performed using 40-63 μm silica gel. All NMR spectra were recorded in $CDCl_3$ (unless otherwise noted) using 400 MHz instrument. Absorption spectra were recorded on CARY 300 Bio UV-Visible spectrometer. Quantum yield was determined using a ferrioxalate chemical actiniometer.[3] Photolyses were conducted in the Rayonet photoreactor equipped with 12 X 4 W 350 nm fluorescent lamps.

Kinetics

Rate measurements in organic solvent were performed using Carry-300 Bio UV-Vis spectrometer, while reactions in aqueous solutions were followed using RX2000 Rapid Kinetics Spectrometer accessory on a Carry-50 Bio UV-Vis spectrometer. The temperature was set to 25.0°C and controlled to 0.1 °C accuracy. Reactions of ODIBO with excess of azide were monitored by following the decay of the characteristic 322 nm absorbance. The experimental data fits the single exponential equation well. Linear dependence of the observed pseudo-first order rate constants on azide concentration was analyzed by the least squares method to obtain the bimolecular rate constants.

3-methoxybenzyl bromide (2.01).[4]

PBr_3 (4.31 mL, 15.92 mmol) was added to a solution of 3-methoxybenzyl alcohol (3.143 g, 22.75 mmol) in CH_2Cl_2 (40 mL) at 0 °C. The solution was then stirred for 30 minutes at 0 °C. Next, the reaction was warmed to room temperature, diluted with ether (150 mL), washed with saturated sodium thiosulfate solution (1 x 50 mL), brine (1 x 50 mL), and dried over $MgSO_4$. The organic layer was then filtered and then concentrated in vacuo to provide 3-methoxybenzyl bromide **2.01** (3.33 g, 73%) as a colorless oil. ^{1}H-NMR: 7.25-7.29 (t, J = 7.9 Hz, 1H), 6.99-7.01 (d, J = 7.6 Hz, 1H), 6.94-6.96 (m, 1H), 6.85-6.88 (dd, J = 8.3, 2.5 Hz, 1H), 4.49 (s, 2H), 3.83 (s, 3H). ^{13}C-NMR: 159.93, 139.33, 129.99, 121.48, 114.62, 114.36, 55.46, 33.69.

1-methoxy-3-((3-methoxybenzyl)oxy)benzene (2.02).

3-methoxybenzyl bromide (1.0 g, 4.97 mmol, 5 mL DMF) was added to a solution of 3-methoxyphenol (0.617 g, 4.97 mmol) in DMF (20 mL) and potassium carbonate (0.687 g, 4.97 mmol). The solution was stirred at 70 °C for 4h. The reaction mixture was cooled to room temperature, diluted with ether (300 mL), washed with water (5 x 100 mL), brine (1 x 100 mL), and dried over $MgSO_4$. The organic layer was then filtered, concentrated in vacuo, and purified via flash chromatography (hexanes: ethyl acetate 10:1) to afford 1-methoxy-3-((3-methoxybenzyl)oxy)benzene **2.02** (0.741 g, 61%) as a colorless oil. ^{1}H-NMR: 7.31-7.35 (t, J = 7.9 Hz, 1H), 7.20-7.24 (t, J = 8.1 Hz, 1H), 7.03-7.06 (m, 2H), 6.89-6.92 (dd, J = 8.2, 2.6 Hz, 1H), 6.55-6.63 (m, 3H), 5.05 (s, 2H), 3.85 (s, 3H), 3.81 (s, 3H). ^{13}C-NMR: 161.00, 160.17, 159.99, 138.73, 130.07, 129.80, 119.85, 113.68, 113.07, 107.08, 106.77, 101.54, 70.06, 55.42, 55.39. HRMS calcd. ($M+H^+$):$C_{15}H_{17}O_3$ 245.1172, found 245.1171.

4,9-dimethoxydibenzo[b,f]cyclopropa[d]oxocin-1(7H)-one (2.03).

A solution of tetrachlorocyclopropene (0.223 g, 1.23 mmol) in CH_2Cl_2 (5 mL) was added to a suspension of aluminum chloride (0.165 g, 1.23 mmol) in CH_2Cl_2 (100 mL). The reaction mixture was stirred for 15 minutes, cooled to -78 °C, and a solution of 1-methoxy-3-((3-methoxybenzyl)oxy)benze **2.03** (0.300 g, 1.23 mmol) in CH_2Cl_2 (10 mL) was added dropwise (over 10 minutes), and stirred for 3 h at -78 °C. The reaction mixture was allowed to warm to room temperature and stirred for an additional 30 min. The reaction was quenched with 5% HCl solution (50 mL) and the organic layer was extracted. The organic layer was washed with brine (1 x 50 mL) and dried over $MgSO_4$. The organic layer was then filtered, concentrated in vacuo, and purified via flash chromatography (CH_2Cl_2 to CH_2Cl_2: methanol 30:1) to afford photo-ODIBO **2.03** (0.041 g, 11%) as a white powder (222-225 °C MP). ^{1}H-NMR: 7.92-7.94 (d, J = 8.0 Hz, 1H), 787-7.89 (m, 1H), 7.02-7.04 (m, 2H), 6.80-6.83 (m, 2H), 5.26-5.29 (d, J – 12.1 Hz, 1H), 4.85-4.88 (d, J = 12.0 Hz, 1H), 3.92 (s, 3H), 3.88 (s, 3H). ^{13}C-NMR: 164.56, 164.12, 162.57, 152.24, 141.96, 140.75, 140.24, 135.56, 135.22, 118.22, 117.13, 114.20, 111.04, 110.50, 108.32, 78.56, 55.95, 55.90. ESI HRMS: calcd. ($M+H^+$): $C_{18}H_{15}O_4$ 295.0965, found 295.0966. IR: 1854 cm^{-1} ($\nu_{C=O}$).

1-((4-(tert-butyl)phenoxy)methyl)-3-methoxybenze (2.04).

3-methoxybenzyl bromide **2.1** (2.87 g, 14.27 mmol, 5 mL DMF) was added to a solution of 4-tert-butylphenol (2.144 g, 14.27 mmol) in DMF (100 mL) and potassium carbonate (1.973 g, 14.27 mmol). The solution was stirred at 70 °C for 4h. The reaction mixture was cooled to room temperature, diluted with ether (200 mL), washed with water (5 x 100 mL), brine (1 x 100 mL) and dried over $MgSO_4$. The organic layer was then filtered, concentrated in vacuo vacuum, and purified via flash chromatography (hexanes: ethyl acetate 5:1) to afford 1-((4-(tert-butyl)phenoxy)methyl)-3-methoxybenze **2.04** (2.31 g, 60%) as a colorless oil. ^{1}H-NMR: 7.29-

7.34 (m, 3H), 7.01-7.04 (m, 2H), 6.92-6.95 (m, 2H), 6.87-6.89 (dd, J = 8.1, 2.4 Hz, 1H), 5.04 (s, 2H), 3.84 (s, 3H), 1.32 (s, 9H). ^{13}C-NMR: 160.04, 156.76, 143.85, 139.14, 129.81, 126.46, 119.87, 114.50, 113.65, 113.09, 70.14, 55.46, 34.30, 31.74. HRMS calcd. ($M+H^+$):$C_{18}H_{23}O_2$ 271.1692, found 271.1697.

3-(tert-butyl)-9-methoxydibenzo[b,f]cyclopropa[d]oxocin-1(7H)-one (Photo-ODIBO, 2.05).

A solution of tetrachlorocyclopropene (0.944 mL, 7.69 mmol) in 5 mL of CH_2Cl_2 was added to a suspension of aluminum chloride (1.026 g, 7.69 mmol) in CH_2Cl_2 (80 mL). The reaction mixture was stirred for 15 minutes, cooled to -78 °C, and 1-((4-(tert-butyl)phenoxy)methyl)-3-methoxybenze **2.04** (2.08g, 7.69 mmol) in CH_2Cl_2 (10 mL) was added dropwise (over ten minutes), and stirred for 3 h at -78 °C. The reaction mixture was allowed to warm slowly to room temperature and stir for an additional 30 min. The reaction was quenched with 5% HCl solution (150 mL) and the organic layer was extracted. The organic layer was washed with brine (1 x 100 mL) and dried over $MgSO_4$. The organic layer was then filtered, concentrated in vacuo, and purified via flash chromatography (CH_2Cl_2 to CH_2Cl_2: methanol 30:1) to afford photo-ODIBO **2.05** (0.720 g, 29%) as a white powder. M.p. = 160-163°C. ^{1}H-NMR: 7.97-7.94 (m, 2H), 7.50-7.52 (dd, J = 8.5, 2.5 Hz, 1H), 7.20-7.22 (d, J = 8.5 Hz, 1H), 7.02-7.05 (m, 2H), 5.27-5.30 (d, J = 12.1 Hz, 1H), 4.78-4.81 (d, J = 12.1 Hz, 1H), 3.92 (s, 3H), 1.36 (s, 9H). ^{13}C-NMR: 162.93, 160.56, 152.82, 148.17, 144.25, 142.41, 140.81, 135.67, 131.24, 130.78, 122.12, 117.99, 117.21, 117.00, 114.17, 78.90, 55.90, 34.78, 31.55. ESI HRMS: calcd ($M+H^+$): $C_{21}H_{21}O_3$ 321.1485, found 321.1504. IR: 1846 cm^{-1} ($\nu_{C=O}$).

3-(tert-butyldimethylsilyloxy)benzaldehyde (2.06).[5]

3-Hydroxybenzaldehyde (15.0 g, 123 mmol) and imidazole (8.36 g, 123 mmol) were dissolved into CH_2Cl_2 (400 mL). While stirring at room temperature TBDMS-Cl (22.22 g, 147 mmol) was added. The reaction was stirred for 3 hours, filtered, concentrated in vacuo, and purified via flash chromatography (hexanes: ethyl acetate, 10:1) to afford 3-(tert-butyldimethylsilyloxy)benzaldehyde **2.06** (28.27 g, 97%) as a colorless oil. ^{1}H-NMR: 9.96 (s, 1H), 7.47-7.49 (d, J = 7.6 Hz, 1H), 7.39-7.43 (t, J = 7.8 Hz, 1H), 7.34 (s, 1H), 7.10-7.13 (m, 1H), 1.00 (s, 9H), 0.22 (s, 6H). ^{13}C-NMR: 192.31, 156.60, 138.13, 130.28, 126.75, 123.76, 120.07, 25.83, 18.41, -4.22.

3-(tert-butyldimethylsilyloxy)benzyl alcohol (2.07).[6]

3-(tert-butyldimethylsilyloxy)benzaldehyde **2.06** (28.27 g, 120 mmol) was dissolved into methanol (300 mL). While stirring, the reaction mixture was cooled to 0 °C. Next, sodium borohydride was added (4.98 g, 132 mmol), stirred for five minutes, and warmed to room temperature. After reaching room temperature the reaction was stirred for 20 minutes, quenched with saturated ammonium chloride (300 mL), diluted with ethyl acetate (600 mL), extracted, and dried over $MgSO_4$. The organic layer was then filtered, concentrated in vacuo, and purified via flash chromatography (hexanes: ethyl acetate, 5:1) to afford 3-(tert-butyldimethylsilyloxy)benzyl alcohol **2.07** (25.82 g, 91%) as a colorless oil. ^{1}H-NMR: 7.20-7.24 (t, J = 7.8 Hz, 1H), 6.94-6.96 (d, J = 7.5 Hz, 1H), 6.87 (s, 1H), 6.76-6.79 (dd, J = 8.1 Hz, 1H), 4.64 (s, 2H), 1.00 (s, 9H), 0.22 (s, 6H). ^{13}C-NMR: 156.05, 142.71, 129.68, 119. 94, 119.40, 118.79, 65.28, 25.87, 18.38, -4.20.

tert-butyl-3-(4-tert-butylphenoxy)methylphenoxydimethylsilane (2.08).

DIAD (14.26 g, 70.5 mmol) was added to a solution of 4-tert-butylphenol (10.59 g, 70.5 mmol), 3-(tert-butyldimethylsilyloxyphenyl)methanol **2.07** (16.81 g, 70.5 mmol), and PPH_3 (18.49 g,

70.5 mmol) in THF (370 mL) at 0 °C. The reaction mixture was stirred for 5 minutes at 0 °C and warmed to room temperature. After warming, the reaction was stirred for 30 minutes, concentrated in vacuo, and purified via flash chromatography (hexanes: ethyl acetate, 10:1) to afford tert-butyl-3-(4-tert-butylphenoxy)methylphenoxydimethylsilane **2.08** (17.11 g, 65.5%) as a colorless oil. ^{1}H-NMR: 7.37-7.38 (d, J = 4.0 Hz, 1H), 7.31-7.33 (dd, J = 6.8, 2.0 Hz, 2H), 7.23-7.25 (m, 1H), 7.03-7.05 (d, J =7.6 Hz, 1H), 6.92-6.94 (m, 3H), 6.80-6.82 (m, 1H), 5.02 (s, 2H), 1.32 (s, 9H), 1.00 (s, 9H), 0.21 (s, 6H). ^{13}C NMR: 156.77, 156.12, 143.82, 139.16, 129.71, 126.41, 120.41, 119.65, 119.18, 114.65, 70.01, 34.29, 31.76, 25.94, 18.44, -4.18. ESI HRMS: calcd. ($M+H^+$): $C_{23}H_{35}O_2Si$ 371.2401, found 371.2393.

3-tert-butyl-9-tert-butyldimethylsilyloxydibenzo[b,f]cyclopropa[d]oxocin-1(7H)-one (photo-ODIBO-TBDMS, 2.09).

A solution of tetrachlorocyclopropene (3.32 g, 18.89 mmol) in 5 mL of CH_2Cl_2 was added to a suspension of aluminum chloride (2.52 g, 18.89 mmol) in CH_2Cl_2 (450 mL). The reaction mixture was stirred for 15 minutes, cooled to -78 °C, and a solution of tert-butyl-3-(4-tert-butylphenoxy)methylphenoxydimethylsilane **2.08** (7.00 g, 18.89 mmol) in CH_2Cl_2 (20 mL) was added dropwise (over 10 minutes), and stirred for 3 h at -78 °C. The reaction mixture was allowed to warm to room temperature and stirred for an additional 30 min. The reaction was quenched with 5% HCl solution (150 mL) and the organic layer was extracted. The organic layer was washed with brine (1 x 150 mL) and dried over $MgSO_4$. The organic layer was then filtered, concentrated in vacuo, and purified via flash chromatography (CH_2Cl_2 to CH_2Cl_2: methanol 50:1) to afford photo-ODIBO-TBDMS **2.09** (3.4 g, 43%) as an off-white amorphous solid. ^{1}H-NMR: 7.95 (d, J = 2.0 Hz, 1H), 7.90-7.92 (d, J =8.9 Hz, 1H), 7.50-7.52 (dd, J = 8.5, 1.8 Hz, 1H), 7.20-7.23 (d, J =8.5 Hz, 1H), 6.97-6.99 (m, 2H), 5.25-5.28 (d, J = 12.1 Hz, 1H),

4.76-4.79 (d, J = 12.1 Hz, 1H), 1.36 (s, 9H), 1.01 (s, 9H), 0.27 (s, 6H). ^{13}C-NMR: 160.57, 159.71, 152.95, 148.14, 144.14, 142.54, 140.85, 135.58, 131.30, 130.86, 122.48, 122.11, 120.86, 118.46, 117.14, 78.80, 34.78, 31.54, 25.76, 18.45, -4.05. ESI HRMS: calcd. ($M+H^+$): $C_{26}H_{33}O_3Si$ 421.2194, found 421.2190. IR: 1842 cm^{-1} ($\nu_{C=O}$).

3-tert-butyl-9-hydroxydibenzo[b,f]cyclopropa[d]oxocin-1(7H)-one (photo-ODIBO-OH, 2.10).

To a solution of photo-ODIBO-TBDMS **2.09** (7.65 g, 18.19 mmol) in THF (80 mL) was added tetrabutylammonium fluoride (18.19 mL, 1.0 M, 18.19 mmol). The solution was stirred for 30 minutes and quenched by saturated ammonium chloride. The reaction was then diluted with CH_2Cl_2 (500 mL), and the aqueous layer was extracted two more times with CH_2Cl_2 (50 mL). The organic layer was then washed with brine and dried over $MgSO_4$. The organic layer was then filtered, concentrated in vacuo, and purified via flash chromatography (CH_2Cl_2: methanol 30:1) to afford photo-ODIBO-OH **2.10** (4.45 g, 80%) of a white powder (170-173 °C MP). ^{1}H-NMR (DMSO-d_6): 10.73 (s, 1H), 7.76 (s, 2H), 7.61-7.63 (d, J = 7.4 Hz, 1H), 7.26-7.28 (d, J = 7.8 Hz, 1H), 7.08 (s, 1H), 6.97 – 6.99 (d, J = 7.0 Hz, 1H), 5.29 – 5.32 (d, J = 11.9 Hz, 1H), 4.81-4.48 (d, J = 12.0 Hz, 1H), 1.32 (s, 9H). ^{13}C-NMR (DMSO-d_6): 161.44, 159.81, 150.83, 147.14, 144.15, 141.18, 140.25, 134.94, 130.57, 129.38, 122.12, 117.89 116.82, 115.92, 115.59, 78.05, 34.13, 30.96. ESI HRMS: calcd. (M+H+). $C_{20}H_{19}O_3$, 307.1329, found 307.1332. IR: 1845 cm^{-1} ($\nu_{C=O}$).

2-(tert-butyl)-11,12-didehydro-8-methoxy-6H-dibenzo[b,f]oxocine (ODIBO, 2.11).

A solution of photo-ODIBO **2.05** (0.016 g, 0.062 mmol) in methanol (125 mL) was irradiated with 350 nm fluorescent lamps (12 x 4W) for 5 min at room temperature. The solution was

concentrated in vacuo and purified via flash chromatography (CH_2Cl_2: methanol 30:1) to provide ODIBO **2.11** (0.016 g, 88%) as a colorless oil. ^{1}H-NMR: 7.24-7.27 (m, 3H), 7.11-7.13 (dd, J = 7.6 Hz, 1.3 Hz, 1H), 7.02-7.03 (d, J = 2.5 Hz, 1H), 6.89-6.92 (dd, J = 8.4, 2.4 Hz, 1H), 5.19-5.22 (d, 12.0 Hz, 1H), 4.55-4.58 (d, J = 12.0 Hz, 1H), 3.85 (s, 3H), 1.33 (s, 9H). ^{13}C-NMR: 167.39, 159.64, 149.21, 147.01, 126.96, 125.58, 123.75, 121.41, 118.25, 117.76, 117.31, 114.28, 113.95, 110.75, 78.11, 55.71, 34.60, 31.61. ESI HRMS: calcd. (M-H+). $C_{19}H_{17}O_2$, 277.1234, found 277.1223.

1-Benzyl-5-(tert-butyl)-11-methoxy-1,9-dihydrodibenzo[2,3:6,7]oxocino[4,5-d][1,2,3]triazole (2.12).

Benzyl azide (0.008 g, 0.066 mmol) was added to a solution of ODIBO **2.11** (0.013 g, 0.044 mmol) in CH_2Cl_2 (2 mL) and stirred overnight. The reaction mixture was then concentrated in vacuo and then purified via flash chromatography (CH_2Cl_2) to give **1**-Benzyl-5-(tert-butyl)-11-methoxy-1,9-dihydrodibenzo[2,3:6,7]oxocino[4,5-d][1,2,3]triazole **2.12** (0.016 g, 85%) as a yellow oil. ^{1}H-NMR: 7.68 (d, J = 2.5 Hz, 1H), 7.28-7.34 (m, 3H), 7.21-7.24 (dd, J = 8.7, 2.6 Hz, 1H), 7.13-7.15 (m, 3H), 7.01-7.02 (d, J = 2.6 Hz, 1H), 6.90-6.93 (dd, J = 8.6, 2.6 Hz, 1H), 6.85-6.87 (d, 8.6 Hz, 1H), 5.56 (s, 2H), 4.86-5.15 (m, 2H), 3.85 (s, 3H), 1.30 (s, 9H). ^{13}C-NMR: 160.84, 152.40, 145.33, 144.37, 138.57, 135.97, 132.62, 130.48, 129.92, 129.08, 128.41, 127.32, 127.24, 120.10, 119.61, 116.82, 115.93, 115.27, 69.72, 55.72, 52.37, 34.40, 31.65. ESI HRMS: calcd. (M-H+). $C_{27}H_{26}N_3O_2$, 424.2031, found 424.2024.

General Procedure for ODIBO formation in Kinetic Experiments. A 0.01 M stock solution of a cyclopropenone derivative in methanol was made. Then 23 µL of the solution was added to either methanol or PBS (pH 7.4) in a cuvette. The solution was then irradiated for 2 minutes and

a solution of azide was added so the total volume was 2 mL and concentration of ODIBO derivative was 0.1 mM.

2.07 References

1. Poloukhtine, A. A.; Mbua, N. E.; Wolfert, M. A.; Boons, G. J.; Popik, V. V. Selective Labeling of Living Cells by a Photo-Triggered Click Reaction. *J. Am. Chem. Soc.*, **2009,** *131*, 15769-15776.

2. Jewett, J. C.; Sletten, E. M.; Bertozzi, C. R. Rapid Cu-free click chemistry with readily synthesized biarylazacyclooctynones. *J Am Chem Soc*, **2010,** *132*, 3688-90.

3. Murov, S. L.; Carmichael, I.; Hug, G. L., *Handbook of Photochemistry*. 2nd ed.; Marcel Dekker: New York, 1993.

4. Mayer, T.; Maier, M. E. Design and Synthesis of a Tag-Free Chemical Probe for Photoaffinity Labeling. *Eur. J. Org. Chem.*, **2007,** *2007*, 4711-4720.

5. Faler, C. A.; Joullie, M. M. The Kulinkovich Reaction in the Synthesis of Constrained N,N-Dialkyl Neurotransmitter Analogues. *Org. Lett.*, **2007,** *9*, 1987-1990.

6. Wu, Y. C.; Liron, M.; Zhu, J. Asymmetric Total Synthesis of (-)-Quinocarcin. *J. Am. Chem. Soc.*, **2008,** *130*, 7148-7152.

CHAPTER 3

EXPLORING THE REACTIVITY OF CYCLOOCTYNES

3.01 Introduction

There have been numerous cyclooctynes reported in the literature and it can be extremely difficult to compare their reactivity and stability. These properties are vital for choosing the correct cyclooctyne for experimental needs. The most commonly used way to determine the rate of SPAAC is NMR, but there are some major drawbacks to this approach. NMR techniques used to determine rates can struggle with accuracy because of the reaction conditions.[1-5] These experiments are done under second order conditions, at a single concentration, and no temperature control. This can lead to high variance in calculated rates. Another problem with how SPAAC rates are determined is that the solvent systems are not uniform. [1-6] We have previously shown that water can have dramatic effects on the rate of SPAAC (*vide supra*) and many of the SPAAC rates reported have different ratios of water. These inconsistencies prompted us to study the rate of SPAAC under numerous directly comparable conditions. We investigated the rate of SPAAC under pseudo-1st order conditions, multiple times, over five different concentrations, and under temperature control. The rate of SPAAC was investigated in methanol, PBS, pH 1.0 and pH 10.0 solutions to determine the extent of the effect solvents have on the reaction. Then we looked into the stability of the cyclooctynes to hydrolysis and glutathione. We envisioned that studying ODIBO, DIBO, ADIBO, and BCN would be most beneficial because of their abundance in the literature (Figure 3.01).

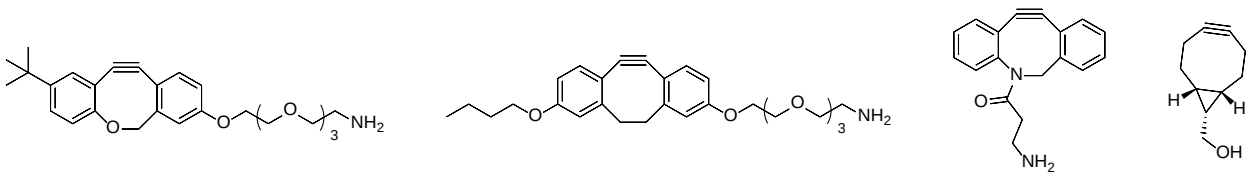

3.01 **3.02** **3.03** **3.04**

Figure 3.01 Cyclooctynes used for SPAAC Kinetics Study.

3.02 Synthesis of the Various Cyclooctynes

We set out to synthesize derivatives of ODIBO and DIBO that would drastically increase their solubility (Scheme 3.01). The first step is tosylation of tetraethylene glycol with triethylamine in dichloromethane to afford monotosyl tetra(ethylene glycol) **3.05**. Next, S_{N2} displacement of the tosyl group with sodium azide, in acetonitrile, under reflux, afforded azido-tetra(ethylene glycol) **3.06**. Reduction of the azide using a Staudinger reaction with triphenylphosphine and water in THF afforded amino-tetra(ethylene glycol) **3.07**. The final step was protection of the amino group with trifluoroacetic anhydride and triethylamine in methanol to afford acetamide-PEG-OH **3.08**.

Scheme 3.01 Synthesis of Acetamide-PEG-OH **3.08**

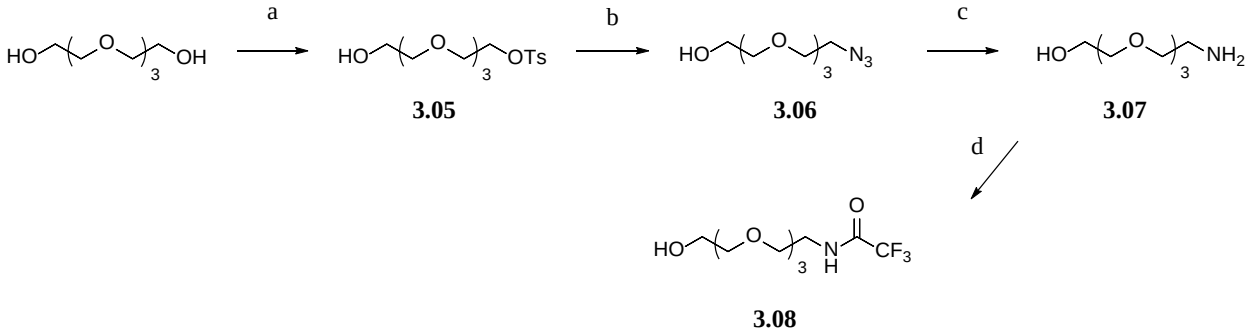

3.05 **3.06** **3.07** **3.08**

Reagents and Conditions: a) p-TsCl, Et_3N, CH_2Cl_2, 42 %; b) NaN_3, 85 °C, CH_3CN, 74 %; c) PPh_3, H_2O, THF, 68 %; d) TFAA, Et_3N MeOH, 87 %.

ODIBO-PEG-NH_2 **3.01** was synthesized by a Mitsunobu reaction with ODIBO-OH **3.09** and acetamide-PEG-OH **3.08**. Unfortunately, ODIBO-PEG-acetamide **3.10** could not be fully

purified from triphenylphosphine oxide but upon deprotection of the trifluoroacetamide with K_2CO_3, water, and methanol isolation of ODIBO-PEG-NH_2 **3.01** was achieved. We have previously reported the synthesis of DIBO-OH[6-7] **3.11** and using a Mitsunobu reaction with acetmide-PEG-OH **3.08** synthesized DIBO-PEG-acetamide **3.12**. Then deprotection of the DIBO-PEG-acetamide **3.12** with K_2CO_3, water, and methanol afforded DIBO-PEG-NH_2 **3.02**. ADIBO and BCN have previously been reported to have sufficient aqueous solubility and no derivatization for improved water solubility was needed.[1, 8]

Scheme 3.02 Synthesis of ODIBO-PEG-NH_2 **3.01**

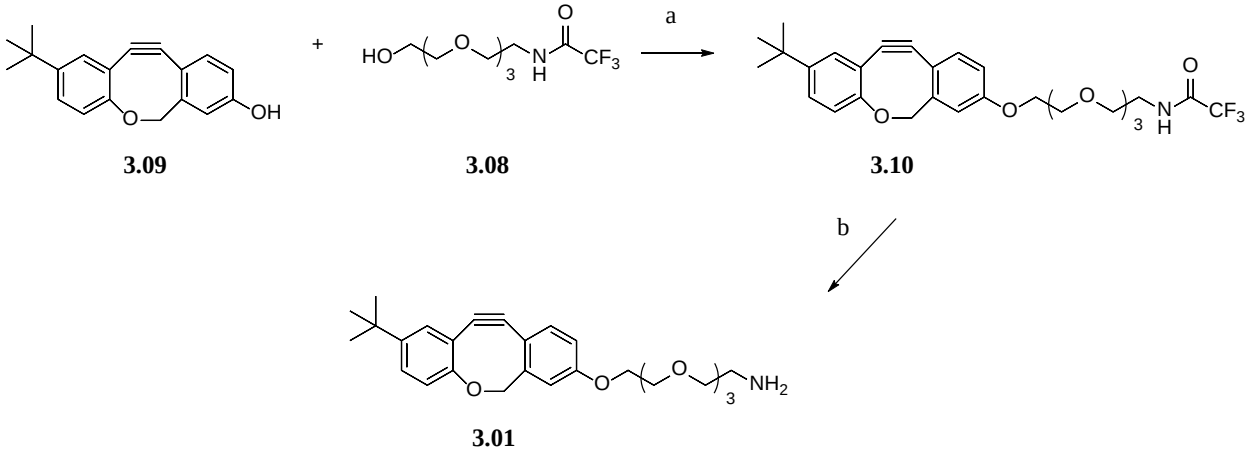

3.09 **3.08** **3.10**

3.01

Reagents and Conditions: a) DIAD, PPh_3, THF; b) K_2CO_3, H_2O, MeOH, 63 %.

Scheme 3.03 Synthesis of DIBO-PEG-NH_2

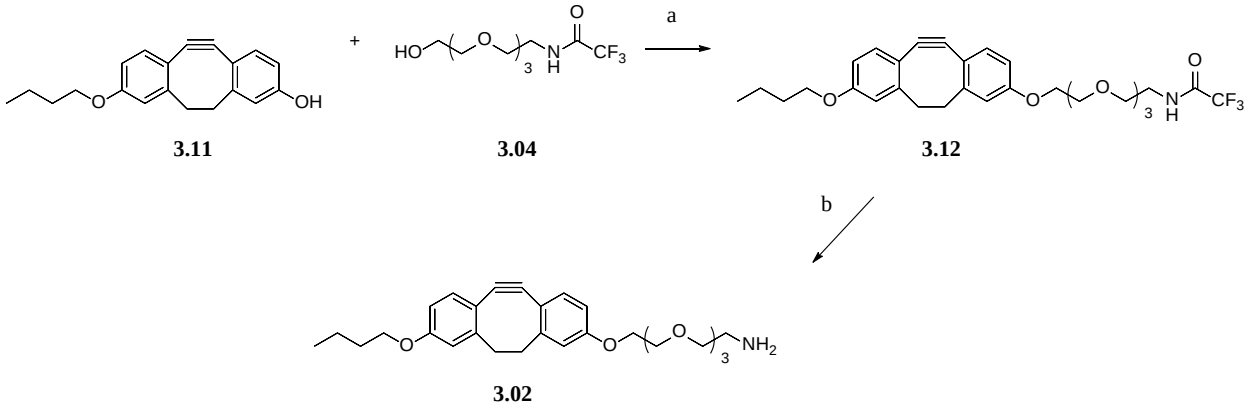

3.11 **3.04** **3.12**

3.02

Reagents and Conditions: a) DIAD, PPh_3, THF, 52 %; b) K_2CO_3, H_2O, MeOH, 82 %.

In order to understand the more than two orders difference in SPAAC reactivity between ODIBO and DIBO, we decided to obtain crystal structures of these compounds. The derivatives that we have studied so far are mostly oily compounds. To enhance crystal formation we prepared 4-iodobenzoyl derivatives of the cyclooctynes (ODIBO-IBA **3.13** and DIBO-IBA **3.14**.) by Steglich esterification of ODIBO-OH **3.09** and DIBO-OH **3.11** with 4-iodobenzoic acid (Scheme 3.04). We were successful in growing crystals of ODIBO-IBA **3.13** (Figure 3.02) and determined that ODIBO had bond angles of 152.6 (C(11)-C(1)-C(2)) and 151.3 ° (C(1)-C(2)-C(3)). Interestingly, BARAC which is half as reactive as ODIBO has symmetrical bond angles of 153 °.[9] This slight change in bond angle further confirms that bond distortion angle is directly responsible for the difference in reactivity.

Scheme 3.04 Synthesis of ODIBO-IBA **3.13** and DIBO-IBA **3.14**

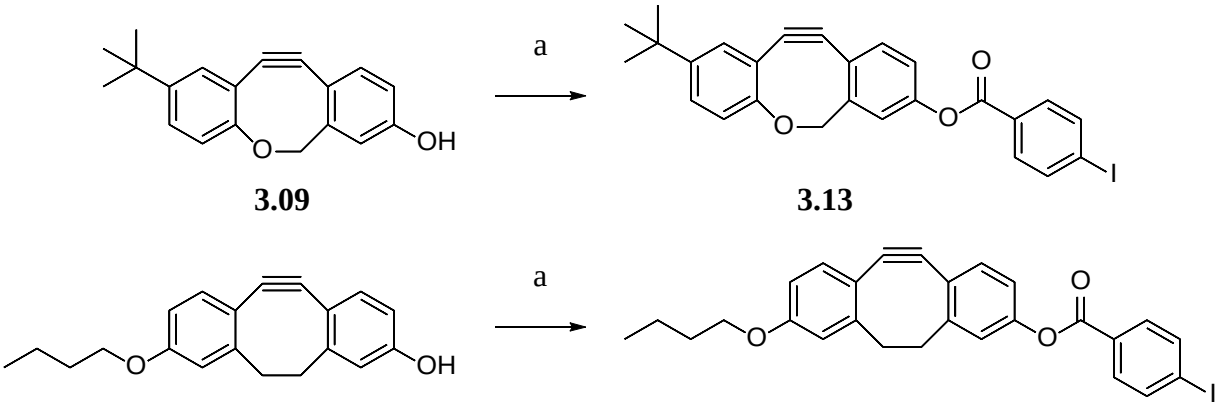

3.09 **3.13**

3.11 **3.14**

Reagents and Conditions: a) 4-iodobenoic acid, DCC, DMAP, CH_2Cl_2, (**3.13**, 56 %), (**3.14**, 56 %).

One piece of information not explained by the bond angles is the stability difference between ODIBO and BARAC. It is intuitive to think the more reactive ODIBO would be less

stable than BARAC. Interestingly, ODIBO is significantly more stable than BARAC. After the preparation of BARAC it must be stored from oxygen, light and at -78 °C or rapid decomposition will occur.[10] In our lab we have experienced that BARAC is not stable for storage in solution even at 0 °C for an extended period of time. Meanwhile ODIBO in crystal form is bench stable and when dissolved can be kept in solution at 0 °C for over a year. This leads us to believe other factors contribute to the uniqueness of ODIBO that go beyond the distortion of the alkyne bond angle. We hope in collaboration with Dr. Wheeler at Texas A&M University to further understand the unique combination of reactivity and stability with ODIBO.

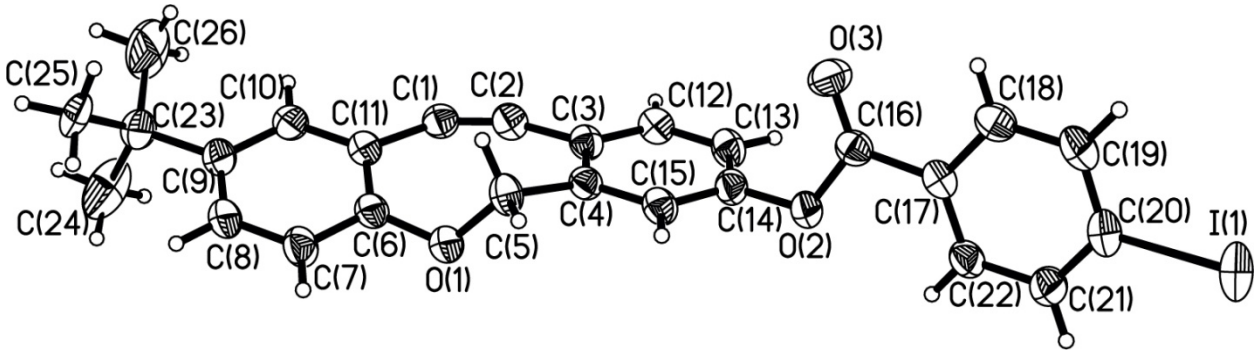

Figure 3.02 ORTEP of ODIBO-IBA **3.13**. The C(11)-C(1)-C(2) bond angel is 152.6 ° and the C(1)-C(2)-C(3) bond angle is 151.3 °.

Unfortunately, we were unable to grow usable crystals of DIBO-IBA **3.14**. A different derivative was synthesized which we hoped would allow us to elucidate the crystal structure. We again used a Steglich esterification with DIBO-OH **3.11** and 2-chloro-4-nitrobenzoic acid to afford DIBO-CNBA **3.15**. After months of growing crystals of both DIBO-IBA **3.14** and DIBO-CNBA **3.15** no crystals have been isolated.

Scheme 3.05 Synthesis of DIBO-CNBA **3.15**

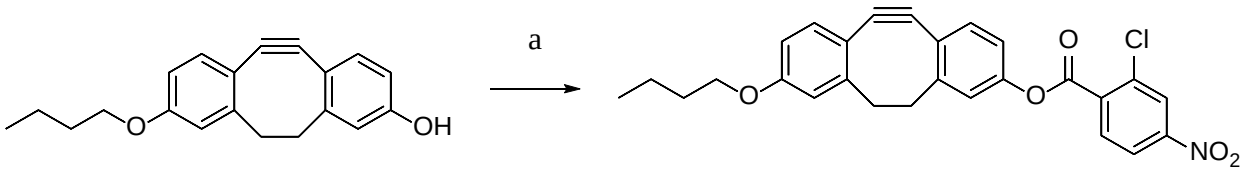

3.11 **3.15**

Reagents and Conditions: a) 2-chloro-4-nitrobenzoic acid, DMAP, DCC, CH_2Cl_2, 79 %.

3.03 Rate Comparison of Cyclooctynes with Azides

We then set out to explore the reactivity of each cyclooctyne in a variety of conditions (Table 3.01). UV spectroscopy was used to determine the reaction kinetics by following the decay of the characteristic alkyne peak under pseudo-first order conditions. The experimental data fits the single exponential equation well, and linear dependence of the pseudo-first order rate constants on azide concentration were analyzed by the least square method to obtain biomolecular rate constants. In the case of BCN **3.04** the formation of triazole was followed. Benzyl azide was chosen because it is the azide standard for SPAAC reactivity determination. Interestingly BCN **3.04** has a second order rate constant that is nearly identical to that of DIBO **3.02**. It has been widely reported that BCN **3.04** is faster than DIBO **3.02** but neither cyclooctyne has been directly compared.[1, 11] Next, the water soluble TEG-N_3 was used and the rate of SPAAC in methanol was determined. These rates were very similar to that of benzyl azide which would be expected. Finally, the rate of SPAAC in PBS buffer was determined. Here, significant rate enhancement of SPAAC for all the cyclooctynes was observed. DIBO **3.02** shows the largest increase in reactivity with a rate of 0.407 ± 0.008 $M^{-1}s^{-1}$ which is 6.7 times

faster in PBS than in methanol. ADIBO **3.03** shows the least amount of change with only a 3.5 times increase in reactivity.

Table 3.01 Rate of SPAAC with Various Cyclooctynes

Cyclooctyne	TEG-N_3 ($M^{-1}s^{-1}$)[a]	TEG-N_3 ($M^{-1}s^{-1}$)[b]	Benzyl Azide ($M^{-1}s^{-1}$)[b]
ODIBO **3.01**	7.89 ± 0.26	1.43 ± 0.04	1.74 ± 0.04
DIBO **3.02**	0.407 ± 0.008	0.061 ± 0.002	0.056 ± 0.003
ADIBO **3.03**	1.30 ± 0.04	0.36 ± 0.01	0.29 ± 0.01
BCN **3.04**	0.28 ± 0.01	0.05 ± 0.004	0.059 ± 0.003

[a] PBS, 5% MeOH; [b] MeOH

Investigation of the reactivity of the cyclooctynes at pH 1.0 and pH 10.0 was also conducted (Table 3.02). Interestingly, in acidic conditions the reactivity of the cyclooctynes is reduced. BCN **3.04** showed the biggest reduction with a rate of 0.90 ± 0.02 $M^{-1}s^{-1}$ which is 1.66 times slower than in PBS. Unfortunately, only DIBO **3.02** has been studied at pH 10.0. The effect looks to be virtually the same as pH 1.0. This would suggest that biological pH is ideal for SPAAC and that potentially higher or lower pH can cause negative changes in the rate of SPAAC. Similar findings have been reported for ADIBO recently where the rate of SPAAC was reduced when ADIBO was used in Tris (pH 8.0) and Mes (pH 6.5) buffer.[12] Our goal is to finish these experiments at pH 10.0 as soon as possible to fully determine the effects of pH on the rate of SPAAC.

Table 3.02 Rate of SPAAC with TEG-N_3 at various pH

Cyclooctyne	pH 1.0 ($M^{-1}s^{-1}$)[a]	pH 10.0 ($M^{-1}s^{-1}$)[a]
ODIBO **3.01**	7.4 ± 0.3	Incomplete
DIBO **3.02**	0.311 ± 0.005	0.309 ± 0.006
ADIBO **3.03**	0.90 ± 0.02	Incomplete
BCN **3.04**	0.169 ± 0.007	Incomplete

[a] HCl, Water, 5 % MeOH; [b] Carbonate Buffer, 5 % MeOH

3.04 Reactivity of Cyclooctynes with NaN_3

Recently we have learned that cyclooctynes are reactive with sodium azide. We were intrigued by this and set out to study the rate of SPAAC and the effects of pH on the reactivity. The first goal was to prove the reaction with sodium azide and DIBO-IBA **3.14** would form a triazole (Scheme 3.06). Interestingly there was only one triazole isolated. We believe that upon formation of the triazole isomerization to the 2H product occurs because of the isolation of one triazole product. Further NMR experiments will be needed to determine the structure of the ODIBO traizole. We also characterized that a triazole formed with ADIBO and BCN by HRMS.

Scheme 3.06 Synthesis of DIBO-IBA triazole **3.16**

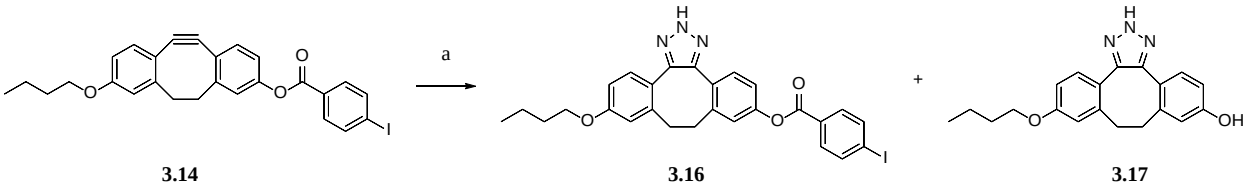

3.14 **3.16** **3.17**

Reagents and Conditions: a) NaN_3, methanol:water (1:1), 79 % **3.16**, 19 % **3.17**.

The hypothesis of the 2*H*-triazole formation was further reinforced by the fact that one triazole isomer is formed when reacting ODIBO with sodium azide. We synthesized ODIBO-PEG-OH **3.22** as our soluble cyclooctyne derivative (Scheme 3.07). ODIBO-PEG-OH was synthesized by taking photo-ODIBO **3.18** and alkylating with linker **3.19** in a Williamson ether reaction to afford photo-ODIBO-TEG-TBS **3.20**. Next, we removed the silyl protecting group by reaction with HF in acetonitrile to afford photo-ODIBO-PEG-OH **3.21**. Finally, irradiation of the cyclopropenone at 350 nm in methanol afforded ODIBO-PEG-OH **3.22**. We then reacted ODIBO-PEG-OH **3.22** and sodium azide to isolate triazole product **3.23**. Another, minor product was isolated as well and this was from nucleophilic attack of methanol. We have previously shown that ODIBO is stable in water and methanol (*vide supra*) but when in the presence of sodium azide a byproduct forms. Unfortunately, we have been unable to determine why this occurs.

Scheme 3.07 Synthesis of ODIBO-PEG-OH triazole **3.23**

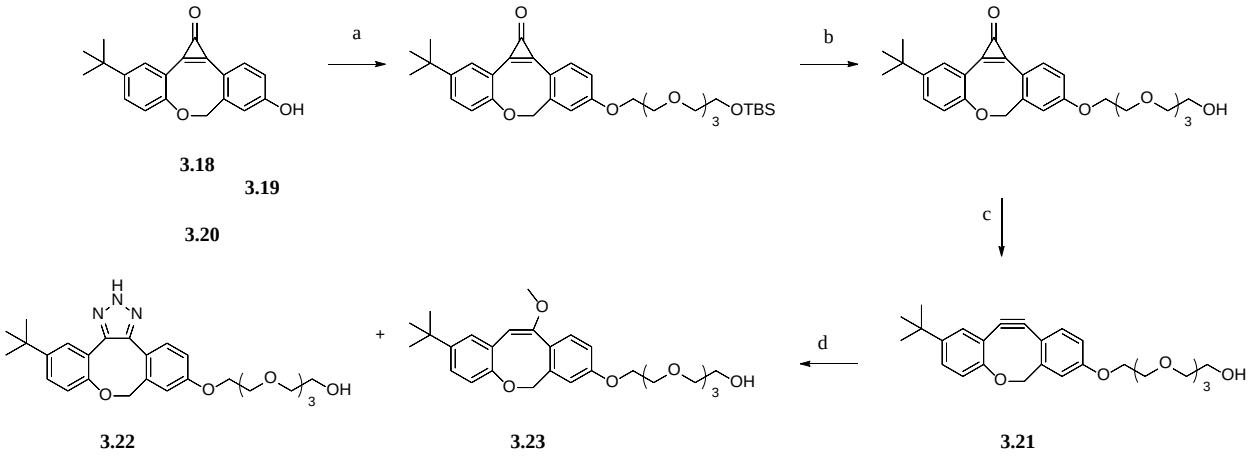

Reagents and Conditions: a) TBDMS protected monotosyl tetra(ethyleneglycol), K_2CO_3, DMF, 58 %; b) HF, CH_3CN, 85 %; c) 350 nm, MeOH, 85 %; d) NaN_3, methanol:water (1:1), 53.4 % **3.22**, 20 % **3.23**.

The rates of SPAAC with sodium azide were then investigated with the various cyclooctynes (Table 3.03). We decided to measure the rates of the reaction of cyclooctynes with azide ion (at pH=7.4) and hydrazoic acid (at pH = 1). The rate of SPAAC for ODIBO **3.01** and ADIBO **3.03** with sodium azide was slightly faster than with TEG-N_3 at pH 7.4. ODIBO **3.01** reacted with sodium azide at 9.0 ± 0.2 $M^{-1}s^{-1}$ and ADIBO **3.03** 1.95 ± 0.03 $M^{-1}s^{-1}$. Interestingly, DIBO **3.02** reacted slower with sodium azide compared to TEG-N_3 with a rate of 0.0198 ± 0.0007 $M^{-1}s^{-1}$. When the pH is lowered to shift the equilibrium towards hydrazoic acid the rate of SPAAC lowers significantly for ODIBO **3.01** and ADIBO **3.03**. Again, DIBO is the outlier and has a rate of 0.074 ± 0.002 $M^{-1}S^{-1}$ which is 3.4 times greater than at pH 7.4. We are still investigating the potential reason for this but it may have to do with sodium azide catalyzing nucleophilic attack of water at pH 7.4. This would lead to observation of a rate that is a

combination of SPAAC and nucleophilic attack. When synthesizing the DIBO triazole **3.16** there was no byproduct isolated like ODIBO vinyl methyl ether **3.23**. The change to the more acidic pH could potentially quench this reaction allowing only SPAAC to be observed for ODIBO **3.01** and ADIBO **3.03**. We will know more information once we finish the reaction kinetics for BCN **3.04**. Its reactivity is very similar to DIBO **3.02** should follow the same trends. We will also have to run HPLC to see if there are multiple products being formed and if so try and determine if sodium azide is catalyzing the nucleophilic attack of water.

Table 3.03 Rate of SPAAC with Sodium Azide at Various pH

Cyclooctyne	pH 1.0[a]	pH 7.4[b]
ODIBO **3.01**	1.68 ± 0.03	9 ± 0.2
DIBO **3.02**	0.074 ± 0.002	0.0198 ± 0.0007
ADIBO **3.03**	0.299 ± 0.004	1.95 ± 0.03
BCN **3.04**	Incomplete	Incomplete

[a] HCl, Water, 5 % MeOH; [b] PBS,5 % MeOH

3.05 Stability of Cyclooctynes to Hydrolysis and Glutathione

The stability of the cycloctynes to hydrolysis were examined to determine if they could be used for experiments that require elevated temperatures (Table 3.04). It was expected that the cyclooctynes of higher SPAAC reactivity would undergo faster hydrolysis. When monitoring the cycloocytnes at 75 °C the decay of the alkyne bond could be observed by UV. ODIBO **3.01** which is the most reactive cyclooctyne had a rate of 1.02×10^{-3} s^{-1}. Interestingly, ADIBO **3.03** was unusually stable to hydrolysis even though it is more reactive towards azides than DIBO **3.02**. Even after heating 24 hours there was no detectable decomposition. When ADIBO **3.03**

was mixed with TEG-N_3 after 24 hours SPAAC was observed by following the decay of the alkyne peak at 309 nm. Unfortunately, we have not completed the experiments with BCN. Next, the reactivity of each cyclooctyne towards glutathione was determined (Table 3.04). Again, it was expected that the more reactive cyclooctyne would have a higher rate. ODIBO **3.01** the most reactive cyclooctyne studied, displayed the fastest rate of 4.15×10^{-4} s^{-1} when reacted with 10 mM of glutathione. The least reactive DIBO **3.02** had displayed a rate of 1.84×10^{-5} under the same conditions. The trend so far is holding true, but the experiments for BCN still must be completed.

Table 3.04 Stability of Various Cyclooctynes

Cyclooctyne	Glutathione 10 mM (s^{-1})[a]	75 ° C (s^{-1})[a]
ODIBO **3.01**	4.15×10^{-4}	1.02×10^{-3}
DIBO **3.02**	1.84×10^{-5}	1.54×10^{-4}
ADIBO **3.03**	1.81×10^{-4}	Stable
BCN **3.04**	Incomplete	Incomplete

[a] PBS, 5% MeOH

3.06 Conclusion

We have successfully determined the rates and stabilities of the most commonly used cyclooctynes in the literature under identical conditions. ODIBO is the fastest of the four cyclooctynes with a rate of 7.89 ± 0.26 $M^{-1}s^{-1}$ with TEG-N_3 in PBS. ADIBO is the most robust of the cyclooctynes studied with exceptional reactivity and stability. This study will allow other researchers to successfully identify which cyclooctyne provides the best properties for their experiment. The data is not fully complete and we will continue to finish the last few

experiments needed for the project. We also hope to include computational support to the experimental data we have collected. Future plans for the project involve testing the reactivity of the cyclooctynes with cyclic nitrones. SPANC has become another powerful tool because of the extremely fast reaction kinetics. There have been no extensive studies into how different cyclooctynes compare in their reactivity of SPANC.

3.07 Experimental Section

All organic solvents were dried and freshly distilled before use; Tetrahydrofuran was distilled from sodium/benzophenone ketyl. Other reagents were obtained from Aldrich or VWR and used as received unless noted. ADIBO and BCN were made using previously reported procedures. Flash chromatography was performed using 40-63 μm silica gel. All NMR spectra were recorded in $CDCl_3$ (unless otherwise noted) using 400 MHz instrument. Absorption spectra were recorded on CARY 300 Bio UV-Visible spectrometer. Photolyses were conducted in the Rayonet photoreactor equipped with 12 X 4 W 350 nm fluorescent lamps.

Kinetics

Rate measurements in organic solvent were performed using Carry-300 Bio UV-Vis spectrometer. The temperature was set to 25.0°C and controlled to 0.1 °C accuracy. Reactions of all cyclocotynes with excess of azide were monitored by following the decay of their characteristic alkyne absorbance. The experimental data fits the single exponential equation well. Linear dependence of the observed pseudo-first order rate constants on azide concentration was analyzed by the least squares method to obtain the bimolecular rate constants.

p-Toluenesulfonic Acid 2-(2-(2-(2-Hydroxyethoxy)ethoxy)ethoxy)ethyl Ester (monotosyl tetra(ethylene glycol), 3.05).[13]

Tetra(ethylene glycol) (20.25 g, 104 mmol) was added to a solution of triethylamine (15.83 g, 156 mmol), p-toluenesulfonyl chloride (22.00 g, 115 mmol), in dichloromethane (200 mL), at 0 °C. The reaction was then stirred for 2 hours at 0 °C, and left overnight at room temperature under inert atmosphere. The precipitate was filtered and the reaction mixture was concentrated in vacuo and purified flash chromatography (hexanes: ethyl acetate 1:4) to provide monotosyl tetra(ethylene glycol) **3.05** (15.28 g, 42%) as a colorless oil. ^{1}H-NMR: 7.79-7.81 (d, J = 8 Hz, 2H), 7.33-3.35 (d, J = 4 Hz, 2H), 4.15-4.18 (t, 2H), 3.59-3.73 (m, 14H), 2.45 (s, 3H). ^{13}C-NMR: 144.80, 132.83, 129.79, 127.84, 72.43, 70.56, 70.50, 70.31, 70.18, 69.27, 68.54, 61.50, 21.53.

2-(2-(2-(2-Azidoethoxy)ethoxy)ethoxy)ethanol (azido-tetra(ethylene glycol), 3.06).[13]

A solution of monotosyl tetra(ethylene glycol) **3.05** (15.285 g, 43.9 mmol) and sodium azide (4.28 g, 65.8 mmol) in acetonitrile (150 mL), was refluxed overnight. After cooling to room temperature, the reaction mixture was concentrated in vacuo and purified via flash chromatography (ethyl acetate) to provide azido-tetra(ethylene glycol) **3.06** (7.09 g, 74%) as a colorless oil. ^{1}H-NMR: 3.60-3.74 (m, 14 H), 3.38-3.41 (t, 2H), 2.55-2.58 (t, 1H). ^{13}C: 72.59, 70.76, 70.72, 70.65, 70.40, 70.11, 61.75, 50.72.

2-(2-(2-(2-Aminoethoxy)ethoxy)ethoxy)ethanol (amino-tetra(ethylene glycol), 3.07).[13]

Triphenylphosphine (9.61 g, 36.7 mmol) was added to a mixture of azido-tetra(ethylene glycol) **3.06** (5.74 g, 26.2 mmol) in THF (53 mL). Once a homogenous solution had been obtained, deionized water (0.660 g, 36.7 mmol) was added, and the contents were stirred at room temperature, open to air, overnight. Next, the reaction mixture was concentrated in vacuo and purified via flash chromatography (chloroform: methanol 1:1) to provide amino-tetra(ethylene

glycol) **3.07** (3.46 g, 68%) as a colorless oil. ^{1}H-NMR: 3.48-3.73 (m, 14H), 2.85-2.87 (t, 2H). ^{13}C-NMR: 73.12, 72.97, 70.54, 70.43, 70.23, 70.07, 61.23, 41.45.

2,2,2-trifluoro-N-(2-(2-(2-(2-hydroxyethoxy)ethoxy)ethoxy)ethyl)acetamide (Acetamide-Peg-OH, 3.08).[13]

Trifluoracetic anhydride (5.26 g, 25.07 mmol) was added dropwise to a reaction mixture of tetraethylene glycol amine **3.07** (3.46 g, 17.91 mmol), triethyl amine (4.53 g, 44.8 mmol), in methanol (35 mL), at 0 °C. The reaction mixture was warmed to room temperature and stirred overnight. The solution was then concentrated in vacuo and purified via flash chromatography (ethyl acetate) to provide acetamide-PEG-OH **3.08** (4.52 g, 87%) as a colorless oil. ^{1}H-NMR: 8.78 (bs, 1H), 3.55-3.71 (m, 16H). ^{13}C-NMR: 157.82 (q, J= 37 Hz), 116.26 (q, J= 286 Hz), 72.61, 70.82, 70.49, 70.18, 69.86, 69.66, 61.40, 39.99.

2-tert-butyl-11,12-didehydro-8-(2-(2-(2-(2-aminoethoxy)ethoxy)ethoxy)ethoxy)-6H-dibenzo[b,f]oxocine (ODIBO-PEG-NH_2, 3.01).

DIAD (1.06 g, 5.23 mmol) was added to a solution of ODIBO-OH **3.09** (1.46 g, 5.23 mmol), acetamide-PEG-OH (1.51 g, 5.23 mmol), and PPH_3 (1.65 g, 6.28 mmol) in THF (50 mL), at 0 °C. The reaction mixture was stirred for 5 minutes at 0 °C and warmed to room temperature. After warming, the reaction was stirred for 30 minutes, concentrated in vacuo, and purified via flash chromatography (CH_2Cl_2: methanol, 40:1) to afford crude product (3.45 g). The crude product (3.45 g) was then dissolved into a solution of methanol (24 mL) and K_2CO_3 (0.722 g, 5.22 mmol) in water (11.60 mL). The solution was then stirred overnight and concentrated in vacuo. The residue was re-dissolved into CH_2Cl_2 (300 mL), washed with water (75 mL), and then brine (75 mL). The organic layer was then dried over $MgSO_4$, filtered, concentrated in vacuo, and purified via flash chromatography (CH_2Cl_2: methanol 40:1 to 10:1) to afford ODIBO-

PEG-NH_2 (1.50 g, 63 % over 2 steps) as a yellow oil. ^{1}H-NMR: 7.20-7.25 (m,3H), 7.09-7.11 (d, J = 9.2 Hz, 1H), 7.03 (d, J = 2.2 Hz, 1H), 6.89-6.92 (dd, J = 8.4, 2.3 Hz, 1H), 5.16-5.19 (d, J = 12 Hz, 1H), 4.51-4.54 (d, J = 12 Hz, 1H), 4.15-4.17 (t, J = 4.7 Hz, 2H), 3.85-3.88 (t, J = 4.7 Hz, 2H), 3.72-3.73 (m, 2H), 3.62-3.69 (m, 6H), 3.51-3.54 (t, J = 5.0 Hz, 2H), 2.88-2.90 (t, J = 5.1 Hz, 2H), 1.31 (s, 9H). ^{13}C-NMR: 167.31, 158.71, 149.13, 146.95, 126.89, 125.57, 123.69, 121.37, 118.37, 117.89, 117.65, 114.65, 114.17, 110.75, 78.02, 72.47, 70.98, 70.75, 70.38, 69.78, 67.93, 41.59, 34.55, 31.56. ESI HRMS: calcd. ($M+H^+$): $C_{27}H_{36}NO_5$ 454.2588, found 454.2572.

2-((2,2,2,-trifluoro-N-(2-(2-(2-(2-(9-butoxy-5,6-didehydro-11,12-dihydrodibenzo[a,e]-[8]annulen-2-yl)oxy)ethoxy)ethoxy)ethoxy)ethyl acetamide (DIBO-PEG-Acetamide, 3.12).

Tributylphosphine (0.305 g, 1.433 mmol, 2 mL THF) was added to a solution of DIBO-OH **3.11** (0.381, 1.303 mmol), acetamide-PEG-OH **3.08** (0.415 g, 1.433 mmol), and 1,1'-(Azodicarbonyl)dipiperidine (ADDP) (0.395 g, 1.564 mmol), in THF (10 mL), at room temperature. The reaction mixture was stirred overnight, concentrated in vacuo, and purified via flash chromatography (dichloromethane: methanol 40:1) to afford DIBO-PEG-Acedatmide **3.12** (0.379 g, 52 %) as a yellow oil. ^{1}H-NMR: 7.59 (s, 1H), 7.18-7.20 (d, J = 8 Hz, 2H), 6.88 (s, 2H), 6.75-6.77 (d, J = 8 Hz, 2H), 4.12-4.14 (m, 2H), 3.95-3.99 (t, 2H), 3.83-3.85 (m, 2H), 3.61-3.74 (m, 10H), 3.51-3.55 (m, 2H), 3.15-3.20 (m, 2H), 2.38-2.47 (m, 2H), 1.74-1.81 (m, 2H), 1.45-1.52 (m, 2H), 0.96-1.00 (t, 3H). ^{13}C-NMR: 158.88, 158.24, 157.46 (q, J= 37 Hz), 155.02, 126.81, 126.77, 116.91, 116.85, 116.81, 116.11 (q, J= 286 Hz), 116.01, 112.02, 112.01, 110.82, 110.31, 70.92, 70.72, 70.67, 70.39, 69.83, 68.90, 67.93, 67.63, 39.92, 36.79, 36.77, 31.45, 19.39, 13.99. ESI HRMS: calcd. ($M+H^+$): $C_{30}H_{37}F_3NO_6$ 564.2567, found 564.2550.

2-(2-(2-(2-(2-(9-butoxy-5,6-didehydro-11,12-dihydrodibenzo[a,e]-[8]annulen-2-yl)oxy)ethoxy)ethoxy)ethoxy)ethyl amine (DIBO-PEG-NH_2, 3.02).

A solution of potassium carbonate (0.093 g, 0.672) in water (1.50 mL), was added to a solution of DIBO-PEG-Acetamide **3.12** (0.379 g, 0.672 mmol) in methanol (3.00 mL) at room temperature. The reaction mixture was stirred overnight, concentrated in vacuo, and the residue was then re-dissolved in dichloromethane/ethyl acetate (1:4). The organic layer was then washed with water, brine, dried over Na_2SO_4, concentrated in vacuo, and purified via flash chromatography (dichloromethane: methanol 10:1 to 10:3) to afford DIBO-PEG-NH_2 **3.02** (0.259 g, 82%) as a yellow oil. ^{1}H-NMR: 7.18-7.20 (d, J = 8 Hz, 2H), 6.87-6.91 (dd, J= 12 Hz & 4 Hz, 2H), 6.74-6.79 (m, 2H), 4.74 (s, 2H), 4.13-4.16 (t, 2H), 3.96-3.99 (t, 2H), 3.84-3.86 (t, 2H), 3.58-3.74 (m, 10H), 3.15-3.20 (m, 2H), 2.96-2.98 (t, 2H), 2.38-2.47 (m, 2H), 1.74-1.81 (m, 2H), 1.55-1.45 (m, 2H), 1.00-0.96 (t, 2H). ^{13}C-NMR: 158.93, 158.28, 155.11, 155.08, 126.68, 116.99, 116.91, 116.08, 112.25, 112.06, 110.88, 110.36, 70.84, 70.66, 70.62 70.55, 70.36, 69.84, 68.00, 67.81, 40.92, 36.83, 31.51, 19.44, 14.03. ESI HRMS: calcd. ($M+H^+$): $C_{28}H_{38}NO_5$ 468.2744, found 468.2727.

2-tert-butyl-11,12-didehydro-6H-dibenzo[b,f]oxocin-8-yl 4-iodobenzoate (ODIBO-IBA, 3.13).

ODIBO-OH **3.09** (0.465 g, 1.67 mmol) was added to a solution of DCC (0.345 g, 1.67 mmol), 4-iodobenzoic acid (0.414 g, 1.67 mmol), and DMAP (cat.) in CH_2Cl_2 (17 mL). The reaction was stirred overnight, filtered, concentrated in vcauo, and purified via flash chromatography (2:1 hexanes: ethyl acetate) to afford ODIBO-IBA **3.13** (0.480 g, 56%) of a white powder (175 °C decomp.). ^{1}H-NMR: 7.89 (s, 4H), 7.34-7.36 (d, J = 8.2 Hz, 1H), 7.23-7.29 (m, 4H), 7.11-7.13 (d, J = 8.2 Hz, 1H), 5.23-5.26 (d, J = 12.2 Hz, 1H), 4.54-4.57 (d, J = 12.1 Hz, 1H), 1.32 (s, 9H).

^{13}C-NMR: 167.78, 164.73, 150.20, 148.96, 147.18, 138.28, 131.76, 128.93, 126.77, 126.23, 124.47, 124.05, 124.00, 122.42, 121.58, 117.13, 113.17, 112.67, 102.09, 77.65, 34.63, 31.60. ESI HRMS: calcd. ($M+H^+$): $C_{26}H_{22}IO_3^+$ 509.0608, found 509.0607.

9-butoxy-5,6-didehydro-11,12-dihydrodibenzo[a,e]-[8]annulen-2-yl 4-iodobenzoate (DIBO-IBA, 3.14).

DIBO-OH[6-7] (0.418 g, 1.43 mmol) was added to a solution of DCC (0.295 g, 1.43 mol), 4-iodobenzoic acid (0.355 g, 1.43 mmol), and DMAP (cat.) in CH_2Cl_2 (15 mL). The reaction was stirred overnight, filtered, concentrated in vcauo, and purified via flash chromatography (2:1 hexanes: ethyl acetate) to afford DIBO-IBA **3.14** (0.417 g, 56 %) of a white powder (154-155 °C MP). ^{1}H-NMR: 7.94 (s, 4H), 7.36-7.38 (d, J= 8.2 Hz, 1H), 7.29-7.30 (d, J = 4.7 Hz, 1H), 7.21 (s, 1H), 7.12-7.15 (dd, J = 8.2, 2.4 Hz, 1H), 6.94 (d, J = 2.7 Hz, 1H), 6.81-6.84 (dd, J = 8.4, 2.6 Hz, 1H), 4.01-4.04 (t, J = 6.4 Hz, 2H), 3.23-3.33 (m, 2H), 2.50-2.53 (d, J = 11.3 Hz, 2H), 1.79-1.86 (m, 2H), 1.50-1.59 (m, 2H), 1.01-1.05 (t, J = 7.3 Hz, 3H). ^{13}C-NMR: 164.93, 159.32, 155.45, 154.73, 149.90, 138.23, 131.73, 129.13, 127.25, 126.70, 123.08, 122.61, 119.80, 116.97, 115.51, 112.50, 112.23, 109.56, 101.93, 68.04, 36.71, 36.67, 31.51, 19.46, 14.06. ESI HRMS: calcd. ($M+H^+$): $C_{27}H_{24}IO_3^+$ 523.0764, found 523.0764.

9-butoxy-5,6-didehydro-11,12-dihydrodibenzo[a,e]-[8]annulen-2-yl 2-chloro-4-nitrobenzoate (DIBO-CNBA, 3.15).

DIBO-OH[6-7] **3.11** (329 g, 1.12 mmol) was added to a solution of DCC (0.232 g, 1.12 mmol), 2-chloro-4-nitrobenzoic acid (0.227 g, 1.12 mmol), and DMAP (cat.) in CH_2Cl_2 (12 mL). The reaction was stirred overnight, filtered, concentrated in vcauo, and purified via flash chromatography (2:1 hexanes: ethyl acetate) to afford DIBO-CNBA **3.15** (0.421 g, 79 %) of a yellow powder (98-101 °C MP). ^{1}H-NMR: 8.39 (s, 1H), 8.23-8.25 (m, 1H), 8.16-8.18 (m, 1H),

7.33-7.35 (d, J = 8.2 Hz, 1H), 7.22-7.25 (m, 2H), 7.15-7.22 (d, J = 8.0 Hz, 1H), 6.90 (s, 1H), 6.77-6.79 (d, J = 8.2 Hz, 1H), 3.97-4.00 (t, J = 6.4 Hz, 2H), 3.19-3.31 (m, 2H), 2.45-2.47 (m, 2H), 1.74-1.81 (m, 2H), 1.46-1.55 (m, 2H), 0.97-1.00 (t, 3H). ^{13}C-NMR: 162.81, 159.37, 155.42, 154.84, 150.01, 149.26, 135.67, 135.14, 132.71, 127.30, 126.79, 126.47, 123.24, 122.68, 121.81, 119.50, 116399, 115.29, 112.87, 112.20, 109.26, 68.01, 36.63, 31.47, 19.44, 14.06. ESI HRMS: calcd. ($M+H^+$): $C_{27}H_{23}ClNO_5^+$ 476.1259, found 476.1252.

DIBO-IBA Triazole and DIBO-OH Triazole (3.16 and 3.17).

Sodium azide (0.012 g, 0.19 mmol) was added to an aqueous methanol solution (1:1) of DIBO-IBA (0.1 g, 0.19 mmol). The reaction was stirred overnight, concentrated in vacuo, and purified via flash chromatography to afford a single isomer of DIBO-IBA triazole (0.086 g, 79%) as a white powder (155 °C decomp.) and the hydrolyzed triazole phenol (0.012 g, 19%) as a colorless oil. DIBO-IBA-Triazole **3.16**: ^{1}H-NMR : 7.87 (s, 4H), 7.50-7.52 (d, J = 8.4 Hz, 1H), 7.32-7.34 (d, J = 8.3 Hz, 1H), 7.13-7.14 (d, J = 2.5 Hz, 1H), 7.05-7.08 (dd, 8.4, 2.4 Hz, 1H), 6.75-6.79 (m, 2H), 3.94-3.97 (t, J = 6.5 Hz, 2H), 3.15-3.22 (m, 4H), 1.72-1.79 (m, 2H), 1.44-1.53 (m, 2H), 0.95-0.99 (t, J = 7.4 Hz, 3H). ^{13}C-NMR: 164.82, 159.72, 151.01, 141.36, 140.79, 138.19, 132.19, 132.13, 131.70, 129.07, 123.21, 119.78, 116.19, 112.93, 101.93, 67.86, 34.94, 34.82, 31.48, 19.44, 14.06. ESI HRMS: calcd. ($M+H^+$): $C_{27}H_{25}IN_3O_3^+$ 566.0935, found 566.0933. DIBO-OH Traizole **3.17**: ^{1}H-NMR (DMSO-d_6, 400 MHz): 7.21-7.23 (d, J = 8.6 Hz, 1H), 7.11-7.13 (d, J = 8.5 Hz, 1H), 6.87-6.88 (d, J = 2.5 Hz, 1H), 6.78-6.81 (dd, J = 8.5, 2.6 Hz, 1H), 6.68-6.69 (d, J = 2.4 Hz, 1H), 6.61-6.64 (dd, J = 8.4, 2.5 Hz, 1H), 3.94-3.97 (t, J = 6.4 Hz, 2H), 3.00-3.04 (m, 4H), 1.64-1.71 (m, 2H), 1.37-1.46 (m, 2H), 0.90-0.94 (t, 3H). ^{13}C-NMR (DMSO-d_6, 125 MHz) DIBO-OH-Traizole: 158.60, 157.42, 140.67, 140.54, 131.72, 131.62, 116.39, 115.52,

113.48, 112.52, 67.12, 34.25, 34.17, 30.78, 18.78, 13.74. ESI HRMS: calcd. ($M+H^+$): $C_{20}H_{22}N_3O_2^+$ 366.1706, found 366.1708.

3-(tert-butyl)-9-((2,2,3,3-tetramethyl-4,7,10,13-tetraoxa-3-silapentadecan-15-yl)oxy)dibenzo[b,f]cyclopropa[d]oxocin-1(7H)-one (photo-ODIBO-TEG-TBS, 3.19).

To a solution of photo-ODIBO-OH[14-15] **3.18** (1.10 g, 3.59 mmol) in DMF (20 mL) was added TBDMS protected monotosyl tetra(ethyleneglycol)[16] (2.492 g, 5.39 mmol) . Next, K_2CO_3 (0.496 g, 3.59 mmol) was added and the solution was stirred and heated to 80 °C for 5 hours. The reaction mixture was then diluted with ethyl acetate (200 mL), washed with water (5 x 50 ml), brine (100 mL), and dried over MgSO4. The organic layer was then filtered, concentrated in vacuo, and purified via flash chromatography (3:1 ethyl acetate: hexanes) to afford photo-ODIBO-TBS **3.19** (1.24 g, 58%) of a colorless oil. ^{1}H-NMR: 7.92-7.94 (m, 2H), 7.48-4.51 (dd, J = 8.5, 2.5 Hz, 1H), 7.19-7.21 (d, J = 8.5 Hz, 1H), 7.02-7.06 (m, 2H), 5.24-5.27 (d, J = 12.1 Hz, 1H), 4.76-4.79 (d, J = 12.1 Hz, 1H), 4.21-4.23 (t, J = 4.7 Hz, 2H), 3.88-3.90 (t, J = 4.7 Hz, 2H), 3.72-3.77 (m, 4H), 3.65-3.69 (m, 6H), 3.53-3.56 (t, J = 5.4 Hz, 2H), 1.34 (s, 9H), 0.87 (s, 9H), 0.05 (s, 6H). ^{13}C-NMR: 162.10, 160.50, 152.79, 148.07, 144310, 142.32, 140.73, 135.56, 131.17, 130.75, 122.09, 117.96, 117.48, 117.13, 114.72, 78.83, 72.82, 71.09, 70.89, 70.87, 70.81, 69.60, 68.06, 62.87, 34.71, 31.49, 26.10, 18.53, -5.08. ESI HRMS: calcd. ($M+H^+$): $C_{34}H_{49}O_7Si^+$ 597.3242, found 597.3241. IR: 1846 cm^{-1} ($\nu_{C=O}$).

3-(tert-butyl)-9-(2-(2-(2-(2-(2-(hydroxyethoxy)ethoxy)ethoxy)ethoxy)dibenzo[b,f]cyclopropa[d]oxocin-1(7H)-one (photo-ODIBO-TEG-OH, 3.20).

HF (0.123 g, 3.07 mmol, 50%) was added to a solution of photo-ODIBO-TBS **3.18** (1.220 g, 2.04 mmol) in acetonitrile (11 mL). The solution was stirred for 30 minutes, diluted with ethyl

acetate (300 mL) and water (100 mL). The organic layer was extracted, dried over MgSO4, filtered, concentrated in vacuo, and purified via flash chromatography (40:1 CH_2Cl_2: methanol) to afford photo-ODIBO-TEG-OH **3.20** (0.835 g, 85 %) as a colorless oil. ^{1}H-NMR: 7.92-7.94 (m, 2H), 7.75-7.50 (dd, J = 8.5, 2.5 Hz, 1H), 7.18-7.20 (d, J = 8.4 Hz, 1H), 7.02-7.05 (m, 2H), 5.24-5.27 (d, J = 12.2 Hz, 1H), 4.74-4.77 (d, J = 12.1 Hz, 1H), 4.21-4.23 (t, J = 4.7 Hz, 2H), 3.86-3.89 (t, J = 4.7 Hz, 2H), 3.65-3.73 (m, 10H), 3.58-3.60 (t, J = 5.4 Hz, 2H), 2.91 (s, 1H), 1.33 (s, 9H). ^{13}C-NMR: 162.05, 160.48, 152.81, 148.05, 144.02, 142.23, 140.72, 135.56, 131.14, 130.46, 122.07, 117.91, 117.48, 117.07, 114.72, 78.80, 72.67, 70.98, 70.77, 70.68, 703.41, 69.57, 67.99, 61.81, 34.69, 31.46. $C_{28}H_{35}O_7^+$ 483.2377, found 483.2388. IR: 1846 cm^{-1} ($\nu_{C=O}$).

2-tert-butyl-11,12-didehydro-8-(2-(2-(2-(2-hydroxyethoxy)ethoxy)ethoxy)ethoxy)-6H-dibenzo[b,f]oxocine (ODIBO-TEG-OH, 3.21).

Photo-ODIBO-TEG-OH **3.20** (0.412 g, 0.85 mmol) was dissolved into methanol (400 mL) and irradiated (16x350) for 25 minutes. The reaction mixture was then concentrated and purified via flash chromatography (1:2 to 1:1 acetone: hexanes) to afford ODIBO-TEG-OH **3.21** (0.343 g, 88%) as a colorless oil. ^{1}H-NMR: 7.23-7.28 (m, 3H), 7.11-7.13 (m, 1H), 7.05 (d, J = 2.5 Hz, 1H), 6.91-6.94 (dd, J = 8.4, 2.5 Hz, 1H), 5.18-5.21 (d, J = 12 Hz, 1H), 4.54-4.57 (d, J = 12 Hz, 1H), 4.17-4.19 (t, J = 4.8 Hz, 2H), 3.87-3.90 (t, J = 4.8 Hz, 2H), 3.68-3.77 (m, J= Hz, 12H), 3.61-3.64 (m, 2H), 1.33 (s, 9H). ^{13}C-NMR: 167.32, 158.76, 149.12, 146.98, 126.92, 125.60, 123.74, 121.39, 118.36, 117.92, 117.69, 114.66, 114.21, 110.74, 78.07, 72.66, 71.07, 70.89, 70.82, 70.57, 69.83, 67.89, 61.98, 34.58, 31.59. $C_{27}H_{35}O_6^+$ 455.2428, found 455.2429.

ODIBO Triazole (3.22) and ODIBO Methyl Vinyl Ether (ODIBO-MVE, 3.23).

Sodium azide (0.037 g, 0.57 mmol) was added to an aqueous methanol solution (1:1) of ODIBO-TEG-OH **3.21** (0.260 g, 0.57 mmol). The reaction was stirred overnight, concentrated in vacuo, and purified via flash chromatography to afford a single isomer of ODIBO triazole **3.22** (0.152 g, 53.4%) as a colorless oil and ODIBO-MVW **3.23** (0.057 g, 20%) side product as a colorless oil. ODIBO Triazole **3.22**: ^{1}H-NMR: 7.68 (s, 1H), 7.48-7.50 (d, J = 8.4 Hz, 1H), 7.24-7.27 (dd, J = 8.6 Hz, 2.5 Hz, 1H), 6.94-6.96 (d, J = 8.6 Hz, 1H), 6.85-6.87 (m, 2H), 5.07 (s, 2H), 4.08-4.10 (t, J = 4.8 Hz, 2H), 3.82-3.84 (m, 2H), 3.73-3.77 (m, 6H), 3.71 (s, 4H), 3.61-3.63 (m, 2H), 1.28 (s, 9H). ^{13}C-NMR: 159.17, 153.73, 145.04, 131.17, 131.25, 128.78, 127.32, 120.59, 115.38, 115.21, 72.92, 71.79, 70.86, 70.76, 70.74, 70.41, 69.81, 67.59, 61.81, 34.40, 31.56. ESI HRMS: calcd. ($M+H^+$): $C_{27}H_{36}N_3O_6^+$ 498.2599, found 498.2602. ODIBO-MVE **3.23**: ^{1}H-NMR: 7.49-7.51 (d, J = 8.4 Hz, 1H), 7.42 (s, 1H), 7.38 (d, 2.5 Hz, 1H), 7.28-7.29 (m, 1H), 6.87-6.92 (m, 3H), 4.65 (s, 2H), 4.17-4.20 (t, J = 8.6 Hz, 2H), 3.86-3.89 (m, 2H), 3.66-3.76 (m, 10H), 3.61-3.63 (m, 2H), 3.36 (s, 3H), 1.31 (s, 9H). ^{13}C-NMR Methyl Vinyl Ether: 158.83, 156.22, 142.70, 140.91, 133.27, 127.70, 127.53, 116.48, 115.19, 114.94, 114.10, 109.20, 93.34, 88.65, 74.09, 72.74, 71.02, 70.84, 70.77, 69.81, 67.74, 61.93, 57.48, 34.24, 31.63. ESI HRMS: calcd. ($M+Na^+$): $C_{28}H_{38}NaO_7^+$ 509.2515, found 509.2508.

ADIBO Triazole.

ESI HRMS: calcd. ($M+H^+$): $C_{18}H_{17}N_3O^+$ 320.1506, found 320.1509.

BCN Triaozle.

ESI HRMS: calcd. ($M+H^+$): $C_{10}H_{16}N_3O^+$ 194.1288, found 194.1290.

3.08 X-Ray Crystal Structure of ODBIO-IBA

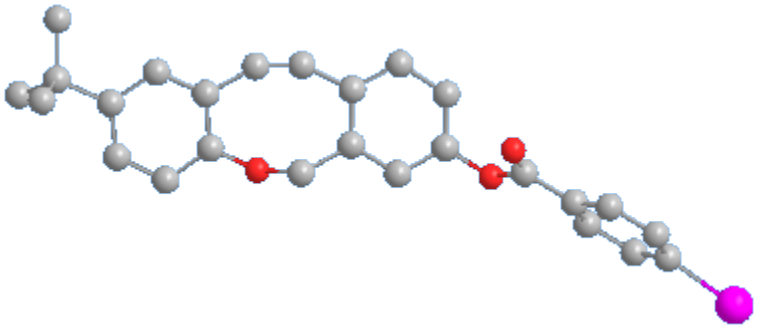

Chemical Formula: $C_{26}H_{21}IO_3$
Formula Weight: 508.35 g/mol
Crystal System: Monoclinic
Space Group: C 2/c
Unit Cell Dimensions: a = 41.004(6) Å alpha = 90 degrees
b = 14.801(2) Å beta = 99.161(2) degrees
c = 7.4267(10) Å gamma = 90 degrees
Cell Volume: 4449.9(10) A^3
Temperature: 296(2) K
Radiation Type:
Radiation Wavelength: 0.71073 Å
Theta Range for Collection: 2.012 to 27.875 degrees
Reflections Collected (Unique): 28369 (5297)
Goodness-of-Fit on F^2: 1.048
Bond Lengths (Å)

I(1)	C(20)	2.094(8)
I(1')	C(20)	2.080(9)
O(1)	C(6)	1.375(7)
O(1)	C(5)	1.452(7)
O(2)	C(16)	1.352(8)
O(2)	C(14)	1.382(7)
O(3)	C(16)	1.195(8)
C(1)	C(2)	1.184(9)
C(1)	C(11)	1.444(9)
C(2)	C(3)	1.424(9)
C(3)	C(12)	1.387(9)
C(3)	C(4)	1.409(9)
C(4)	C(15)	1.390(8)
C(4)	C(5)	1.517(8)
C(6)	C(7)	1.391(9)
C(6)	C(11)	1.403(9)
C(7)	C(8)	1.396(9)
C(8)	C(9)	1.386(11)
C(9)	C(10)	1.396(10)

C(9)	C(23)	1.522(9)
C(10)	C(11)	1.389(9)
C(12)	C(13)	1.407(10)
C(13)	C(14)	1.360(10)
C(14)	C(15)	1.393(9)
C(16)	C(17)	1.488(9)
C(17)	C(22)	1.375(9)
C(17)	C(18)	1.402(8)
C(18)	C(19)	1.375(10)
C(19)	C(20)	1.394(10)
C(20)	C(21)	1.361(9)
C(21)	C(22)	1.382(9)
C(23)	C(26)	1.50(4)
C(23)	C(25')	1.52(2)
C(23)	C(24')	1.53(2)
C(23)	C(26')	1.523(16)
C(23)	C(24)	1.50(4)
C(23)	C(25)	1.57(2)

Bond Angles (degrees):

C(6)	O(1)	C(5)	118.6(5)
C(16)	O(2)	C(14)	116.5(5)
C(2)	C(1)	C(11)	152.6(7)
C(1)	C(2)	C(3)	152.4(7)
C(12)	C(3)	C(4)	120.4(6)
C(12)	C(3)	C(2)	126.2(6)
C(4)	C(3)	C(2)	113.4(5)
C(15)	C(4)	C(3)	119.6(5)
C(15)	C(4)	C(5)	118.6(5)
C(3)	C(4)	C(5)	121.4(5)
O(1)	C(5)	C(4)	114.5(5)
O(1)	C(6)	C(7)	118.5(6)
O(1)	C(6)	C(11)	122.0(6)
C(7)	C(6)	C(11)	119.4(6)
C(6)	C(7)	C(8)	118.6(7)
C(9)	C(8)	C(7)	123.3(7)
C(8)	C(9)	C(10)	117.1(6)
C(8)	C(9)	C(23)	121.4(7)
C(10)	C(9)	C(23)	121.5(7)
C(11)	C(10)	C(9)	121.1(7)
C(10)	C(11)	C(6)	120.5(6)
C(10)	C(11)	C(1)	127.2(6)
C(6)	C(11)	C(1)	112.3(6)
C(13)	C(12)	C(3)	118.9(6)
C(14)	C(13)	C(12)	120.4(6)
C(13)	C(14)	O(2)	120.0(6)

C(13)	C(14)	C(15)	121.4(6)
O(2)	C(14)	C(15)	118.6(6)
C(4)	C(15)	C(14)	119.2(6)
O(3)	C(16)	O(2)	123.5(6)
O(3)	C(16)	C(17)	125.1(6)
O(2)	C(16)	C(17)	111.3(5)
C(22)	C(17)	C(18)	119.8(6)
C(22)	C(17)	C(16)	123.1(5)
C(18)	C(17)	C(16)	117.1(6)
C(19)	C(18)	C(17)	119.9(7)
C(18)	C(19)	C(20)	119.3(6)
C(21)	C(20)	C(19)	120.7(7)
C(21)	C(20)	I(1')	119.2(6)
C(19)	C(20)	I(1')	120.0(5)
C(21)	C(20)	I(1)	122.0(6)
C(19)	C(20)	I(1)	117.4(5)
C(20)	C(21)	C(22)	120.3(7)
C(17)	C(22)	C(21)	119.9(6)
C(25')	C(23)	C(24')	115.1(16)
C(26)	C(23)	C(9)	110(2)
C(25')	C(23)	C(9)	106.0(19)
C(24')	C(23)	C(9)	107.7(13)
C(25')	C(23)	C(26')	107(2)
C(24')	C(23)	C(26')	108.1(17)
C(9)	C(23)	C(26')	112.9(15)
C(26)	C(23)	C(24)	113(3)
C(9)	C(23)	C(24)	111(2)
C(26)	C(23)	C(25)	104(2)
C(9)	C(23)	C(25)	108.6(13)
C(24)	C(23)	C(25)	111(2)

3.09 References

1. Dommerholt, J.; Schmidt, S.; Temming, R.; Hendriks, L. J. A.; Rutjes, F. P. J. T.; van Hest, J. C. M.; Lefeber, D. J.; Friedl, P.; van Delft, F. L. Readily Accessible Bicyclononynes for Bioorthogonal Labeling and Three-Dimensional Imaging of Living Cells. *Angew. Chem. Int. Ed.*, **2010,** *49*, 9422-9425.

2. Sletten, E. M.; Bertozzi, C. R. A Hydrophilic Azacyclooctyne for Cu-Free Click Chemistry. *Org. Lett.*, **2008,** *10*, 3097-3099.

3. Jewett, J. C.; Bertozzi, C. R. Synthesis of a Fluorogenic Cyclooctyne Activated by Cu-Free Click Chemistry. *Org. Lett.*, **2011,** *13*, 5937-5939.

4. Codelli, J. A.; Baskin, J. M.; Agard, N. J.; Bertozzi, C. R. Second-Generation Difluorinated Cyclooctynes for Copper-Free Click Chemistry. *J. Am. Chem. Soc.*, **2008,** *130*, 11486-11493.

5. Debets, M. F.; van Berkel, S. S.; Schoffelen, S.; Rutjes, F. P. J. T.; van Hest, J. C. M.; van Delft, F. L. Aza-Dibenzocyclooctynes for Fast and Efficient Enzyme PEGylation via Copper-Free (3+2) Cycloaddition. *Chem. Commun.*, **2010,** *46*, 97-99.

6. Poloukhtine, A. A.; Mbua, N. E.; Wolfert, M. A.; Boons, G. J.; Popik, V. V. Selective Labeling of Living Cells by a Photo-Triggered Click Reaction. *J. Am. Chem. Soc.*, **2009,** *131*, 15769-15776.

7. Arnold, R. M.; McNitt, C. D.; Popik, V. V.; Locklin, J. Direct Grafting of Poly(pentafluorophenyl acrylate) onto Oxides: Versatile Substrates for Reactive Microcapillary Printing and Self-Sorting Modification. *Chem. Commun.*, **2014,** *50*, 5307-5309.

8. Kuzmin, A.; Poloukhtine, A.; Wolfert, M. A.; Popik, V. V. Surface Functionalization Using Catalyst-Free Azide−Alkyne Cycloaddition. *Bioconjugate Chem.*, **2010,** *21*, 2076-2085.

9. McKay, C. S.; Chigrinova, M.; Blake, J. A.; Pezacki, J. P. Kinetics Studies of Rapid Strain-Promoted [3 + 2]-Cycloadditions of Nitrones with Biaryl-Aza-Cyclooctynone. *Org. Biomol. Chem.*, **2012,** *10*, 3066-3070.

10. Gordon, C. G.; Mackey, J. L.; Jewett, J. C.; Sletten, E. M.; Houk, K. N.; Bertozzi, C. R. Reactivity of Biarylazacyclooctynones in Copper-Free Click Chemistry. *J. Am. Chem. Soc.*, **2012,** *134*, 9199-9208.

11. Jewett, J. C.; Bertozzi, C. R. Cu-Free Click Cycloaddition Reactions in Chemical Biology. *Chem. Soc. Rev.*, **2010,** *39*, 1272-1279.

12. Davis, D. L.; Price, E. K.; Aderibigbe, S. O.; Larkin, M. X. H.; Barlow, E. D.; Chen, R.; Ford, L. C.; Gray, Z. T.; Gren, S. H.; Jin, Y.; Keddington, K. S.; Kent, A. D.; Kim, D.; Lewis, A.; Marrouche, R. S.; O'Dair, M. K.; Powell, D. R.; Scadden, M. l. H. C.;

Session, C. B.; Tao, J.; Trieu, J.; Whiteford, K. N.; Yuan, Z.; Yun, G.; Zhu, J.; Heemstra, J. M. Effect of Buffer Conditions and Organic Cosolvents on the Rate of Strain-Promoted Azide–Alkyne Cycloaddition. *J. Org. Chem.*, **2016,** *81*, 6816-6819.

13. Wang, W.; Li, L.-S.; Helms, G.; Zhou, H.-H.; Li, A. D. Q. To Fold or to Assemble? *J. Am. Chem. Soc.*, **2003,** *125*, 1120-1121.

14. McNitt, C. D.; Popik, V. V. Photochemical generation of oxa-dibenzocyclooctyne (ODIBO) for metal-free click ligations. *Org. Biomol. Chem.*, **2012,** *10*, 8200-2.

15. Brooks, K.; Yatvin, J.; McNitt, C. D.; Reese, R. A.; Jung, C.; Popik, V. V.; Locklin, J. Multifunctional Surface Manipulation Using Orthogonal Click Chemistry. *Langmuir*, **2016,** *32*, 6600-6605.

16. Wagner, H.; Brinks, M. K.; Hirtz, M.; Schafer, A.; Chi, L.; Studer, A. Chemical surface modification of self-assembled monolayers by radical nitroxide exchange reactions. *Chem. Eur. J.*, **2011,** *17*, 9107-12.

CHAPTER 4

APPLICATION AND DEVELOPMENT OF PHOTO-SPAAC AND SPAAC REAGENTS

4.01 Introduction

The mild reaction conditions, selectivity, and reaction kinetics of SPAAC has expanded its application beyond the labeling of biomolecules. SPAAC has become prominent in a variety of different fields.[1-5] These include the functionalization of metal-organic frameworks (MOF) and branched nanomaterials.[6-7] The combination of SPANC and SPAAC has also been used to create complex surfaces.[8] In our group we have employed photo-SPAAC in collaboration with Dr. Locklin at the University of Georgia to functionalize polymer brushes with photo-DIBO.[9] Upon irradiation through a photo-mask selective deprotection and functionalization of the surface was achieved. The continued development of new SPAAC derivatives is instrumental for application in new chemistries. This chapter describes the design and synthesis of various novel photo-SPAAC and SPAAC reagents and their application.

4.02 Photo-DIBO-TEG-SH for Nano-Particle Functionalization

It was recently reported that interfacial-SPAAC (I-SPAAC) could be used for the efficient functionalization of gold nanoparticles (AuNP) with azide functionalized polymersomes.[10] The cyclooctyne ADIBO was attached to the surface of AuNPs using a multi-step process. This strategy is cumbersome and requires purification of the AuNPs to remove coupling reagents. A more efficient strategy would be direct functionalization of the AuNPs with ADIBO. Unfortunately, thiol group that is required for the immobilization of substrates on AuNPs adds to ADIBO in a thiol-yne click reaction. In collaboration with Dr. Workentin at

Western University we developed a procedure for the direct functionalization of AuNPs with photo-caged cyclooctynes.[11] Cyclopropenones are stable in the presence of thiols and allow for spatial and temporal control of SPAAC. To achieve this, we have synthesized a thiol-functionalized photo-caged dibenzocyclooctyne **4.06** (photo-DIBO-TEG-SH), which could be directly attached to AuNPs. Then, upon irradiation of the functionalized AuNPs, I-SPAAC can be achieved.

To make photo-DIBO-TEG-SH **4.06,** a tetraethylene glycol linker was prepared with a trityl protected thiol for attachment to photo-DIBO-OH **4.01** (Scheme 4.01).[12] The first step was tosylation of commercially available tetraethylene glycol to afford mono-tosylated tetraethylene glycol **4.02**. Then, S_N2 displacement of the tosyl group with triphenylmethanethiol afforded trityl protected thiol **4.03**. Finally, tosylation of alcohol **4.03** produced linker **4.04** which can then be attached to photo-DIBO-OH **4.01** by a Williamson Ether reaction to afford trityl protected photo-DIBO derivative **4.05**. The last step was removal of the trityl group by acid cleavage with trifluoroacetic acid and triisopropyl silane in dichloromethane to afford photo-DIBO-TEG-SH **4.06**.

Scheme 4.01 Synthesis of Photo-DIBO-SH **4.06**

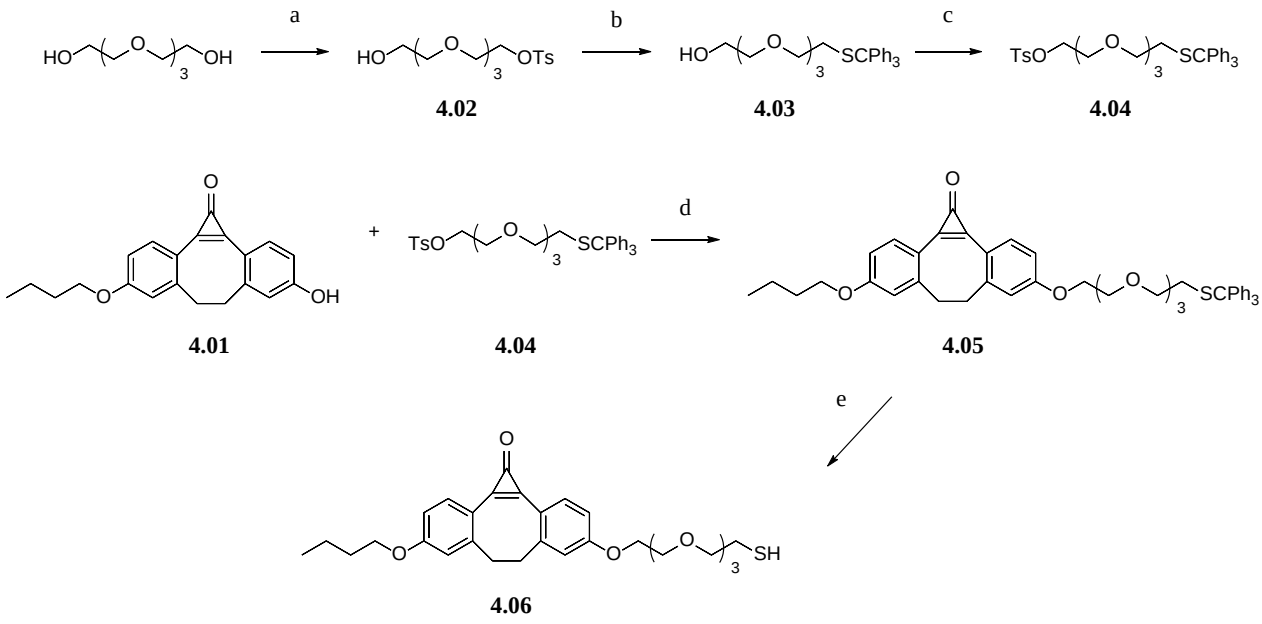

Reagents and Conditions: a) p-TsCl, EtN_3, CH_2Cl_2, 42%; b) triphenylmethanethiol, NaOH, EtOH, Toluene, H_2O, 82%; c) p-TsCl, imidazole, EtN_3, CH_2Cl_2, 83%; d) K_2CO_3, DMF, 72%; e) TFA, *i*-Pr3SiH, CH_2Cl_2, 92%.

AuNPs were functionalized with photo-DIBO-TEG-SH **4.06** through a place exchange reaction. It is important to note that changing the incubation time and concentration of photo-DIBO-TEG-SH **4.06** with the AuNPs control the amount of functionalization. A 1:5 ratio of photo-DIBO-TEG-SH **4.06** and AuNPs were incubated for 15 minutes to achieve optimal functionalization. Characterization of the AuNPs determined the amount of photo-DIBO-TEG-SH **4.06** attached to the surface was 0.136 μmol mg^{-1}. Upon irradiation of the functionalized AuNPs, the DIBO cyclooctyne was successfully formed, and the rate of I-SPAAC with benzyl azide was measured (0.053 $M^{-1}s^1$). The generality of the chemistry was showcased by reacting the AuNPs with a variety of azide compounds that included 3'-Azido-3'-deoxythymidine (AZT),

4-methoxyphenyl azide, and 3-azidopropan-1-ol. In addition, the efficient coupling of N-phenyl-α-phenynitrone to AuNPs demonstrated the possibility of I-SPANC.

4.03 Solvent and Catalyst-Free Generation of Polymer Brushes

The two main strategies for the construction of polymer brushes are the "grafting from" and "grafting to" approach.[1-2, 13] The "grafting from" approach utilizes polymerization directly from an immobilized substrate on a surface. The "grafting to" approach works by attaching fully synthesized polymer to a surface through a chemical reaction. The latter allows for a higher degree of polymerization control and characterization.[1, 13] Unfortunately, it is difficult to create densely packed brushes because of the steric interactions of the large polymers being attached. A way to improve the grafting density in the "grafting to" approach is to use polymer melts.[14-15] We envisioned that SPAAC could be used with a polymer melt to create highly dense polymer brushes. In collaboration with Dr. Minko's group at the University of Georgia, we have developed a solvent-free "grafting to" approach that utilizes SPAAC to create high density poly(ethylene glycol) polymer brushes.[16]

A photo-DIBO amine (photo-DIBO-NH_2) **4.09** derivative was chosen to functionalize a poly(glycidyl methacrylate) polymer (PGMA) anchored to a silicon plate. We envisioned that the spatial and temporal control of photo-DIBO coupled with the high thermal stability of DIBO were a perfect combination to achieve our goals. After functionalization of the plates they can then be reacted with a polymer melt of azide functionalized poly(ethyelen glycol) (PEG-N_3). The synthesis of photo-DIBO-NH_2 **4.09** is accomplished in several steps (Scheme 4.02). The first step is tosylation of commercially available N-boc-ethanol amine to form alkylating agent **4.07**. Then, a Williamson Ether reaction between previously synthesized photo-DIBO-OH **4.01**

and linker **4.07** afforded photo-DIBO-Boc **4.08**. Removal of the Boc group was achieved with trifluoracetic acid in dichloromethane to afford photo-DIBO-NH_2 **4.09**.

Scheme 4.02 Synthesis of Photo-DIBO-NH_2 **4.09**

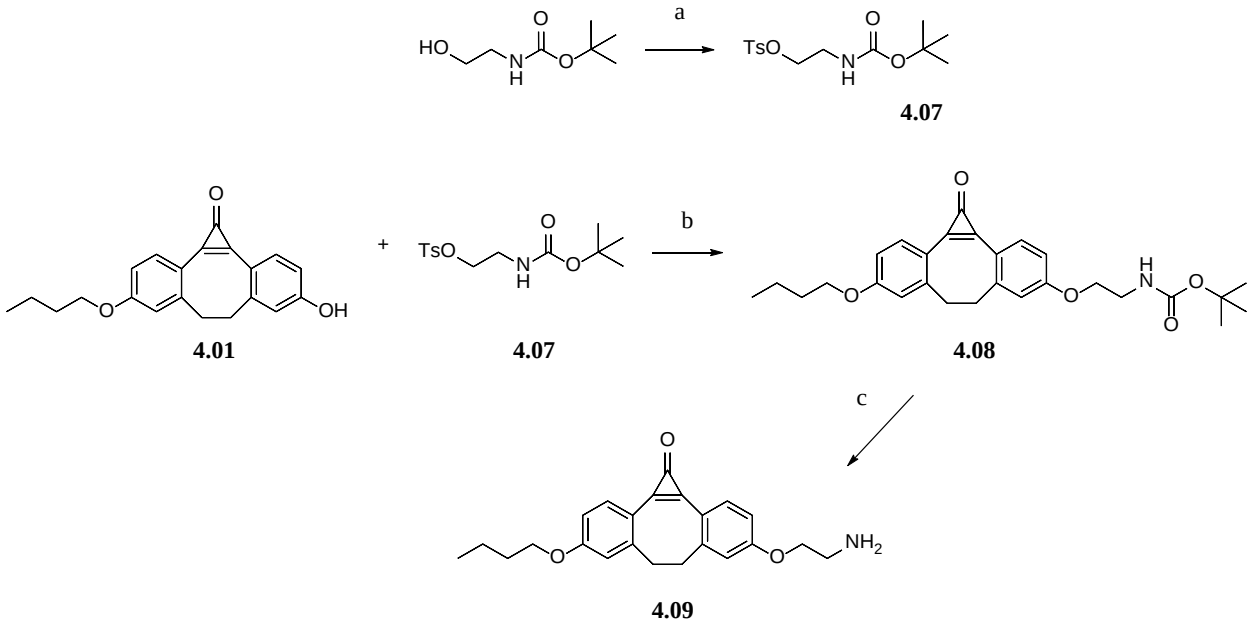

Reagents and Conditions: a) p-TsCl, imidazole, CH_2Cl_2, 96 %; b) K_2CO_3, DMF, 97 %; c) TFA, CH_2Cl_2, 91 %.

After attachment of photo-DIBO-NH_2 **4.09** to the PGMA through an epoxide ring opening reaction, DIBO was formed by irradiation at 350 nm. Then, under varying temperatures, PEG-N_3 of 5, 10, 20 kg/mol were melted and reacted with DIBO. In all cases it was observed that after heating for 12-24 hours over 50% grafting thickness was achieved. The rate of thickness would then slow over time. It was determined that PEG-N_3 of 5 kg/mol at 130 °C for 96 hours gave the highest density with 1.2 chains/nm^2. The polymer brushes generated from SPAAC polymer melt procedure had high anti-fowling properties and were stable in PBS over 2 months.

4.04 Development of Hydrophilic Photo-ADIBO Derivatives

The hydrophobic nature of cyclooctynes is problematic for biological application. To alleviate these problems, we have explored the utility of structural modifications of DIBO by introducing sulfates or ethylene glycol substituents. Unfortunately, there are no examples of photo-caged cyclooctynes with significant water solubility. We set out to synthesize several photo-ADIBO derivatives that not only more hydrophilic than photo-DIBO, but after irradiation have SPAAC rates five times faster than DIBO. We believed that these compounds could find use in biological applications in the future.

Using a previously known procedure for the preparation of photo-ADIBO, we have desined and synthesized tetrahydroxy-photo-ADIBO (TH-photo-ADIBO) **4.13** (Scheme 4.03).[17] The first step was reductive amination of commercially available 3,4,5-trimethoxyaniline and m-anisaldehyde with $NaBH_4$ in methanol to afford aniline **4.10**. Then, alkylation of aniline **4.10** with succinic anhydride, DMAP, and triethylamine in chloroform afforded cyclopropenone precursor **4.11**. A double Friedel-Crafts alkylation of **4.11** with tetrachlorocyclopropene subsequently followed by hydrolysis with 5% HCl afforded tetramethoxy-photo-ADIBO (TM-photo-ADIBO) **4.12**. Finally, demethylation of the methoxy groups was done by using BBr_3 in dichloromethane to afford trimethoxy-photo-ADIBO (TH-photo-ADIBO) **4.13**. Unfortunately, the methoxy group ortho to the cyclopropenone was inert under these conditions. We believe that the strong interactions of the cyclopropenone with this methoxy group significantly reduce its reactivity.

Scheme 4.03 Synthesis of TH-Photo-ADIBO **4.13**

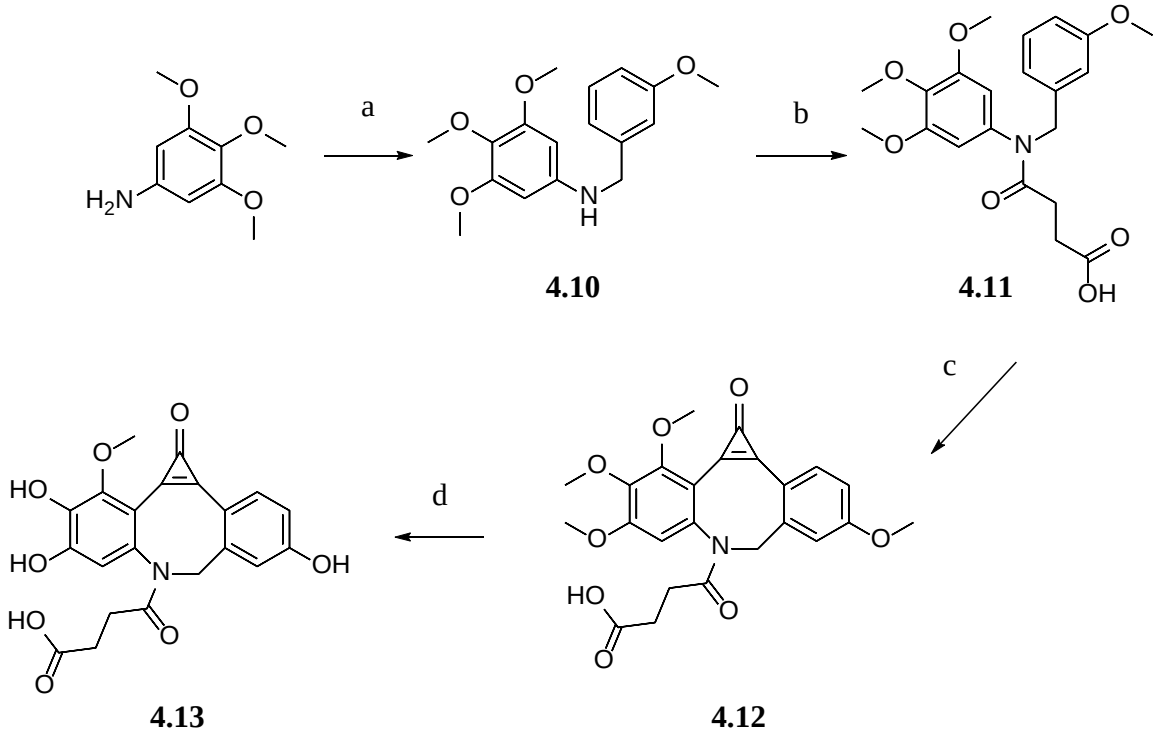

Reagents and Conditions: a) m-anisaldehyde, $NaBH_4$, MeOH, 97 %; b) succinic anhydride, DMAP, Et_3N, $CHCl_3$, 90 %; c) C_3Cl_4, $AlCl_3$, CH_2Cl_2, 51 %; d) BBr_3, CH_2Cl_2, 55 %.

The second photo-ADIBO derivative was prepared using a similar procedure (Scheme 4.04).[18] Reductive amination of commercially available m-methoxyaniline and m-anisaldehdye with $NaBH_4$ in methanol afforded aniline **4.14**. Next, alkylation with succinic anhydride, DMAP, and triethylamine in chloroform afforded cyclopropenone precursor **4.15**. A Friedel-Crafts alkylation with **4.11** and tetrachlorocyclopropene subsequently followed by hydrolysis with 5% HCl afforded dimethoxy photo-ADIBO (DM-photo-ADIBO) **4.16**. Gratifyingly, the demethylation of cyclopropenone **4.16** was successful with BBr_3 in dichloromethane to afford dihydroxy-photo-ADIBO (DH-photo-ADIBO) **4.17**.

Scheme 4.04 Synthesis of DH-Photo-ADIBO **4.17**

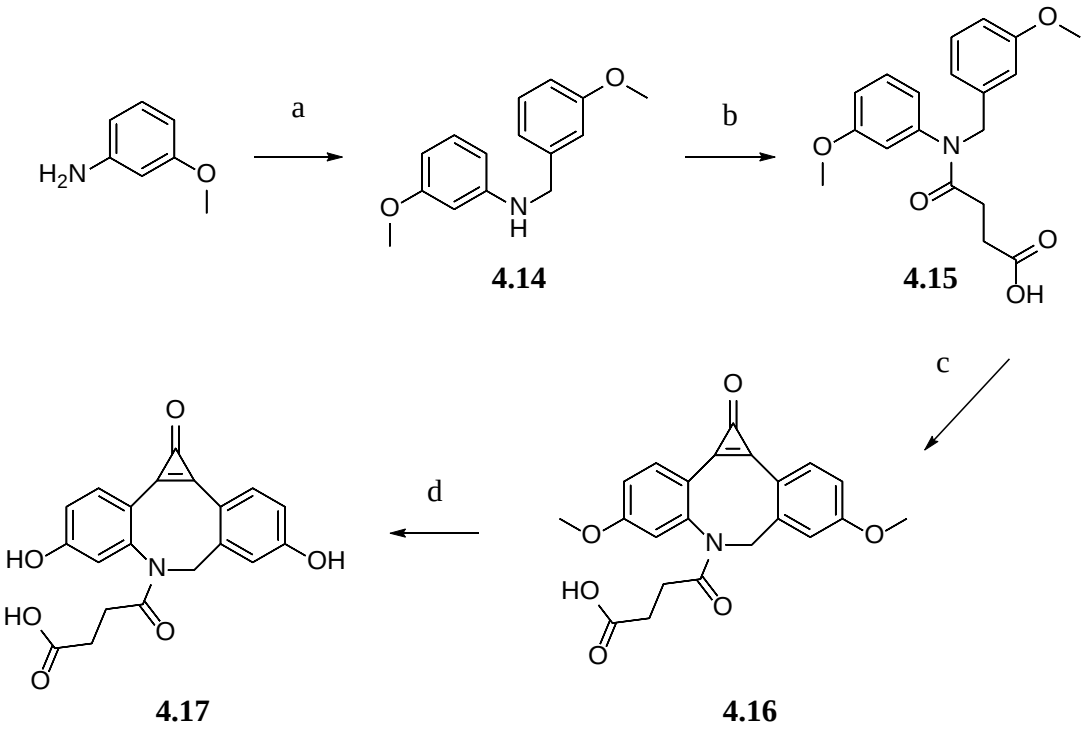

Reagents and Conditions: a) m-anisaldehyde, $NaBH_4$, MeOH, 65 %; b) succinic anhydride, DMAP, Et_3N, $CHCl_3$, 82 %; c) C_3Cl_4, $AlCl_3$, CH_2Cl_2, 28 %; d) BBr_3, CH_2Cl_2, 71 %.

We first investigated the solubility of both photo-ADIBO derivatives **4.13** and **4.17**. Both were exceptionally soluble in water and concentrations could be made up to 1 mM with PBS. The rate of SPAAC was then investigated for trihydroxy-ADIBO (TH-ADIBO) **4.18** (Scheme 4.05) to determine the steric effects of the ortho methoxy substituent. Generation of TH-ADIBO **4.18** was done *in situ* by irradiation of TM-photo-ADIBO with 350 nm light, and reacted with 1-Amino-11-azido-3,6,9-trioxaundecane (TEG-N_3) and benzyl azide (BnN3) in various solvents (Scheme 4.06). As expected the rate of SPAAC in methanol with BnN_3 (0.00585 ± 0.00002 M^{-1} s^{-1}) and TEG-N_3 (0.0067 ± 0.0002 M^{-1} s^{-1}) matches the previously reported rate (0.008 M^{-1} s^{-1}). The ortho methoxy substituent causes significant reduction in the rate of SPAAC. Unfortunately, we were unable to determine the rate in PBS buffer because TM-ADIBO **4.18**

would decompose faster than its reactivity with azides. We were unable to determine the reason for the decomposition of TH-ADIBO **4.18** and decided to move onto DH-photo-ADIBO **4.17** because of its faster kinetics. DH-Photo-ADIBO **4.17** showed no problems in aqueous solvent and after photolysis showed similar rates to that of ADIBO (0.29 ± 0.01). Also, we observed that DH-ADIBO was stable in PBS buffer for over 24 hours.

Scheme 4.05 Photodecarbonylation of TM-Photo-ADIBO and Reaction Kinetics

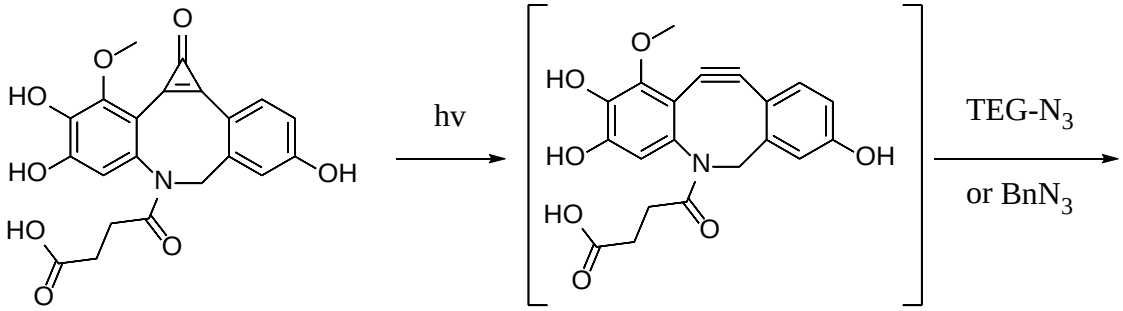

4.13 **4.18**

ADIBO	Solvent	Azide	Rate ($M^{-1}s^{-1}$)
4.18	MeOH	BnN_3	0.00585 ± 0.00002
4.18	MeOH	TEG-N_3	0.0067 ± 0.0002

4.05 ADIBO-CO_2H for Functionalization of Pt^{IV} Prodrugs and Lipid Analogues for Drug Delivery

The Pt^{IV} prodrug of cisplatin has become widely studied because its relative chemical inertness and accessibility to introduce functionality.[19] When Pt^{IV} drugs enter cells they are reduced and generate biologically active Pt^{II}. The active Pt^{II} species then goes through displacement of the chlorines to generate highly electrophilic plantium (II) complexes which can then crosslink with DNA and induce cell death. Unfortunately, the reactivity of Pt^{IV} and weakly nucleophilic hydroxyl groups limit the chemistry that can be used to make derivatives. A

popular way to functionalize Pt^{IV} prodrugs is with alkylation of the hydroxyl groups with anhydrides.[19-20] We envisioned that a simple anhydride with an azide handle would allow for rapid generation of Pt^{IV} derivatives through SPAAC coupling. SPAAC is ideal method because of its mild reaction conditions, high chemical yields, and large abundance of commercially available derivatives. In collaboration with Dr. Dhar at the University of Miami we developed a procedure for bis-functionalization of cisplatin with ADIBO-acid **4.20** (AIDO-CO_2H).[21] The use of SPAAC allows for easy attachment of various targeting ligands, antibodies, fluorescence reporters, or therapeutics (Scheme 4.06).

The synthesis of ADIBO-CO_2H **4.20** can be done in one step from ADIBO-NH_2 **4.19** by reacting with succinic anhydride and trimethylamine in chloroform (Scheme 4.06). After synthesis of ADIBO-CO_2H **4.20** it was reacted with a new terminal-azide-appended Pt^{IV} compound (Platin-Az) **4.21** to form functionalized cisplatin (Platin-CLK) **4.22**. Platin-CLK **4.22** was then examined for its therapeutic properties. Platin-CLK **4.22** exhibited no change in the redox potential and very favorable antiproliferative properties compared to Platin-Az **4.21**.

To showcase the applicability of the system, two different experiments were performed. The first experiment of Platin-CLK's **4.22** was encapsulation by poly(lactide-co-glycolide)-b-polyethyleneglycol (PLGA-b-PEG) nanoparticles for controlled drug delivery. The results concluded that the highly hydrophobic nature of ADIBO substantially increased loading into the hydrophobic core. These results were promising for future drug delivery application. The second experiment was visualization of the internalization of Platin-CLK **4.22** in cells. This was done by functionalization of ADIBO-CO_2H **4.20** with cell reporter Cy5.5. The newly synthesized ADIBO derivative was then reacted with Platin-Az **4.21** and upon visualization

showed internalization of the platin compound. We believe this robust system will allow for endless possibilities of Pt^{IV} prodrugs to be made.

Scheme 4.06 Synthesis of Platin-CLK 4.22

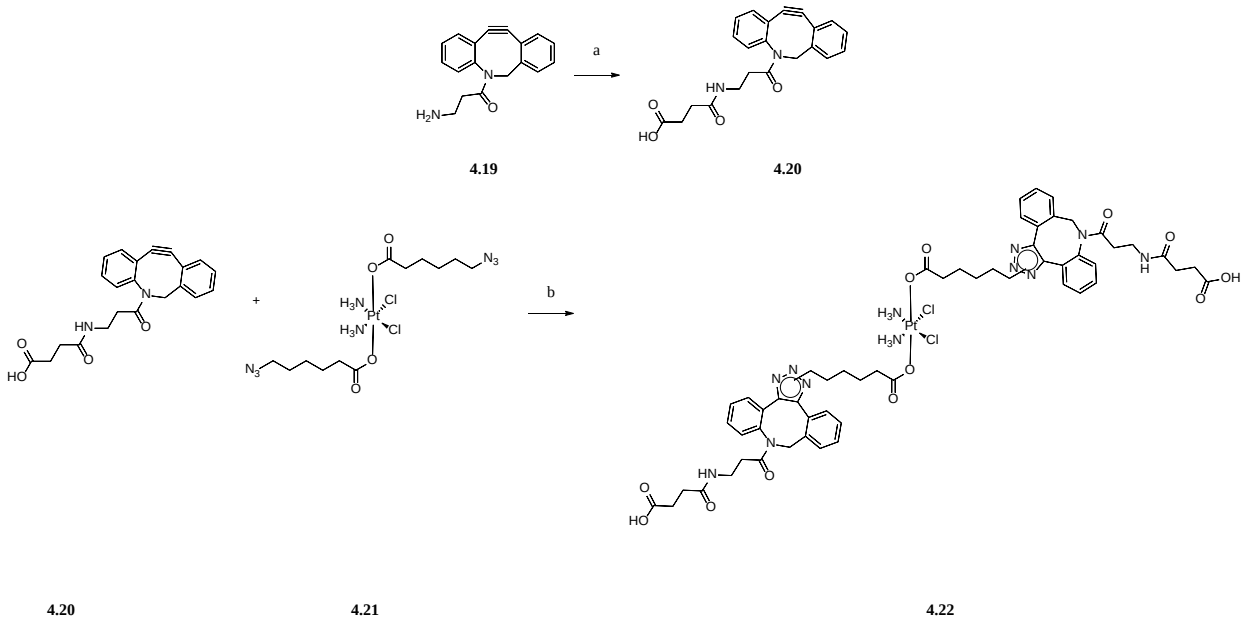

Reagents and Conditions: a) succinic anhydride, Et_3N, $CHCl_3$ 83%; b) DMF, 79%.

Another application of ADIBO-CO_2H **4.20** was for the development of a clickable and photo-cleavable lipid analogue for drug delivery.[22] Lipids have become an effective drug deliver agent because of their biocompatibility and ability to target cells through insertion and fusion of cell membranes. Click Reactions like CuAAC have been used to functionalization lipids with therapeutics but copper can cause lipid degradation and is not biocompatible. SPAAC offers an alternative because of its mild reaction conditions and biocompatibility. In collaboration with Dr. Best at the University of Tennessee we have developed an ADIBO lipid with a 2-nitrobenzyl headgroup for a clickable and photocleavable lipid analog **4.24**. Through a simple amide coupling reaction between ADIBO-CO_2H **4.20** and lipid **4.23** with HBTU, HOBt, DIPEA, and CH_2Cl_2 lipid derivative **4.24** was synthesized.

Scheme 4.07 Synthesis of Clickable and Photocleavable Lipid Delivery Agent

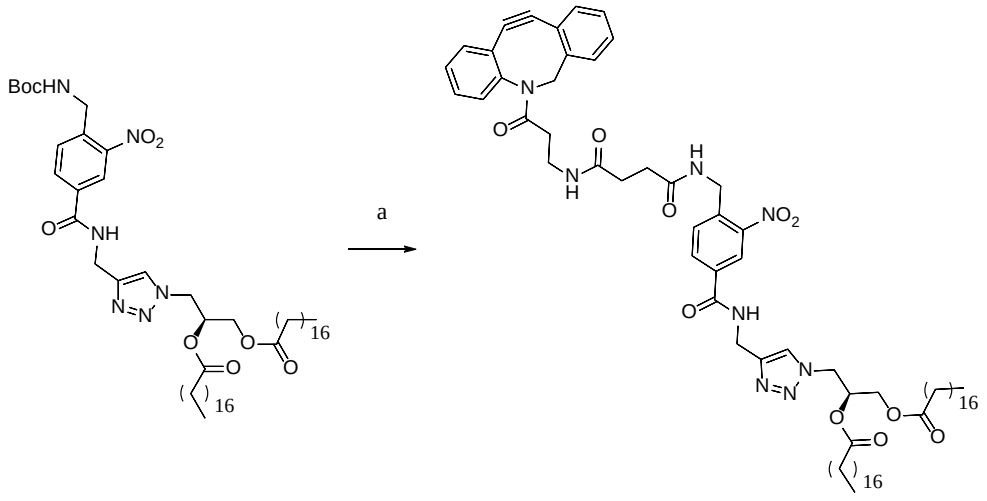

4.23 **4.24**

Reagents and Conditions: a) 1. TFA, CH_2Cl_2 2. **4.20**, HBTU, HOBt, DIPEA, CH_2Cl_2, 38 %.

Clickable and photocleavable lipid **4.24** was then tested for delivery and release with a model liposome (Scheme 4.08). Lipid **4.24** (4%) was then incubated with unilamellar liposomes (~200 nm) composed primarily of phosphatdylcholine (96%) and derivatized with a SPAAC-activated coumarin fluorophore **4.25**. The reaction was then followed by the increase in fluorescent intensity over time. After 40 minutes, the fluorescent intensity had plateaued signifying the completion of the SPAAC reaction. When compared to an unfunctionalized control, the coumarin labeled liposome showed over six-fold increase in fluorescence intensity. The ability to release therapeutics was then examined by incorporation of lipid **4.24** in live *Saccharomyces cerevisiae* cells. The cells were functionalized with the fluorescent azide azide-Fluor 488. Fluorescent images of the cells showed successful labeling through SPAAC. The cells were then irradiated for 1, 2, 3, and 12 hours which resulted in decreases in fluorescence intensities of 70, 60, 57, and 42 %. Lipid **4.24** was successful in its application of delivery and drug release.

Scheme 4.08 Incorporation of Lipid 4.24 into Liposomes

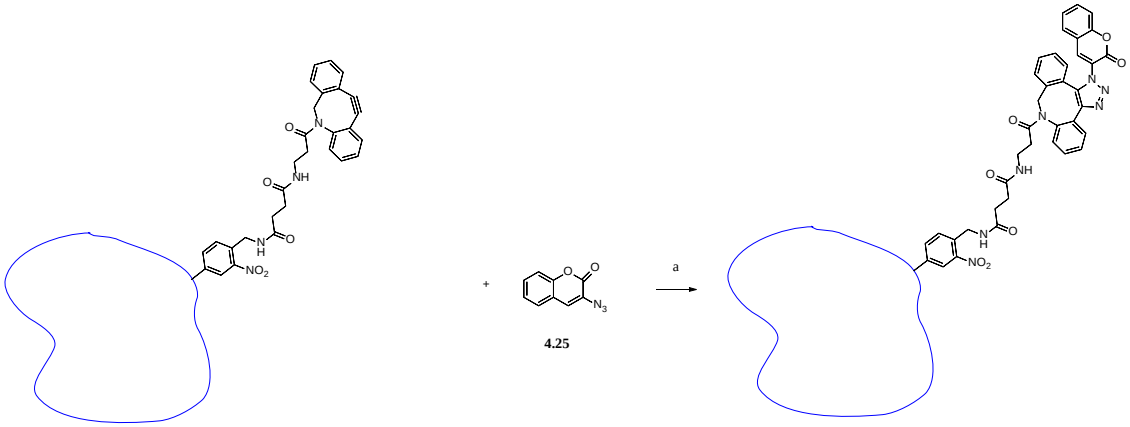

Reagents and Conditions: a) DMSO, HEPES buffer

4.06 Applications of ODIBO and DIBO-NH_2 for Surface Functionalization

The use of SPAAC has become instrumental in surface functionalization because of the mild reaction conditions, reaction kinetics, and orthogonality.[1-2] In collaboration with Dr. Locklin at the University of Georgia we have completed several projects that revolve around postpolymerization modifications of polymer brushes. Project one entails one-pot dual functionalization of poly(pentafluoro-phenyl acrylate) (poly(PFPA)) polymer brushes with fluorogenic azides and amines.[23] The poly(PFPA) polymers are made from a "grafting to" approach to a silanol surface. Using microcaplliary printing, selective functionalization of the brushes were done with DIBO-PEG-NH_2 **4.23** (Figure 4.01). The brushes were then functionalized in a one-pot manner with azido-Texas Red and amino-Fluorescein. Upon fluorescent imaging, detailed channels were observed with no cross contamination. The use of aminolysis and SPAAC were very successful orthogonal partners in brush functionalization.

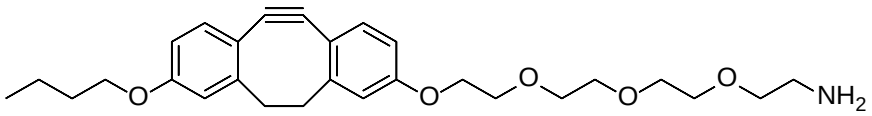

4.23

Figure 4.01 DIBO-PEG-NH_2 for Surface Functionalization

The second project revolved around the development of tri-functionalized brush surface that uses SPAAC, SuFEx and aminolysis (Figure 4.02).[24] Again, poly(PFPA) polymer brushes were used with microcapillary printing to partially functionalize the brushes with ODIBO-PEG-NH_2 **4.24** and aryl sulfonyl fluoride **4.25** (PEFABLOC). The polymer brushes were placed in a solution of azido-texas red, TBDMS fluorescein methyl ester, and aminomethyl pyrene. After the reactions were completed the brushes were imaged and showed successful self-sorting of the three fluorophores. There was no cross contamination between the various channels for each click reaction. This showcased how easy it can be to create complex surfaces using the correct orthogonal reactions.

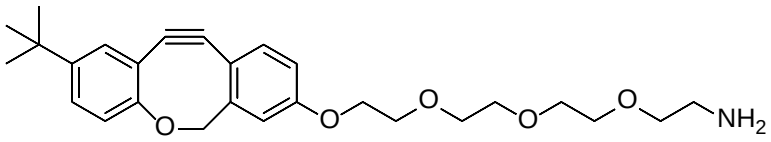

4.24

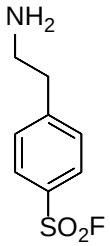

4.25

Figure 4.02 ODIBO-PEG-NH_2 for Tri-Surface Functionalization

The last project revolves around using SPAAC to functionalize polymer brushes with multiple azide fluorophores without the use of a photo-labile protecting group. To achieve this, we used two different cyclooctynes that differed in reactive of about 30 times. ODIBO has a second order rate constant of $1.74 \pm 0.04\ M^{-1}s^{-1}$ and DIBO has a rate constant of 0.0567 ± 0.0027

$M^{-1}s^{-1}$ with benzyl azide in methanol. We first examined the effect of attaching the cyclooctynes to the surface of the polymer brushes. The pseudo-1st order rates of SPAAC were determined by individually functionalizing poly(PFPA) brushes with ODIBO-PEG-NH_2 **4.24** and DIBO-PEG-NH_2 **4.23**. Two different experiments were done for each ODIBO and DIBO polymer brushes (Table 4.01). The first was the rate of SPAAC on each brush freely dissolved into solution, and the second was the rate of SPAAC of the brush bound to a silicon wafer. Both ODIBO and DIBO showed significant reduction in their rate when bound to the poly(PFPA) brush. Fortuitously, ODIBO increases from 24 times to 83 times faster than DIBO when the polymer brush is bound to a silicon wafer. This large rate difference allowed for the functionalization of the brushes using kinetic resolution.

Table 4.01 Pseudo-First Order Rates of SPAAC with Poly(PFPA)

Cyclooctyne	Pseudo-1st Order Rate Bound[a]	Pseudo-1st Order Rates Unbound[b]
ODIBO	0.0005 s^{-1}	0.00262 s^{-1}
DIBO	0.0418 s^{-1}	0.06375 s^{-1}

[a] 4 mM azido-disperse red 1, DMF, 25 ° C; [b] 45 mM BnN_3, DMF, 25 ° C

To showcase the ability to functionalize a surface based on kinetic resolution poly(PFPA) brushes bound to a silicon wafer were functionalized by microcapillary printing with ODIBO-PEG-NH_2 **4.24** and DIBO-PEG-NH_2 **4.23**. Next, the wafer was placed in a solution of 4 mM of azidomethylpyrene for 10 minutes. The wafer was then washed with DMF and reacted with 4 mM of azido-fluoresceine for 1 hour. After washing the wafer, it was imaged using fluorescent microscopy to show well defined channels (Figure 4.03). We were successful in designing a system that allows for selective functionalization of polymer brushes based off their rates. This significantly simplifies the preparation of surfaces because only SPAAC chemistry is required.

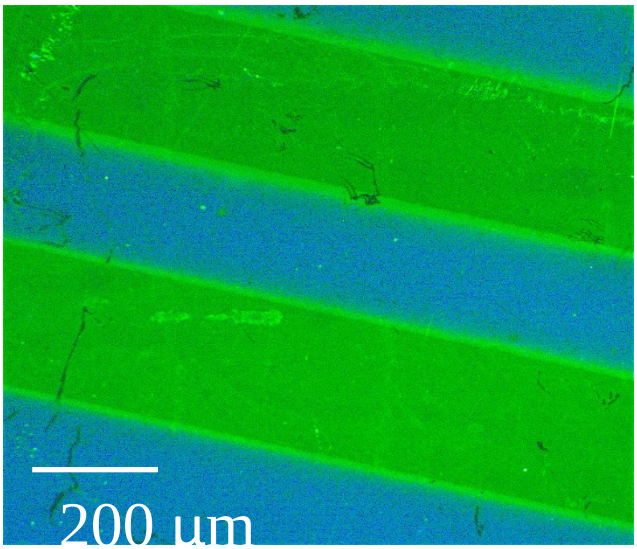

Figure 4.03 Fluorescent microscope images of patterned surfaces generated through microcapillary printing of ODIBO and DIBO. ODIBO was reacted with azidomethylpyrene (blue) for 10 minutes and DIBO was reacted with azdio-fluoresceine (green) for 1 hour.

4.07 Conclusion

The application of photo-SPAAC and SPAAC reagents has expanded to a variety of research fields. We have shown SPAAC to be a powerful tool in creating a variety of complex surfaces. The application of SPAAC to functionalizing AuNPs, Pt^{IV} complexes, and derivatization of lipids for drug delivery further showcase its robustness. Also, we developed highly hydrophilic photo-ADIBO-CO_2H derivatives that can be applied in biological application. We are currently working on the application of SPAAC for RNA labeling and two-photon excitation of photo-SPAAC reagents for labeling of muscle tissue.

4.08 Experimental Section

All organic solvents were dried and freshly distilled before use; Tetrahydrofuran was distilled from sodium/benzophenone ketyl. Other reagents were obtained from Aldrich or VWR and used as received unless noted. Photo-DIBO-OH and Tos-N-Boc-ethanolamine were

prepared using standard procedures. Flash chromatography was performed using 40-63 μm silica gel. All NMR spectra were recorded in $CDCl_3$ (unless otherwise noted) using 400 MHz instrument. Absorption spectra were recorded on CARY 300 Bio UV-Visible spectrometer. Photolyses were conducted in the Rayonet photoreactor equipped with 12 X 4 W 350 nm fluorescent lamps.

Kinetics

Rate measurements in organic solvent were performed using Carry-300 Bio UV-Vis spectrometer. The temperature was set to 25.0°C and controlled to 0.1 °C accuracy. Reactions of ADIBO and DIBO with excess of azide were monitored by following the decay of the characteristic alkyne peak at 309 nm. Reactions with ODIBO were done with excess of azide and monitored by following the decay of the characteristic alkyne peak at 321 nm. The experimental data fits the single exponential equation well. Linear dependence of the observed pseudo-first order rate constants on azide concentration was analyzed by the least squares method to obtain the bimolecular rate constants.

p-Toluenesulfonic Acid 2-(2-(2-(2-Hydroxyethoxy)ethoxy)ethoxy)ethyl Ester (4.02).

Please See Chapter 3 for the synthesis of Tosylated Linker **4.02**.

1,1,1-triphenyl-5,8,11-trioxa-2-thiatridecan-13-ol (4.03).

Triphenylmethanethiol (4.12 g, 14.91 mmol) was dissolved in a solution of EtOH/toluene (1:1, 40 mL) and NaOH (0.596 g, 14.91 mmol) in H_2O (8 mL) was added. To this mixture was added a solution of 2-(2-(2-(2-hydroxyethoxy)ethoxy)ethoxy)ethyl 4-methylbenzenesulfonate (4.155 g, 11.93 mmol) in EtOH/toluene (1:1, 40 mL). The reaction mixture was stirred at room temperature for 18 h. Once the reaction was completed, the mixture was poured into a $NaHCO_3$ saturated solution. The organic layer was washed with $NaHCO_3$ (3x) and brine (3x). The organic

portion was then dried over $MgSO_4$ and concentrated in vacuo. The crude product was then purified via silica gel chromatography (hexanes: ethyl acetate 1:1 to 1:3) to provide 1,1,1-triphenyl-5,8,11-trioxa-2-thiatridecan-13-ol **4.03** (4.44 g, 82%) as a colorless oil. ^{1}H-NMR: 7.40-7.42 (d, 6H), 7.24-7.28 (m, 6H), 7.17-7.21 (m, 3H), 3.67-3.69 (m, 2H), 3.60-3.64 (m, 5H), 3.55-3.58 (m, 4H), 3.43-3.45 (m, 2H), 3.27-3.31 (t, J = 6.9 Hz, 2H), 2.41-2.45 (t, J = 6.9 Hz, 2H). ^{13}C-NMR: 144.91, 129.73, 127.99, 126.76, 72.67, 70.73, 70.51, 70.41, 70.22, 69.74, 66.73, 61.81, 31.73.

1,1,1-triphenyl-5,8,11-trioxa-2-thiatridecan-13-yl 4-methylbenzenesulfonate (4.04).

To a solution of p-toluenesulfonyl chloride (1.873 g, 9.83 mmol) in CH_2Cl_2 (100 mL) at 0 °C, was added **4.03** (4.447, 9.83 mmol) and dry triethylamine (4.97 g, 49.1 mmol). The reaction was then stirred for 2 hours at 0 °C, and left overnight at room temperature under nitrogen. The precipitate was filtered, and the solution was concentrated in vacuo. The residue was purified via silica gel chromatography (hexanes: ethyl acetate 1:1 to 1:3) to provide 1,1,1-triphenyl-5,8,11-trioxa-2-thiatridecan-13-yl 4-methylbenzenesulfonate **4.04** (4.92, 83 %) as a colorless oil. ^{1}H-NMR: 7.78-7.80 (d, J = 8.3 Hz, 2H), 7.40-7.42 (m, 6H), 7.31-7.33 (m, 2H), 7.25-7.29 (m, 6H), 7.18-7.22 (m, 3H), 4.12-4.15 (t, J = 4.8 Hz, 2H), 3.65-3.67 (t, J = 4.8 Hz, 2H), 3.51-3.55 (m, 6H), 3.41-3.44 (m, 2H), 3.27-3.31 (t, J = 6.9 Hz, 2H), 2.40-2.43 (m, 5H).^{13}C-NMR: 144.99, 144.97, 133.17, 130.01, 129.81, 128.18, 128.08, 126.85, 70.92, 70.73, 70.68, 70.33, 69.80, 69.44, 68.87, 66.79, 31.83, 21.86.

4-butoxy-9-((1,1,1-triphenyl-5,8,11-trioxa-2-thiatridecan-13-yl)oxy)-6,7-dihydro-dibenzo[a,e]cyclopropa[c][8]annulen-1-one (4.05).

To a solution of **4.01**[12] (1.186 g, 3.70 mmol) in DMF (40 mL) was added **4.04** (3.37 g, 5.55 mmol). Next, portionwise was added K_2CO_3 (0.512 g, 3.70 mmol) and the solution was stirred

and heated to 80 °C for 5 hours. The reaction was cooled to room temperature, diluted with ethyl acetate (400 mL), washed 5x with water (75 ml), brine (100 mL), and dried over $MgSO_4$. The organic layer was then filtered, concentrated in vacuo, and purified via silica gel chromatography (hexanes: ethyl acetate 3:1 to CH_2Cl_2: MeOH 30:1) to provide 4-butoxy-9-((1,1,1-triphenyl-5,8,11-trioxa-2-thiatridecan-13-yl)oxy)-6,7-dihydro-dibenzo[a,e]cyclopropa[c][8]annulen-1-one **4.05** (2.01 g, 72% yield) as a yellow oil. ^{1}H-NMR: 7.92-7.95 (m, 2H), 7.40-7.42 (m, 6H), 7.25-7.29 (m, 6H), 7.18-7.21 (m, 3H), 6.88-6.90 (m, 4H), 4.17-4.19 (t, J = 4.7 Hz, 2H), 4.03-4.06 (t, J = 6.5, 2H), 3.86-3.88 (t, J = 4.7 Hz, 2H), 3.71-3.73 (m, 2H), 3.64-3.65 (m, 2H), 3.57-3.60 (m, 2H), 3.45-3.3.47 (t, J = 4.7 Hz, 2H), 3.29-3.32 (m, 4H), 2.60-2.63 (d, J = 10.7 Hz, 2H), 2.41-2.44 (t, J = 6.9 Hz, 2h), 1.75-1.84 (m, 4H), 1.47-1.56 (m, 2H), 0.98-1.01 (t, J = 7.4 Hz, 3H). ^{13}C-NMR: 162.77, 161.77, 153.99, 147.99, 147.97, 144.99, 142.61, 142.21, 136.03, 135.91, 129.80, 128.07, 126.85, 116.81, 116.56, 116.44, 116.39, 112.54, 112.45, 71.06, 70.89, 70.72, 70.37, 69.81, 69.71, 68.20, 67.86, 66.79, 37.38, 37.35, 31.86, 31.35, 19.41, 14.03. ESI HRMS: calcd. ($M+H^+$): $C_{48}H_{51}O_6S$ 755.3401, found 755.3401.

4-butoxy-9-(2-(2-(2-(2-mercaptoethoxy)ethoxy)ethoxy)ethoxy)-6,7-dihydro-dibenzo[a,e]cyclopropa[c][8]annulen-1-one (photo-DIBO-TEG-SH, 4.06).

Photo-DIBO **4.05** (1.45 g, 1.921 mmol) was dissolved in CH_2Cl_2 (20 mL) and TFA (1.850 mL, 24.01 mmol). IPr_3SiH (0.866 mL, 4.23 mmol) was added and the reaction mixture was stirred at room temperature under argon for 3 hours. The reaction was concentrated in vacuo and purified via silica gel chromatography (CH_2Cl_2: MeOH 30:1) to provide photo-DIBO-TEG-SH **4.06** (0.910 g, 92%) as a yellow oil. ^{1}H-NMR: 7.92-7.95 (d, J = 8.7 Hz, 2H), 6.88-6.92 (m, 4H), 4.20-4.23 (m, 2H), 4.03-4.06 (t, J = 6.5 Hz, 2H), 3.88-3.91 (m, 2H), 3.74-3.76 (m, 2H), 3.59-3.71 (m, 8H), 3.32-3.35 (d, J = 10.6, 2H), 2.61-2.64 (d, J = 10.7 Hz, 2H), 2.87-2.72 (m, 2H), 1.77-1.84

(m, 2H), 1.58-1.63 (t, J = 7.4 Hz, 1H), 1.47-1.56 (m, 2H), 0.98-1.01 (t, 3H).^{13}C-NMR: 162.27, 161.76, 153.97, 147.98, 142.63, 142.19, 136.02, 135.91, 116.83, 116.55, 116.43, 116.37, 112.55, 112.46, 73.07, 71.11, 70.90, 10.79, 70.43, 69.74, 68.20, 67.86, 37.39, 37.36, 31.34, 24.49, 19.40, 14.02. ESI HRMS: calcd. ($M+H^+$): $C_{29}H_{37}O_6S$ 513.2305, found 513.2303.

4-(2-((tert-butoxycarbonyl)aminoethoxy)-9-butoxy-6,7-dihydro-dibenzo[a,e]cyclopropa[c][8]annulen-1-one (photo-DIBO-Boc, 4.08).

To a solution of photo-DIBO-OH[12] **4.01** (0.700 g, 2.185 mmol) in DMF (40 mL) was added 2-((tert-butoxycarbonyl)amino)ethyl 4-methylbenzenesulfonate[25] **4.07** (0.689 g, 2.185 mmol). Next, K_2CO_3 (0.302 g, 2.185 mmol) was added and the solution was stirred and heated to 80 °C for 3 hours. The reaction was then diluted with CH_2Cl_2 (200 mL), washed with water (5 x 50 ml), brine (100 mL), and dried over $MgSO_4$. The organic layer was filtered, concentrated in vacuo, and purified via silica flash chromatography (40: 1 CH_2Cl_2: methanol) to provide photo-DIBO-Boc-amine **4.08** (0.985 g, 97% yield) as a white solid (147-150 °C MP). ^{1}H-NMR: 7.89-7.91 (dd, J = 8.4, 2.4 Hz, 2H), 6.86-6.87 (m, 4H), 4.08-4.10 (t, J = 5.2 Hz, 2H), 4.01-4.04 (t, J = 6.5 Hz, 2H), 3.55-3.56 (m, 2H), 3.29-3.32 (d, J = 10.6 Hz, 2H), 2.57-2.60 (d, J = 11.8 Hz, 2H), 1.75-1.82 (m, 2H), 1.44-1.54 (m, 11H), 0.96-0.99 (t, J = 7.4 Hz, 3H). ^{13}C-NMR: 162.25, 161.48, 156.04, 153.84, 148.00, 147.89, 142.71, 142.02, 135.93, 135.82, 116.90, 116.34, 116.25, 116.11, 112.64, 112.45, 79.78, 68.15, 67.57, 40.13, 37.31, 37.29, 31.28, 28.54, 19.34, 13.97. ESI HRMS: calcd. ($M+H^+$): $C_{28}H_{34}NO_5^+$ 464.2432, found 464.2421. IR: 1845 cm^{-1} ($\nu_{C=O}$).

4-(2-aminoethoxy)-9-butoxy-6,7-dihydro-dibenzo[a,e]cyclopropa[c][8]annulen-1-one (photo-DIBO-NH_2, 4.09).

TFA (0.980 g, 8.51 mmol) was added to a solution of Photo-DIBO-Boc-amine **4.08** (0.493 g, 1.063 mmol) in CH_2Cl_2 (6 mL) at rt. The reaction mixture was stirred overnight, quenched with

water (50 mL), and diluted with CH_2Cl_2 (200 mL). The organic layer was extracted, concentrated in vacuo, and purified via flash chromatography (10: 1 CH_2Cl_2: methanol) to afford photo-DIBO-NH_2 **4.09** (0.353 g, 91% yield) as an off white powder (133-136 °C MP). ^{1}H-NMR: 7.90-7.92 (d, J = 8.5 Hz, 2H), 6.86-6.89 (m, 4H), 4.01-4.07 (m, 4H), 3.30-3.32 (d, J = 10.6 Hz, 2H), 3.10-3.13 (t, J = 5.1 Hz, 2H), 2.58-2.61 (d, J = 10.6 Hz, 2H), 1.75-1.82 (m, 2H), 1.45-1.54 (m, 2H), 0.96-1.00 (t, J = 7.4 Hz, 3H). ^{13}C-NMR: 162.26, 161.87, 153.88, 147.99, 147.92, 142.60, 142.15, 135.94, 135.88, 116.78, 116.39, 116.36, 112.55, 112.46, 70.54, 68.18, 41.53, 37.34, 37.32, 31.31, 19.35, 13.96. ESI HRMS: calcd. ($M+H^+$): $C_{23}H_{26}NO_3^+$ 364.1907, found 364.1900. IR: 1843 cm^{-1} ($\nu_{C=O}$).

4-oxo-4-(3,4,9-trihydroxy-2-methoxy-1-oxo-1H-dibenzo[b,f]cyclopropa[d]azocin-6(7H)-yl)butanoic acid (TH-photo-ADIBO, 4.13).

BBr_3 (5.22 g, 20.82 mmol) was added dropwise to a solution of 4-oxo-4-(2,3,4,9-tetramethoxy-1-oxo-1H-dibenzo[b,f]cyclopropa[d]azocin-6(7H)-yl)butanoic acid (1.180 g, 2.60 mmol), in dichloromethane (50 mL), at -78 °C, under inert atmosphere. The reaction mixture was warmed to room temperature and stirred for 3 days. Quenching of the reaction was done by pouring the reaction mixture onto ice (50 mL). The crude product was then filtered and purified via flash chromatography to afford TH-photo-ADIBO **4.13** (0.59 g, 55.1 %) as a light tan solid. ^{1}H-NMR (DMSO-d_6): 7.60-7.62 (d, J = 8.0 Hz, 1H), 7.02 (s, 1H), 6.79-6.84 (m, 2H), 4.88-4.92 (d, J = 14.6 Hz, 1H), 4.12-4.15 (d, J = 14.4 Hz, 1H), 3.94 (s, 3H), 2.42-2.54 (m, 1H), 2.16-2.27 (m, 2H), 1.82-1.86 (m, 1H). ^{13}C-NMR (DMSO-d_6): 173.58, 171.14, 160.63, 150.80, 150.68, 149.16, 142.77, 141.68, 138.36, 136.21, 135.80, 135.18, 119.08, 114.81, 113.85, 112.57, 108.65, 62.09, 55.84, 29.05, 28.95. ESI HRMS: calcd. ($M+H^+$): $C_{21}H_{18}NO_8^+$ 412.1027, found 412.1031.

4-(4,9-dihydroxy-1-oxo-1H-dibenzo[b,f]cyclopropa[d]azocin-6(7H)-yl)-4-oxobutanoic acid (DH-photo-AIDBO, 4.17).

BBr_3 (10.97 g, 43.8 mmol) was added dropwise to a solution of methyl 4-(4,9-dimethoxy-1-oxo-1H-dibenzo[b,f]cyclopropa[d]azocin-6(7H)-yl)-4-oxobutanoic acid (1.435 g, 3.65 mmol), in dichloromethane (40 mL), at -78 °C, under inert atmosphere. The reaction mixture was warmed to room temperature and stirred for 3 days. Quenching of the reaction was done by pouring the reaction mixture onto ice (50 mL). The crude product was then filtered and purified via flash chromatography to afford DH-photo-ADIBO **4.17** (0.941 g, 71 %) as a light yellow powder. ^{1}H-NMR (DMSO-d_6): 7.74-7.76 (m, 1H), 7.57-7.59 (d, J = 8.3 Hz, 1H),7.04-7.06 (m, 2H), 6.97-6.99 (m, 1H), 6.83-6.85 (d, J = 8.4 Hz, 1H), 4.90-4.94 (m, 1H), 4.12-4.16 (m, 1H), 2.48-2.50 (m, 1H), 2.17-2.26 (m, 2H), 1.83-1.89 (m, 1H). ^{13}C-NMR (DMSO-d_6): 171.29, 162.35, 160.83, 151.03, 146.00, 142.41, 141.23, 140.93, 138.37, 134.87, 134.39, 119.55, 116.89, 115.96, 114.96, 113.92, 112.75, 55.38, 29.71, 29.56. ESI HRMS: calcd. ($M+H^+$): $C_{20}H_{16}NO_6^+$ 366.0972, found 366.0961.

Aza-Dibenzocyclooctyne-Acid (ADIBO-CO_2H, 4.20).

Succinic anhydride (0.207 g, 2.070 mmol) was added to a solution of ADIBO-NH_2[26] **4.19** (0.440 g, 1.592 mmol), triethylamine (0.444 mL, 3.18 mmol), and chloroform (30 mL). The reaction mixture was stirred for 4 hours, concentrated in vacuo, and purified via silica gel chromatography (CH_2Cl_2/MeOH 20:1) to afford ADIBO-CO_2H **4.20** (0.496 g, 1.319 mmol, 83% yield) as an off white crystal. ^{1}H-NMR: 7.65-7.67 (d, J = 7.67 Hz, 1H), 7.27-7.40 (m, 7H), 6.54 (bs, 1H), 5.11-5.15 (d, J = 13.9 Hz, 1H), 3.69-3.73 (d, J = 13.9 Hz, 1H), 3.34-3.41 (m, 1H), 3.15-3.21 (m, 1H), 2.56-2.66 (m, 2H), 2.44-2.51 (m, 1H), 2.28-2.39 (m, 2H), 1.94-2.01 (m, 1H). ^{13}C-NMR: 175.68, 172.62, 172.32, 151.12, 148.01, 132.36, 129.23, 128.89, 128.76, 128.54, 128.13,

127.48, 125.82, 123.12, 122.75, 115.05, 107.91, 55.86, 35.72, 34.69, 30.86, 30.04, 34.5. ESI HRMS: calcd. ($M+H^+$): $C_{22}H_{20}N_2O_4$ 377.1495, found: 377.1492

2-(2-(2-(2-(2-(9-butoxy-5,6-didehydro-11,12-dihydrodibenzo[a,e]-[8]annulen-2-yl)oxy)ethoxy)ethoxy)ethoxy)ethyl amine (DIBO-PEG-NH_2, 4.23).

Please See Chapter 3 for the synthesis of DIBO-PEG-NH_2 **4.23**.

2-tert-butyl-11,12-didehydro-8-(2-(2-(2-(2-aminoethoxy)ethoxy)ethoxy)ethoxy)-6H-dibenzo[b,f]oxocine (ODIBO-PEG-NH_2, 4.24).

Please See Chapter 3 for the synthesis of ODIBO-PEG-NH_2 **4.24**.

4.09 References

1. Arnold, R. M.; Huddleston, N. E.; Locklin, J. Utilizing Click Chemistry to Design Functional Interfaces Through Post-Polymerization <odification. *J. Mater. Chem.*, **2012,** *22*, 19357-19365.

2. Arnold, R. M.; Patton, D. L.; Popik, V. V.; Locklin, J. A Dynamic Duo: Pairing Click Chemistry and Postpolymerization Modification To Design Complex Surfaces. *Acc. Chem. Res.*, **2014,** *47*, 2999-3008.

3. Zeng, D.; Zeglis, B. M.; Lewis, J. S.; Anderson, C. J. The Growing Impact of Bioorthogonal Click Chemistry on the Development of Radiopharmaceuticals. *J. Nucl. Med.*, **2013,** *54*, 829-832.

4. Thirumurugan, P.; Matosiuk, D.; Jozwiak, K. Click Chemistry for Drug Development and Diverse Chemical–Biology Applications. *Chem. Rev.*, **2013,** *113*, 4905-4979.

5. Sapsford, K. E.; Algar, W. R.; Berti, L.; Gemmill, K. B.; Casey, B. J.; Oh, E.; Stewart, M. H.; Medintz, I. L. Functionalizing Nanoparticles with Biological Molecules: Developing Chemistries that Facilitate Nanotechnology. *Chem. Rev.*, **2013,** *113*, 1904-2074.

6. Wang, Z.; Liu, J.; Arslan, H. K.; Grosjean, S.; Hagendorn, T.; Gliemann, H.; Bräse, S.; Wöll, C. Post-Synthetic Modification of Metal–Organic Framework Thin Films Using Click Chemistry: The Importance of Strained C–C Triple Bonds. *Langmuir*, **2013,** *29*, 15958-15964.

7. Ledin, P. A.; Xu, W.; Friscourt, F.; Boons, G.-J.; Tsukruk, V. V. Branched Polyhedral Oligomeric Silsesquioxane Nanoparticles Prepared via Strain-Promoted 1,3-Dipolar Cycloadditions. *Langmuir*, **2015,** *31*, 8146-8155.

8. Wendeln, C.; Singh, I.; Rinnen, S.; Schulz, C.; Arlinghaus, H. F.; Burley, G. A.; Ravoo, B. J. Orthogonal, Metal-Free Surface Modification by Strain-Promoted Azide-Alkyne and Nitrile Oxide-Alkene/Alkyne Cycloadditions. *Chem. Sci.*, **2012,** *3*, 2479-2484.

9. Orski, S. V.; Poloukhtine, A. A.; Arumugam, S.; Mao, L.; Popik, V. V.; Locklin, J. High Density Orthogonal Surface Immobilization via Photoactivated Copper-Free Click Chemistry. *J. Am. Chem. Soc.*, **2010,** *132*, 11024-11026.

10. Gobbo, P.; Mossman, Z.; Nazemi, A.; Niaux, A.; Biesinger, M. C.; Gillies, E. R.; Workentin, M. S. Versatile Strained Alkyne Modified Water-Soluble AuNPs for Interfacial Strain Promoted Azide-Alkyne Cycloaddition (I-SPAAC). *J. Mater. Chem. B.*, **2014,** *2*, 1764-1769.

11. Luo, W.; Gobbo, P.; McNitt, C.; Sutton, D.; Popik, V.; Workentin, M. 'Shine & Click' Photoinduced Interfacial Unmasking of Strained-Alkynes on Small Water Soluble Gold Nanoparticles. *Chem. Eur. J.*, **2016**, *Accepted*.

12. Poloukhtine, A. A.; Mbua, N. E.; Wolfert, M. A.; Boons, G. J.; Popik, V. V. Selective Labeling of Living Cells by a Photo-Triggered Click Reaction. *J. Am. Chem. Soc.*, **2009,** *131*, 15769-15776.

13. Barbey, R.; Lavanant, L.; Paripovic, D.; Schüwer, N.; Sugnaux, C.; Tugulu, S.; Klok, H.-A. Polymer Brushes via Surface-Initiated Controlled Radical Polymerization: Synthesis, Characterization, Properties, and Applications. *CHem. Rev.*, **2009,** *109*, 5437-5527.

14. Luzinov, I.; Julthongpiput, D.; Malz, H.; Pionteck, J.; Tsukruk, V. V. Polystyrene Layers Grafted to Epoxy-Modified Silicon Surfaces. *Macromolecules*, **2000,** *33*, 1043-1048.

15. Jones, R. A. L.; Lehnert, R. J.; Schonherr, H.; Vancso, J. Factors Affecting the Preparation of Permanently End-Grafted Polystyrene Layers. *Polymer*, **1999,** *40*, 525-530.

16. Laradji, A. M.; McNitt, C. D.; Yadavalli, N. S.; Popik, V. V.; Minko, S. Robust, Solvent-Free, Catalyst-Free Click Chemistry for the Generation of Highly Stable Densely Grafted Poly(ethylene glycol) Polymer Brushes by the Grafting To Method and Their Properties. *Macromolecules*, **2016,** *49*, 7625-7631.

17. Starke, F.; Walther, M.; Pietzsch, H.-J. A Novel Dibenzoazacyclooctyne Precursor in Regioselective Copper-Free Click Chemistry. An Innovative 3-Step Synthesis. *ARKIVOC*, **2010,** *xi*, 350-359.

18. Debets, M. F.; Prins, J. S.; Merkx, D.; van Berkel, S. S.; van Delft, F. L.; van Hest, J. C. M.; Rutjes, F. P. J. T. Synthesis of DIBAC Analogues with Excellent SPAAC Rate Constants. *Org. Biomol. Chem.*, **2014,** *12*, 5031-5037.

19. Hall, M. D.; Mellor, H. R.; Callaghan, R.; Hambley, T. W. Basis for Design and Development of Platinum(IV) Anticancer Complexes. *J. Med. Chem.*, **2007,** *50*, 3403-3411.

20. Pathak, R. K.; Marrache, S.; Choi, J. H.; Berding, T. B.; Dhar, S. The Prodrug Platin-A: Simultaneous Release of Cisplatin and Aspirin. *Angew. Chem. Int. Ed.*, **2014,** *53*, 1963-1967.

21. Pathak, R. K.; McNitt, C. D.; Popik, V. V.; Dhar, S. Copper-Free Click-Chemistry Platform to Functionalize Cisplatin Prodrugs. *Chem. Eur. J.*, **2014,** *20*, 6861-6865.

22. Alam, S.; Alves, D. S.; Whitehead, S. A.; Bayer, A. M.; McNitt, C. D.; Popik, V. V.; Barrera, F. N.; Best, M. D. A Clickable and Photocleavable Lipid Analogue for Cell Membrane Delivery and Release. *Bioconjugate Chem.*, **2015,** *26*, 1021-1031.

23. Arnold, R. M.; McNitt, C. D.; Popik, V. V.; Locklin, J. Direct Grafting of Poly(pentafluorophenyl acrylate) onto Oxides: Versatile Substrates for Reactive Microcapillary Printing and Self-Sorting Modification. *Chem. Commun.*, **2014,** *50*, 5307-5309.

24. Brooks, K.; Yatvin, J.; McNitt, C. D.; Reese, R. A.; Jung, C.; Popik, V. V.; Locklin, J. Multifunctional Surface Manipulation Using Orthogonal Click Chemistry. *Langmuir*, **2016,** *32*, 6600-6605.

25. Loison, S.; Cottet, M.; Orcel, H.; Adihou, H.; Rahmeh, R.; Lamarque, L.; Trinquet, E.; Kellenberger, E.; Hibert, M.; Durroux, T.; Mouillac, B.; Bonnet, D. Selective fluorescent nonpeptidic antagonists for vasopressin V(2) GPCR: application to ligand screening and oligomerization assays. *J Med Chem*, **2012,** *55*, 8588-602.

26. Kuzmin, A.; Poloukhtine, A.; Wolfert, M. A.; Popik, V. V. Surface Functionalization Using Catalyst-Free Azide−Alkyne Cycloaddition. *Bioconjugate Chem.*, **2010,** *21*, 2076-2085.

APPENDIX A

^{1}H NMR, ^{13}C NMR

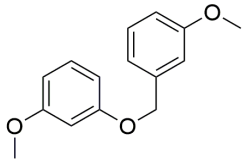

2.02

3.85
3.81
5.05
6.92
6.91
6.91
6.91
6.90
6.89
6.89
6.89
6.63
6.63
6.63
6.63
6.61
6.61
6.61
6.60
6.59
6.59
6.58
6.58
6.58
6.57
6.56
6.56
6.56
6.55
6.55
6.56
6.56
6.56
6.57
6.58
6.58
6.58
6.59
6.59
6.60
6.61
6.61
6.61
6.61
6.61
6.63
6.63
6.63
6.63
6.91
7.03
7.03
7.04
7.06
7.06
7.20
7.22
7.24
7.31
7.33
3.17
3.04
2.08
2.84
0.99
1.91
0.97
1.00
f1 (ppm)

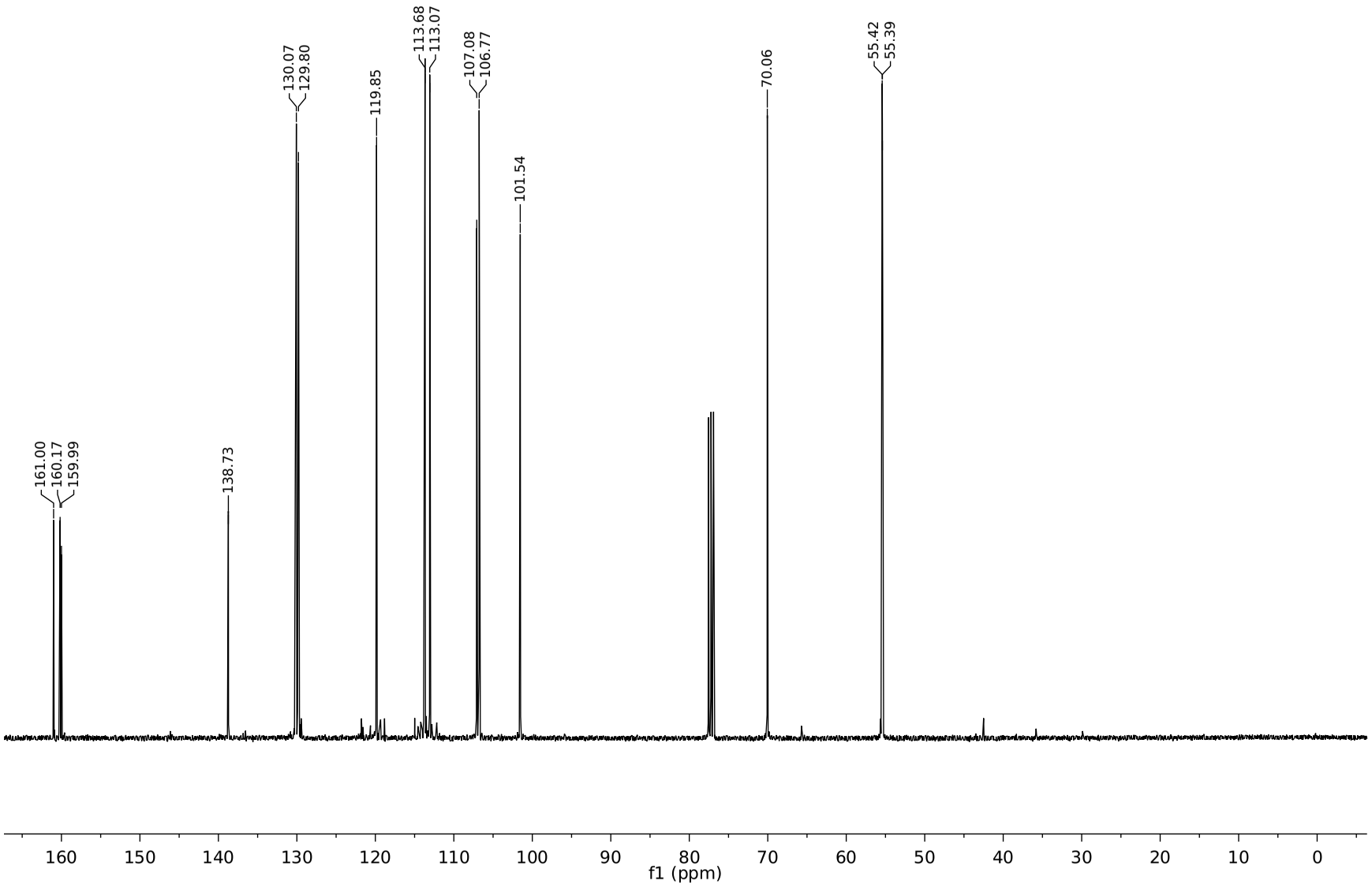
161.00
160.17
159.99
138.73
130.07
129.80
119.85
113.68
113.07
107.08
106.77
101.54
70.06
55.42
55.39
160
150
140
130
120
110
100
90
80
70
60
50
40
30
20
10
0
f1 (ppm)

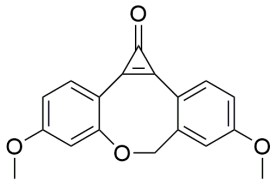

2.03

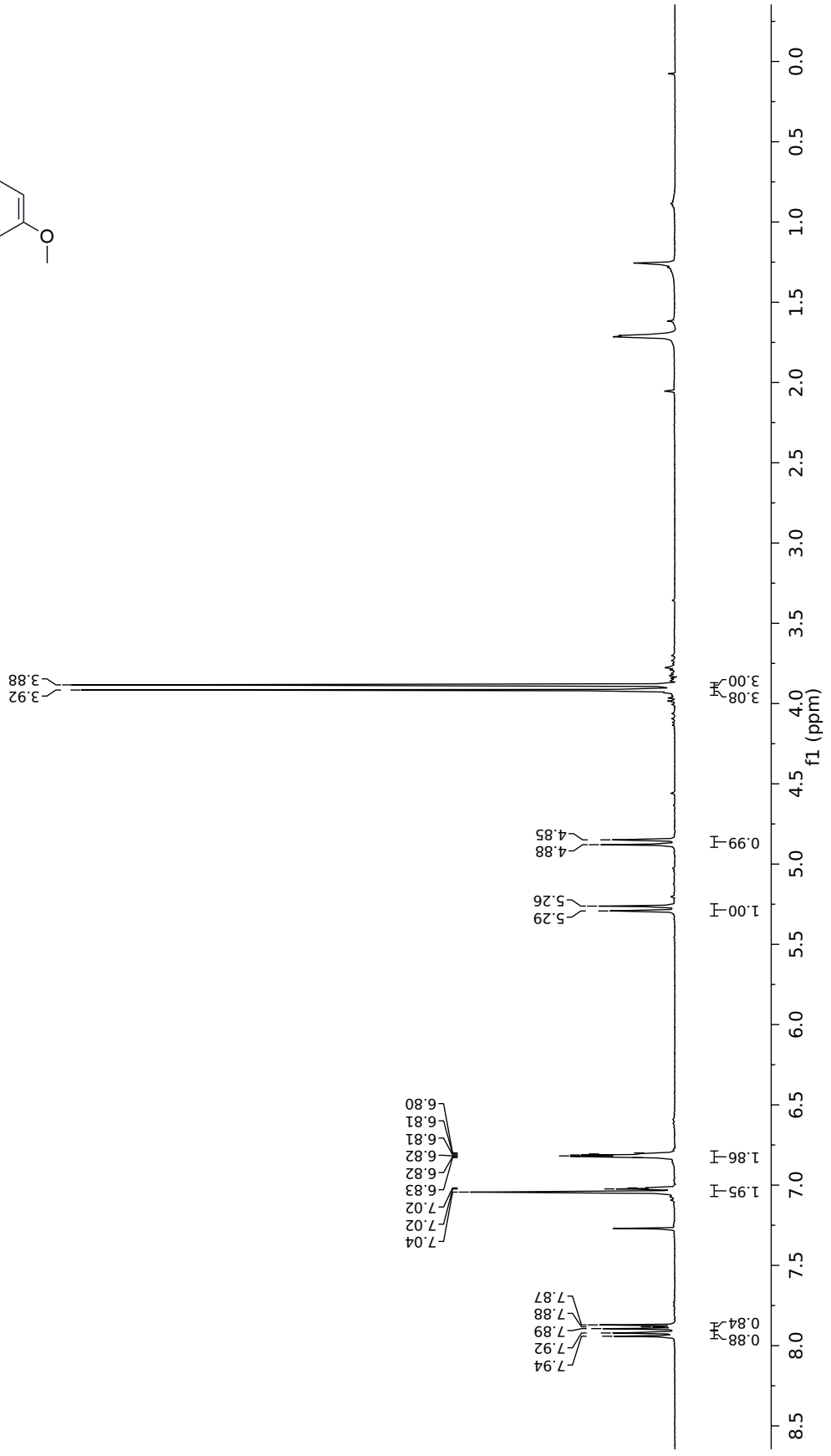
3.92
3.88
4.88
4.85
5.29
5.26
7.94
7.92
7.89
7.88
7.87
7.04
7.02
7.02
7.02
6.83
6.82
6.82
6.81
6.81
6.80
3.08
3.00
0.99
1.00
1.86
1.95
0.88
0.84
f1 (ppm)

164.57
164.13
162.59
152.25
141.97
140.76
140.25
135.58
135.23
118.23
117.14
114.21
111.05
110.51
108.33
78.67
55.97
55.91
f1 (ppm)

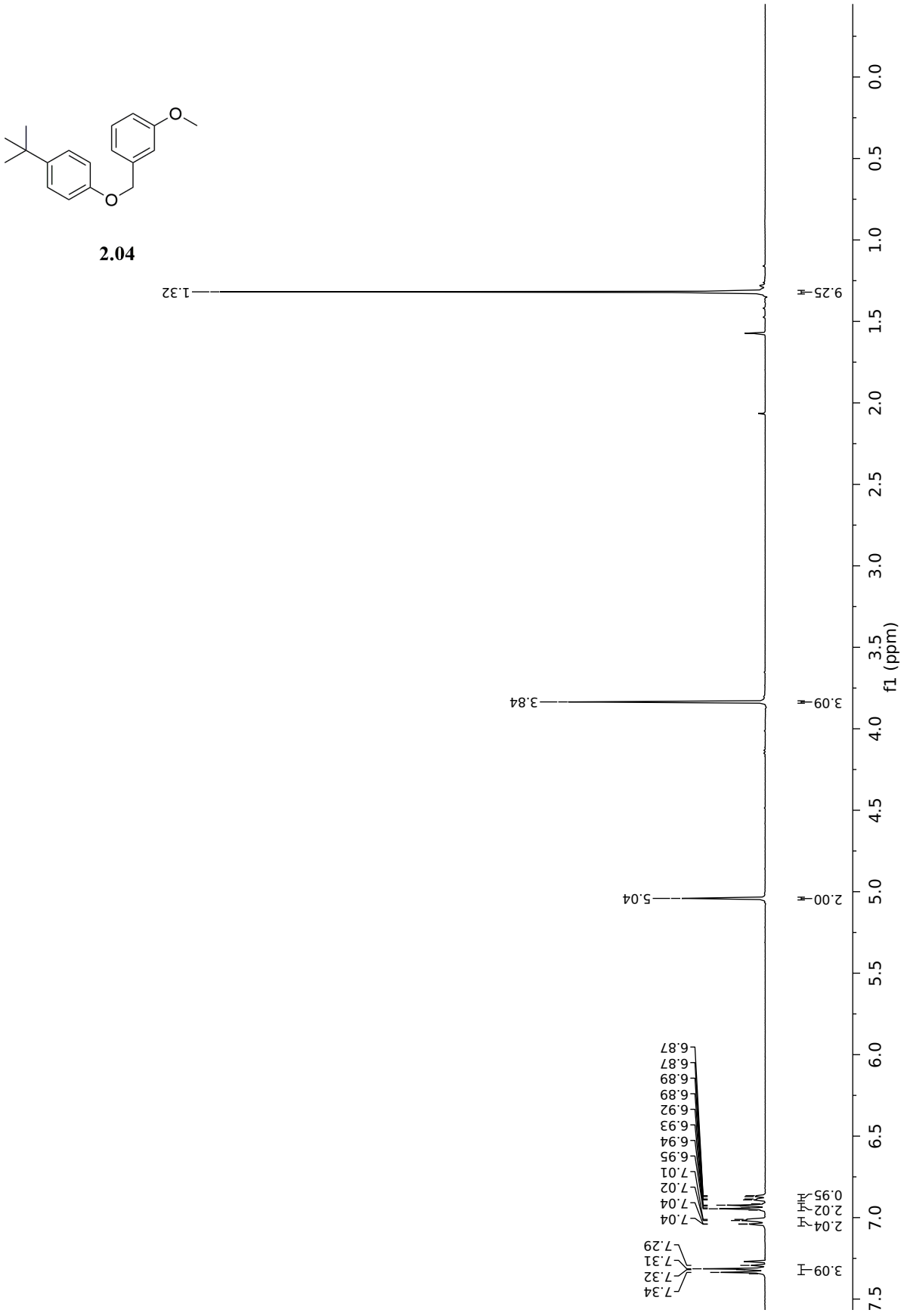
2.04
1.32
3.84
5.04
7.34
7.32
7.31
7.29
7.04
7.04
7.02
7.01
6.95
6.94
6.93
6.92
6.89
6.89
6.87
6.87
9.25
3.09
2.00
3.09
2.04
2.02
0.95
f1 (ppm)

160.04
156.76
143.85
139.14
129.81
126.46
119.87
114.50
113.65
113.09
70.14
55.46
34.30
31.74
f1 (ppm)

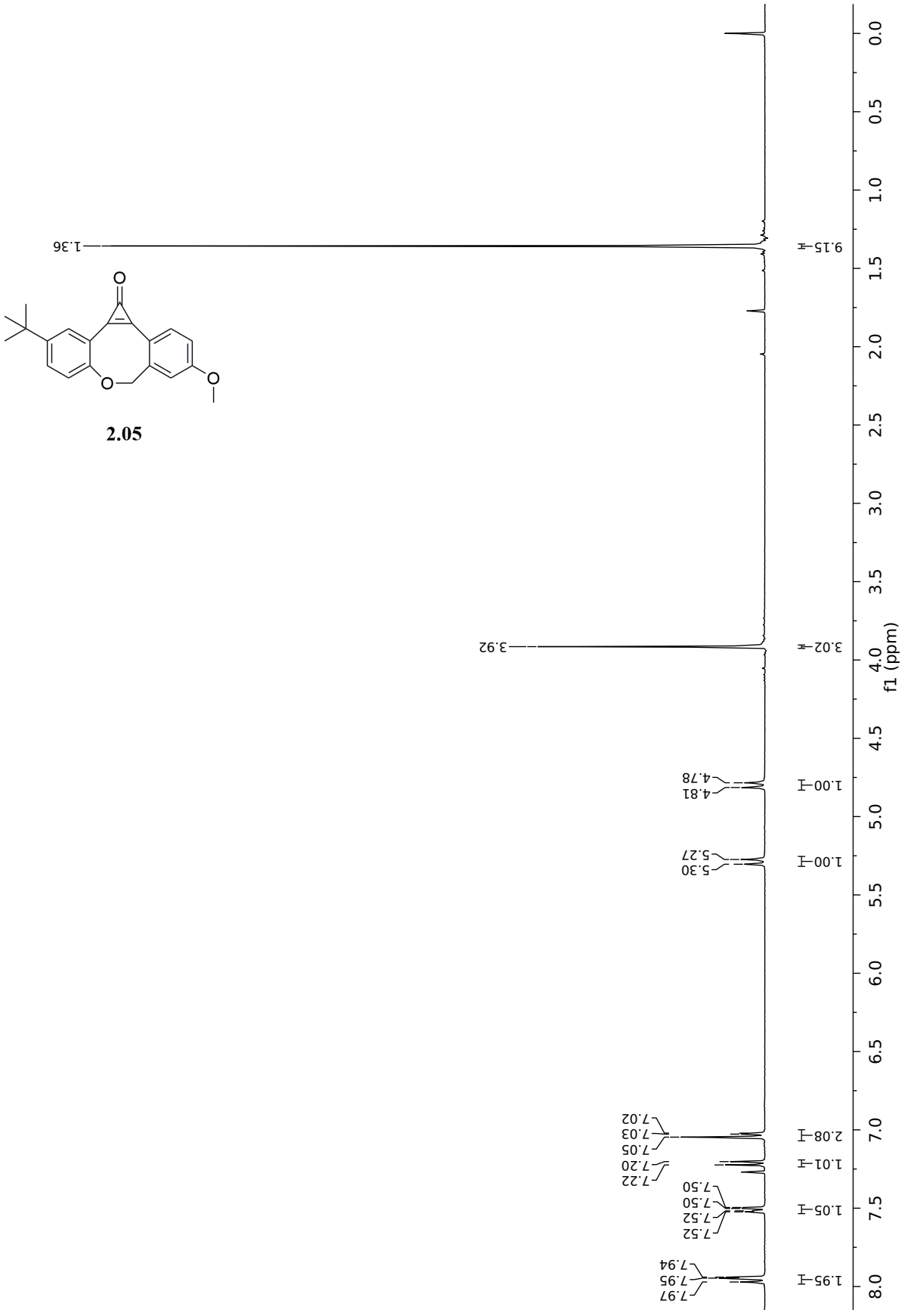
1.36
3.92
4.78
4.81
5.27
5.30
7.02
7.03
7.05
7.20
7.22
7.50
7.50
7.52
7.52
7.94
7.95
7.97
9.15
3.02
1.00
1.00
2.08
1.01
1.05
1.95
f1 (ppm)

2.05

162.93
160.56
152.82
148.17
144.25
142.41
140.81
135.67
131.24
130.78
122.12
117.99
117.21
117.00
114.17
78.90
55.90
34.78
31.55
f1 (ppm)

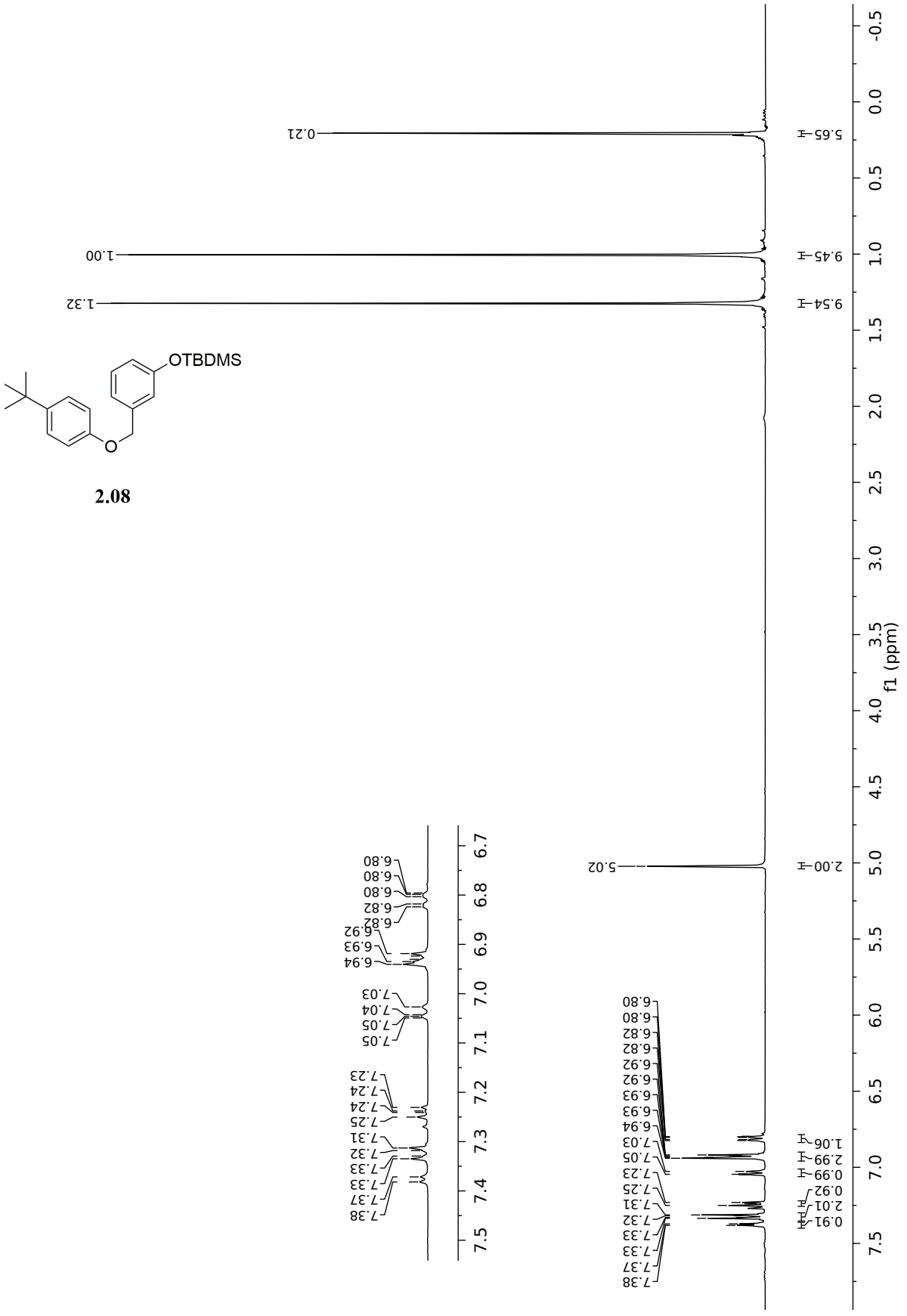
OTBDMS
O
2.08
f1 (ppm)

156.77
156.11
143.81
139.16
129.71
126.41
120.40
119.65
119.28
114.65
70.01
34.29
31.76
25.94
18.44
-4.18
f1 (ppm)

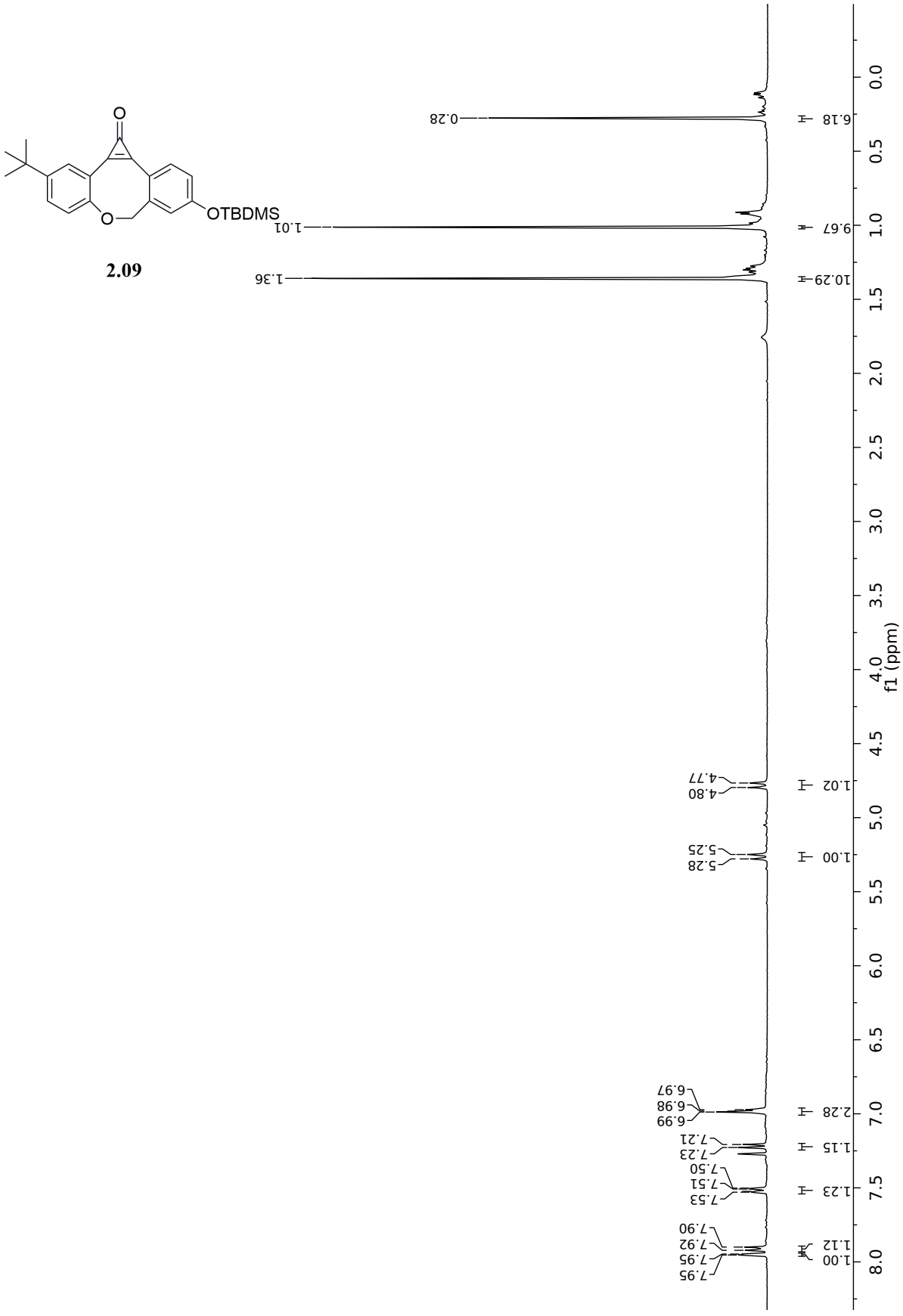
O
OTBDMS
O
2.09
0.28
1.01
1.36
4.77
4.80
5.25
5.28
6.97
6.98
6.99
7.21
7.23
7.50
7.51
7.53
7.90
7.92
7.95
7.95
6.18
9.67
10.29
1.02
1.00
2.28
1.15
1.23
1.12
1.00
f1 (ppm)

160.57
159.71
152.95
148.14
144.14
142.54
140.85
135.58
131.30
130.86
122.48
122.11
120.86
118.46
117.14
78.80
34.78
31.54
25.76
18.45
-4.09
f1 (ppm)

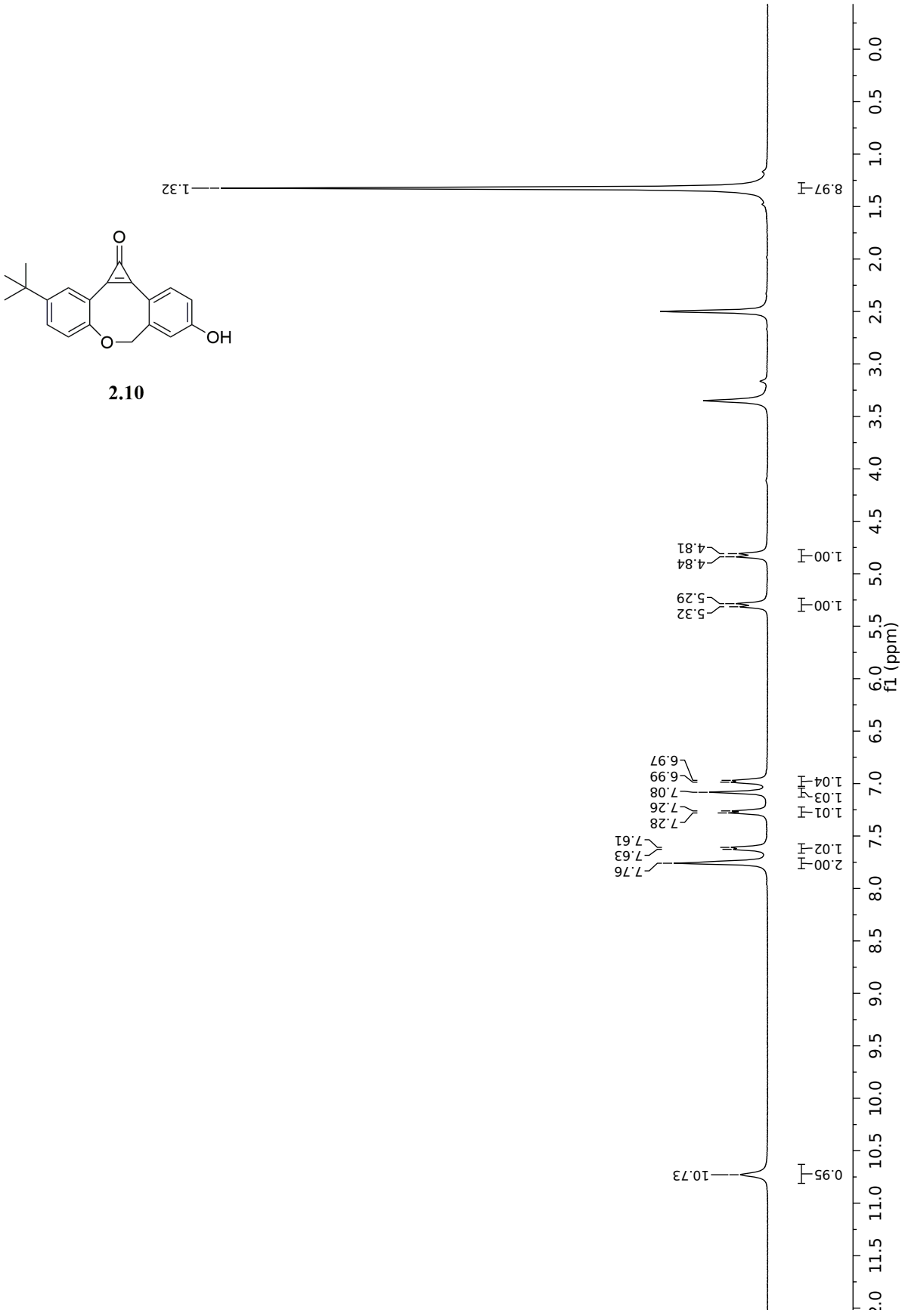
O
O
OH
1.32
8.97
4.81
4.84
5.29
5.32
6.97
6.99
7.08
7.26
7.28
7.61
7.63
7.76
10.73
1.00
1.00
1.04
1.03
1.01
1.02
2.00
0.95
f1 (ppm)

2.10

161.44
159.81
150.83
147.14
144.15
141.18
140.25
134.94
130.57
129.38
122.12
117.89
116.82
115.92
115.59
78.05
34.13
30.96
f1 (ppm)

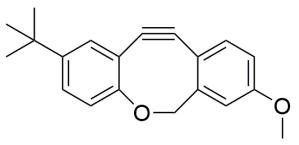

2.11

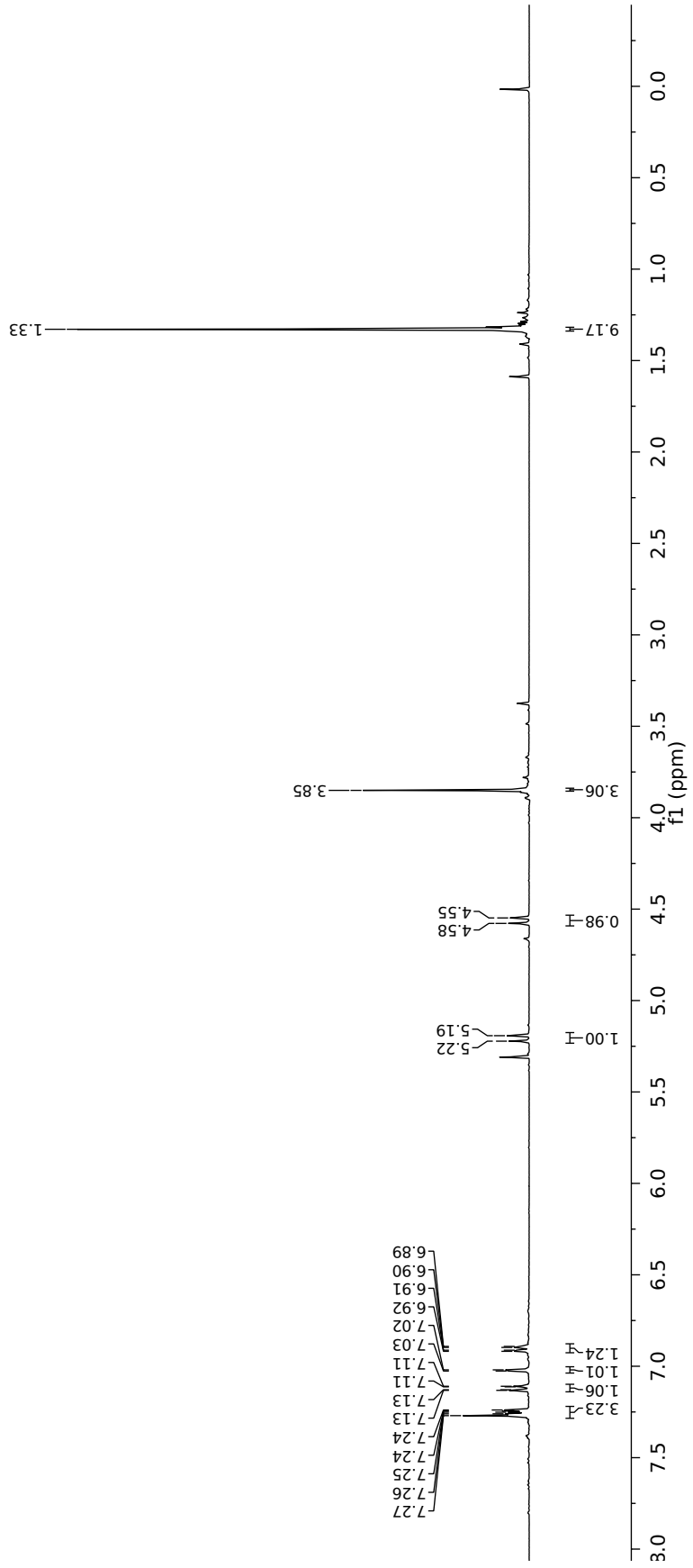
1.33
3.85
4.58
4.55
5.22
5.19
7.27
7.26
7.25
7.24
7.24
7.13
7.13
7.11
7.11
7.03
7.02
6.92
6.91
6.90
6.89
9.17
3.06
0.98
1.00
3.23
1.06
1.01
1.24
f1 (ppm)

167.39
159.64
149.21
147.01
126.96
125.58
123.75
121.41
118.25
117.76
117.31
114.28
113.95
110.75
78.11
55.71
34.60
31.61
f1 (ppm)

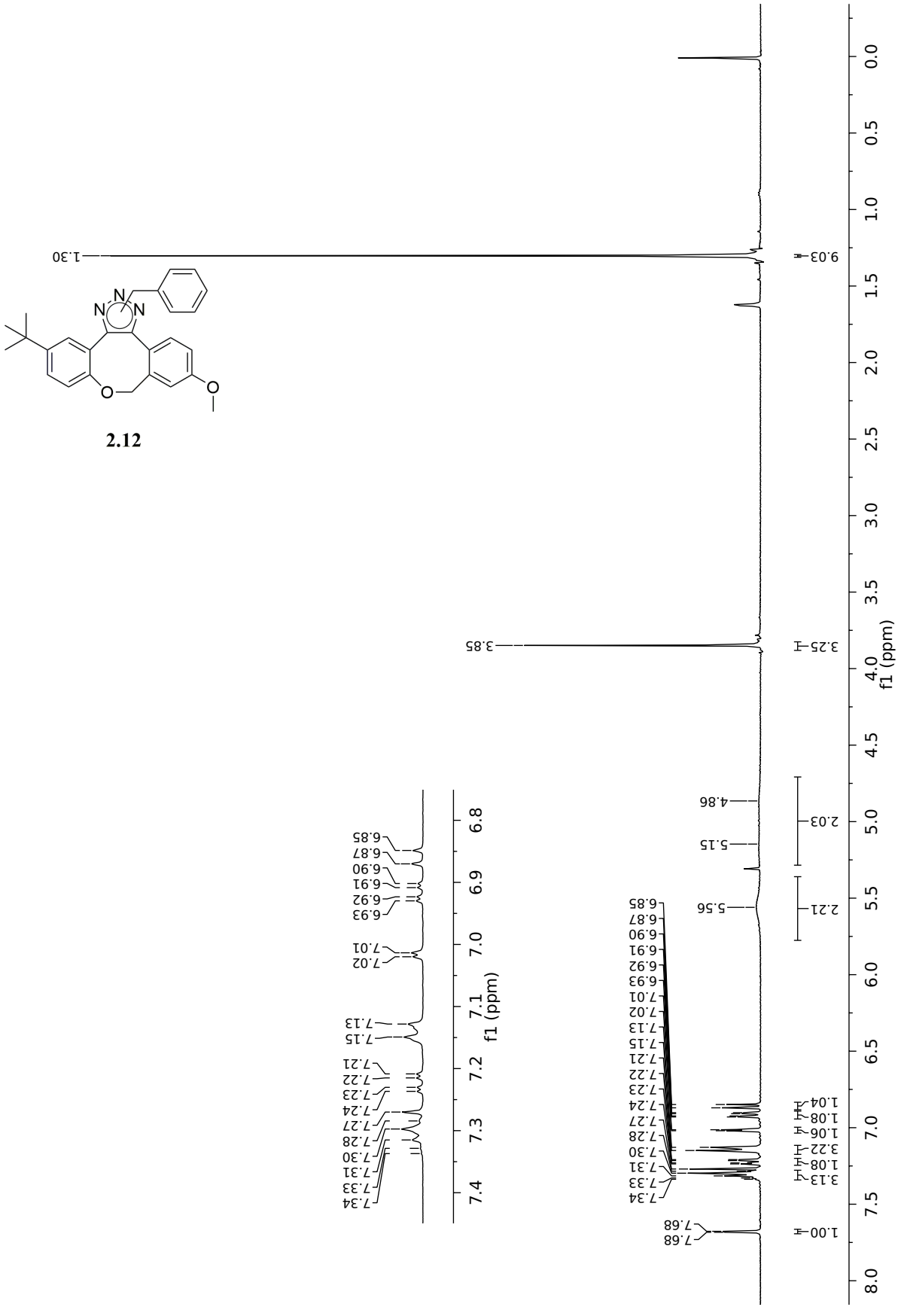
1.30
9.03
3.85
3.25
2.03
2.21
4.86
5.15
5.56
1.00
3.13
1.08
3.22
1.06
1.04
7.68
7.34
7.33
7.31
7.30
7.28
7.27
7.24
7.23
7.22
7.21
7.15
7.13
7.02
7.01
6.93
6.92
6.91
6.90
6.87
6.85
f1 (ppm)

2.12

160.80
152.36
145.49
144.33
138.53
135.93
132.58
130.44
129.88
129.04
128.37
127.28
127.20
120.06
119.57
116.78
115.89
115.23
69.68
55.68
52.33
34.36
31.61
f1 (ppm)

1.31
9.15
2.88
2.89
2.90
2.98
2.14
1.72
3.53
3.62
3.64
3.67
3.69
3.72
3.73
3.86
2.20
6.18
2.14
2.19
4.15
4.16
4.17
2.10
4.51
4.54
0.98
5.16
5.19
1.00
6.89
6.90
6.91
6.92
7.03
7.03
7.09
7.11
7.20
7.22
7.23
7.25
1.08
1.01
1.04
3.04
O
O
O
3
NH2
0.5
1.0
1.5
2.0
2.5
3.0
3.5
4.0
4.5
5.0
5.5
6.0
6.5
7.0
7.5
f1 (ppm)

3.01

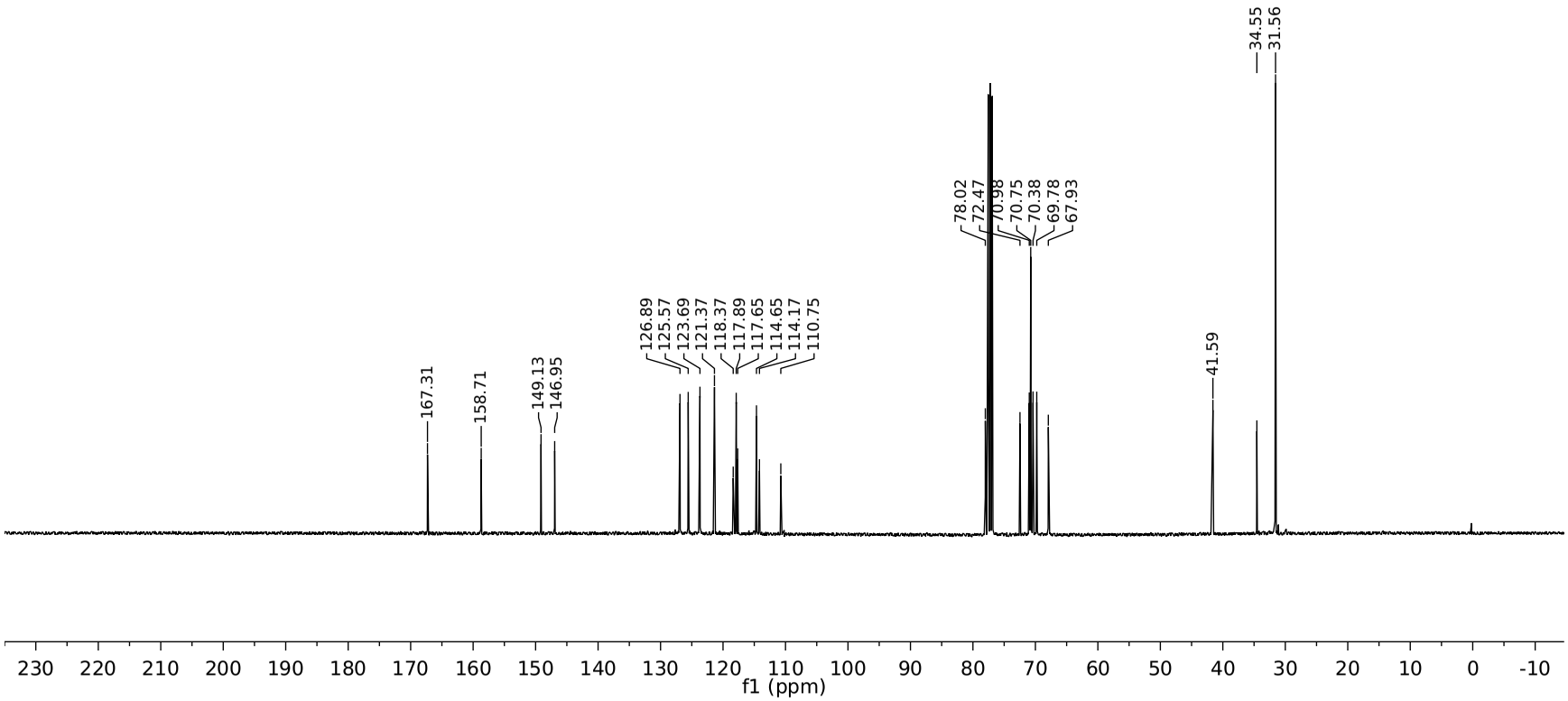
167.31
158.71
149.13
146.95
126.89
125.57
123.69
121.37
118.37
117.89
117.65
114.65
114.17
110.75
78.02
72.47
70.98
70.75
70.38
69.78
67.93
41.59
34.55
31.56
230 220 210 200 190 180 170 160 150 140 130 120 110 100 90 80 70 60 50 40 30 20 10 0 -10
f1 (ppm)

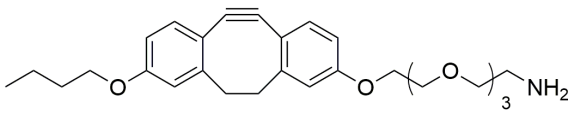

3.02

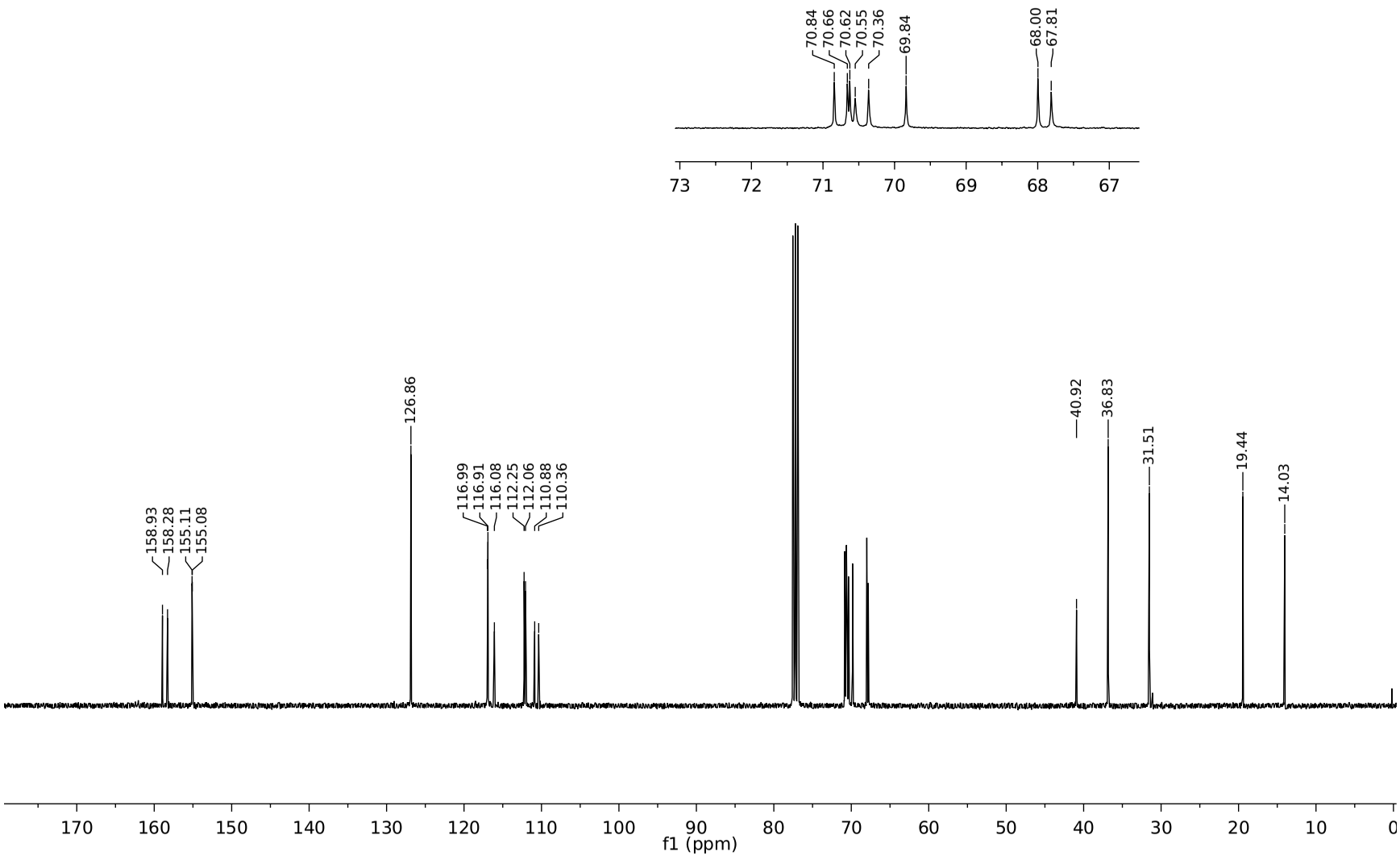
70.84
70.66
70.62
70.55
70.36
69.84
68.00
67.81
73
72
71
70
69
68
67
158.93
158.28
155.11
155.08
126.86
116.99
116.91
116.08
112.25
112.06
110.88
110.36
40.92
36.83
31.51
19.44
14.03
170
160
150
140
130
120
110
100
90
80
70
60
50
40
30
20
10
0
f1 (ppm)

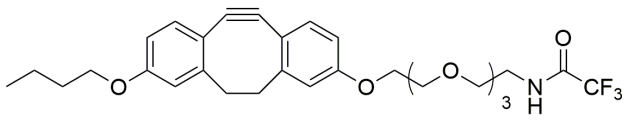

3.12

7.59
7.20
7.18
6.88
6.77
6.75
4.14
4.13
4.12
3.99
3.97
3.95
3.85
3.84
3.83
3.74
3.73
3.73
3.72
3.72
3.69
3.69
3.68
3.68
3.67
3.65
3.63
3.62
3.61
3.55
3.53
3.52
3.51
3.20
3.17
2.44
2.41
1.81
1.79
1.77
1.75
1.74
1.54
1.52
1.51
1.49
1.47
1.45
1.00
0.98
0.96
0.88
1.95
1.99
1.79
2.22
1.97
2.03
10.24
2.08
2.00
1.89
2.02
1.93
3.01
f1 (ppm)

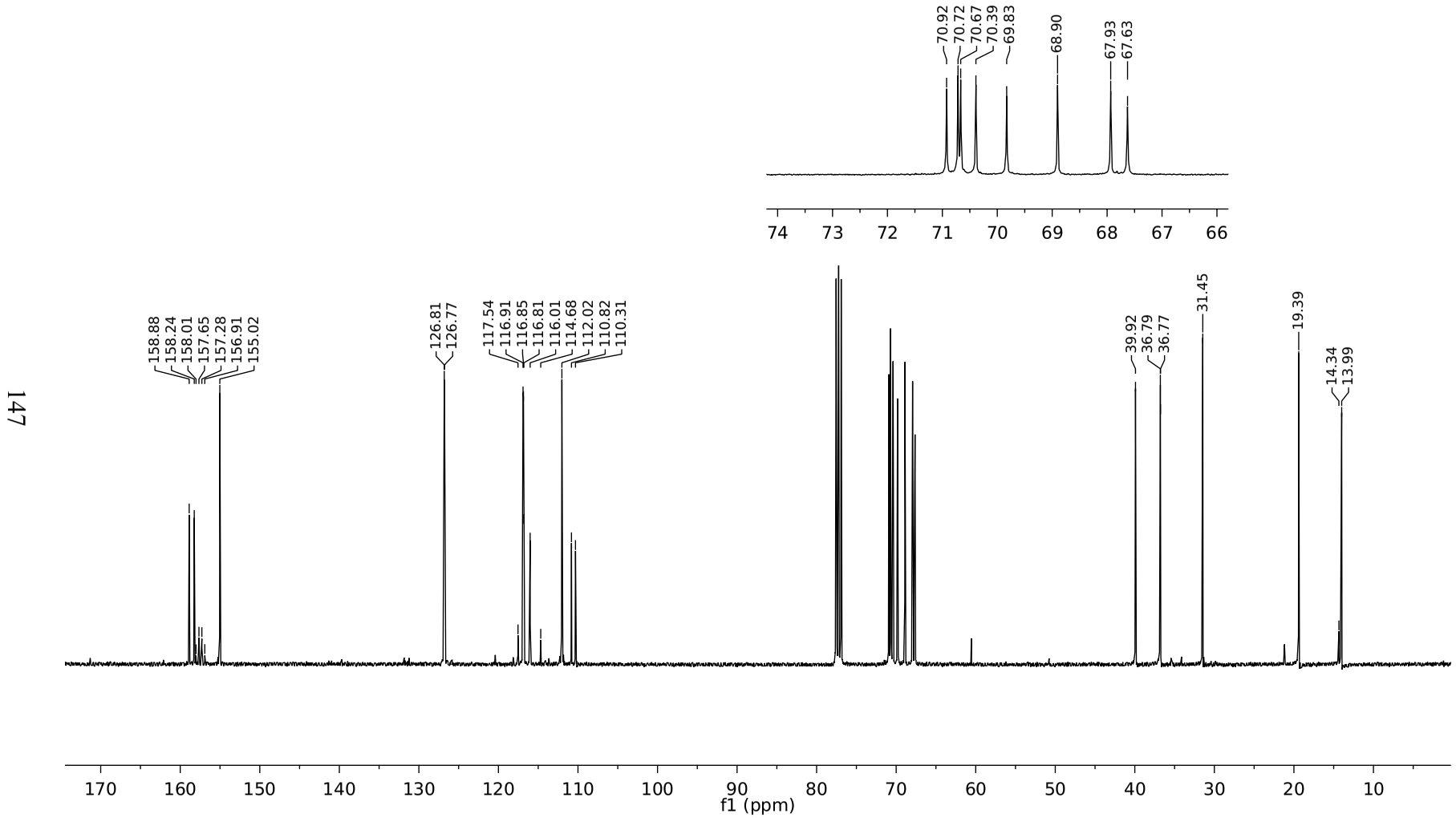
70.92
70.72
70.67
70.39
69.83
68.90
67.93
67.63
74
73
72
71
70
69
68
67
66
158.88
158.24
158.01
157.65
157.28
156.91
155.02
126.81
126.77
117.54
116.91
116.85
116.81
116.01
114.68
112.02
110.82
110.31
39.92
36.79
36.77
31.45
19.39
14.34
13.99
170
160
150
140
130
120
110
100
90
80
70
60
50
40
30
20
10
f1 (ppm)

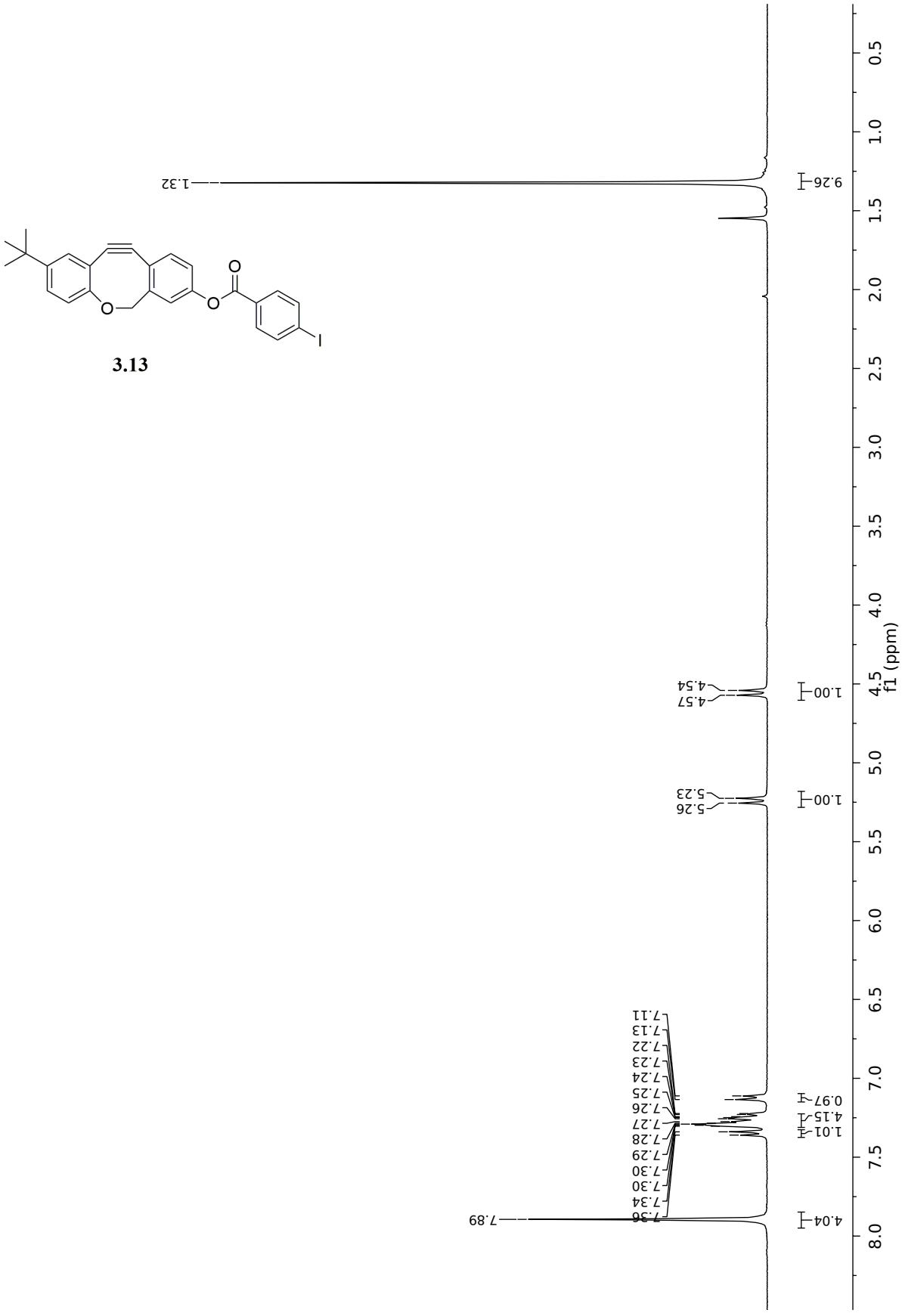
3.13
1.32
9.26
7.89
7.36
7.34
7.30
7.30
7.29
7.28
7.27
7.26
7.25
7.24
7.23
7.22
7.13
7.11
5.26
5.23
4.57
4.54
1.00
1.00
0.97
4.15
1.01
4.04
f1 (ppm)

167.78
164.73
150.20
148.96
147.18
138.28
131.76
128.93
126.77
126.23
124.47
124.05
124.00
122.42
121.58
117.13
113.17
112.67
102.09
77.65
34.63
31.60
f1 (ppm)

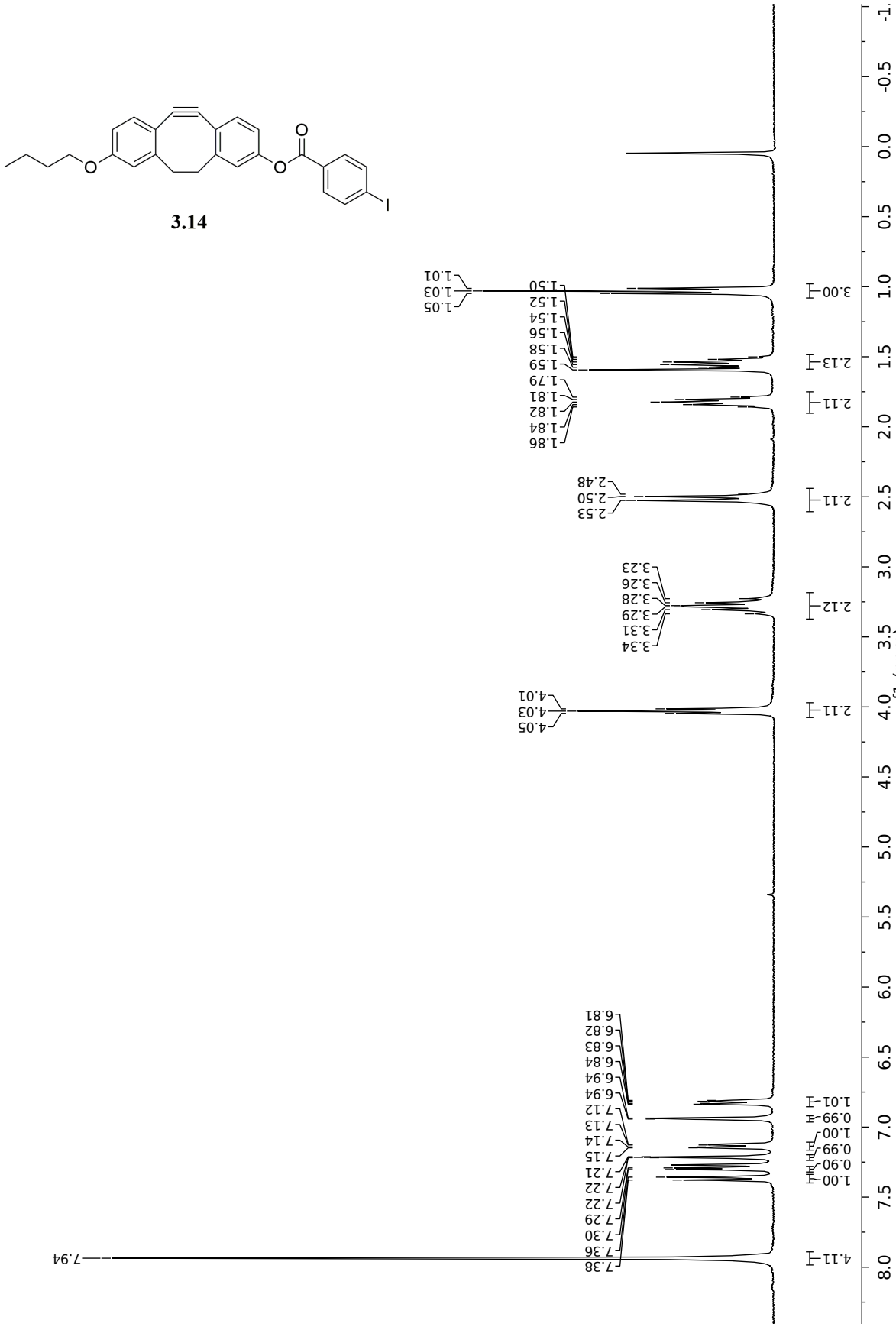
3.14
7.94
7.38
7.36
7.30
7.29
7.22
7.22
7.21
7.15
7.14
7.13
7.12
6.94
6.94
6.84
6.83
6.82
6.81
4.05
4.03
4.01
3.34
3.31
3.29
3.28
3.26
3.23
2.53
2.50
2.48
1.86
1.84
1.82
1.81
1.79
1.59
1.58
1.56
1.54
1.52
1.50
1.05
1.03
1.01
4.11
1.00
0.90
0.99
1.00
0.99
1.01
2.11
2.12
2.11
2.11
2.13
3.00
f1 (ppm)

164.93
159.32
155.46
154.73
149.90
138.23
131.73
129.13
127.25
126.71
123.08
122.61
119.80
116.97
115.51
112.50
112.23
109.56
101.94
68.04
36.71
36.67
31.51
19.46
14.06
f1 (ppm)

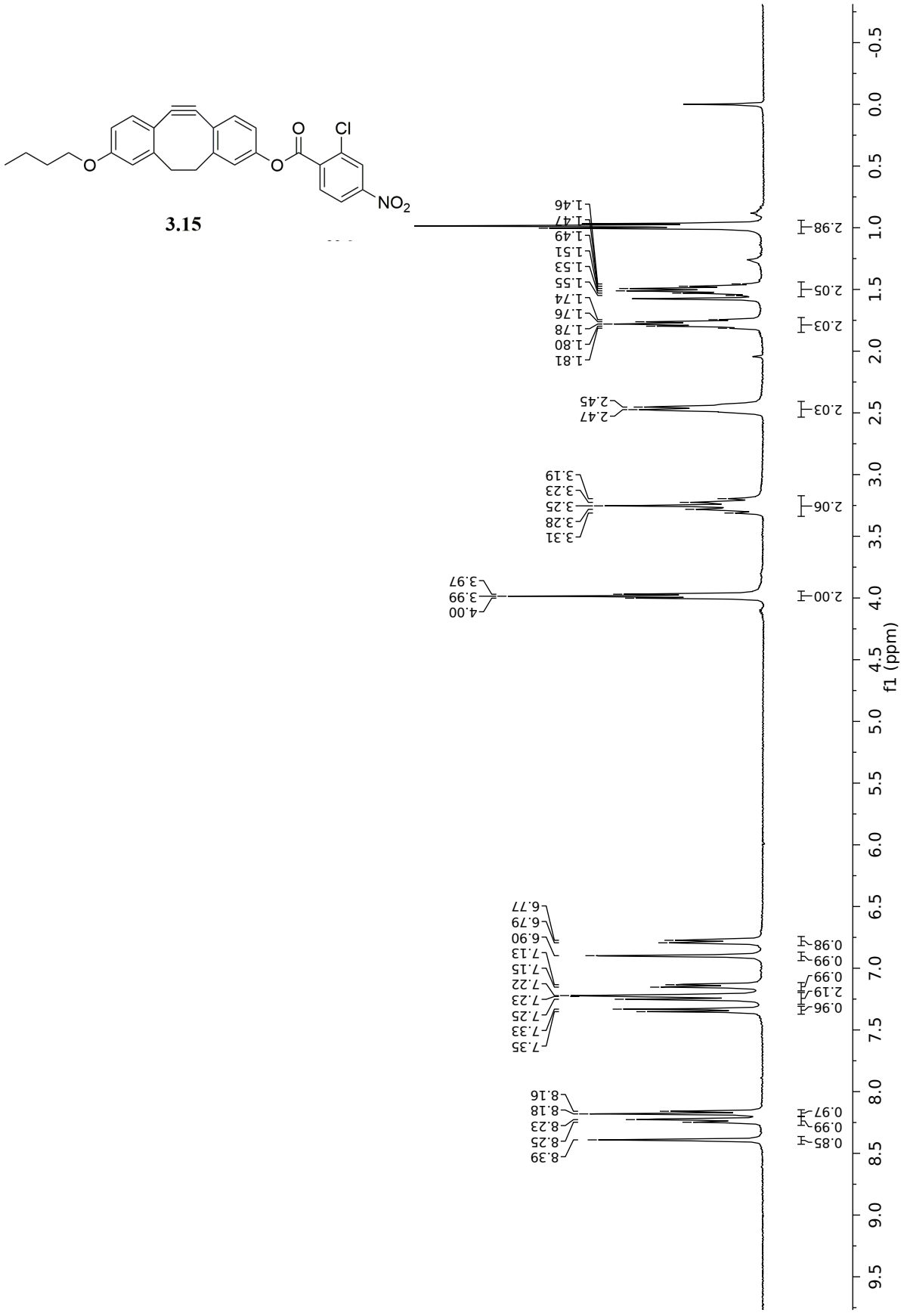
O
Cl
O
O
NO2
8.39
8.25
8.23
8.18
8.16
7.35
7.33
7.25
7.23
7.22
7.15
7.13
6.90
6.79
6.77
4.00
3.99
3.97
3.31
3.28
3.25
3.23
3.19
2.47
2.45
1.81
1.80
1.78
1.76
1.74
1.55
1.53
1.51
1.49
1.47
1.46
0.85
0.99
0.97
0.96
2.19
0.99
0.99
0.98
2.00
2.06
2.03
2.03
2.05
2.98
f1 (ppm)

3.15

162.81
159.37
155.42
154.84
150.01
149.26
135.67
135.14
132.71
127.30
126.79
126.47
123.24
122.68
121.81
119.50
116.99
115.29
112.87
112.20
109.26
68.01
36.63
31.47
19.44
14.06
f1 (ppm)

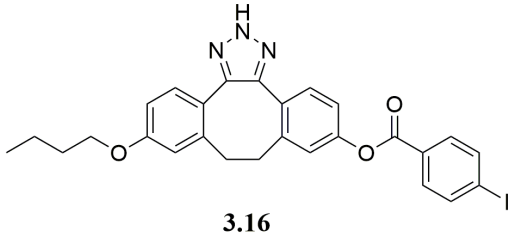

3.16

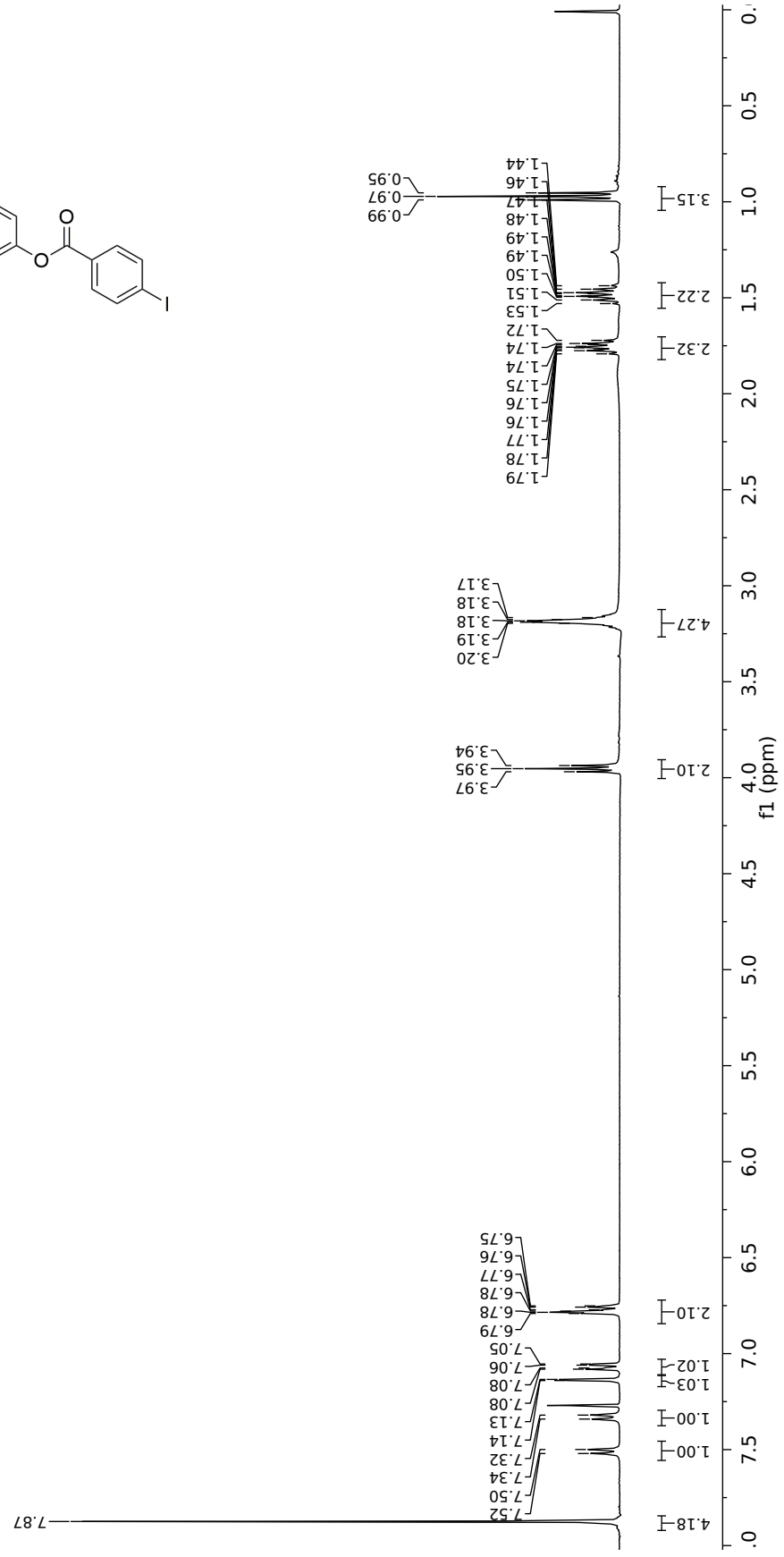
7.87
7.52
7.50
7.34
7.32
7.14
7.13
7.08
7.08
7.06
7.05
6.79
6.78
6.78
6.77
6.76
6.75
3.97
3.95
3.94
3.20
3.19
3.18
3.18
3.17
1.79
1.78
1.77
1.76
1.76
1.75
1.74
1.74
1.72
1.53
1.51
1.50
1.49
1.49
1.48
1.47
1.46
1.44
0.99
0.97
0.95
4.18
1.00
1.00
1.03
1.02
2.10
4.27
2.32
2.22
3.15
f1 (ppm)

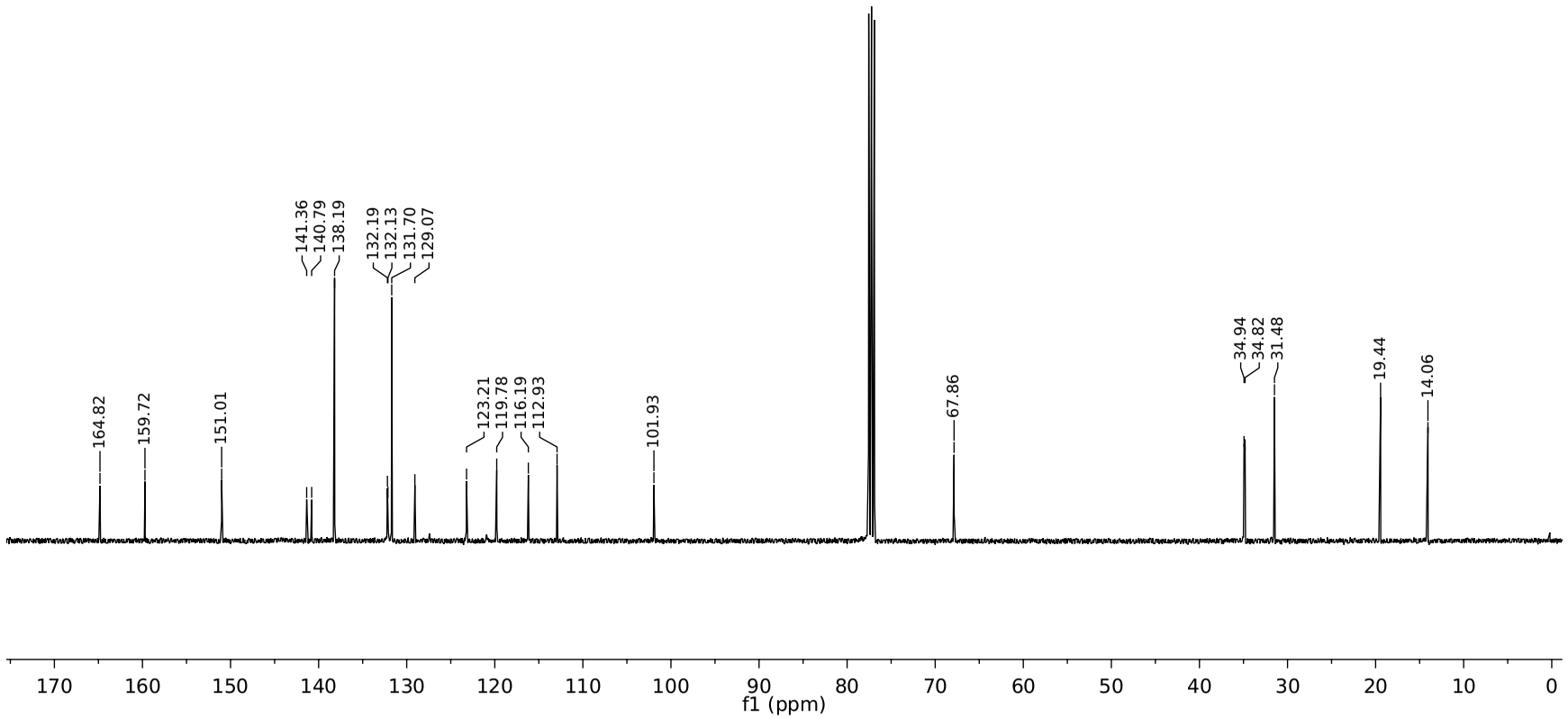
164.82
159.72
151.01
141.36
140.79
138.19
132.19
132.13
131.70
129.07
123.21
119.78
116.19
112.93
101.93
67.86
34.94
34.82
31.48
19.44
14.06
170
160
150
140
130
120
110
100
90
80
70
60
50
40
30
20
10
0
f1 (ppm)

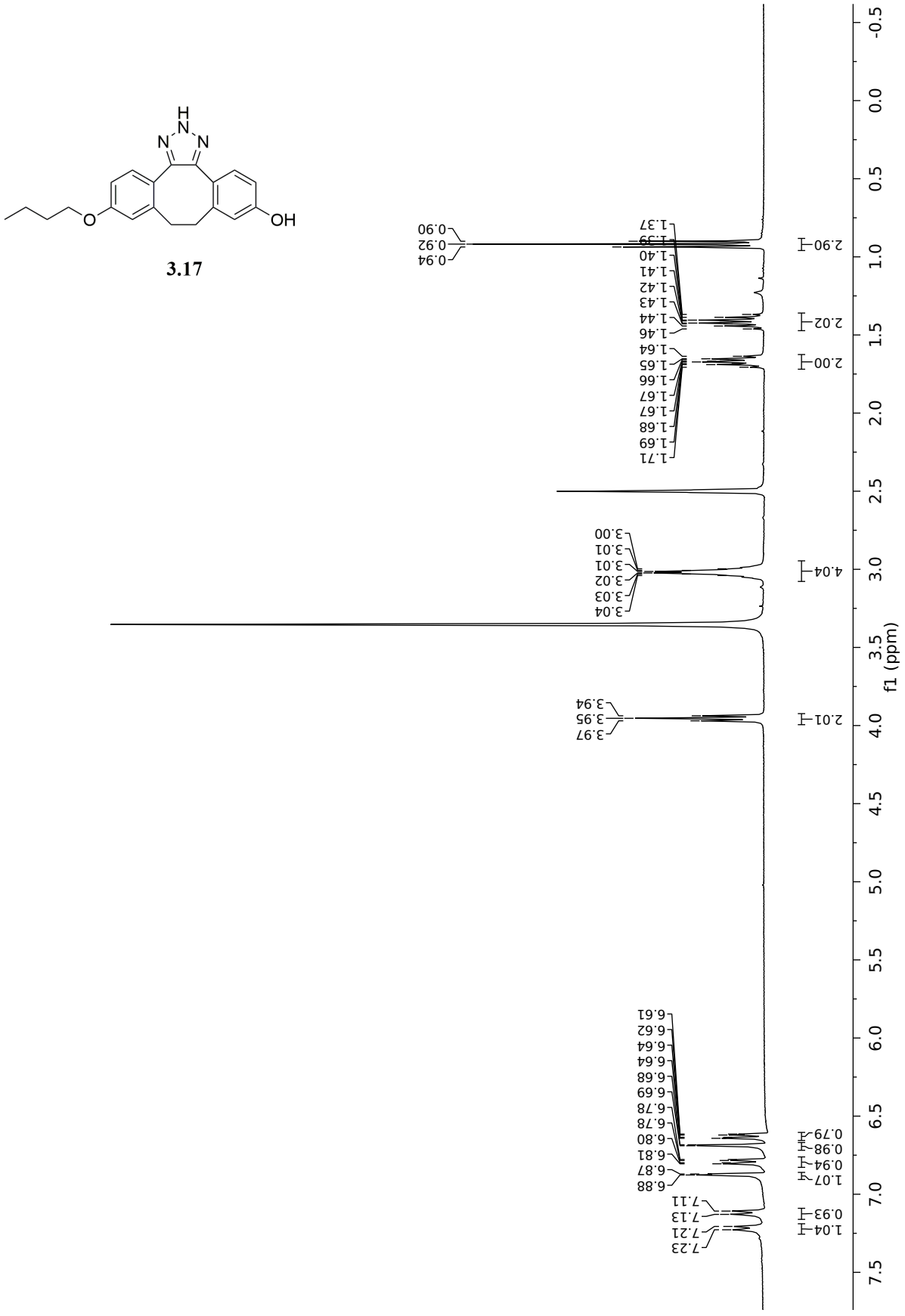
H
N
N
N
O
OH
3.17
0.94
0.92
0.90
1.71
1.69
1.68
1.67
1.67
1.66
1.65
1.64
1.46
1.44
1.43
1.42
1.41
1.40
1.39
1.37
3.04
3.03
3.02
3.01
3.01
3.00
3.97
3.95
3.94
6.88
6.87
6.81
6.80
6.78
6.78
6.69
6.68
6.64
6.64
6.62
6.61
7.23
7.21
7.13
7.11
2.90
2.02
2.00
4.04
2.01
1.04
0.93
1.07
0.94
0.98
0.79
f1 (ppm)

13.74
18.78
30.78
34.17
34.25
67.12
112.52
113.48
115.52
116.39
131.62
131.72
140.54
140.67
157.42
158.60
0
10
20
30
40
50
60
70
80
90
100
110
120
130
140
150
160
170
f1 (ppm)

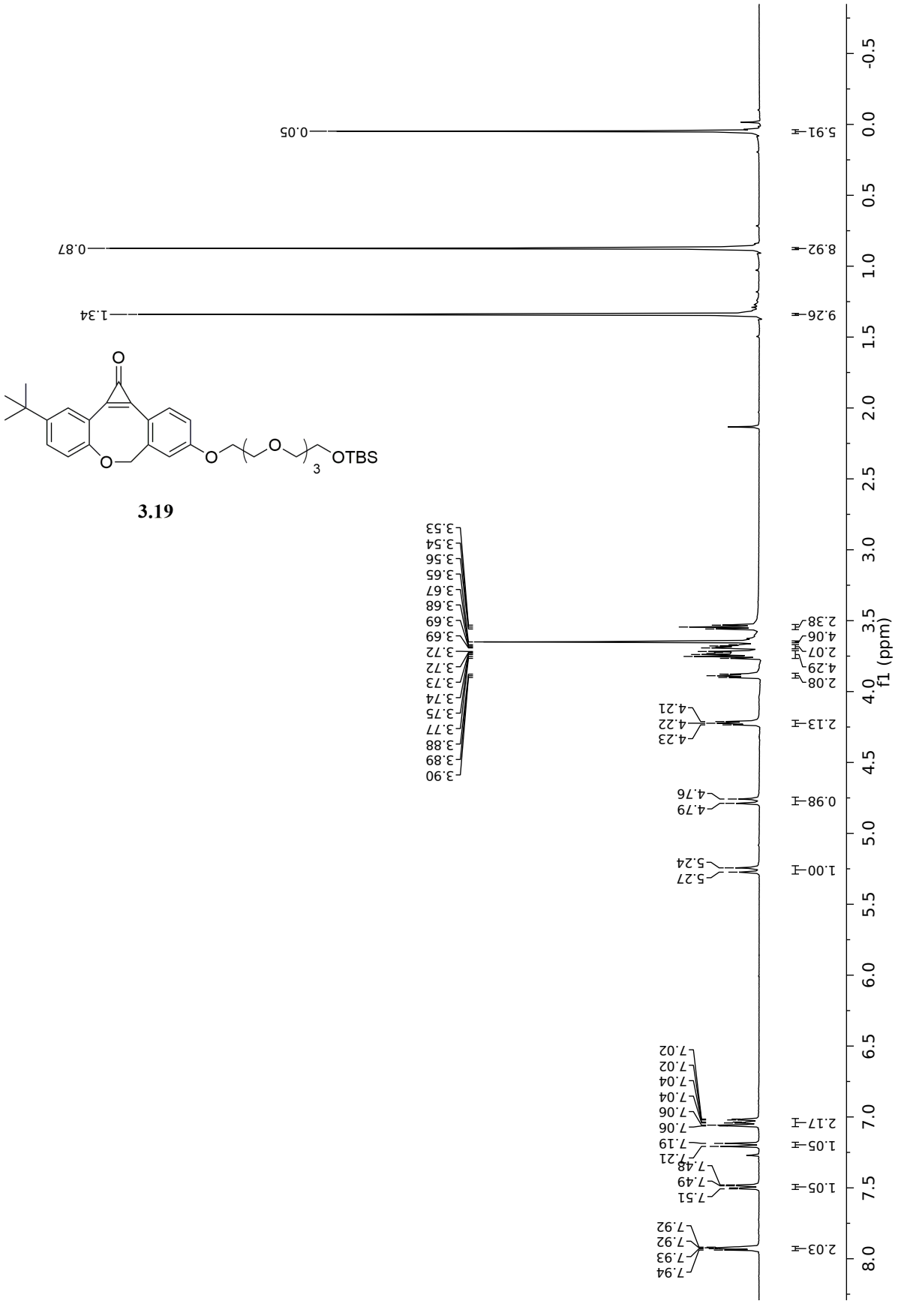
O
O
O
O
3
OTBS
1.34
0.87
0.05
9.26
8.92
5.91
2.38
4.06
2.07
4.29
2.08
2.13
4.23
4.22
4.21
0.98
4.79
4.76
1.00
5.27
5.24
2.03
7.94
7.93
7.92
7.92
1.05
7.51
7.49
7.48
7.21
1.05
7.19
2.17
7.06
7.06
7.04
7.04
7.02
7.02
3.90
3.89
3.88
3.77
3.75
3.74
3.73
3.72
3.72
3.69
3.69
3.68
3.67
3.65
3.56
3.54
3.53
f1 (ppm)

3.19

162.10
160.50
152.79
148.07
144.10
142.32
140.73
135.56
131.17
130.75
122.09
117.96
117.48
117.13
114.72
78.83
72.82
71.09
70.89
70.87
70.81
69.60
68.06
62.87
34.71
31.49
26.10
18.53
-5.08
f1 (ppm)

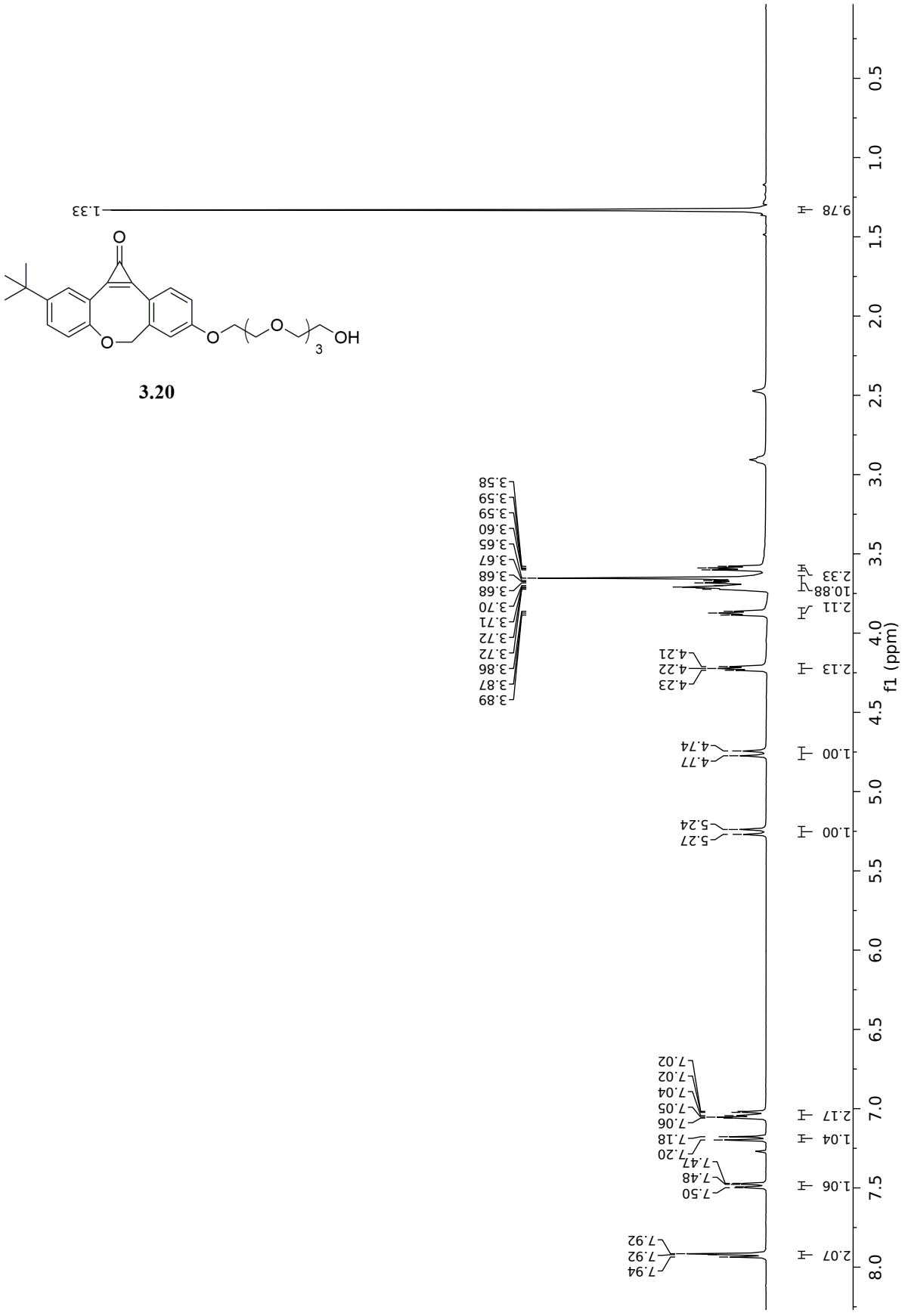
1.33
3.20
3.89
3.87
3.86
4.23
4.22
4.21
3.72
3.72
3.71
3.70
3.68
3.68
3.67
3.65
3.60
3.59
3.59
3.58
4.77
4.74
5.27
5.24
7.94
7.92
7.92
7.50
7.48
7.47
7.20
7.18
7.06
7.05
7.04
7.02
7.02
9.78
2.33
10.88
2.11
2.13
1.00
1.00
2.07
1.06
1.04
2.17
f1 (ppm)

162.04
160.48
152.81
148.05
144.02
142.23
140.72
135.57
131.14
130.76
122.07
117.91
117.48
117.07
114.72
78.80
72.67
70.98
70.77
70.68
70.41
69.57
67.98
61.81
34.69
31.46
f1 (ppm)

1.33
O
O
O
3
OH
7.28
7.27
7.27
7.25
7.25
7.23
7.25
7.13
7.13
7.11
7.11
7.05
7.05
6.94
6.93
6.92
6.91
5.21
5.18
4.57
4.54
3.90
3.89
3.87
3.76
3.75
3.74
3.74
3.72
3.72
3.71
3.69
3.68
3.68
3.64
3.62
3.61
3.82
1.07
1.00
1.10
1.00
2.00
2.27
13.02
2.46
9.03
7.0
6.5
6.0
5.5
5.0
4.5
4.0
3.5
3.0
2.5
2.0
1.5
1.0
f1 (ppm)

3.21

167.32
158.76
149.12
146.98
126.92
125.60
123.74
121.39
118.36
117.92
117.69
114.66
114.21
110.74
78.07
77.23
72.66
71.07
70.89
70.82
70.57
69.83
67.89
61.98
34.58
31.59
f1 (ppm)

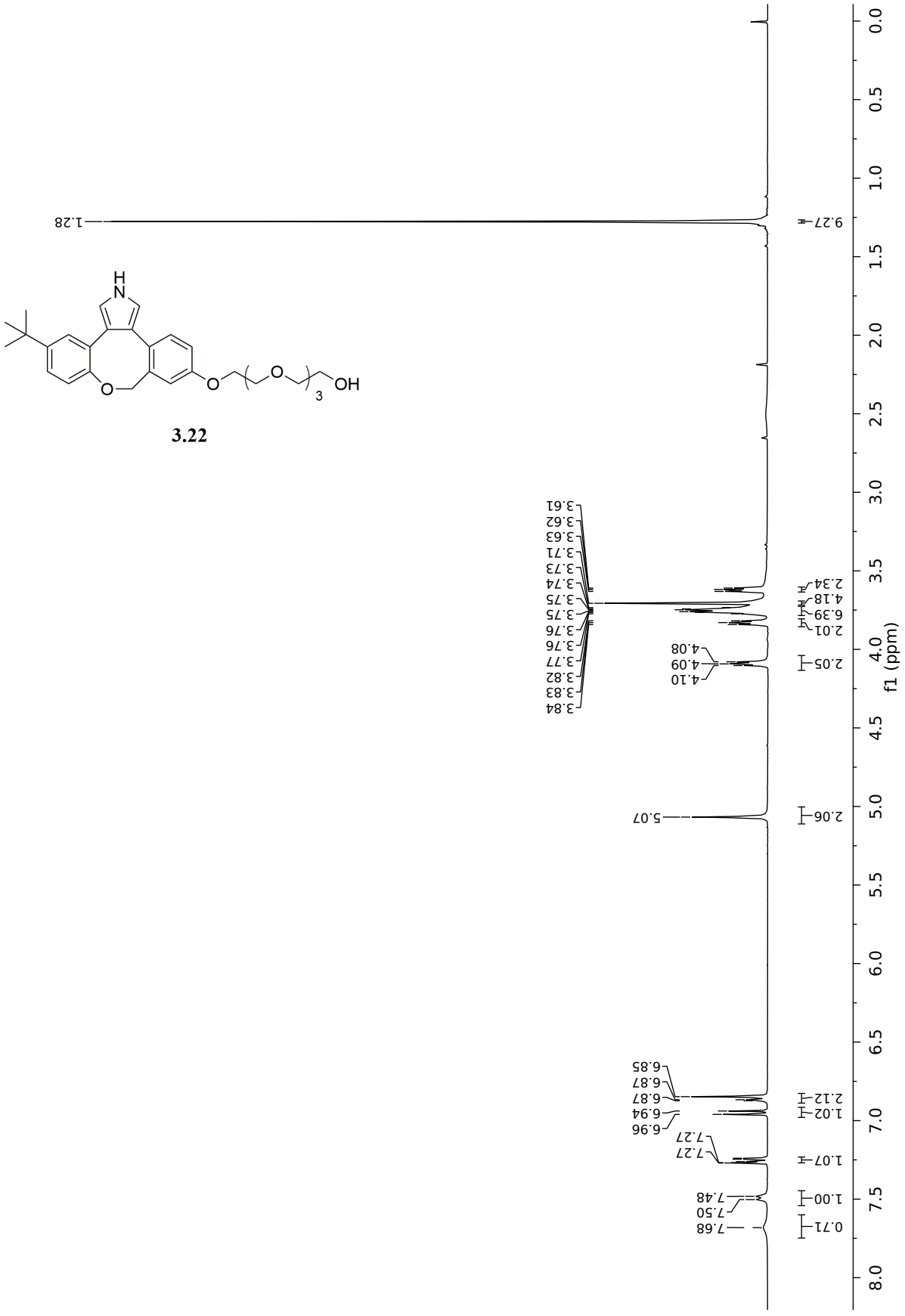
H
N
O
O
O
3
OH
3.22
1.28
9.27
7.68
7.50
7.48
7.27
6.96
6.94
6.87
6.87
6.85
5.07
4.10
4.09
4.08
3.84
3.83
3.82
3.77
3.76
3.76
3.75
3.75
3.74
3.73
3.71
3.63
3.62
3.61
2.34
4.18
6.39
2.01
0.71
1.00
1.07
1.02
2.12
2.05
2.06
f1 (ppm)

159.17
153.73
145.04
137.17
131.25
128.78
127.32
120.59
115.38
115.21
72.92
71.79
70.86
70.76
70.74
70.41
69.81
67.59
61.81
34.40
31.56
f1 (ppm)

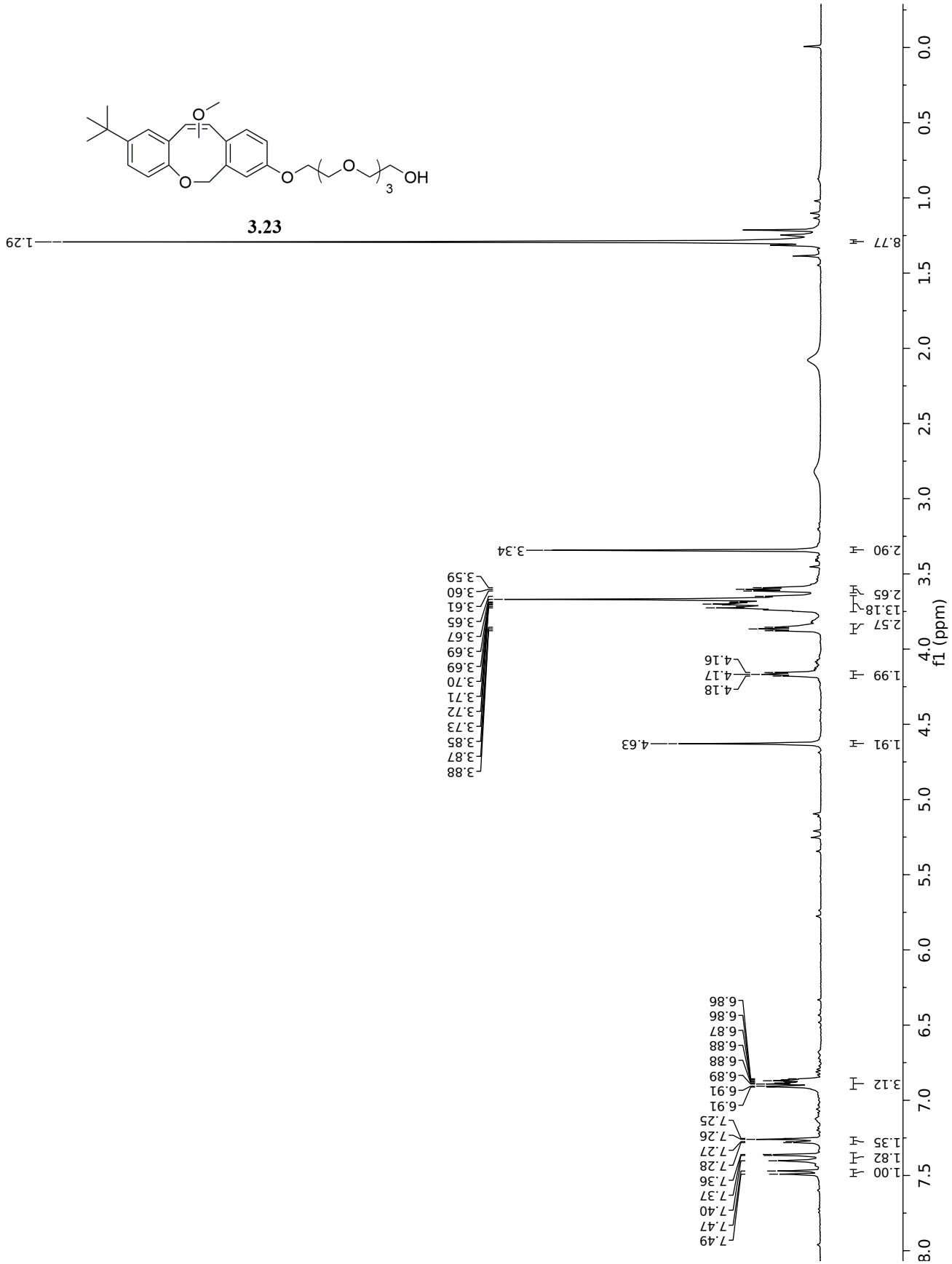
3.23
1.29
3.34
3.88
3.87
3.85
3.73
3.72
3.71
3.70
3.69
3.69
3.67
3.65
3.61
3.60
3.59
4.63
4.18
4.17
4.16
6.91
6.91
6.89
6.88
6.88
6.87
6.86
6.86
7.49
7.47
7.40
7.37
7.36
7.28
7.27
7.26
7.25
8.77
2.90
2.65
13.18
2.57
1.99
1.91
3.12
1.35
1.82
1.00
f1 (ppm)

158.83
156.22
142.70
140.91
133.27
127.70
127.53
116.48
115.19
114.94
114.10
109.20
93.34
88.66
74.09
72.74
71.02
70.84
70.77
70.49
69.81
67.74
61.93
57.48
34.24
31.63
f1 (ppm)

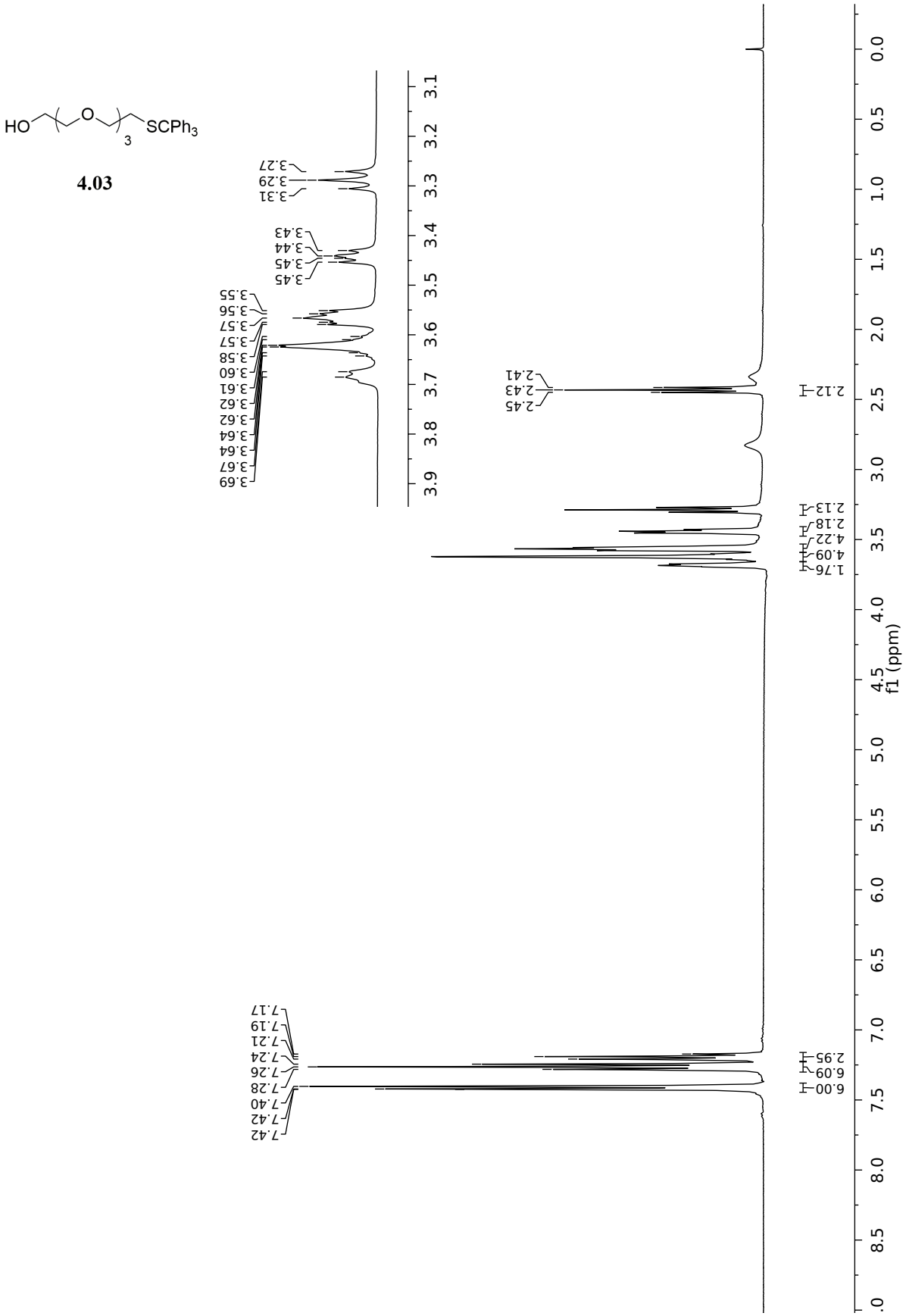
HO
O
3
SCPh3
4.03
7.42
7.42
7.40
7.28
7.26
7.24
7.21
7.19
7.17
3.69
3.67
3.64
3.64
3.62
3.62
3.61
3.60
3.58
3.57
3.57
3.57
3.56
3.55
3.45
3.45
3.44
3.43
3.31
3.29
3.27
2.45
2.43
2.41
6.00
6.09
2.95
2.12
4.09
4.22
2.18
2.13
1.76
f1 (ppm)

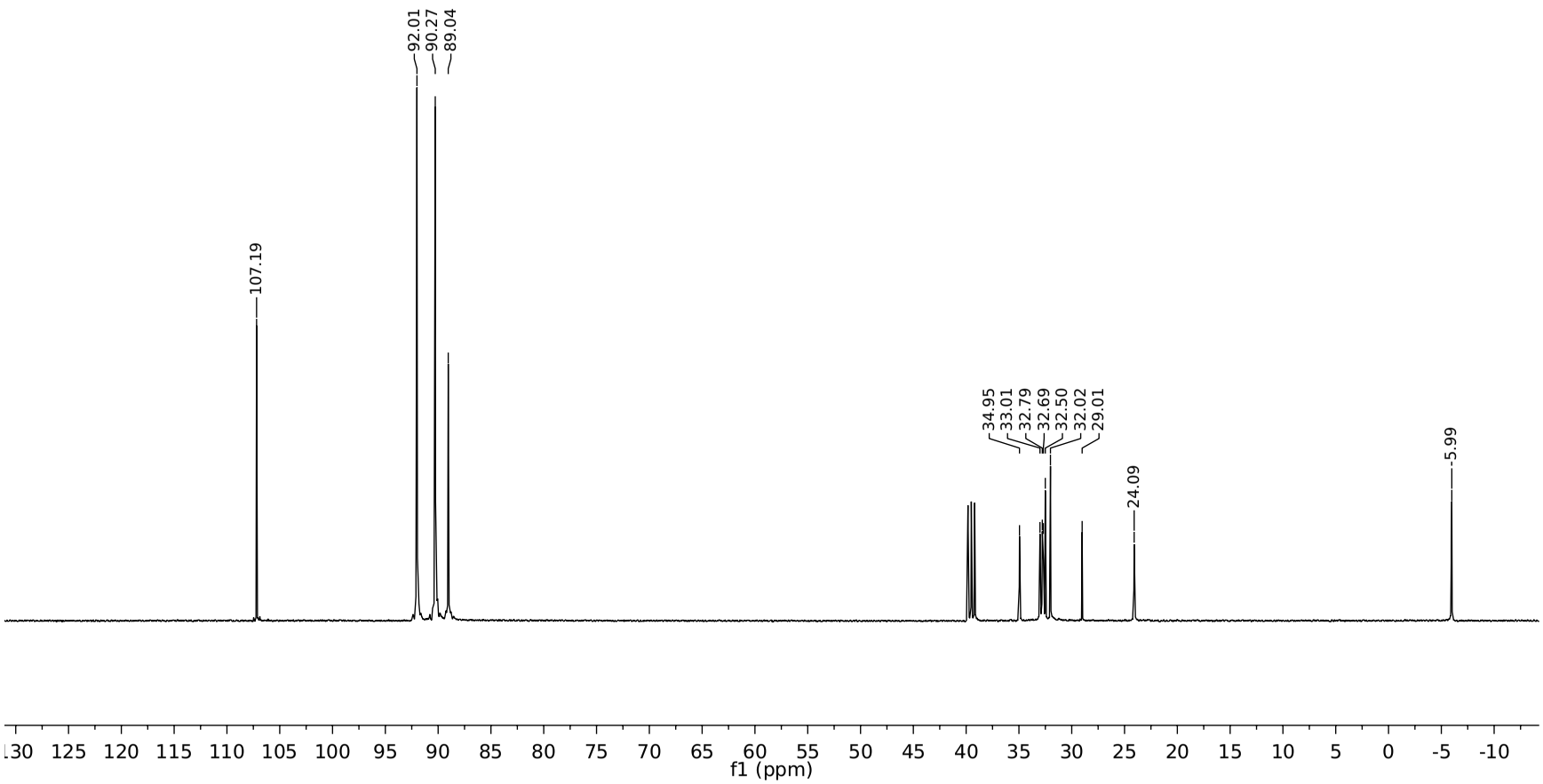
169
92.01
90.27
89.04
107.19
34.95
33.01
32.79
32.69
32.50
32.02
29.01
24.09
5.99
130 125 120 115 110 105 100 95 90 85 80 75 70 65 60 55 50 45 40 35 30 25 20 15 10 5 0 -5 -10
f1 (ppm)

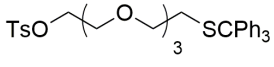
TsO
O
3
SCPh3

4.04

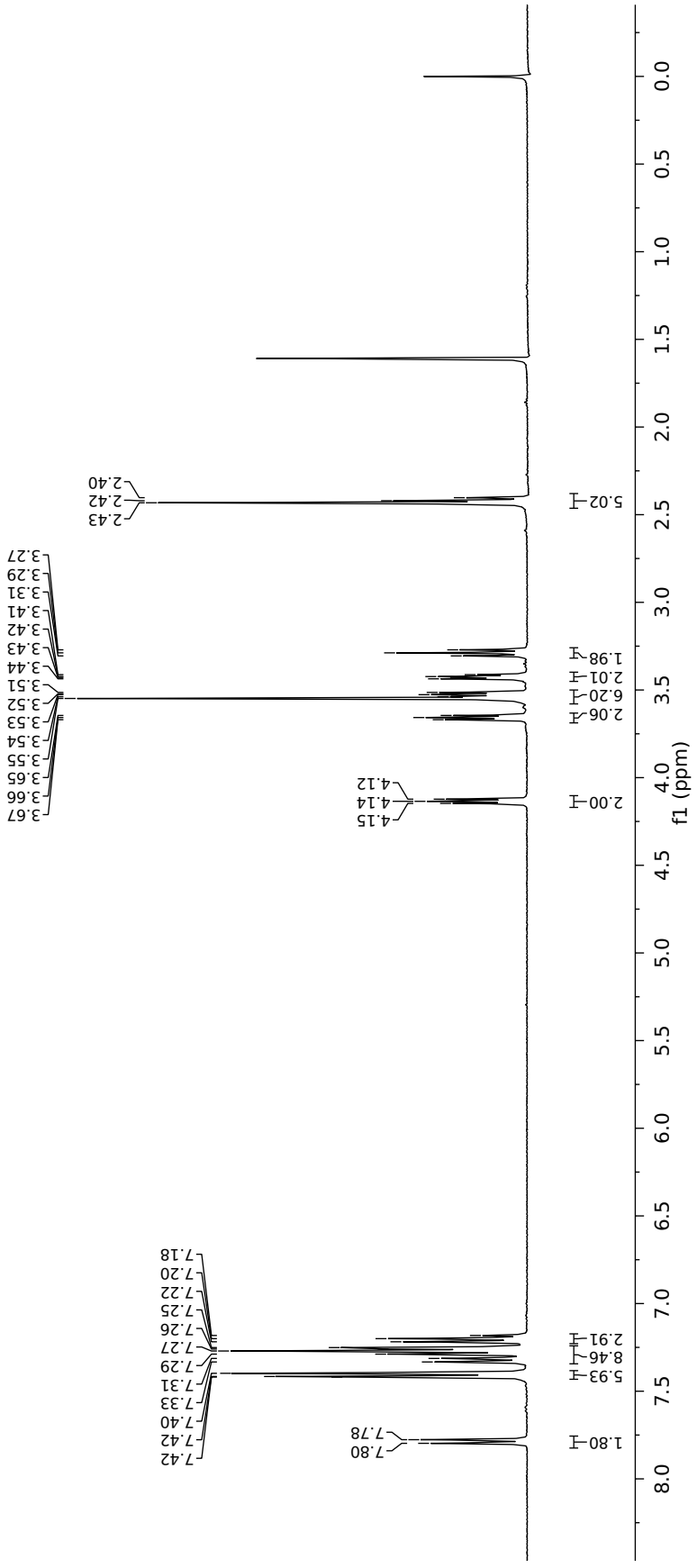
7.80
7.78
7.42
7.42
7.40
7.40
7.33
7.31
7.29
7.27
7.26
7.25
7.22
7.20
7.18
4.15
4.14
4.12
3.67
3.66
3.65
3.55
3.54
3.53
3.52
3.51
3.44
3.43
3.42
3.41
3.31
3.29
3.27
2.43
2.42
2.40
5.02
1.98
2.01
6.20
2.06
2.00
1.80
5.93
8.46
2.91
f1 (ppm)

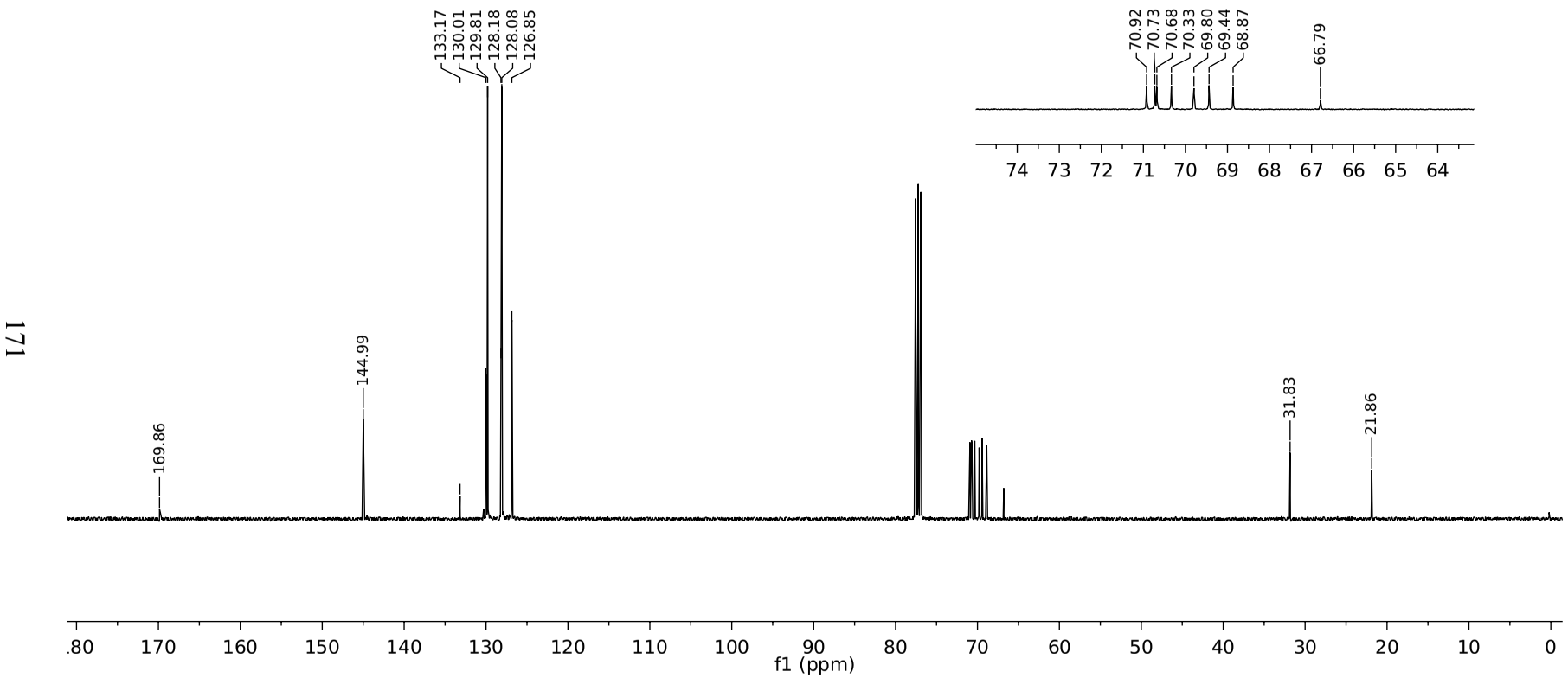
133.17
130.01
129.81
128.18
128.08
126.85
70.92
70.73
70.68
70.33
69.80
69.44
68.87
66.79
169.86
144.99
31.83
21.86
74 73 72 71 70 69 68 67 66 65 64
.80 170 160 150 140 130 120 110 100 90 80 70 60 50 40 30 20 10 0
f1 (ppm)

171

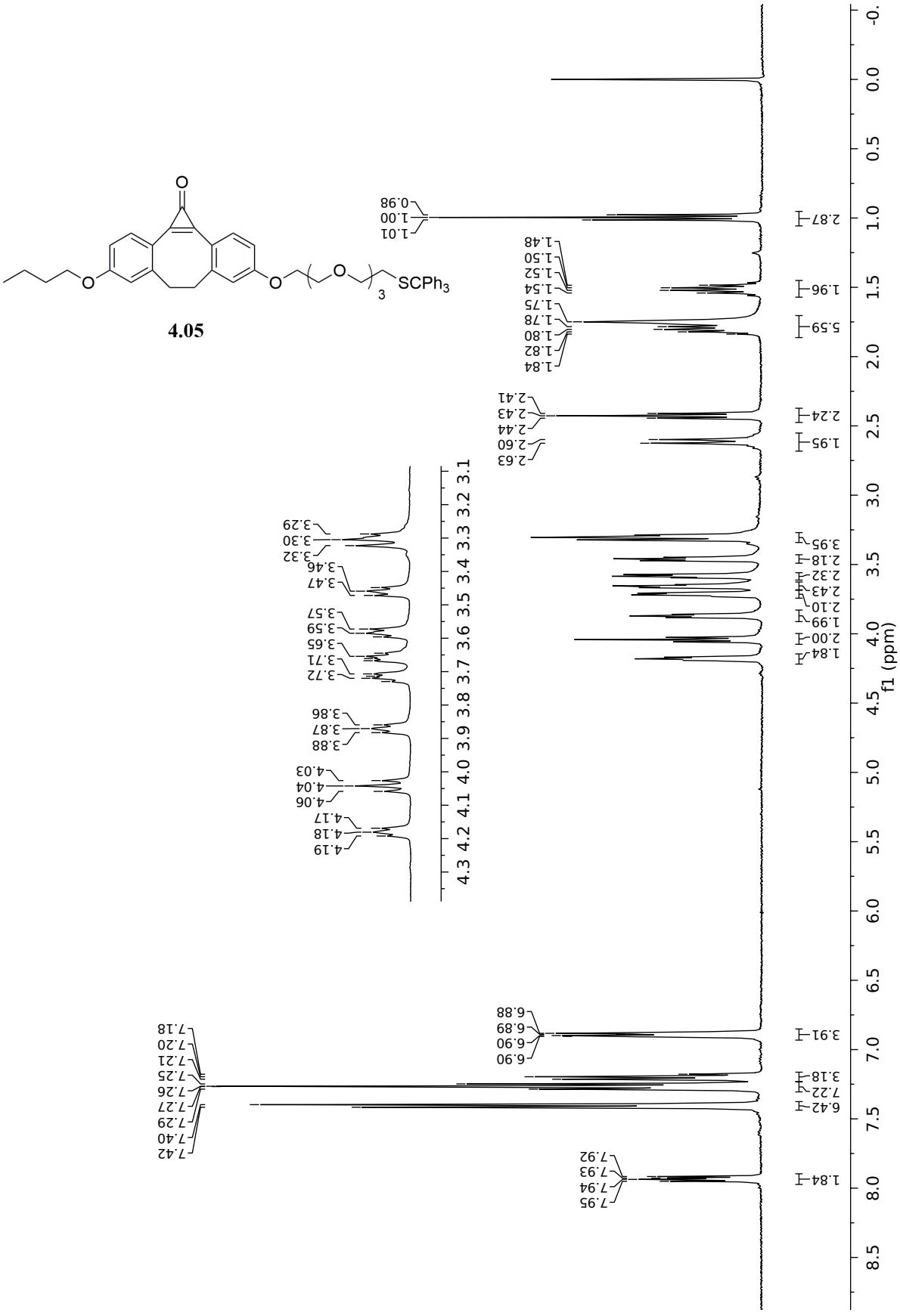

4.05

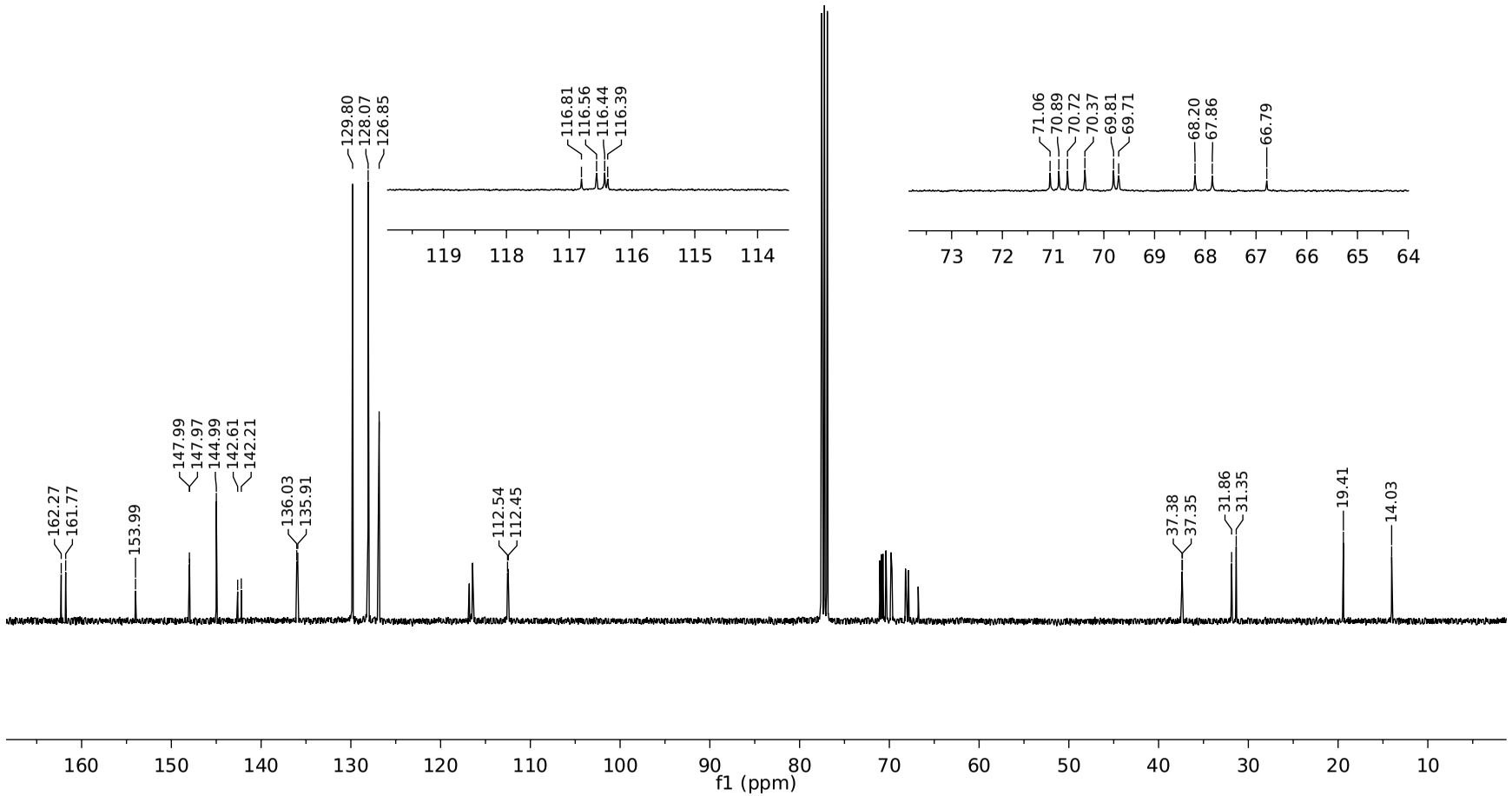
162.27
161.77
153.99
147.99
147.97
144.99
142.61
142.21
136.03
135.91
129.80
128.07
126.85
112.54
112.45
116.81
116.56
116.44
116.39
71.06
70.89
70.72
70.37
69.81
69.71
68.20
67.86
66.79
37.38
37.35
31.86
31.35
19.41
14.03
f1 (ppm)

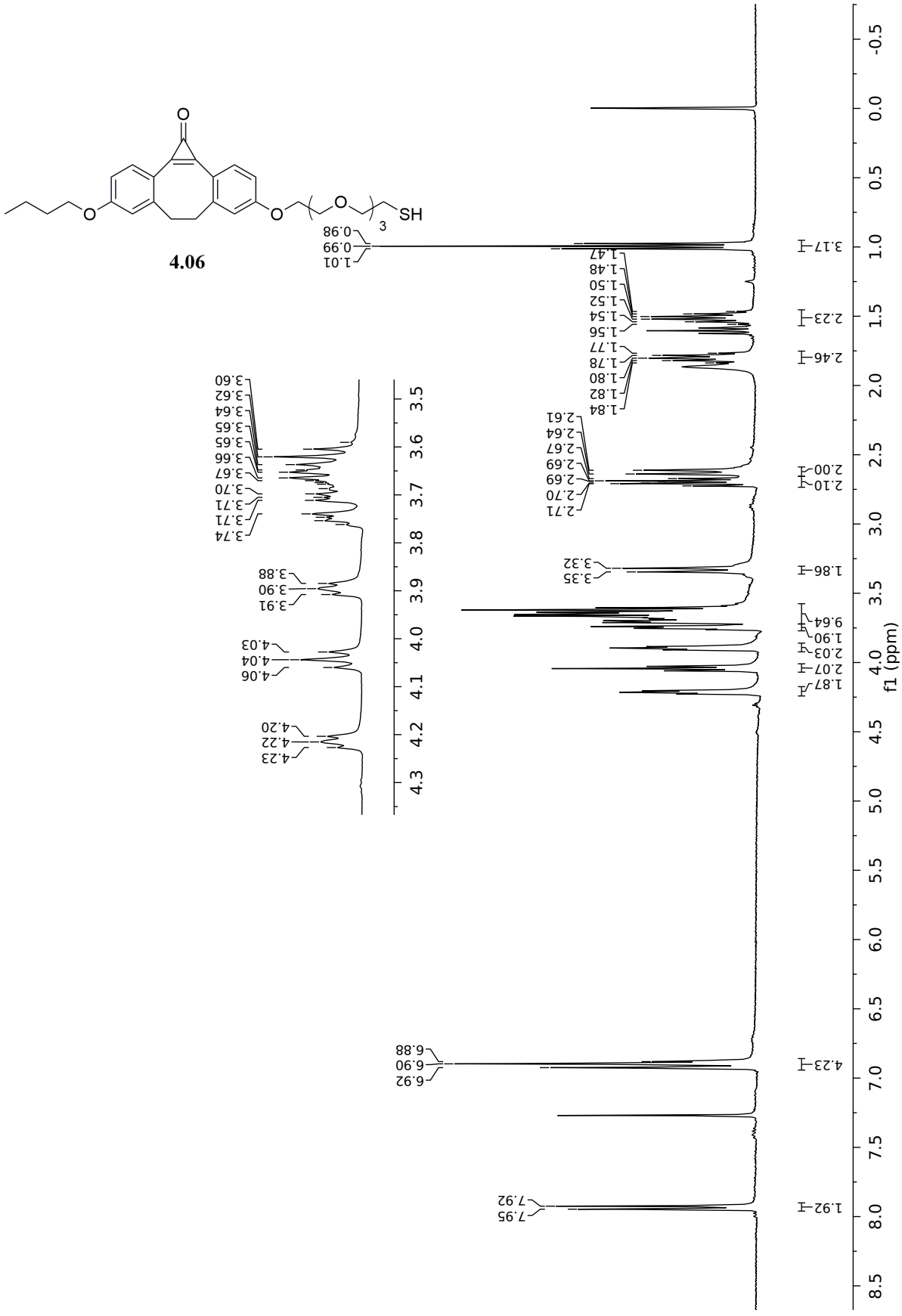
O
O
O
O
SH
3
4.06
f1 (ppm)

162.27
161.76
153.97
147.98
142.63
142.19
136.02
135.91
116.83
116.55
116.43
116.37
112.55
112.46
37.39
37.36
31.34
24.49
19.40
14.02
73.07
71.11
70.90
70.79
70.43
69.74
68.20
67.86
f1 (ppm)
f1 (ppm)

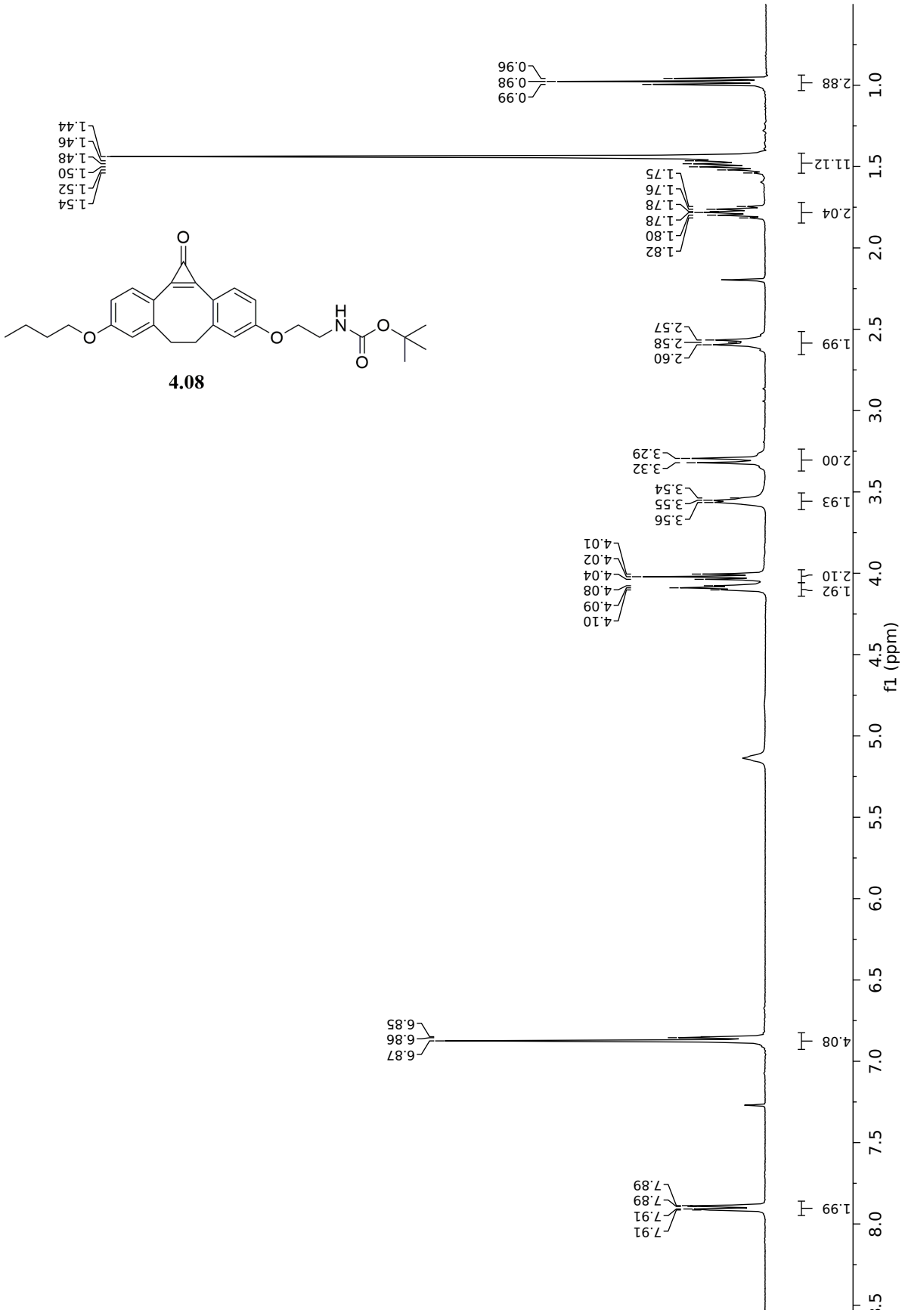
4.08
f1 (ppm)

162.07
161.30
155.86
153.66
147.82
147.71
142.53
141.84
135.75
135.64
116.72
116.16
116.07
115.93
112.46
112.27
79.60
67.97
67.39
39.95
37.13
37.10
31.10
28.36
19.16
13.79
0
10
20
30
40
50
60
70
80
90
100
110
120
130
140
150
160
170
f1 (ppm)

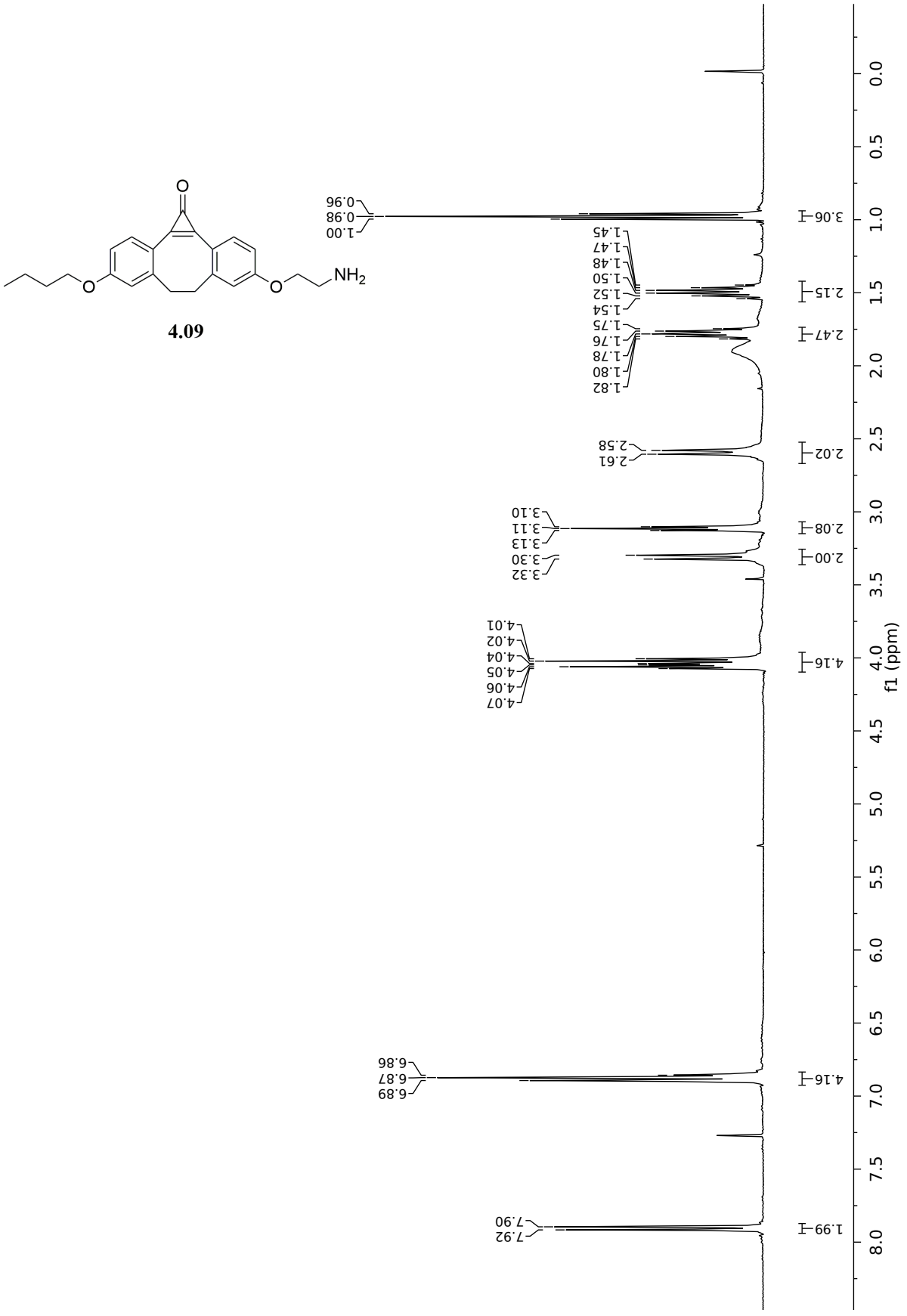
O
O
O
NH2
4.09
0.96
0.98
1.00
1.45
1.47
1.48
1.50
1.52
1.54
1.75
1.76
1.78
1.80
1.82
2.58
2.61
3.10
3.11
3.13
3.30
3.32
4.01
4.02
4.04
4.05
4.06
4.07
6.86
6.87
6.89
7.90
7.92
3.06
2.15
2.47
2.02
2.08
2.00
4.16
4.16
1.99
f1 (ppm)

13.96
19.35
31.31
37.32
37.34
41.53
68.18
70.54
112.46
112.55
116.33
116.36
116.39
116.78
135.88
135.94
142.15
142.60
147.92
147.99
153.88
161.87
162.26
f1 (ppm)

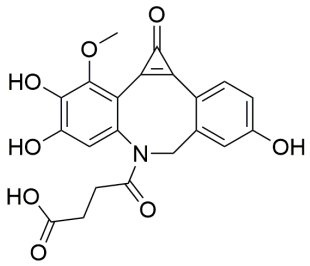
O
O
HO
HO
N
OH
HO
O
O

4.13

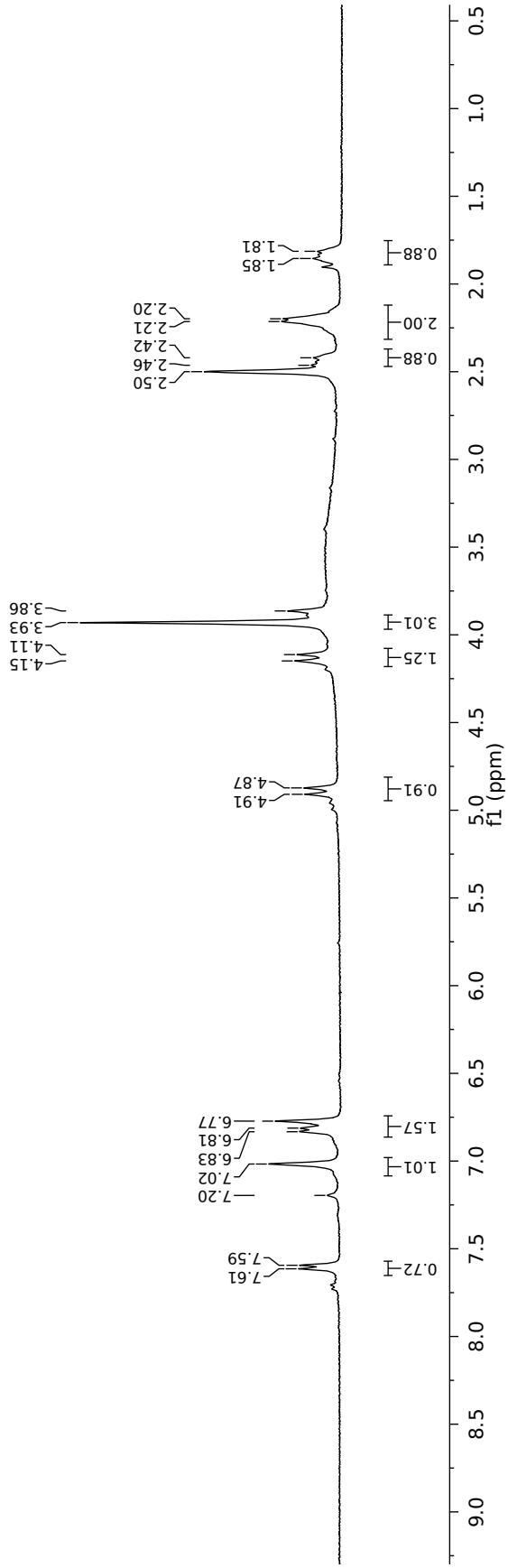
7.61
7.59
7.20
7.02
6.83
6.81
6.77
4.91
4.87
4.15
4.11
3.93
3.86
2.50
2.46
2.42
2.21
2.20
1.85
1.81
0.72
1.01
1.57
0.91
1.25
3.01
2.00
0.88
0.88
f1 (ppm)

173.60
171.13
160.60
150.94
150.65
149.09
142.74
141.56
138.38
136.21
135.81
135.14
119.06
114.78
113.84
112.55
108.53
62.05
55.82
29.04
28.97
20
30
40
50
60
70
80
90
100
110
120
130
140
150
160
170
180
f1 (ppm)

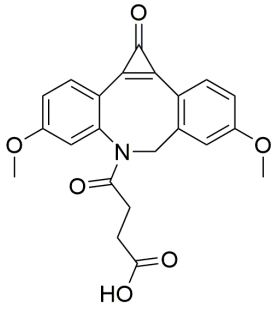

4.16

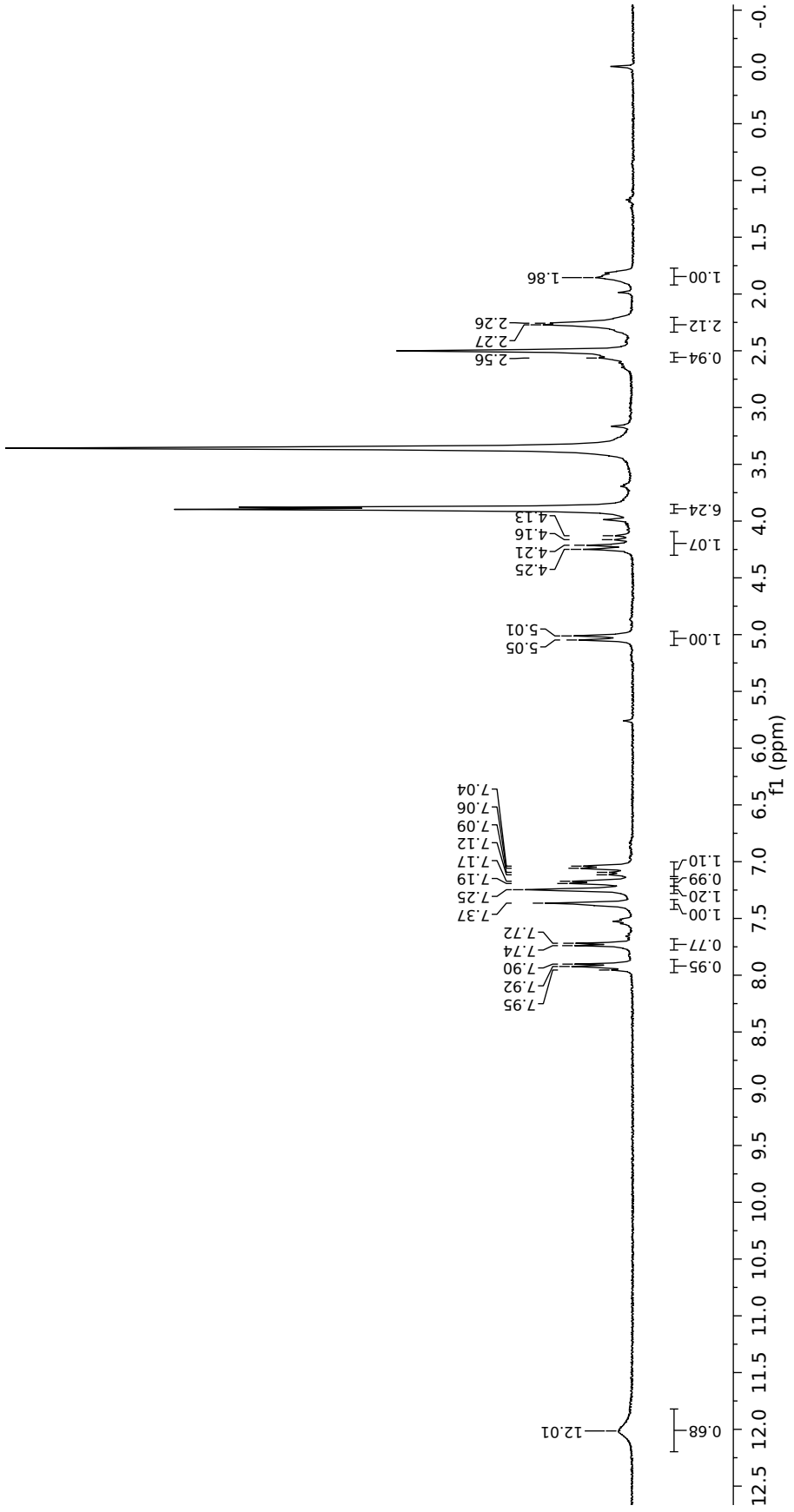
12.01
7.95
7.92
7.90
7.74
7.72
7.37
7.25
7.19
7.17
7.12
7.09
7.06
7.04
5.05
5.01
4.25
4.21
4.16
4.13
2.56
2.27
2.26
1.86
0.68
1.00
0.77
0.95
1.00
1.20
0.99
1.10
1.00
2.12
0.94
6.24
1.07
f1 (ppm)

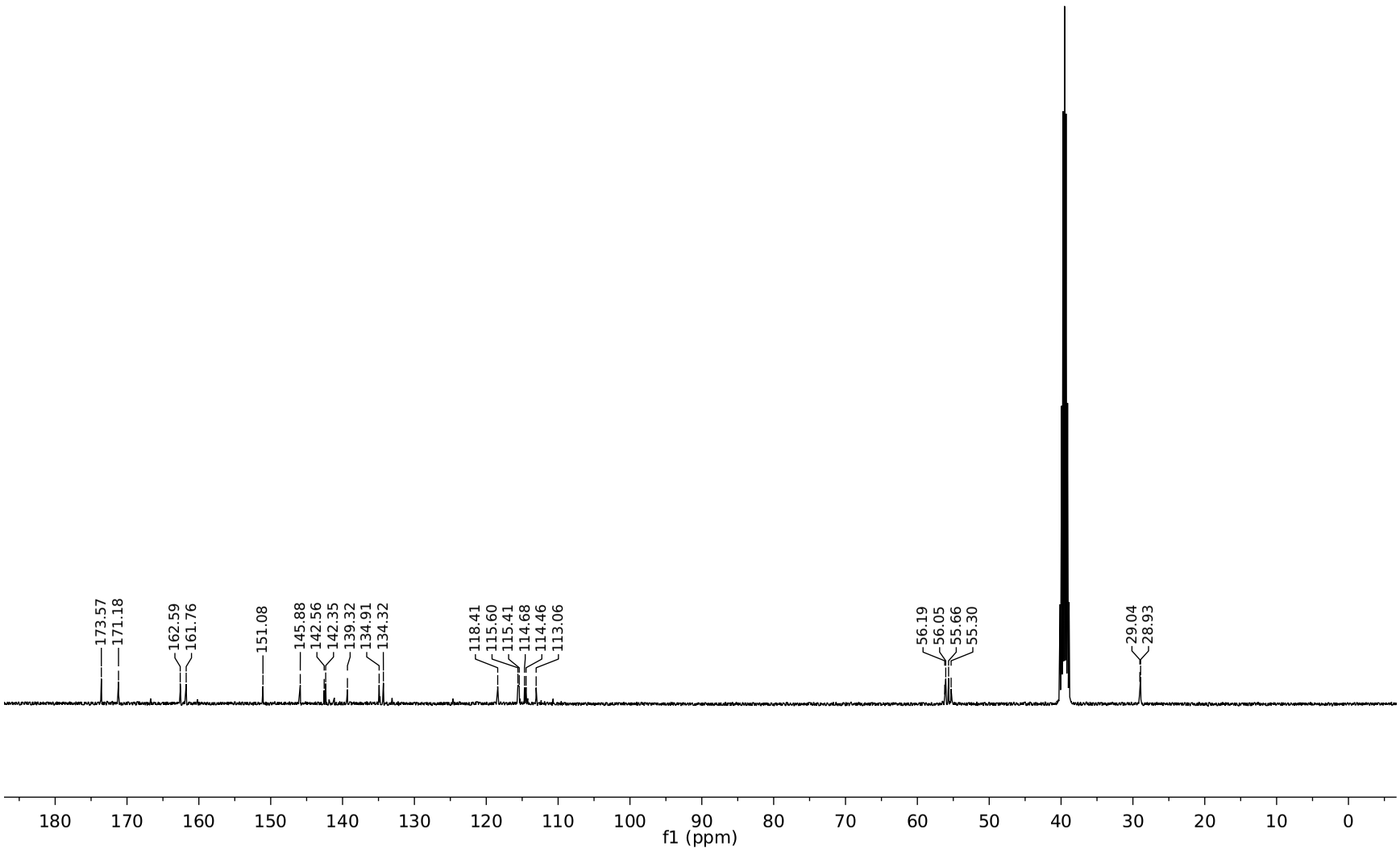
173.57
171.18
162.59
161.76
151.08
145.88
142.56
142.35
139.32
134.91
134.32
118.41
115.60
115.41
114.68
114.46
113.06
56.19
56.05
55.66
55.30
29.04
28.93
180
170
160
150
140
130
120
110
100
90
80
70
60
50
40
30
20
10
0
f1 (ppm)

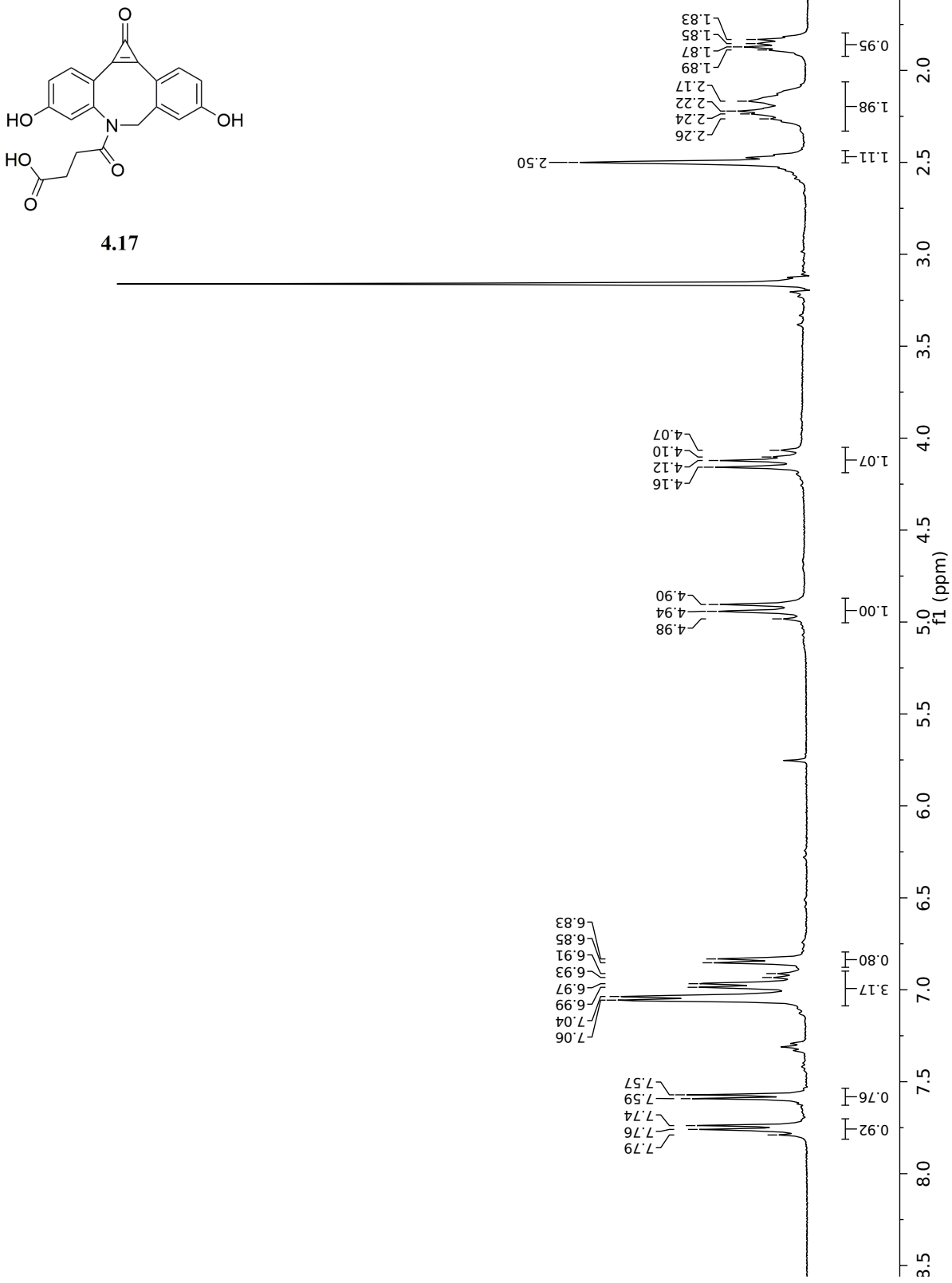
HO
OH
HO
N
O
O
O
O
4.17
7.79
7.76
7.74
7.59
7.57
7.06
7.04
6.99
6.97
6.93
6.91
6.85
6.83
4.98
4.94
4.90
4.16
4.12
4.10
4.07
2.50
2.26
2.24
2.22
2.17
1.89
1.87
1.85
1.83
0.92
0.76
0.80
3.17
1.00
1.07
1.11
1.98
0.95
f1 (ppm)

29.71
29.56
48.64
55.38
112.75
113.92
114.96
115.96
116.89
119.55
134.39
134.87
138.37
140.93
141.23
142.41
146.00
151.03
160.83
162.35
171.29
f1 (ppm)

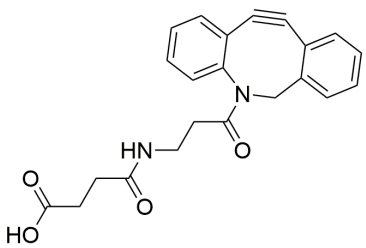

4.20

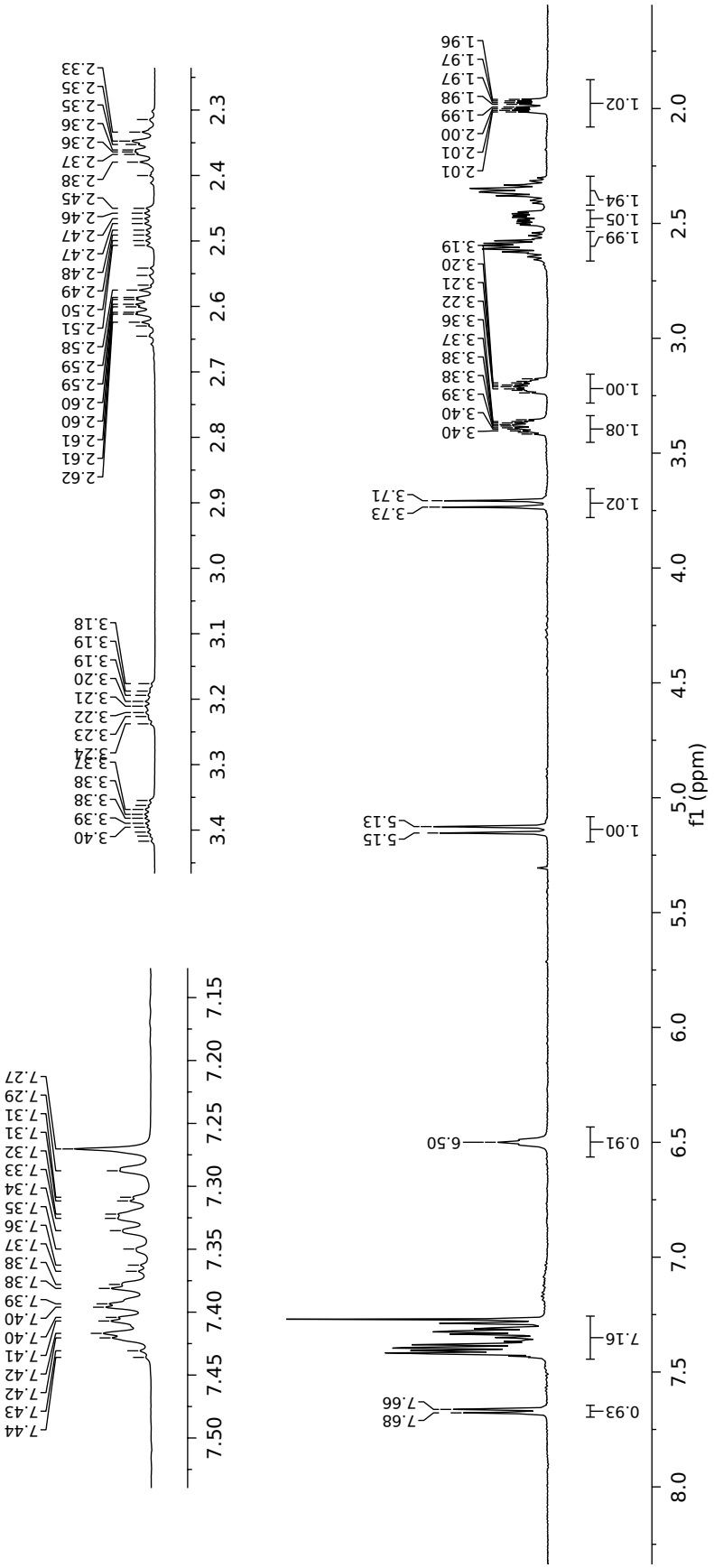

175.68
172.62
172.32
151.12
148.01
132.36
129.23
128.89
128.76
128.54
128.13
127.48
125.82
123.12
122.75
107.91
115.05
55.86
35.72
34.69
30.86
30.04
f1 (ppm)